To the Graduate Council:

I am submitting herewith a dissertation written by Mickey Charles McBrayer entitled "Clay Barriers: Laboratory Study of Hydraulic Defects and Preferential Flow Paths." I have examined the final copy of this dissertation for form and content and recommend that it be accepted in partial fulfillment of the requirements for the degree of Master of Science, with a major in Civil Engineering.

Matthew Mauldon, Major Professor

We have read this dissertation
and recommend its acceptance:

Accepted for the Council:

Associate Vice Chancellor and
Dean of the Graduate School

In presenting this thesis in partial fulfillment of the requirements for a Master's degree at the University of Tennessee, Knoxville, I agree that the Library shall make it available to borrowers under rules of the Library. Brief quotations from this thesis are allowable without special permission, provided that accurate acknowledgment of the source is made.

Permission for extensive quotation from or reproduction of this thesis may be granted by the major professor, or in his absence, by the Head of Interlibrary Services when, in the opinion of either, the proposed use of the material is for scholarly purposes. Any copying or use of the material in this thesis for financial gain shall not be allowed without my written permission.

Signature Mindy C McBrayer

Date 4/28/95

CLAY BARRIERS: LABORATORY STUDY OF HYDRAULIC DEFECTS AND PREFERENTIAL FLOW PATHS

A Thesis

Presented for the

Master of Science

Degree

The University of Tennessee, Knoxville

Mickey Charles McBrayer

May 1995

DEDICATION

This thesis is dedicated to

Almighty God

Who Created me in His Own Image

and has made everything possible,

and to my parents,

James M. McBrayer and Laura K. McBrayer,

whose support, encouragement, and prayers have

inspired and enabled me to complete my thesis and degrees.

For by Him all things were created that are in heaven and that are on earth,

visible and invisible, whether thrones or dominions or principalities or powers.

All things were created through Him and for Him (Colossians 1:16).

ACKNOWLEDGMENTS

I would like to thank Dr. Matthew Mauldon for his help and guidance throughout this project. I also would like to thank Dr. Eric Drumm and Dr. Glenn Wilson for their assistance and input, and for their service on my committee. The help provided by Curtis Allin and Ken Thomas in the laboratory is also greatly appreciated. I am also grateful to the J.M. Huber Corporation for providing the commercial kaolinite which is produced under the trade name Barden AG-1. This research was carried out under the DOE-UTK Joint Education Program in Environmental Restoration and Waste Management, Gregory D. Reed (P.I.). This work was supported, in whole or in part, by a DOE cooperative agreement DE-FC05-920R22056. This support does not constitute an endorsement by DOE of the views expressed herein.

ABSTRACT

A laboratory testing program was carried out to evaluate the importance of preferential flow in fractured clay. The saturated hydraulic conductivity was found to be insufficient in capturing the contribution of preferential flow paths during flow, especially for smaller samples. The reason for this is that these pathways closed as the sample swelled upon saturation. These pathways seem to be much more hydraulically active during the dynamic stage of infiltration before the cracks close. Three series of tests were conducted to evaluate the development of preferential flow paths, show the dynamics of flow through clay fractures, and explore the importance of preferential flow paths during infiltration.

Flow tests were performed on desiccated slurry samples to investigate the impact of swelling on fractures. An apparent hydraulic conductivity defined for unsaturated conditions in fractured clay was shown to decrease by as much as three orders of magnitude as the fractures closed. Digital images of the samples before and after the flow tests showed closing of the fractures. Flow interruptions were used to show how the head can influence the rate at which fractures closed. Infiltration tests performed with a red dye showed the influence of preferential flow in compacted kaolinite samples. The dye stains dramatically illustrated the importance of preferential flow paths during infiltration. Fractures and clod size were found to have a strong influence on both the rate and depth of infiltration. These pathways may be especially important in governing contaminant transport in compacted clay barriers.

TABLE OF CONTENTS

PART 1

INTRODUCTION

COMPACTED CLAY BARRIERS 2

PREFERENTIAL FLOW 4

Development of Preferential Flow Paths

in Clay Barriers 6

Flow Through Preferential Flow Paths 8

SATURATED HYDRAULIC CONDUCTIVITY MEASUREMENTS 11

PART 2

THE NATURE OF CLAY FRACTURES

PREFERENTIAL FLOW PATHS IN COMPACTED CLAY LINERS 19

Chemical Attack 19

Differential Settlement 20

Plant Roots and Animals 21

Desiccation 21

Desiccation Tests 24

Freeze / Thaw 32

Freeze / Thaw Tests 36

Clod Size 39

Interlift Transport 40

CLAY SWELLING 40

Crack Development Tests 42

PART 3

FLOW TESTS IN FRACTURED CLAY

FLOW TESTING 47

Apparent Conductivity 50

Rising Head 51

Constant Head 53

Falling Head 53

FLOW TEST RESULTS 55

Side-Wall Leakage 55

Presentation of Flow Test Results 56

Decrease in Apparent Conductivity 60

Effect of Average Fracture Area on Short Term Fracture Flow 60

Fracture Geometry 63

Closing of Fractures 67

Effect of Head on Fracture Closure 69

PART 4

INFILTRATION TESTS IN FRACTURED CLAY

INFILTRATION 77

INFILTRATION TESTS 79

Influence of Fractures on Infiltration 82

Influence of Clods on Infiltration 84

Closing of Fractures 86

PART 5

DEVELOPMENTAL STUDY IN USING ELECTRICAL RESISTIVITY TO PREDICT SUBSURFACE CRACKING

INTRODUCTION 90

THEORY OF ELECTRICAL RESISTIVITY SURVEYS 91

THE ELECTRICAL RESISTIVITY OF EARTH MATERIALS 93

The Effect of Fractures on Electrical Resistivity 95

Resistivity Studies in Compacted Clay Barriers 97

DESIGN OF A LABORATORY RESISTIVITY SURVEY 98

Resistivity Test Results 102

PART 6

SUMMARY

INTRODUCTION 104

OBJECTIVES 108

MATERIALS AND METHODS 108

Crack Development Tests 109

Flow Tests 109

Infiltration Tests 112

RESULTS AND DISCUSSION 114

Crack Development Tests 114

Flow Tests 116

Infiltration Tests 121

CONCLUSIONS 127

PART 7

CONCLUSIONS AND RECOMMENDATIONS

CONCLUSIONS 131

RECOMMENDATIONS FOR FURTHER RESEARCH 134

REFERENCES 135

APPENDICES

APPENDIX 1: FLOW TEST RESULTS 141

APPENDIX 2: INFILTRATION TEST RESULTS 189

VITA 215

LIST OF TABLES

TABLE PAGE

1-1 Summary of desiccation cracks in various liner sections 6

1-2 Hydraulic conductivity of FWP samples 13

1-3 Results of constant head conductivity tests 15

2-1 Kaolinite properties 25

2-2 Summary of results from desiccation tests 25

3-1 Estimated percent fracture closure 68

LIST OF FIGURES

FIGURE		PAGE
1-1	Schematic of solid waste landfill (after Tchobanoglous, 1993)	2
1-2	Schematic of a typical Darcy experiment	3
1-3	Hydraulic conductivity and compaction relationships	4
1-4	Preferential Flow (after Beven and Germann, 1982)	5
1-5	Typical Liner / Cover Sections (after Corser and Cranston, 1991)	7
1-6	Stages of water flow in a macropore (Beven & Germann, 1981)	10
1-7	Procedure for constant head hydraulic conductivity tests	14
2-1	Batch #4 Drying Stages	27
2-2	Batch #5 Drying Stages	28
2-3	Batch #6 Drying Stages	30
2-4	Batch #7 Drying Stages	31
2-5	Batch #8 Drying Stages	33
2-6	Batch #9 Drying Stages	34
2-7	Crack Development: Sample FT-8	37
2-8	Crack Development: Sample FT-9	38
2-9	Decrease in hydraulic conductivity (after Leeds-Harrison, et al., 1986)	41
2-10	Crack Development: Sample D-4 (small clod size)	43
2-11	Crack Development: Sample D-5 (large clod size)	44
3-1	Sampling Procedure for Flow Tests	48

3-2 Schematic of flow test system 49

3-3 Bingham flow effects 51

3-4 Apparent Conductivity 52

3-5 Tests for Batch #5, Sample #4 57

3-6 Short Term Flow Tests 61

3-7 Long Term Flow Tests 62

3-8 Relationship Between Apparent Conductivity and Average Fracture Area 64

3-9 Effect of head on fracture closure 70

3-10 Pressure equilibrium / disequilibrium at crack surface 74

4-1 Macropore effects on infiltration (Beven & Germann, 1981) 78

4-2 Procedure of Exposing Fracture Stains 80

4-3 Schematic of Infiltration system 81

4-4 Fracture effects on infiltration 83

4-5 Clod size effects on infiltration 85

4-6 Fracture stains: Sample FT-6 87

5-1 Measuring Resistivity 91

5-2 The Electrical Resistivity of Earth Materials 94

5-3 Variation of Soil Resistivity with Moisture Content (McCarter, 1994) 96

5-4 Four-probed Wenner array 99

5-5 Design of Electrical Resistivity Test 101

6-1 Sample preparation for flow tests 110

6-2 Schematic of flow test system 111

6-3 Apparent Conductivity 112

6-4 Infiltration test procedure 113

6-5 Cracking due to desiccation and freeze/thaw 115

6-6 Flow test results 117

6-7 Flow interruptions 119

6-8 Pressure equilibrium / disequilibrium at crack surface 121

6-9 Fracture effects on infiltration 124

6-10 Clod size effects on infiltration 126

6-11 Fracture stains: Sample FT-6 127

PART 1

INTRODUCTION

COMPACTED CLAY BARRIERS

Compacted clay barriers are used in solid waste landfills to isolate the waste from infiltrating water and to minimize the flow of leachate from the waste. Figure 1-1 shows a cross section of a typical municipal solid waste landfill. The final cover system is designed to limit percolation through the waste and minimize the generation of leachate. The daily cover and bottom liner provide further protection from the migration of leachate into the subsurface. The effectiveness of these barriers depends on their ability to limit the movement of water and contaminants. The saturated hydraulic conductivity (K_s) of the clay is used to quantify this. The hydraulic conductivity in Darcy's Law describes the ability of water to flow through soil. A schematic of a typical Darcy experiment is given in Figure 1-2.

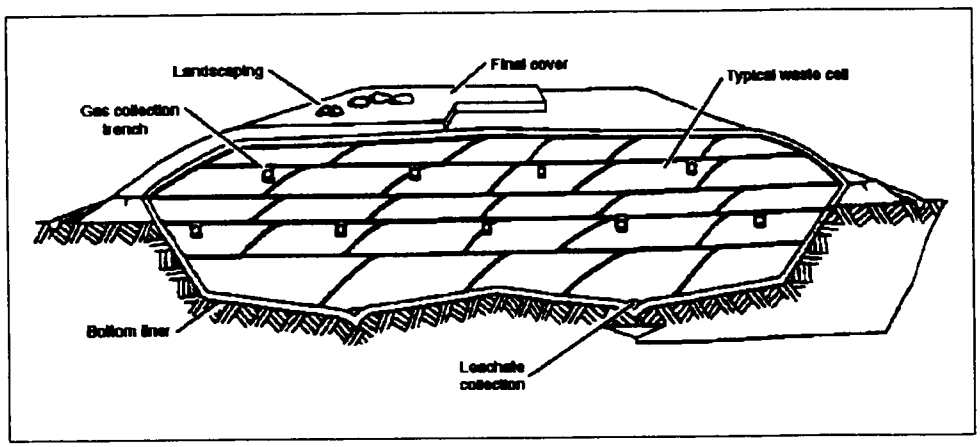


Fig. 1-1. Schematic of solid waste landfill (after Tchobanoglous, 1993)

Darcy's Law is usually given by the following equation,

$$Q = - K i A = K \frac{\Delta H}{\Delta x} A \qquad (1\text{-}1)$$

where,

Q = rate of flow (cm^3 / s)
K = hydraulic conductivity (cm / s)
i = hydraulic gradient (dimensionless) = $\frac{\Delta H}{\Delta x}$
ΔH = head loss across specimen (cm)
Δx = length of specimen (cm)
A = cross-sectional area of specimen perpendicular to direction of flow (cm^2)

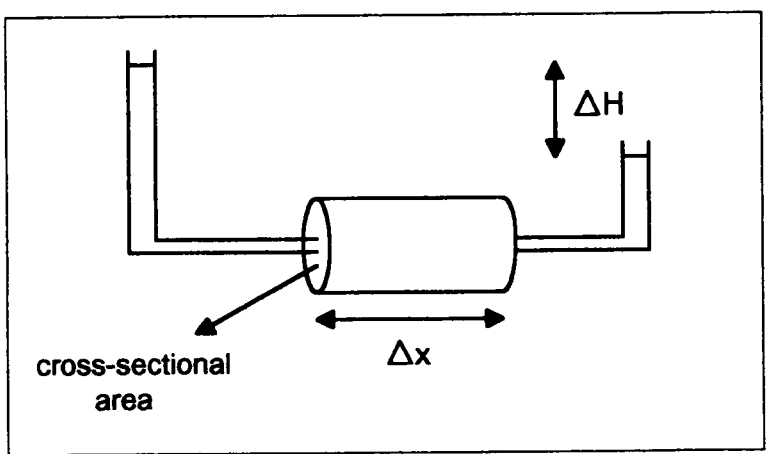


Fig. 1-2. Schematic of a typical Darcy experiment

The U.S. Environmental Protection Agency (EPA) requires liner materials to achieve a K_s of less than $1x10^{-7}$ cm/sec (EPA, 1989). Factors most affecting the hydraulic conductivity include: (1) soil structure; (2) soil texture; (3) fluid characteristics; and (4) entrapped air. The impact of structure, or pore size distribution, on the long term saturated conductivity has received increased attention in recent years. Daniel and Benson (1990) showed that water content

and compactive effort are critical when constructing a barrier for minimum hydraulic conductivity. The general relationships among these parameters are illustrated in Figure 1-3. It can be seen from the figure that the hydraulic conductivity decreases significantly for water contents wet of optimum for each compactive effort. Furthermore, the hydraulic conductivity decreases as compactive effort increases for a given water content. Mundell and Bailey (1985) propose that the hydraulic conductivity of soil compacted dry of optimum can be 10 to 1000 times larger than for soil compacted wet of optimum.

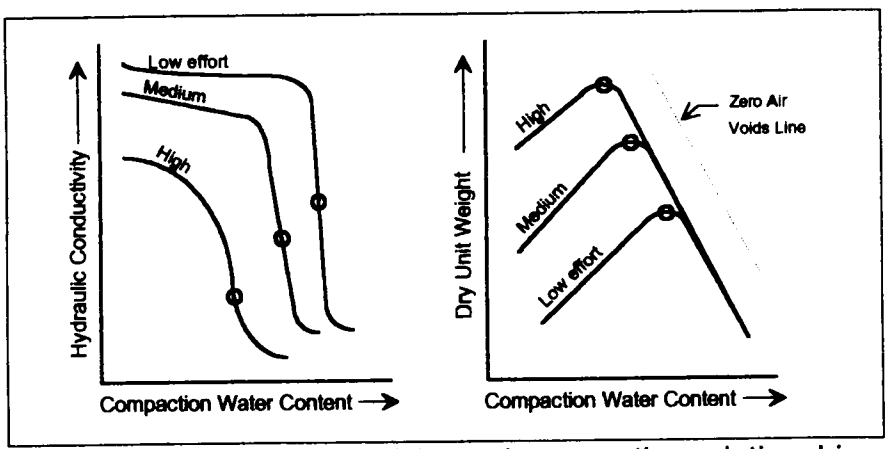


Fig. 1-3. Hydraulic conductivity and compaction relationships (after Mundell & Bailey, 1985)

PREFERENTIAL FLOW

The flow domain through a compacted clay barrier is often assumed to be homogeneous and continuous. However, the presence of cracks and other defects can render this assumption inappropriate (see Figure 1-4). Preferential flow paths can allow contaminants to migrate and spread rapidly, sometimes

referred to as "short-circuiting." Bouma and Dekker (1978) define "short-circuiting" as the "rapid downward movement of water through initially air-filled large, vertical pores, thereby bypassing dry or moist soil inside peds." This water can carry contaminants during dry periods in which there is little adsorption to the soil, resulting in pollution of the groundwater. These preferential flow paths can develop by a number of different means. Beven and Germann (1982) divided these flow paths into four groups based on morphology: (1) pores formed by the soil fauna, (2) pores formed by plant roots, (3) cracks and fissures between aggregates, and (4) natural soil pipes. Of particular interest here is the development of cracks and fissures. Two principal processes which can lead to the formation of cracks are desiccation and freeze/thaw cycles.

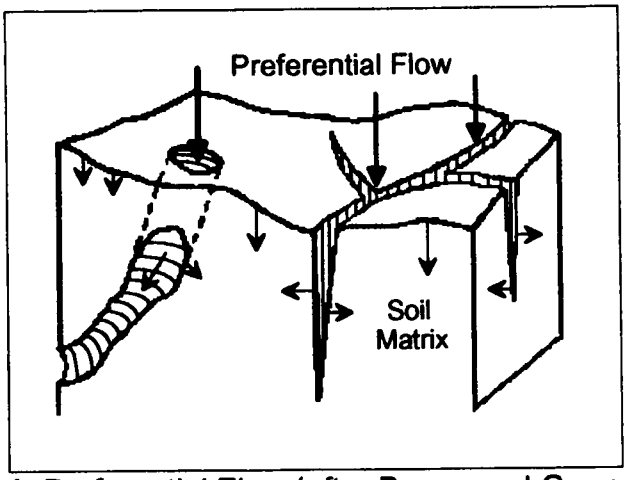


Fig. 1-4. Preferential Flow (after Beven and Germann, 1982)

Development of Preferential Flow Paths in Clay Barriers

Although clay compacted wet of optimum can initially serve well as a barrier to contaminant transport, it is also susceptible to post compaction structure changes that can alter the integrity of the liner. Kleppe (1981) showed that high plasticity clays placed wet of optimum have the highest potential to crack due to the high shrink-swell characteristics. It has generally been assumed that covering or burying these liners will prevent these cracks from developing. The rationale for this is that the liner will be protected from atmospheric processes and that the overburden pressures will tend to keep cracks from opening at depth.

However, Corser and Cranston (1991) have shown that desiccation can occur even with a protective soil cover and/or geomembrane. Figure 1-5 outlines some typical liner/cover sections. Corser and Cranston (1991) performed tests on each of these combinations and their results are summarized in Table 1-1. The liner section with the HDPE (high density polyethylene) cover and vegetative soil cover performed the best at limiting desiccation. The section with only the vegetative cover was found to crack significantly over the course of the summer

Table 1-1. Summary of Desiccation cracks in various liner sections

Type of Liner Section	Observed Desiccation	Size of Cracks
HDPE and Vegetative Cover	Minor or limited desiccation	hairline fractures
Vegetative Cover only	fairly extensive cracking	up to 0.4" width and 4" depth
HDPE only	cracking in some areas and none in others	up to 0.25" width and 3" depth

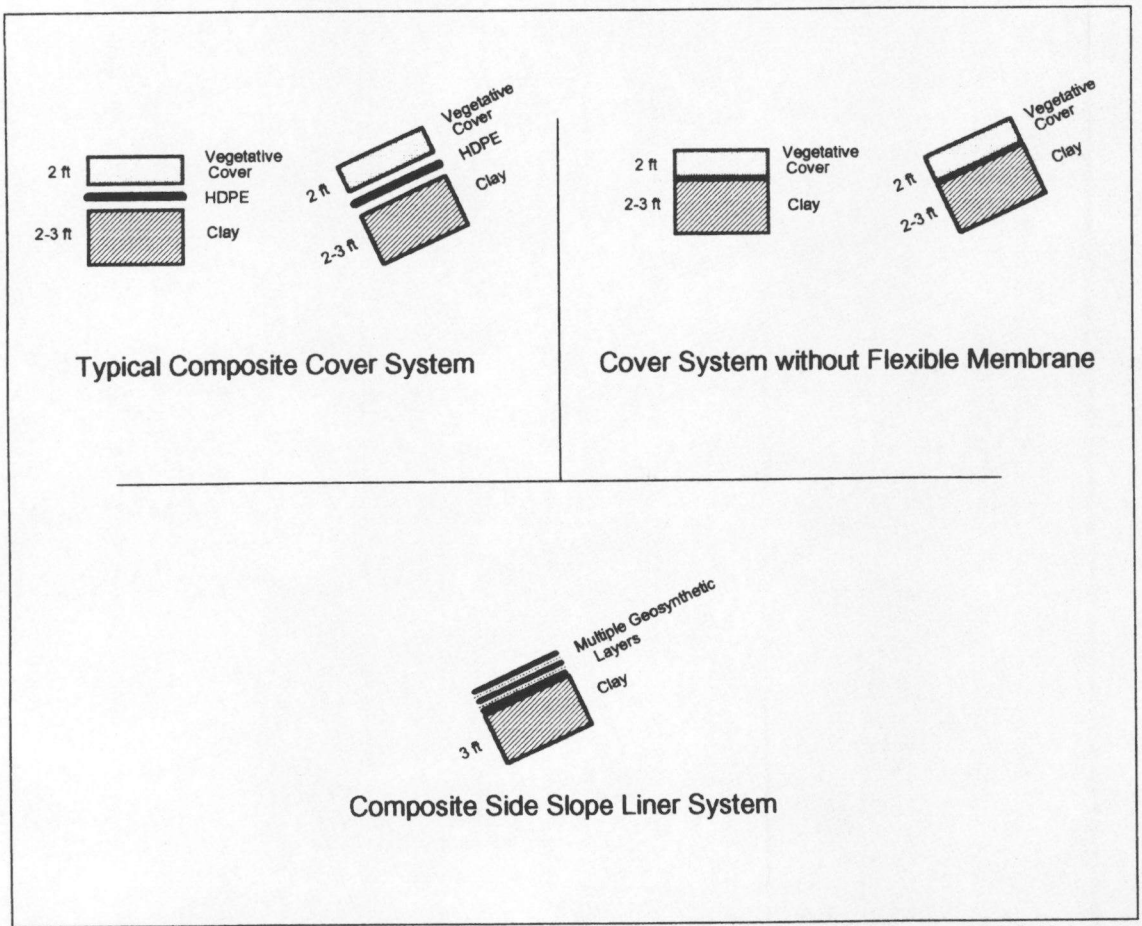


Fig. 1-5. Typical Liner/Cover Sections (after Corser and Cranston, 1991)

it was monitored. This suggests that simply burying a liner does not necessarily protect it from desiccation. The section with only the HDPE liner best represents a side slope liner section. The HDPE layer was black and exposed to direct sunlight over the course of a summer. It was suggested that the variable cracking pattern found for this section was due to irregular evaporation from the liner system. Water loss and cracking seemed to occur in air pockets where the HDPE was not in contact with the clay. Areas where the HDPE was in contact with the clay actually showed increases in water content and no desiccation.

There is limited information on the development of preferential flow paths in compacted clay liners due to freezing and thawing. However, this process is gaining increased attention and is recognized as a serious potential problem. Desiccation can be limited by adding water to the liner to keep it moist. However, this same water can be the source of significant cracking during freezing temperatures. These effects will be discussed in a later section.

Flow Through Preferential Flow Paths

The presence of preferential flow paths close to the surface is particularly important during unsaturated infiltration. Infiltration is the process of water entering a soil profile at the boundary. During vertical infiltration, as the soil becomes wetter with time, water at the wetting front advances into the drier soil ahead of the front under the influence of matric potential gradients as well as

gravity. The matric potential gradients generally control infiltration during the early stages when the wetting front is near the surface. The importance of preferential flow during this process was recognized as far back as 1864 by Schumacher, who wrote, "The permeability of a soil during infiltration is mainly controlled by big pores, in which the water is not held under the influence of capillary forces."

Beven and Germann (1981) described the various stages of water flow in a fracture, or macropore. Their conceptual model, Figure 1-6, illustrates the dynamics of this process. It is assumed that infiltration into a fracture does not begin until the infiltration capacity of the surface matrix is reached since fractures contribute very little to the total surface area. At this point, flow will begin to take place in the fracture followed by lateral infiltration into the matrix at deeper depths. The flow of water in the fracture can greatly increase the surface area available for infiltration into the soil matrix. In this way, the infiltration capacity of a soil can increase significantly with the presence of preferential flow paths. These processes also may not be adequately described by Darcy's Law since the hydraulic properties of the soil are not homogeneous over some representative cross-sectional area. Water fluxes can vary significantly over small distances, and the hydraulic gradient may not be properly defined for the soil due to turbulence in the preferential flow paths.

During infiltration into a dry clay soil, the soil becomes wetter, resulting in a gradual decrease of the infiltration rate due to a decrease in the hydraulic

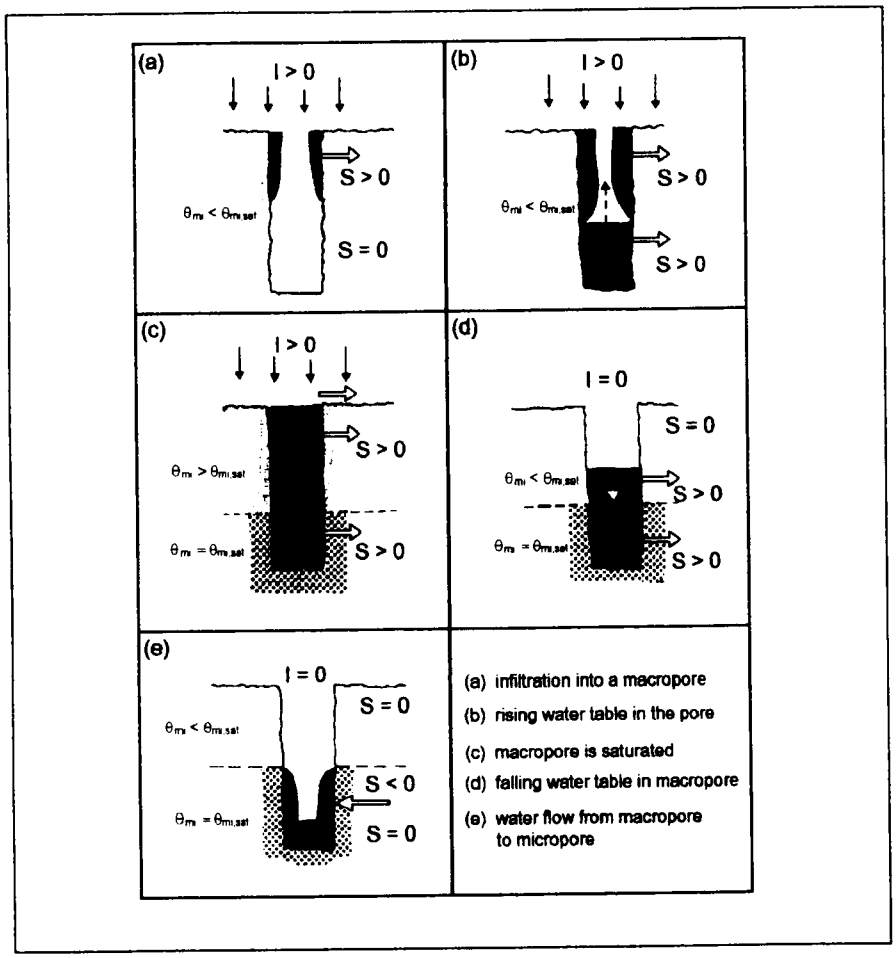


Fig. 1-6. Stages of water flow in a macropore (Beven & Germann, 1981)

gradient and partly due to swelling. Swelling may ultimately close some of the preferential flow paths forcing water to flow through the matrix and restoring the integrity of a clay barrier. However, although preferential flow paths may make up only a small portion of the total soil voids, they can dominate vertical flow during infiltration before the fractures are closed.

SATURATED HYDRAULIC CONDUCTIVITY MEASUREMENTS

As noted before, the saturated hydraulic conductivity is the parameter used to judge the quality and integrity of compacted clay liners. Hydraulic conductivity is given in Darcy's law, which was originally applied for saturated flow only, but was extended by Richards (1931) to unsaturated flow. Hydraulic conductivity is typically a maximum at saturation so that the saturated conductivity is generally believed to be a conservative parameter for barrier evaluation. This would be true of course except that the formation and closure of fractures in clay media is highly dynamic. Preferential flow paths tend to open during unsaturated conditions and close following saturation. These pathways can make unsaturated flow the more critical condition. Furthermore, due to the presence of matric potential gradients in unsaturated flow, the unsaturated hydraulic conductivity is necessarily lower than the saturated hydraulic conductivity given the same outflow. Thus the suggestion that the unsaturated

condition is not conservative is very misleading with regard to the flow of water or contaminants.

There are several additional problems with the use and measurement of the saturated hydraulic conductivity. One problem is the difficulty of obtaining laboratory samples that are representative of field conditions. One reason for this is the difference in structure, possibly due to desiccation, between laboratory compacted soil and field compacted soil. The chances of obtaining small samples with representative preferential flow paths are unlikely. Another reason suggested by Daniel (1984) is the possible influence of clod size on the hydraulic conductivity. Clods of clay are broken down into small aggregates in the laboratory whereas clod sizes in the field can reach diameters of 0.3 m. Larger clod sizes possibly result in larger preferential flow paths thereby increasing the hydraulic conductivity of the soil. As a result, laboratory measurements of hydraulic conductivity typically underestimate the in situ hydraulic conductivity by an order of magnitude or more.

Boles (1994) suggested that the size of laboratory samples introduces geometric effects which influence the pattern of cracking during desiccation. The experiments described by Boles involved two series of tests which measured hydraulic conductivity using a Flexible Wall Permeameter (FWP) on small diameter samples and lysimeters for larger samples. After cycles of saturation and drying, the smaller samples actually experienced a slight decrease in hydraulic conductivity whereas the larger samples saw higher conductivity

values (Table 1-2). Boles suggested the reason for this behavior is that the smaller samples represent intact portions of a clay liner separated by preferential flow paths, whereas the larger samples correspond to the liner as a whole including both the intact clay and the surrounding defects. He also found that the FWP samples experienced a decrease in dry density after the dry back cycles. Perhaps an additional factor is that the FWP tests were conducted with a confining stress that effectively closed any desiccation cracks upon saturation. There was no external confining stress on the lysimeter samples and desiccation cracks were perhaps less affected during testing. The lysimeter samples were subjected to an overburden stress but perhaps it was not large enough to keep cracks closed at depth. Although the lysimeters were designed to intercept side wall leakage, these effects could also affect the results.

Table 1-2. Hydraulic Conductivity of FWP Samples (Boles, 1994)

Sample	Initial Hydraulic Conductivity (cm/s)	Final Hydraulic Conductivity (cm/s)
Optimum	3.6×10^{-7}	1.7×10^{-8}
Optimum +3	6.9×10^{-7}	2.0×10^{-8}

To test the hypothesis that the fractures closed upon saturation, hydraulic conductivity measurements were made by this author on three samples compacted at standard energy with 4" diameters. One of the samples was tested after compaction while the other two were tested after a series of three wet-dry cycles. These cycles consisted of drying the sample completely under a heat

lamp at 150° F and resaturating it through submergence. A flexible membrane was placed on the samples to maintain the integrity of the samples during the wet-dry cycles. The samples were visibly cracked after the drying cycles. A constant head test was performed for each of the three samples as outlined in Figure 1-7.

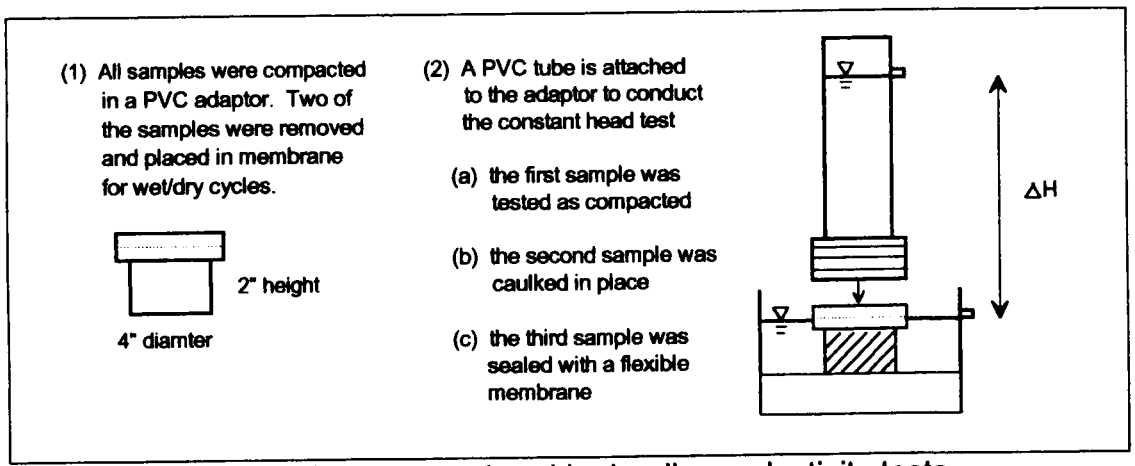


Fig. 1-7. Procedure for constant head hydraulic conductivity tests

Results in Table 1-3 indicate little difference in hydraulic conductivity between cracked and uncracked samples. Perhaps the slight increase in hydraulic conductivity for cracked samples suggest that after desiccation, the dry density actually increased and the preferential flow paths closed upon saturation resulting in a lower hydraulic conductivity. No cracks could be seen in the desiccated samples after the tests, which further suggests, closure. Although there was no direct confining stress, an indirect confinement was achieved since the samples were confined in a dry state. As the sample became saturated,

swelling was limited laterally and the soil essentially collapsed inward, closing any fractures.

Table 1-3. Results of constant head conductivity tests

	Description	Saturated Hydraulic Conductivity (cm/s)
Sample A	Uncracked	5.4×10^{-7}
Sample B	Desiccated and sealed in caulk	2.7×10^{-7}
Sample C	Desiccated and sealed with flexible membrane	2.2×10^{-7}

McKay et al. (1993) also argue for a scale dependence on hydraulic conductivity measurements. Small scale samples displayed a greater variability in hydraulic conductivity than larger scale samples. This further illustrates the importance of preferential flow paths and the variability of which they can close upon saturation. Also, the lateral confinement may or may not cut off some of the connected pores that run in non-vertical directions leading to wide variability. This can be especially critical for small samples in that critical pathways can be blocked along the perimeter. It is less likely that all of these critical pathways will be blocked for larger samples, and hence their higher conductivity. Pyrak-Nolte and Montemagno (1994) showed the importance of the critical path on the permeability of fractured coal seams. They found that permeability was less affected by effective porosity but was controlled by the geometry and interconnectedness of the void spaces. Similar results should be expected for

clay soils as well. The presence of a few well connected large aperture fractures can greatly influence permeability.

These results suggest that saturated hydraulic conductivity of laboratory samples is perhaps not the best parameter to judge how resistant a clay barrier is to contaminant transport, especially with the presence of preferential flow paths. These pathways seem to be much more hydraulically active during the dynamic stage of infiltration. Infiltration tests should better demonstrate the impact of preferential flow paths on the flow of water and contaminants through compacted clay barriers in landfills. There have been numerous studies that show an increase in hydraulic conductivity due to the presence of preferential flow paths. Bowders et al. (1994) report an increase in hydraulic conductivity after the development of fractures due to freeze/thaw cycles. However, the measured increase was not as great as expected given the observed severity of the cracks. They comment, "given the appearance of the specimens one might have anticipated much larger increases in permeability than were measured." The most likely reason for this is that the cracks began to close upon permeation. Bowders et al. (1994) also report that the ratios of permeability after freeze/thaw to those before, decreased as the effective confining stress increased. This further supports the previous suggestion that the confining stress plays a large role in the degree to which the fractures will close. At higher confining stresses, the fractures close more completely resulting in a lower impact on the saturated hydraulic conductivity.

Anderson and Bouma (1973) showed that very small variations in pore size have a significant impact on the amount of water that can be conducted at a given hydraulic gradient. Shrinking and swelling of clays can contribute greatly to this variation in pore size. Although there are many studies that show an increase in hydraulic conductivity due to preferential flow, they still have not fully examined the impact of these flow paths. The pathways contribute most before saturation. The hydraulic conductivity at best underestimates the role of these pathways during transport.

PART 2

THE NATURE OF CLAY FRACTURES

PREFERENTIAL FLOW PATHS IN COMPACTED CLAY LINERS

Preferential flow paths may develop in compacted clay barriers through a number of different mechanisms. Some of these include damage incurred by chemical attack from retained fluids, fractures developed due to differential settlement, macropores caused by plant roots and animals, desiccation, and freeze/thaw cycles. The size of clods during compaction can also affect preferential flow zones. Flow between poorly bonded lifts of a compacted liner provides further means of preferential transport. Preferential flow paths through any of these processes can impair the ability of a liner to prevent the migration of contaminants into the subsurface.

Chemical Attack

The structure of clay used for compacted barriers can be significantly altered due to chemical attack from retained contaminants. Shackelford (1994) gives three mechanisms by which the hydraulic conductivity of clay soils can increase upon permeation of acid permeants: (1) flocculation of the clay, (2) dissolution of the clay minerals (aluminosilicates), and (3) dissolution of other minerals (eg., $CaCO_3$) in the clay soil. These mechanisms can lead to voids through which water and contaminants can rapidly migrate. Further research is needed to evaluate the importance of chemical attack with respect to the other means of preferential flow path development.

Differential Settlement

Fractures can also develop as a result of differential landfill settlements. These fractures can in turn provide pathways through which contaminants may rapidly travel. Cheng et al. (1994) found that hydraulic conductivity increased with an increase in flexural stress. In addition, they found that the compacted water content is very important in this evaluation. As indicated before, compaction wet of optimum results in a favorable decrease in hydraulic conductivity. However, stiffness and compressive and tensile strengths are higher for clays compacted dry of optimum. This can be important for withstanding damage resulting from developing flexural stresses during differential settlement. Leonards and Narain (1963), however, have suggested that clayey soils compacted wet of optimum are more flexible thus more resistant to cracking than if compacted dry of optimum. Thus the decision in design is, whether to concentrate on minimizing the initial conductivity, or providing strength for long term durability.

Compacted clay caps in landfills are especially susceptible to differential settlements due to the variable compressibility of waste material. This variability is enhanced along the side slopes due to the changing thickness of compressible fill. The resulting differential settlement leads directly to the formation of cracks providing pathways for rapid infiltration into the landfill.

Plant Roots and Animals

Preferential pathways may also develop from plant roots and burrowing animals. These pores are generally tubular in shape and found near the surface. They can be especially important in compacted clay caps which are used to limit infiltration into the waste fill. Voids left by decaying roots or soil fauna such as earthworms and ants can allow more water to infiltrate into the waste for the formation of additional leachate. This not only leads to additional contaminants available for transport into the subsurface, but can lead to an increased pressure head in the landfill. This can also lead to additional contaminants being transported through the clay barriers.

Desiccation

Desiccation cracking can occur when soil is exposed to drying, resulting in shrinkage. The tensile stresses that cause cracking are produced by negative pore water pressures that develop as water evaporates from the soil. These negative pore water pressures lead to an increase in effective stress resulting in a volume reduction. As a result, cracking occurs to accommodate this shrinkage. If water is then added, the soil will swell, possibly closing the cracks. However, these cracks can still corrupt the integrity of a compacted clay cap or liner.

Haines (1923) defined three different shrinkage phases for drying clay:

(1) Normal shrinkage - the change in volume of soil is equal to the loss in volume of water.

(2) Residual shrinkage - the change in volume of soil is less than the volume of water lost as air enters the pores of the soil.

(3) No shrinkage - the soil reaches its densest configuration with no further volume change with loss of water.

Stirk (1954) defined a fourth phase of shrinkage termed structural shrinkage. As large water-filled pores are emptied, the soil aggregates can reach a denser packing. This phase was likely captured by Boles (1994) where a decrease in dry density was found for the intact portion of the samples. The process of desiccation can initiate these phases of shrinkage as water evaporates from the soil. This shrinkage directly results in cracking and the development of preferential flow paths.

Corte and Higashi (1964) performed an extensive series of tests investigating desiccation cracking in soil. Some factors that affect the cracking pattern include the type of soil, the rate of desiccation, the thickness of the soil, the nature of the material below the soil, and the presence of foreign matter. The thickness of the sample seemed to be the most significant of these factors. The total length of cracks decreases as the sample thickness increases. Further, the water content at the initiation of cracking is dependent upon the soil thickness. They also found that the cracks propagate slowly when the soil layer is thick, but reach final form much more quickly when the soil layer is thin. The cracking

pattern for thin samples formed hexagonal patterns, whereas thicker layers formed square patterns. Due to the adhesion of the soil to the bottom of the container, this bottom material was also found to affect the nature of the desiccation cracks. Foreign matter such as stones was found to serve as nucleating points where desiccation cracks begin. Another interesting relationship found was that the cracking water content decreased as the rate of desiccation increased. The authors did a probabilistic analysis and found that the probability of the formation of a crack at a high water content was small at higher desiccation rates due to low internal stresses. This probability only becomes high enough as the water content gets smaller. On the other hand, for slow desiccation rates, the probability is higher because of the long duration of higher water content. Lima and Grismer (1992) concluded that soil salinity also affected soil crack morphology. They found that crack width, crack area, and crack volume increased as soil salinity increased, whereas crack depth decreased. Many of these factors and explanations will become important in interpreting results from experiments performed for this research.

Kleppe and Olson (1985) also investigated desiccation cracking and its impact on clay barriers. The authors attempted to find a soil blend, such as the addition of sand to the clay, to minimize the cracking potential while maintaining sufficiently low hydraulic conductivity. They found that cyclic wetting and drying led to the formation of cracks to progressively greater depths. Cracks were more severe for samples at higher water contents and typically formed one large crack

across the sample. Saturating the sample before desiccation also led to an increase in cracking. They also found that desiccation shrinkage increased linearly with compaction water content but was not dependent on dry density. Typically, mixtures with about 75% sand were needed to limit cracking. Although this may limit the development of preferential flow paths, the hydraulic conductivity as mixed may not meet the EPA's requirement for barrier material.

Desiccation Tests

A series of desiccation tests was performed on kaolinite slurry samples to evaluate the formation of desiccation cracks. Pertinent material properties are listed in Table 2-1. The soil was mixed to the desired water content in 0.5 cubic yard concrete mixer until the slurry was smooth and uniform. The slurry was then spread into a 30 cm x 60 cm pan lined with wax paper to a uniform thickness of about 3.2 cm. The pan was then placed in an oven at a specific temperature until significant desiccation occurred. Digital images of the sample were taken at intervals to observe the onset and development of desiccation cracks. Among the factors varied for the investigation were water content, desiccation temperature, desiccation time, thickness, and artificial defects (see Table 2-2).

Table 2-1. Kaolinite properties (after Phifer, 1994)

Mineral Composition	Kaolinite	94.6 -97.2 %
	Silica, quartz	1.5 - 3.8 %
	Titanium dioxide	1.3 - 1.6 %
Particle size	> 45 μm	0.0 - 0.1 %
	> 5 μm	0.3 - 3.5 %
	< 2 μm	92.0 - 97.0 %
Atterberg Limits	Plastic Limit	29.9
	Liquid Limit	75.0
	Plasticity Index	45.1
	Shrinkage Limit	17
Standard Proctor	Optimum water content	31.6 %
	Maximum dry density	1.37 g / cm^3
Modified Proctor	Optimum water content	26.3 %
	Maximum dry density	1.52 g / cm^3

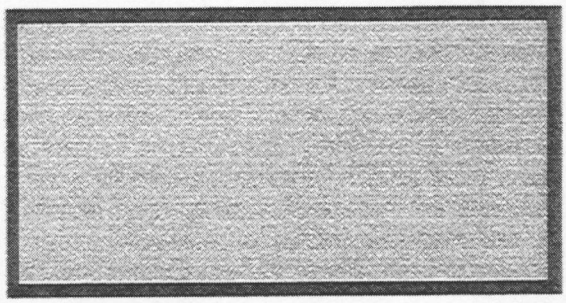
Table 2-2. Summary of Results from Desiccation Tests

Sample	Initial Water Content	Final Water Content	Desiccation Temperature	Variable Investigated	Cracking Pattern
Batch 4	64.3%	54.0%	300° F	Smaller water content	Moderate orthogonal cracking after three hours
Batch 5	71.9%	56.0%	300° F	Larger water content	Minor orthogonal cracking after three hours
Batch 6	71.4%	48.0%	225° F	Lower oven temperature	Only two notable orthogonal cracks after seven hours
Batch 7	75.3%	35.7%	78° F	air-dry desiccation	No cracking with only shrinkage
Batch 8	70.4%	41.6%	375° F	Higher oven temperature	Heavy, mildly orthogonal cracking after three hours
Batch 9	74.1%	47.7%	275° F	Artificial defect	Large fracture developed along artificial sample defect

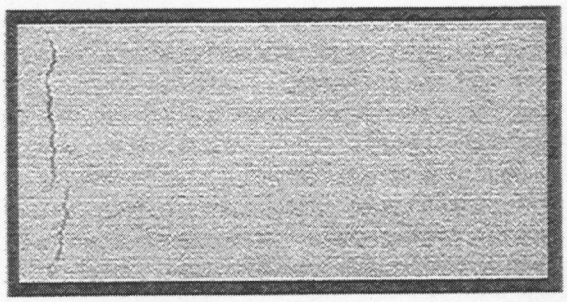
The images for Batch 4 (Figure 2-1) indicate most that the degree of cracking increases with time in the oven. The reason for this is that more and more water was evaporated from the soil causing shrinkage cracks. The apertures of the developed cracks also increased with time. Another obvious characteristic of the images was the boundary effect on the cracking pattern. The developing cracks tended to develop parallel to the boundaries of the pan. However, Lachenbruch (1962) gives further explanation for this orthogonal cracking pattern. He defines a "zone of stress relief" that forms as the component of stress normal to the crack diminishes. Thus a band of reduced horizontal tension surrounds the crack. However, the tension parallel to the crack is minimally affected, leading to large horizontal stress differences in the "zone of stress relief." Lachenbruch writes, "A second crack entering this zone tends to align itself perpendicular to the direction of greatest tension and, hence, tends to intersect the first crack at right angles." It would seem reasonable to assume then that the boundary dictates the alignment of the first developing cracks, and the stress conditions dictate the alignment of the secondary cracks.

Batch 5 (Figure 2-2) was prepared at a higher initial water content and was desiccated at the same oven temperature as the previous sample. The cracking pattern for this sample was similar to the previous example except that the onset of cracking was delayed. The studies of Corte and Higashi (1964) suggested that the water content at the onset of cracking is dependent on the desiccation speed. Since the desiccation rate for these two samples was the

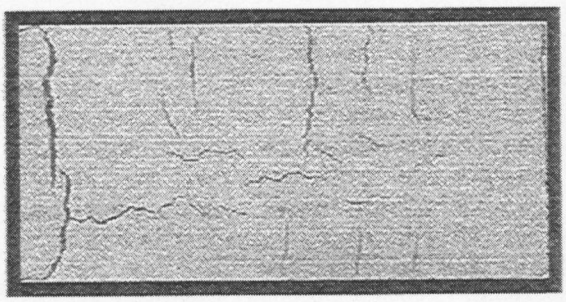
Initial Water Content = 64.3% Oven Temp. = 300° F Final Water Content=54.0%



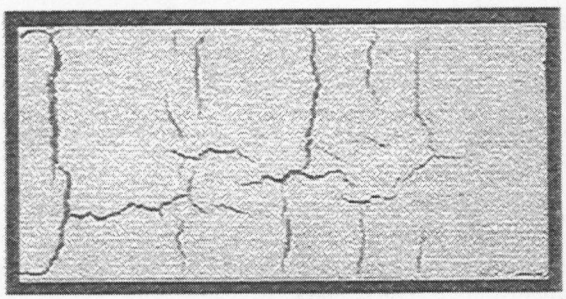
Time = 0 hours



Time = 1 hour



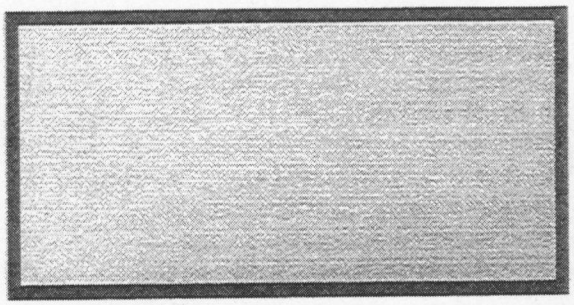
Time = 2 hours



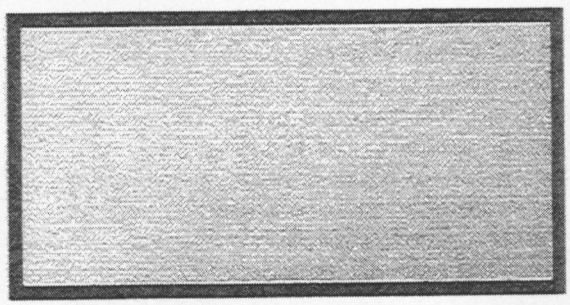
Time = 3 hours

Fig. 2-1. Batch #4 Drying Stages

Initial Water Content = 71.9% Oven Temp. = 300° F Final Water Content=56.0%



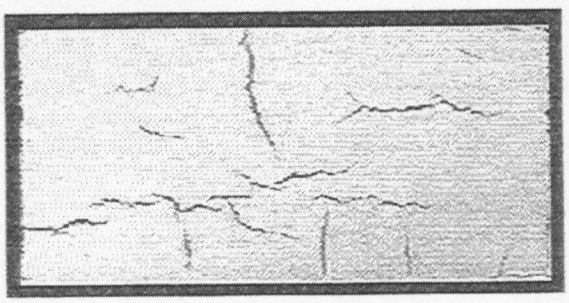
Time = 0 hours



Time = 1 hour



Time = 2 hours



Time = 3 hours

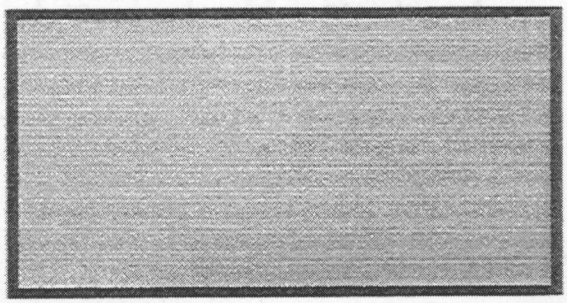
Fig. 2-2. Batch #5 Drying Stages

same, it would seem appropriate to assume that it would take longer to reach the cracking water content for the sample with the larger initial water content. This could explain why Batch 4 with the lower initial water content cracked earlier than Batch 5. Since cracking began sooner, it would also seem logical that the degree of cracking would be slightly higher for Batch 4 at the end of the three hour interval. The orthogonal cracking pattern was still evident for Batch 5.

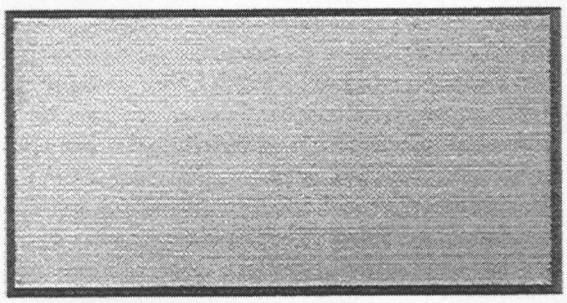
Batch 6 (Figure 2-3), in comparison to Batch 5, was mixed at a similar water content but desiccated at a lower oven temperature. The desiccation interval was seven hours instead of three as the slower desiccation rate led to the necessity of longer desiccation times. There were fewer cracks formed at this lower temperature with much more shrinkage of the sample as a whole. Although Corte and Higashi (1964) concluded that the cracking pattern was not strongly dependent on temperature, the results reported here suggest that temperature does have an impact. This relationship will be further explored in the later examples.

Batch 7 (Figure 2-4) was mixed at a slightly higher water content than the previous examples and was desiccated at room temperature for 70 hours. No cracks formed in the interior of the sample as it only experienced shrinkage. This lends itself to the notion that slower desiccation rates lead to fewer and wider spaced cracks. It is likely that if the sample was large enough, large cracks would have formed. Also, if the sample was thinner, more cracks would have formed. This was verified as the slurry was remixed and placed in the pan to a

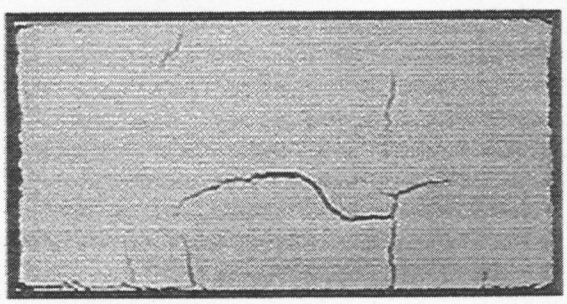
Initial Water Content = 71.4% Oven Temp. = 225° F Final Water Content=48.0%



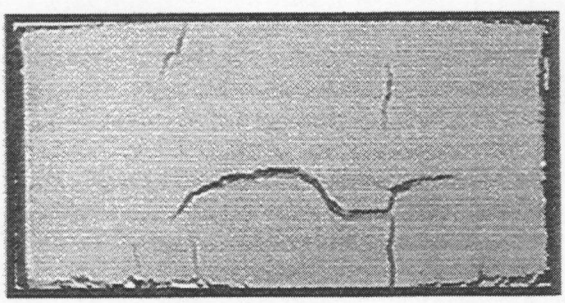
Time = 0 hours



Time = 2 hours



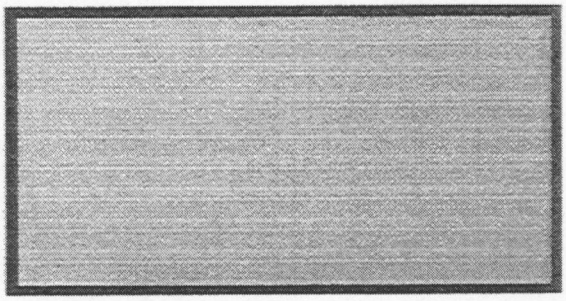
Time = 5 hours



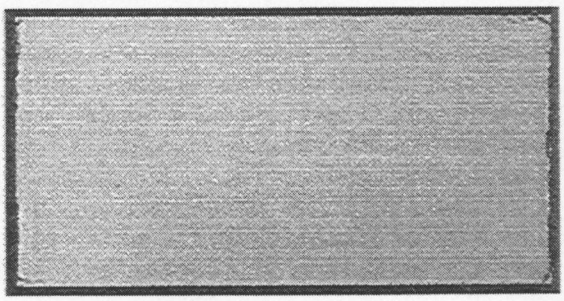
Time = 7 hours

Fig. 2-3. Batch #6 Drying Stages

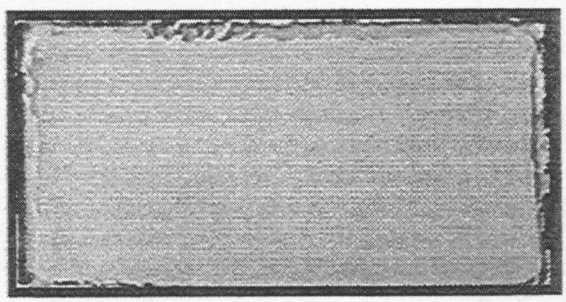
Initial Water Content = 75.3% Oven Temp. = 78° F Final Water Content=35.7%



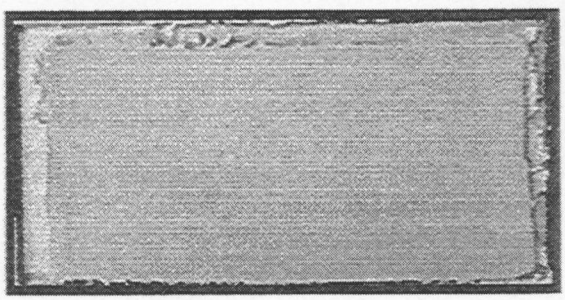
Time = 0 hours



Time = 18 hours



Time = 52 hours



Time = 70 hours

Fig. 2-4. Batch #7 Drying Stages

thickness of about 1.5 cm and exposed to room temperature. This sample was found to crack extensively forming more of a hexagonal cracking pattern such as found by Corte and Higashi (1964).

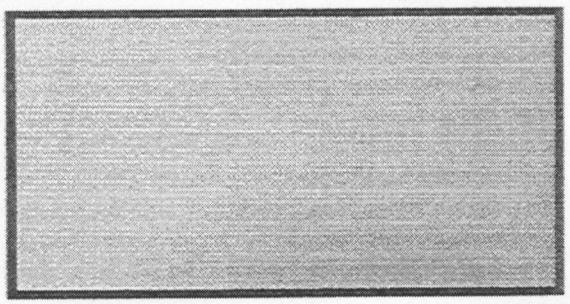
Batch 8 (Figure 2-5) was again mixed at a similar water content as the first three examples but desiccated at a higher oven temperature. This higher desiccation rate led to extensive cracking after just three hours further demonstrating the impact of desiccation rate on cracking pattern. The higher this rate, the more numerous and closely spaced the cracks formed. The initiation of cracking was also earlier for the greater oven temperatures.

Batch 9 (Figure 2-6) illustrates the role pre-desiccated defects have on the cracking pattern. A thin diagonal slice was cut into the sample to a depth of 0.5 cm. Upon desiccation, a large fracture propagated from this defect across the sample. A diagonal crack of this nature was not generated in any of the other tests, so that it is reasonable to conclude that the pre-desiccated defect controlled the initiation and alignment of the developing crack. The presence of a defect in clay can serve as a starting point from which fractures can develop when subjected to desiccation.

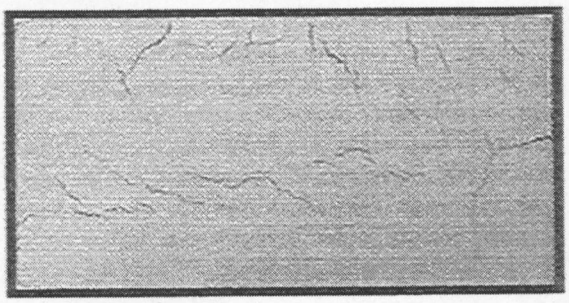
Freeze/Thaw

Cracking resulting from freeze/thaw cycles can also lead to significant preferential flow paths. The volume of a soil can increase about 10% due to the

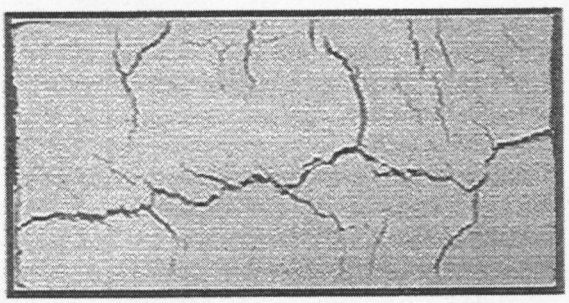
Initial Water Content = 70.4% Oven Temp. = 375° F Final Water Content=41.6%



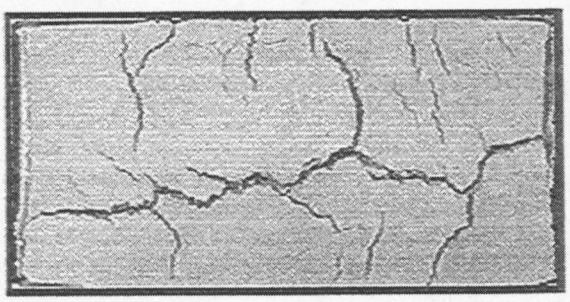
Time = 0 hours



Time = 1 hour



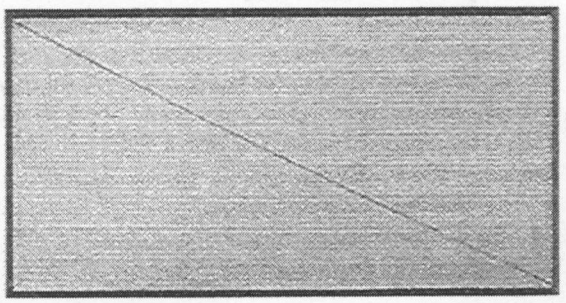
Time = 2 hours



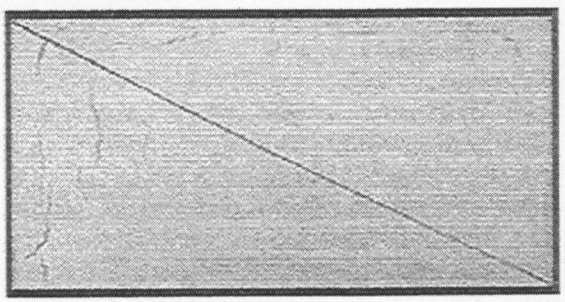
Time = 3 hours

Fig. 2-5. Batch #8 Drying Stages

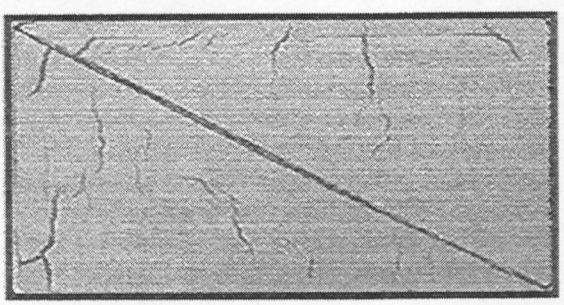
Initial Water Content = 74.1% Oven Temp. = 275° F Final Water Content=47.7%



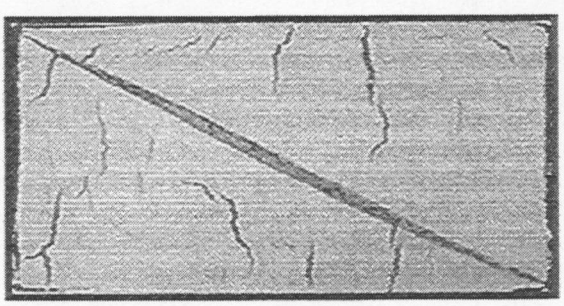
Time = 0 hours



Time = 1 hour



Time = 2 hours



Time = 3 hours

Fig. 2-6. Batch #9 Drying Stages

volumetric expansion of water upon freezing (Holtz & Kovacs, 1981). More importantly, the freezing of some soil is accompanied by the formation of ice crystals or lenses. Thermodynamic processes produce hydraulic gradients as more water migrates to these lenses. These lenses can range from a millimeter to several centimeters in thickness (Holtz & Kovacs, 1981). When these lenses melt, a void or preferential flow path is left through which contaminants may travel.

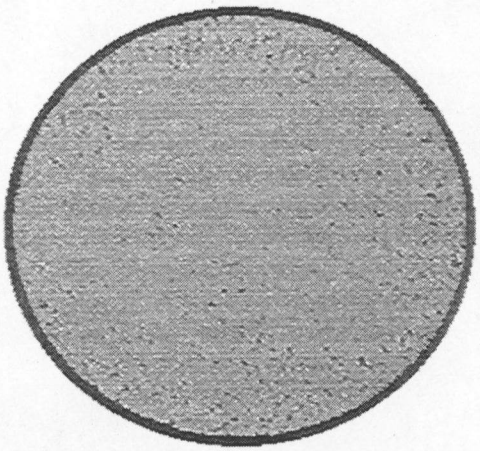
Several recent studies have investigated the phenomenon of freeze/thaw and its impact on the hydraulic conductivity. Benson and Othman (1993) found increases of one to two orders of magnitude in hydraulic conductivity due to freezing and thawing. They also found that cracks were more numerous near the surface and decreased in frequency with depth. However, deep vertical cracks were noted to be caused by a decrease in water content as water was drawn nearer to the surface by the developing gradients. Thus, desiccation processes can be initiated even during freezing. Large overburden pressures were found to limit the formation of ice lenses and close any developing cracks after thawing. Kim and Daniel (1992) also found increases in hydraulic conductivity due to the formation of preferential flow paths during freeze/thaw cycles. They concluded that molding water content was the most important factor affecting this change, and compactive energy had very little impact. The increases in hydraulic conductivity were also found to be almost eliminated at higher confining stresses. Again, the reason for this is that the fractures are more likely to fully

closed at higher confining stress resulting in little impact on hydraulic conductivity. Bowders and McClelland (1994) also found very similar results.

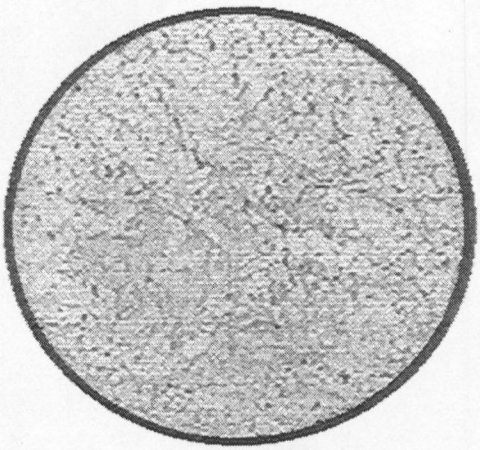
Freeze/Thaw Tests

Freeze/thaw tests were performed to evaluate the initiation and development of preferential flow paths in compacted kaolinite resulting from freeze/thaw cycles. Digital images for two of these samples are given in Figures 2-7 and 2-8. Figure 2-7 shows a sample compacted with a clod size passing the #4 sieve, whereas Figure 2-8 is for a sample in which all clods were retained on the #4 sieve. The maximum clod size was about 1.3 cm in diameter. The samples were compacted in 10.2 cm diameter PVC molds (5.1 cm thick). They were then extracted and placed in a rubber flexible membrane. The samples were subjected to three cycles, 24 hours per cycle, of freezing and thawing. Othman et al. (1994) concluded that three-dimensional freezing, as used for these samples, gives similar results as one-dimensional freezing. The samples were also not exposed to an external water supply; the water during compaction being the only water available throughout the cycles. Again, Othman et al. (1994) concluded that the availability of an external water supply is relatively unimportant.

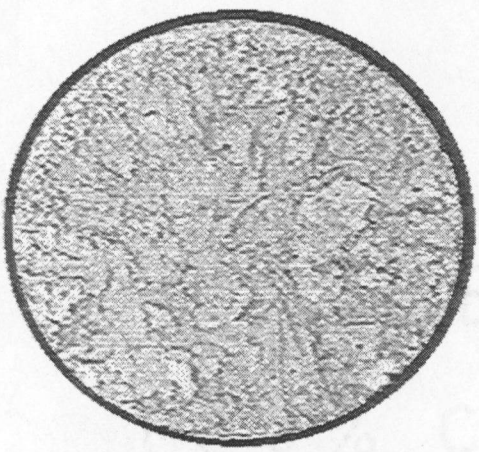
Both samples cracked extensively after three freeze/thaw cycles. The most significant change in the samples occurred after the first cycle. Othman et al. (1994) support this when they stated, "the network of cracks formed during



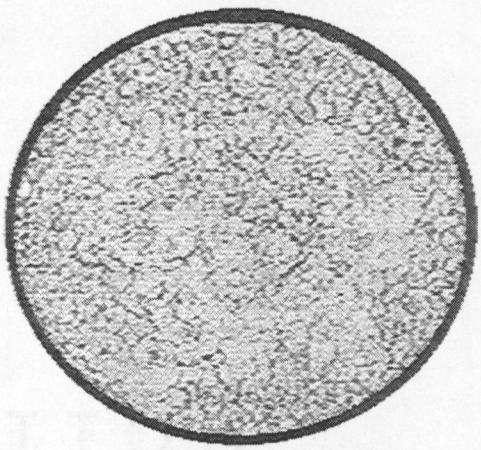
Sample as compacted



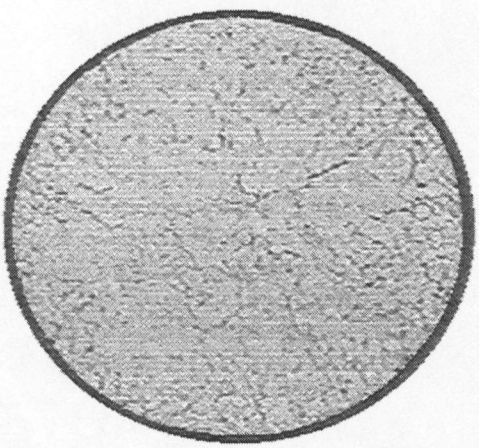
Second freeze cycle



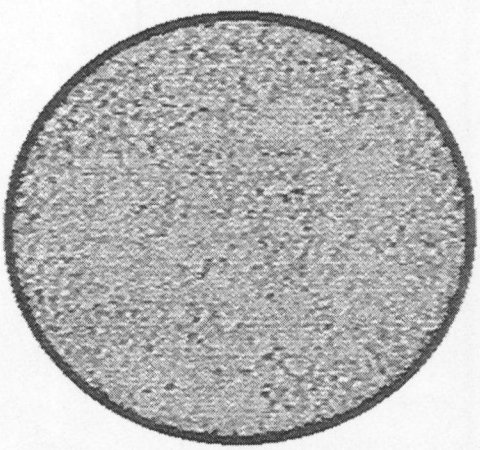
First freeze cycle



Thawed after second cycle



Thawed after first cycle



Third freeze cycle

Fig. 2-7. Crack Development: Sample FT-8

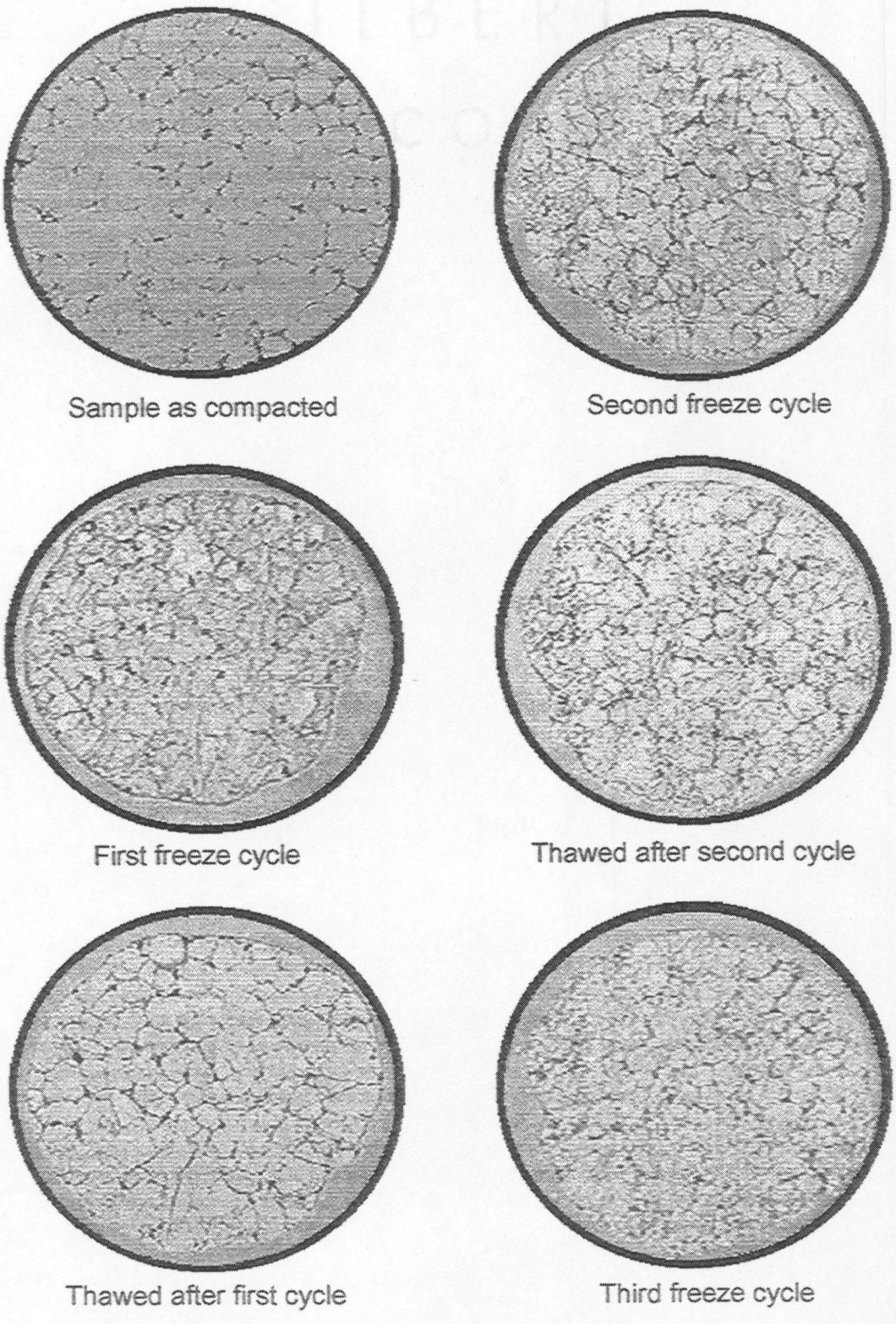


Fig. 2-8. Crack Development: Sample FT-9

the first cycle of freeze-thaw causes the greatest change in a soil's fabric." The surface of both samples appeared as if they had been sliced with a sharp object. The formation of ice lenses in the sample was the probable cause of this. As these lenses melted during the thaw cycle, a fracture or preferential flow path was left. These fractures were also observed on the bottom of both samples. For the sample compacted with the larger clods, the fractures typically formed between clods. The fractures in the sample with the smaller clods seemed less restricted. In any event, significant pathways were formed through the cycles of freeze/thaw.

Clod Size

Benson and Daniel (1990) performed an extensive investigation on the impact of clod size on the hydraulic conductivity. They found hydraulic conductivities as much as six orders of magnitude higher for samples with large clods (19 mm) than for samples with small clods (4.8 mm) when compacted dry of optimum. This difference was eliminated when compacted wet of optimum as the clods were softer and more easily molded to remove interclod voids. The large clods used in field situations can certainly lead to significant preferential flow paths that can be critical regarding compacted clay caps and barriers for landfills. The influence of clod size on preferential flow will be examined further in a later section.

Interlift Transport

Horizontal flow along poorly bonded lifts in a compacted barrier can serve to connect vertical flow paths and increase transport. Scarifying the surface and thereby increasing the cohesion between two lifts can serve to significantly reduce the connectivity of any developing preferential flow paths. Benson and Daniel (1994) concluded that four to six lifts (60 cm to 90 cm) provided adequate redundancy to minimize the probability of connected pathways through the liner. Providing good bonding between lifts is also important from a stability perspective, especially along the side slopes.

CLAY SWELLING

As water is lost from a soil, the soil will decrease in volume leading to the formation of shrinkage cracks. In the same manner, when water is added to a soil, the soil will increase in volume and possibly close any shrinkage cracks. This can be beneficial for compacted clay barriers as the clay will tend to heal itself if damaged. Although some of the cracks can completely heal, they are nevertheless conductive in the interim period before the clay is saturated. Saturated hydraulic conductivity is a parameter found after any preferential flow paths have had an opportunity to close. For this reason, it gives little insight into the effect of preferential flow paths during their most conductive state.

Leeds-Harrison et al. (1986) investigated the effects swelling have on hydraulic conductivity. They found decreases in hydraulic conductivity, Figure 2-9, especially near the surface, of large cores of Eversham clay soil after a period of continuous ponding. They note that these decreases were "accompanied by changes in the size and extent of cracks at the soil surface." The decrease in hydraulic conductivity was initially rapid but decreased with time. The authors found that the soil swelled fully and reached a "quasi-equilibrium" after about 40 days of saturation. While the authors attributed the general decrease in hydraulic conductivity to swelling, the brief increases were credited to a release of gas pressure buildup. In any event, the significance of swelling during water flow is readily seen.

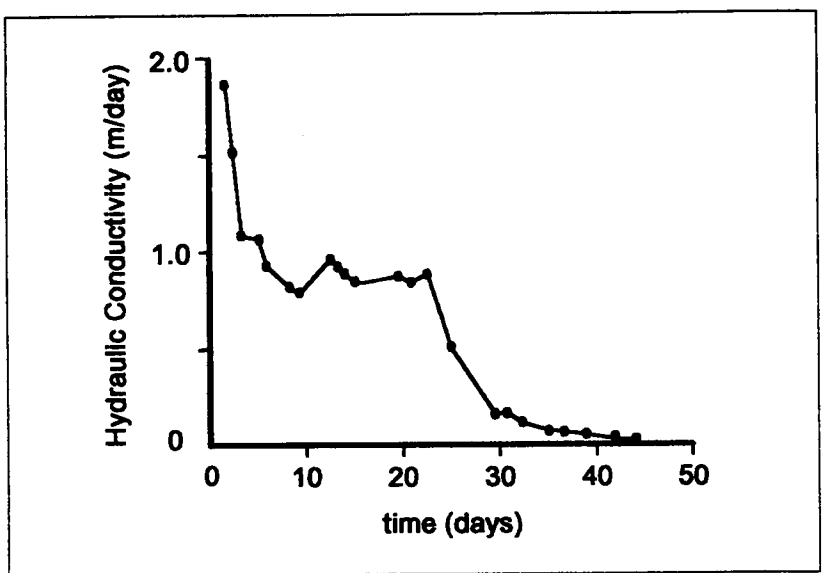


Fig. 2-9. Decrease in hydraulic conductivity (after Leeds-Harrison et al., 1986)

Soil also has a "memory", or hysteresis effects, in that any cracks closed upon saturation, can re-open in the same configuration if exposed to any of the damaging processes discussed earlier. Not only may they re-open, they tend to grow larger with each successive cycle. Othman et al. (1994) suggested that cracks become fully formed with no additional cracking after about five freeze/thaw cycles. A similar number could perhaps be assumed for desiccation cycles. In any event, the cracks can again become conductive, which may subvert the purpose of compacted clay barriers.

Crack Development Tests

Digital images of the surface of two compacted samples were captured during each stage of three cycles of desiccation. Both samples were compacted at 3% above optimum water content with standard energy. Sample D-4 (Figure 2-9) was compacted with a clod size passing the #4 sieve, whereas sample D-5 (Figure 2-10) was compacted with a clod size retained on the #4 sieve. Each desiccation cycle was 24 hours, consisting of 12 hours under a heat lamp and 12 hours saturating in a water bath. The temperature under the heat lamp averaged about 150° F. Both of the samples cracked during the desiccation cycles. The cracks in Sample D-5 developed typically along interclod boundaries due to the large clod size, whereas the cracks formed more freely for Sample D-4 with the smaller clod size. Also, Sample D-4 experienced less shrinkage along the

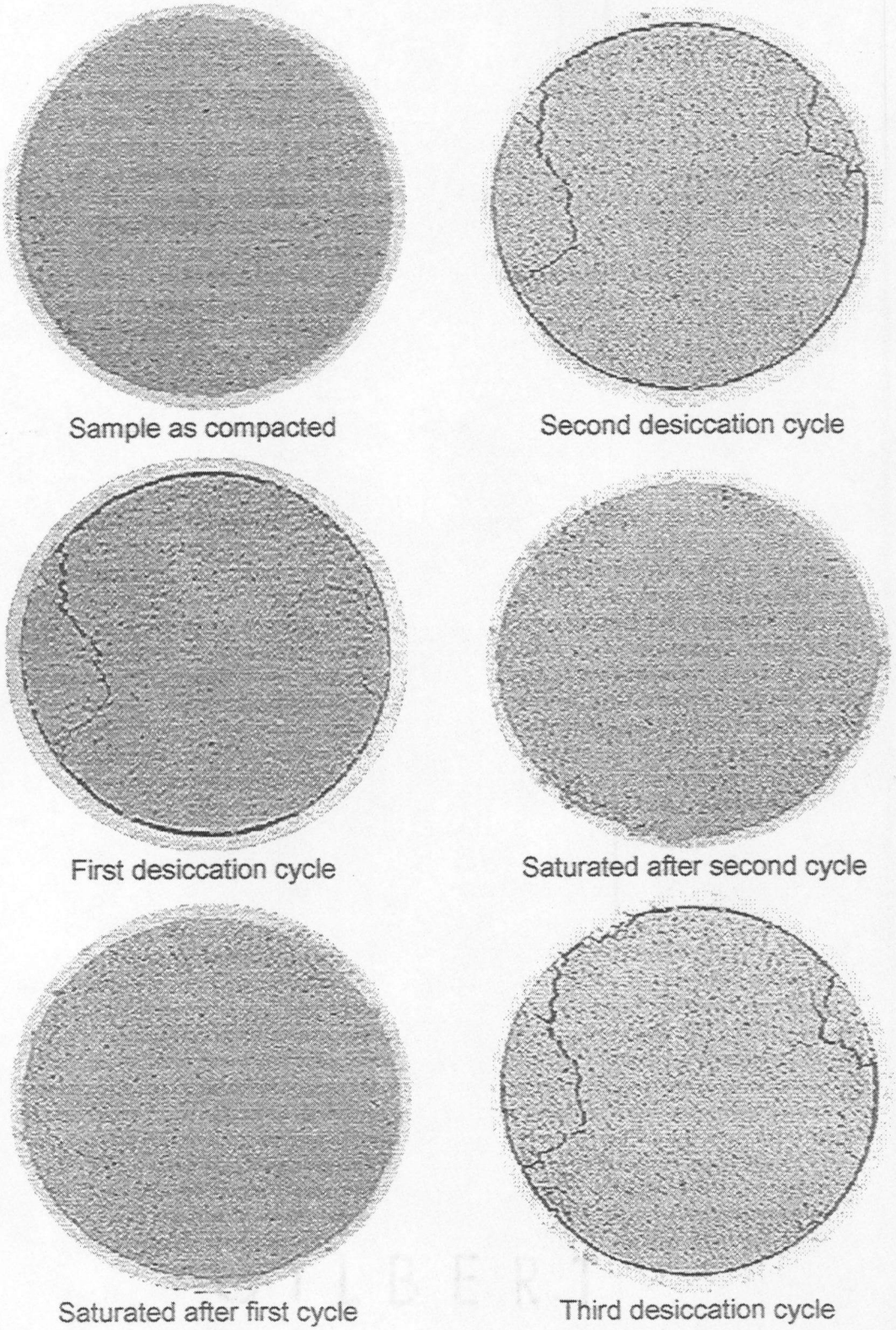


Fig. 2-10. Crack Development: Sample D-4 (small clod size)

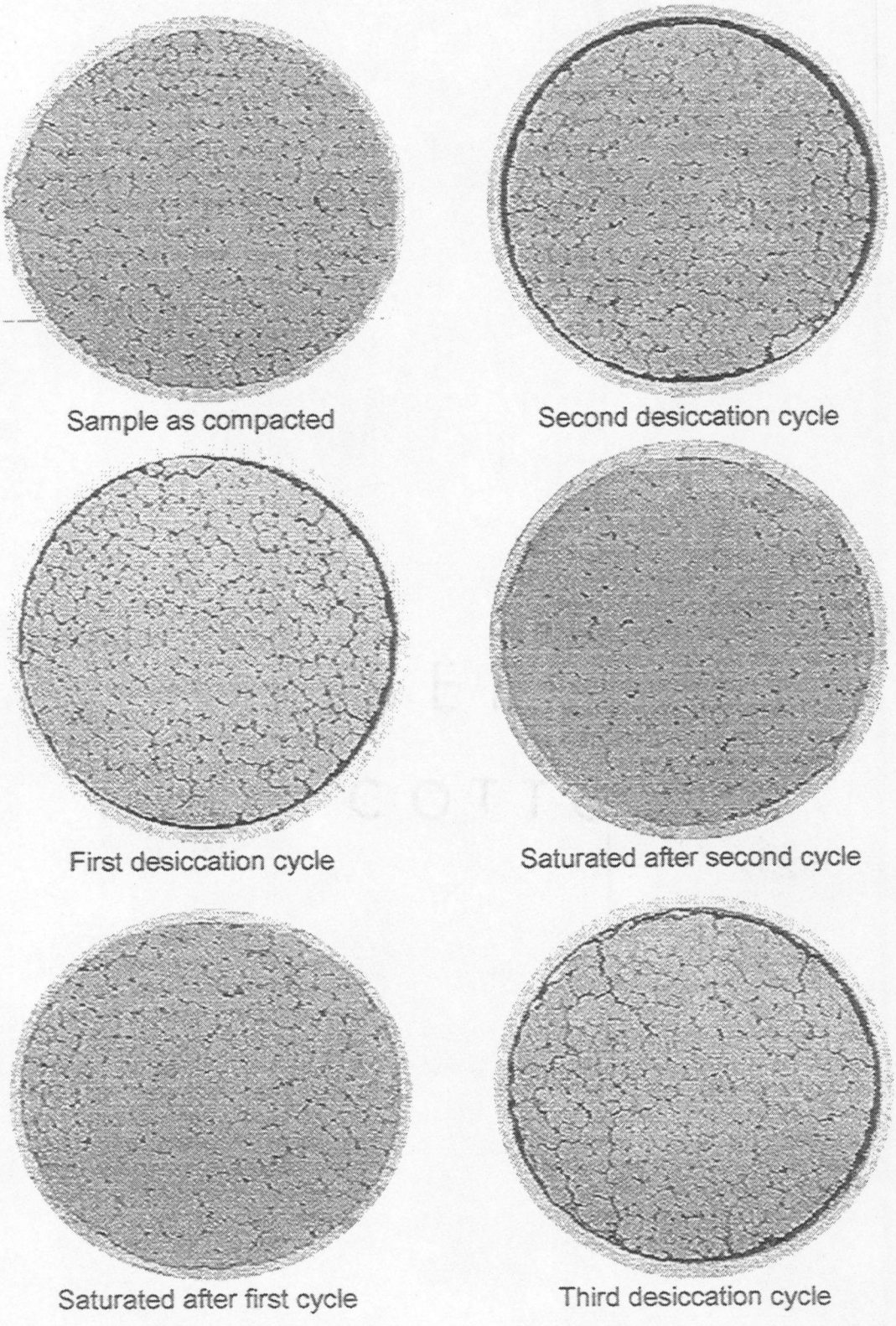


Fig. 2-11. Crack Development: Sample D-5 (large clod size)

perimeter due to the wider aperture cracks developed in the interior. The significance of clod size during preferential flow will be investigated further in a later section.

The most significant characteristic for both of the samples was the healing of the cracks after saturation. As the sample absorbed more water and increased in volume, the interior cracks and perimeter voids closed. Further, these same cracks opened up again to greater lengths and wider apertures during the next cycle. New cracks were also created during succeeding cycles. It is reasonable to conclude that more energy is necessary to create a crack than it is to open a previously existing one. For this reason, the first cycle of desiccation is the most important to the structure of a clay soil. With respect to clay barriers, it is very important to protect them from desiccation, or any other process leading to cracking, during and immediately after construction. If they become damaged during construction, or early in their design life, it will be increasingly more difficult to maintain their function.

PART 3

FLOW TESTS IN FRACTURED CLAY

FLOW TESTING

As discussed before, fractures tend to close as the soil expands due to water being absorbed into the matrix. A testing plan was formulated to evaluate the response of fractures in partially saturated clay after the application of water. The objective of this experiment was to examine how this dynamic process influenced the flow of water. Flow tests were performed on specimens from the desiccated slurry samples discussed earlier. These specimens were retrieved by cutting out a portion of the sample using a steel cylinder with a beveled edge much like a cookie cutter as illustrated in Figure 3-1. Because the samples were fairly moist, a good cohesion was established with the wall of the cylinder. Experiments on uncracked sections proved side-wall leakage to be negligible.

A flow pump was used to supply water to the sample at a constant flow rate. The system, illustrated in Figure 3-2, eventually reaches a point at which the fracture network is unable to conduct flow at the rate at which water is being applied. This can occur immediately or with time as the fractures close depending on the flow rate and the fracture system. At this point, the system will begin to "back up" and the height of water on the sample increases. A floating depth meter was used to measure the depth of water at any given time on the sample. The water can rise to the top of the cylinder where additional water will

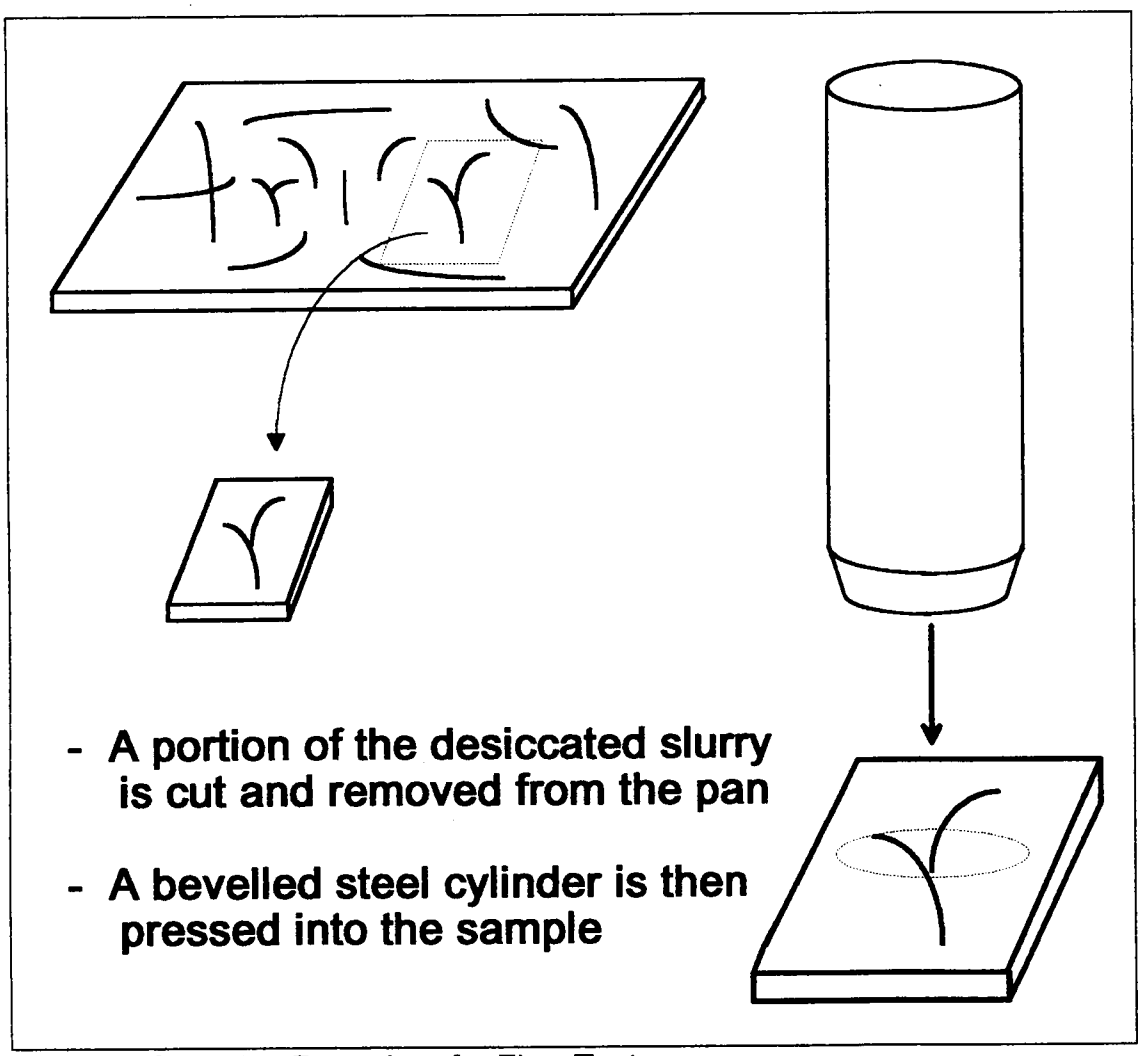


Fig. 3-1. Sampling Procedure for Flow Tests

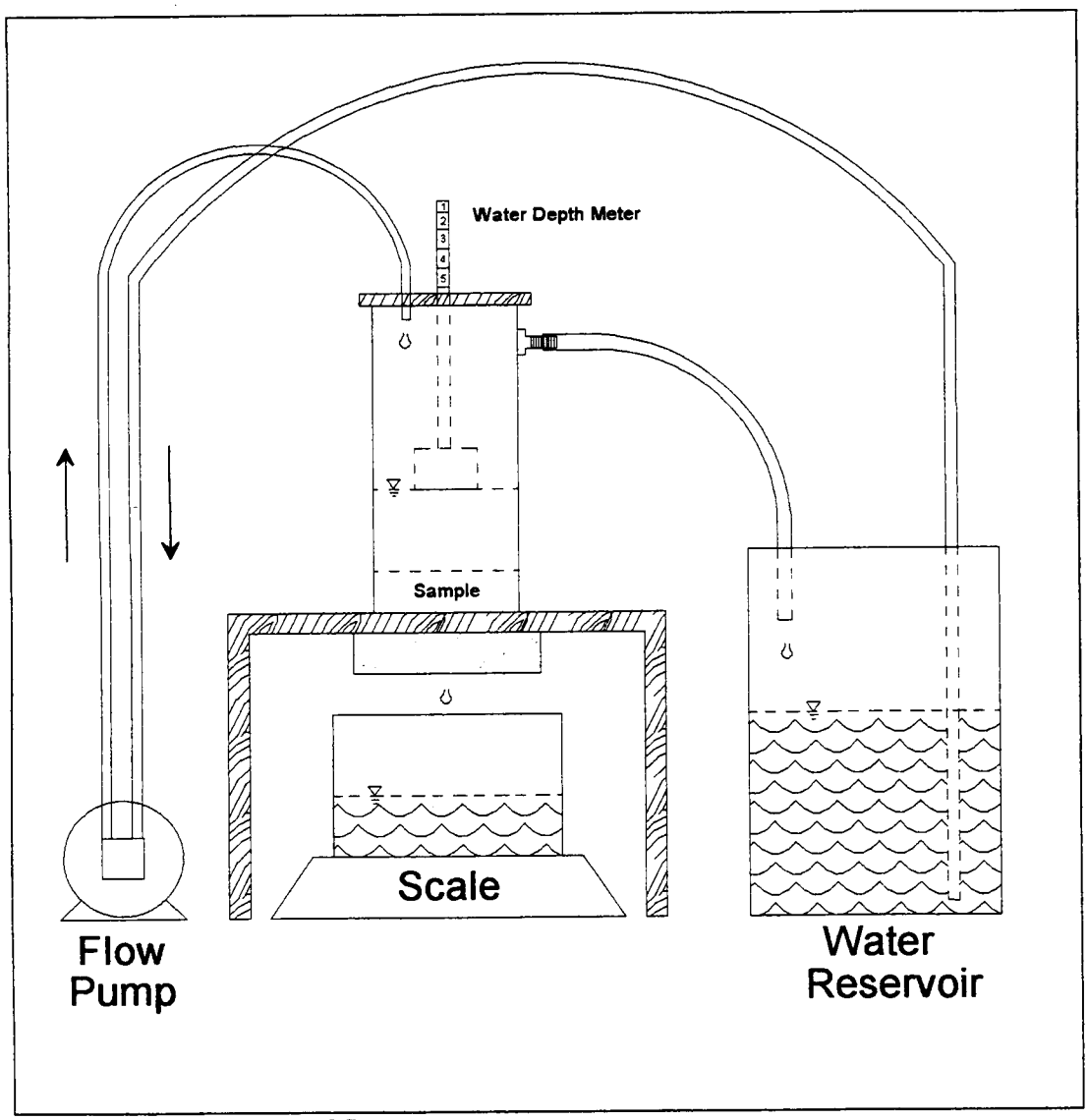


Fig. 3-2. Schematic of flow test system

be diverted such that constant head conditions can be maintained. An electronic scale was used to measure the outflow.

Apparent Conductivity

From these flow tests, a parameter termed the apparent conductivity was defined. The term 'apparent' is used to distinguish this conductivity from that obtained in a true Darcy experiment. Darcy's law is based on a number of assumptions and may not be valid under certain situations. For instance, Darcy's law is a macroscopic law giving an averaged description of microscopic behavior. In other words, the presence of features such as cracks and fissures can make this "averaging" less informative. Also, studies have shown that flow through fractures becomes very non-linear at small hydraulic gradients, which can not be described by Darcy's law. Other factors leading to non-Darcian behavior include the degree of saturation, internal swelling, dispersion of clay particles, and the Bingham flow effect. Some researches (Swartzendruber, 1962; Miller and Low, 1963; Nerpin et al., 1966) have proposed "Bingham flow" at low hydraulic gradients, in which no flow or flow less than proportional to the gradient may result (Figure 3-3). This theory calls for a threshold gradient below which the flow is zero or at least lower than that predicted by Darcy's law. Flow only becomes proportional to the gradient at hydraulic gradients exceeding this threshold value. All of these factors are involved in the flow tests conducted, thus

the need to define an apparent conductivity. The apparent conductivity was defined for three cases: rising head, constant head, and falling head (Figure 3-4).

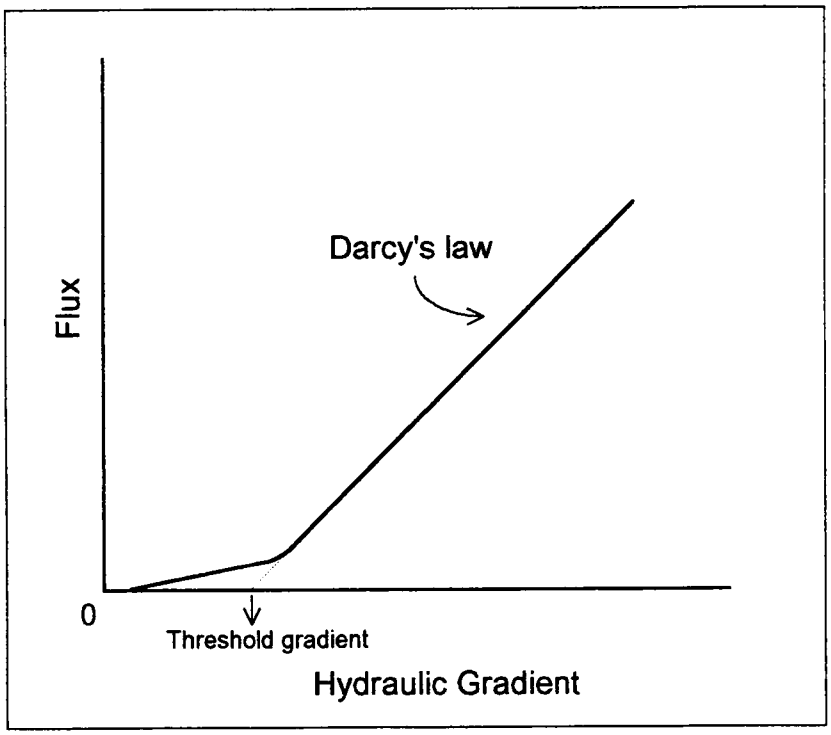
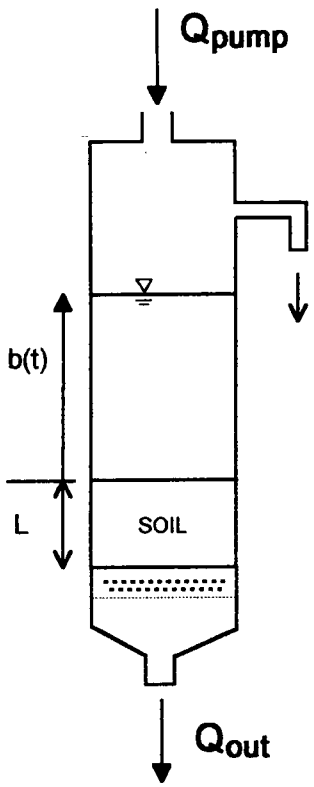


Fig. 3-3. Bingham flow effects

Rising Head

At the beginning of the test, the water level on the sample begins to rise as the fracture network becomes unable to conduct all the water. An exact solution for apparent conductivity during the rising head condition would include solving a complex differential equation. Due to the small time intervals, an approximate solution was deemed adequate and employed for simplicity. This



z = elevation head

ψ = pressure head

H = hydraulic head

$\{z_2 = L, \psi_2 = b(t), H_2 = L + b(t)\}$

$\{z_1 = 0, \psi_1 = 0, H_1 = 0\}$

Rising Head:
$$K_{app} = \frac{\left[\frac{Q_{pump}}{A} - \frac{\Delta b}{\Delta t}\right]}{\left[\frac{L + \bar{b}}{L}\right]}$$

Constant Head:
$$K_{app} = \frac{\left[\frac{Q_{out}}{A}\right]}{\left[\frac{L + b}{L}\right]}$$

Falling Head:
$$K_{app} = \frac{\left[\frac{Q_{out}}{A}\right]}{\left[\frac{L + \bar{b}}{L}\right]}$$

A = cross-sectional area; Δb = change in water level during time interval Δt; $\bar{b} = \frac{b(t) + b(t + \Delta t)}{2}$

Fig. 3-4. Apparent Conductivity

approximate solution included using an average value of head during a given time interval in the Darcy equation. The outflow for the rising head condition was found in such a way as to include water absorbed into the matrix (i.e., outflow equals inflow minus volume of water on sample).

Constant Head

As the water level neared the top of the cylinder, excess water was drained away to maintain a constant head on the sample. The equation for constant head condition is well established and generally accepted such that no simplifying assumptions were necessary. Direct measurements of outflow were used in the equation as the sample is assumed to be fully saturated during the constant head condition.

Falling Head

During flow interruptions and at the end of the test, the flow pump is shut off and water is allowed to drain freely through the sample. An exact solution from Darcy's law for apparent conductivity during falling head conditions is given by the equation

$$K_{Darcy} = \frac{L}{\Delta t} \ln \left[\frac{b(t) + L}{b(t+\Delta t) + L} \right] \qquad (3\text{-}1)$$

In order to maintain consistency, however, an approximate solution was used as given by the equation

$$K_{app} = \frac{\left[\frac{Q_{out}}{A}\right]}{\left[\frac{L+\bar{b}}{L}\right]} = \frac{\frac{b(t) - b(t+\Delta t)}{\Delta t}}{\frac{L + \left[\frac{b(t) + b(t+\Delta t)}{2}\right]}{L}} \qquad (3\text{-}2)$$

The ratio of these two equations is given by

$$\frac{K_{Darcy}}{K_{app}} = \frac{\ln\left[\frac{b(t)+L}{b(t+\Delta t)+L}\right] \times \left[L + \left[\frac{b(t) + b(t+\Delta t)}{2}\right]\right]}{b(t) - b(t+\Delta t)} \qquad (3\text{-}3)$$

For short time intervals, mathematical derivation shows

$$\lim_{(b(t) - b(t+\Delta t)) \to 0} \left[\frac{K_{Darcy}}{K_{app}}\right] = 1 \qquad (3\text{-}4)$$

Thus the exact and approximate solution approach the same value as Δt goes to zero. Comparisons were made between the exact and approximate solutions and were found to be the same for three significant digits. Thus, the use of the approximate solution for the rising and falling head seems reasonable. This approximate solution, just as in the rising head condition, included using an average water head during a given interval. Again, direct measurements of outflow were used in calculating the apparent conductivity. Only small "jumps", if any, occurred in the calculated apparent conductivity when transferring from one condition to another.

FLOW TEST RESULTS

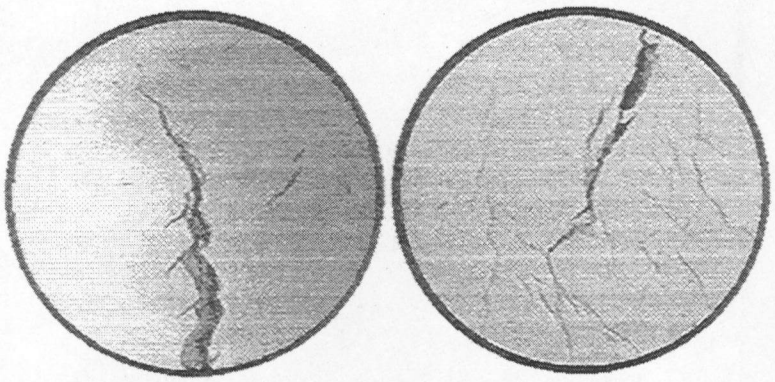
The flow tests included investigations into the flow properties of twenty desiccated kaolin slurry samples. The results include digital images of the sample before and after the test, and plots of head, flow rate, and apparent conductivity versus time. This information for all of the tests is given in Appendix 1. The following discussion will encompass side-wall leakage effects, short-term and long-term tests, influence of total fracture area, fracture closure, and the effect of head on fracture closure.

Side-Wall Leakage

In order to isolate the flow of water through the clay fractures, flow along the wall of the cylinder must be kept negligible. Due to the beveled edge of the sampling cylinder and the relatively moist clay, good adhesion between the soil and the tube was visually observed. An unfractured sample was tested to verify that side-wall leakage was negligible (see Sample 5-6 in Appendix 1). There was no observed outflow for over five days, a duration longer than any of the other tests. Thus it seems reasonable to assume that the outflow is predominantly due to fracture flow.

Presentation of Flow Test Results

The flow test data for all of tests are presented in Appendix 1. Sample 5-4 gave results (Figure 3-5) typical of all the tests. The inflow rate was calibrated before and after the test and the average value was plotted. The outflow and the head are measured every two minutes for the first sixty minutes. The rising head indicated that the fracture system could not conduct water at a sufficient rate to keep up with the inflow rate. Results for the first hour of the test, illustrated in Figure 3-5 (a), showed a decrease in apparent conductivity. This was typical of all the samples. Closing of the fractures as the clay swelled likely caused this decrease. These effects will be discussed more fully in a later section. Some of the early tests were only run for sixty minutes and thus do not include the long term plots illustrated in Figure 3-5 (b). Longer duration tests were performed to determine if the flow would reach an equilibrium. It was found that there was a limit to how fully the fractures would close, resulting in no further decrease in apparent conductivity. Breaks in the apparent conductivity plot represent flow interruptions, which will be further discussed later. Digital images of the top and bottom of the sample shown in Figure 3-5 (c) vividly illustrate the closing of the fractures during the test. Flow through the sample was controlled by the smallest fracture area, which was generally found on the bottom of the sample.



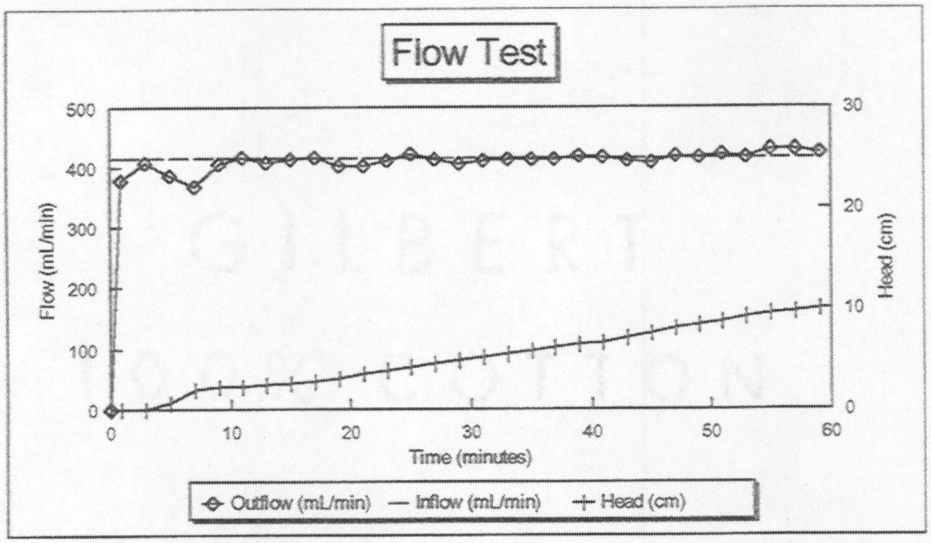
Top of Sample Bottom of Sample

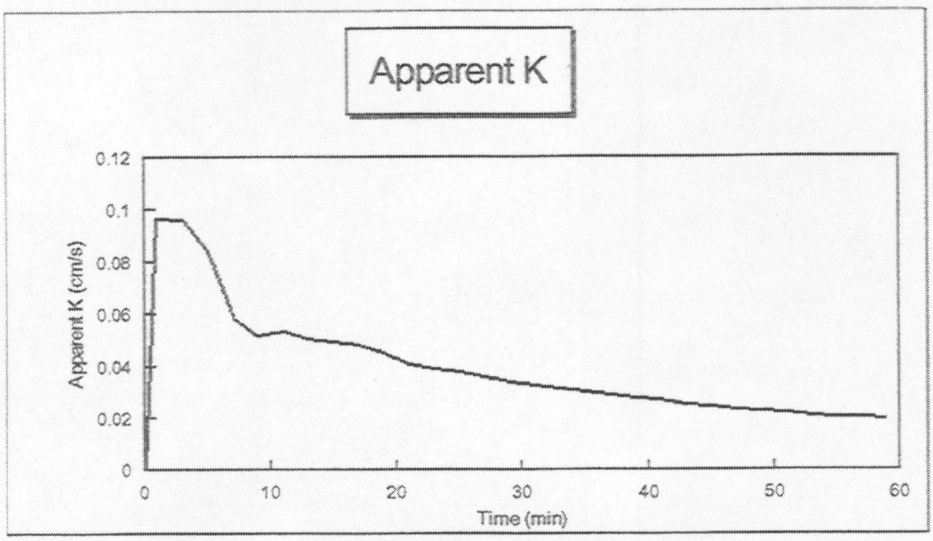
Initial Batch w%= 71.9%
Initial Sample w%= 50.0%

Thickness = 2.65 cm
Diameter = 9.5 cm

Maximum Aperture = 7.2 mm

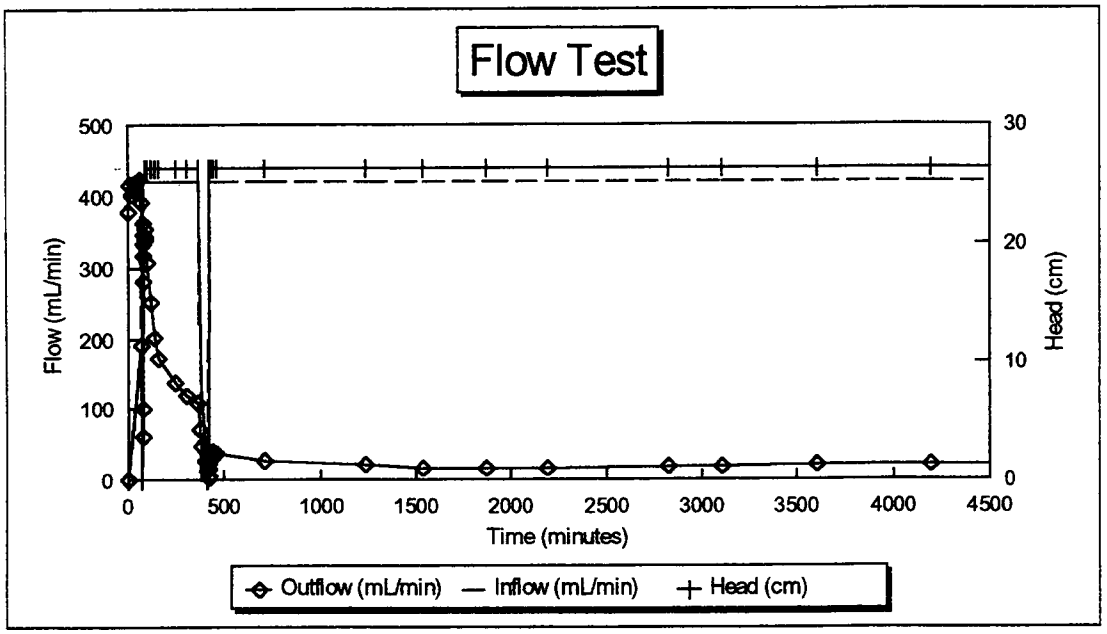
Fracture Area Percentage
Top of Sample = 4.9%
Bottom of Sample = 2.5%

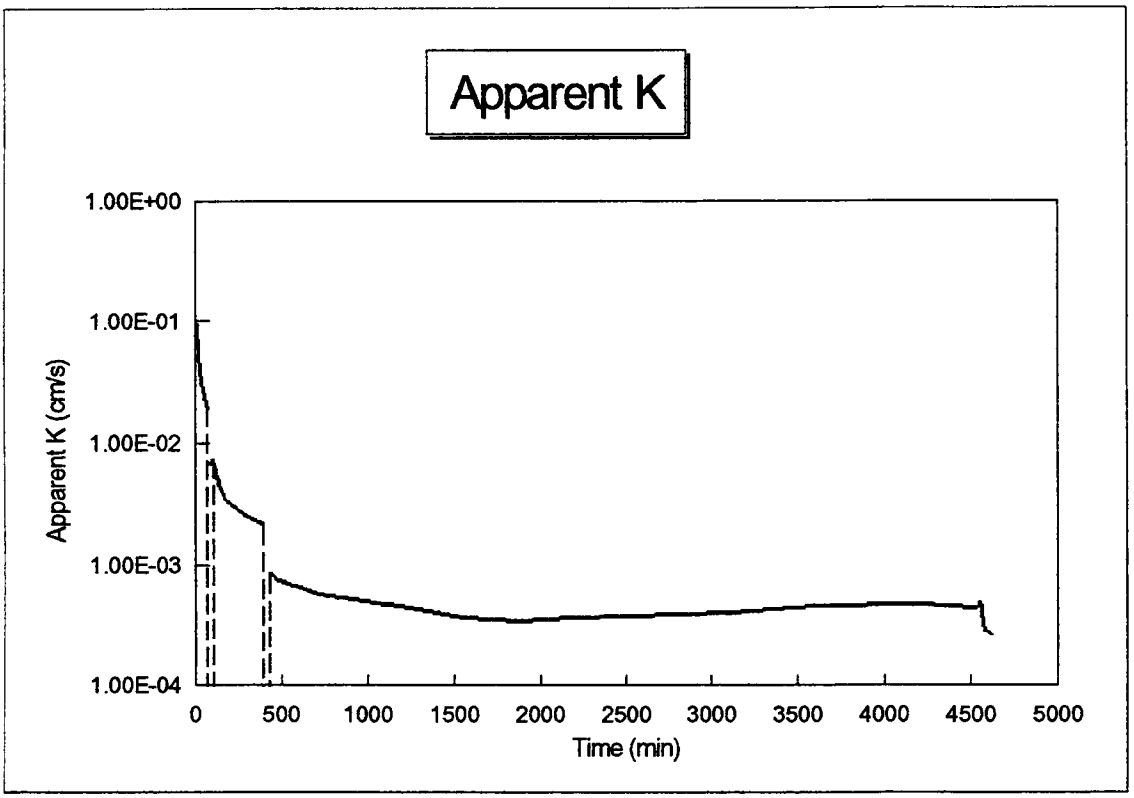




(a) Short term results

Fig. 3-5. Tests for Batch #5, Sample #4





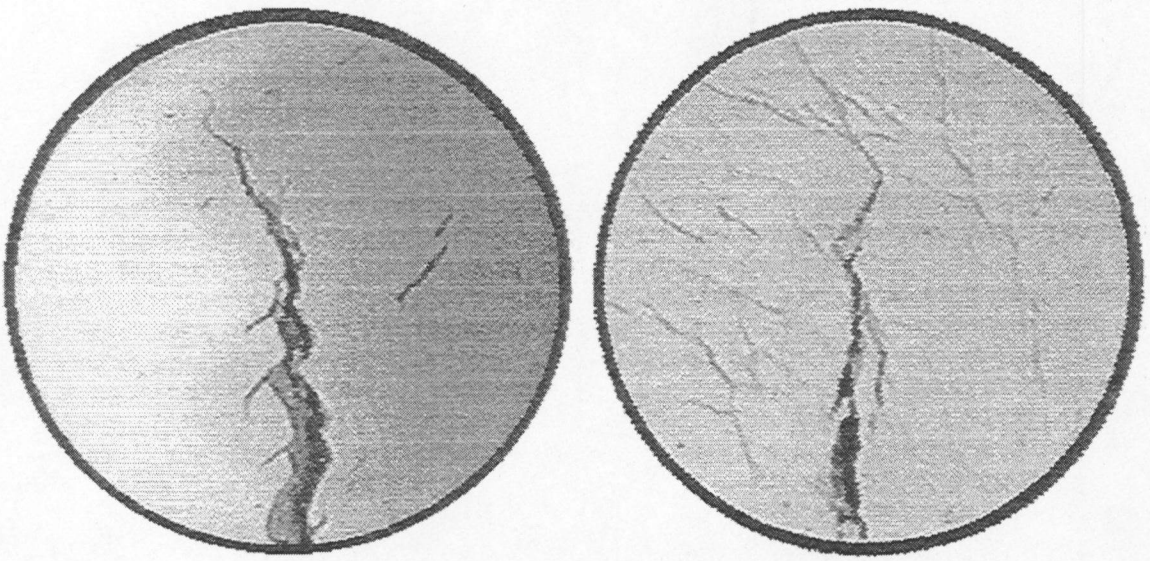
(b) Long term results

Fig. 3-5. (continued)

Before Testing

Top of Sample

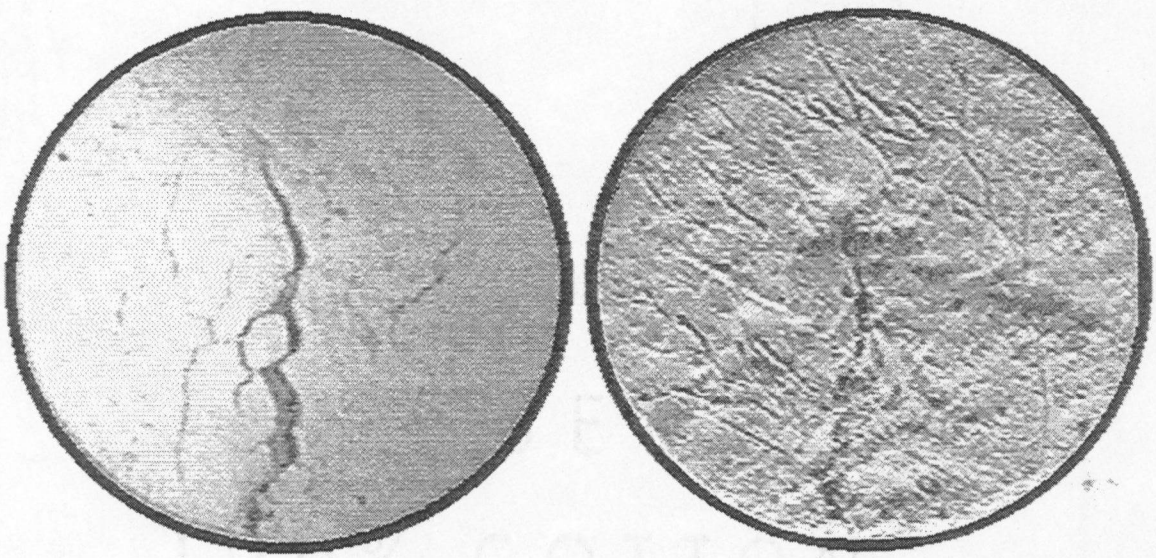
Bottom of Sample



After Testing

Top of Sample

Bottom of Sample



(c) Sample fractures

Fig. 3-5. (continued)

Decrease in Apparent Conductivity

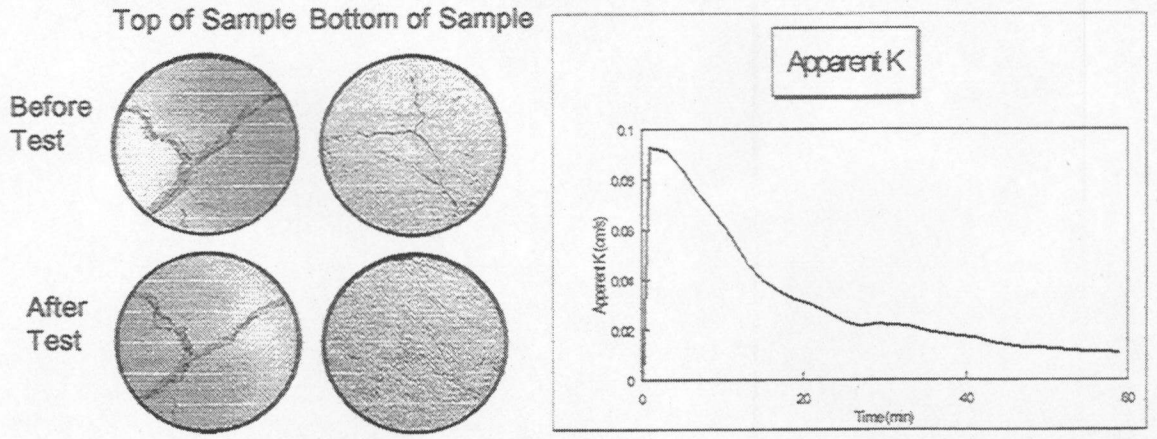
As mentioned before, a measured decrease in apparent conductivity was found for all of the samples. This decrease is reflected in both the short term and long term tests, as shown in Figures 3-6 and 3-7. Images of the samples also showed the closing of the fractures. The apparent conductivity decreased rapidly during the early stages of the test and slowly reached a steady value. The short term tests, Figure 3-6, are plotted on a normal scale, whereas the long term tests, Figure 3-7, are plotted on a semi-log scale. The decrease in apparent conductivity for each of these examples is almost three orders of magnitude.

Effect of Average Fracture Area on Short Term Fracture Flow

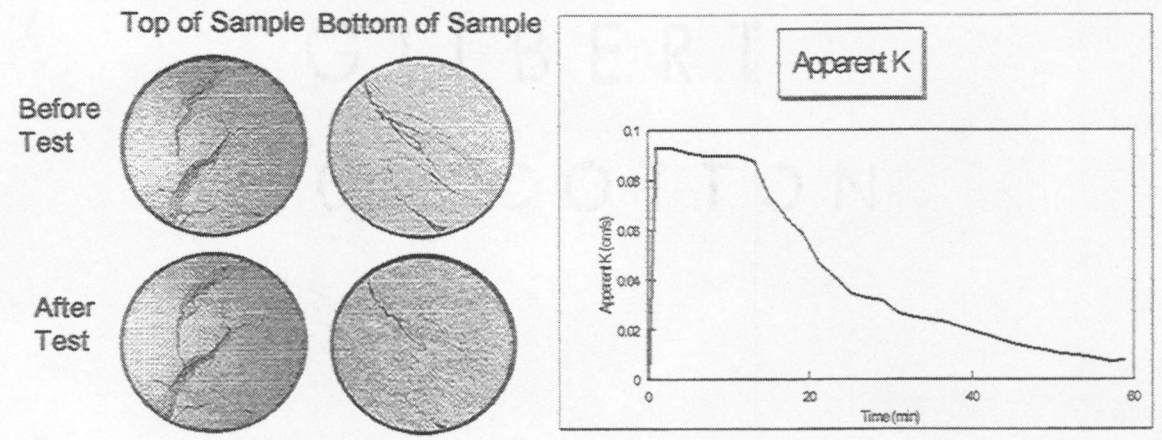
Snow (1968) showed that flow through a fracture in rock followed a cubic law in which the flow rate was proportional to the cube of the fracture aperture. The same general idea should apply to soils except that fracture aperture is a dynamic property; it changes with time. For this reason, the cubic law could not be explicitly applied to predict or model flow. However, the flow tests conducted do show a general relationship between the magnitude of a fracture and the resulting flow.

The fracture area, expressed as a percentage of the total sample area, was used to show this relationship. The fracture area of the top and bottom of the sample were estimated using the method of squares. A grid of 0.2 cm

(a) Sample 4-3



(b) Sample 5-1



(c) Sample 5-2

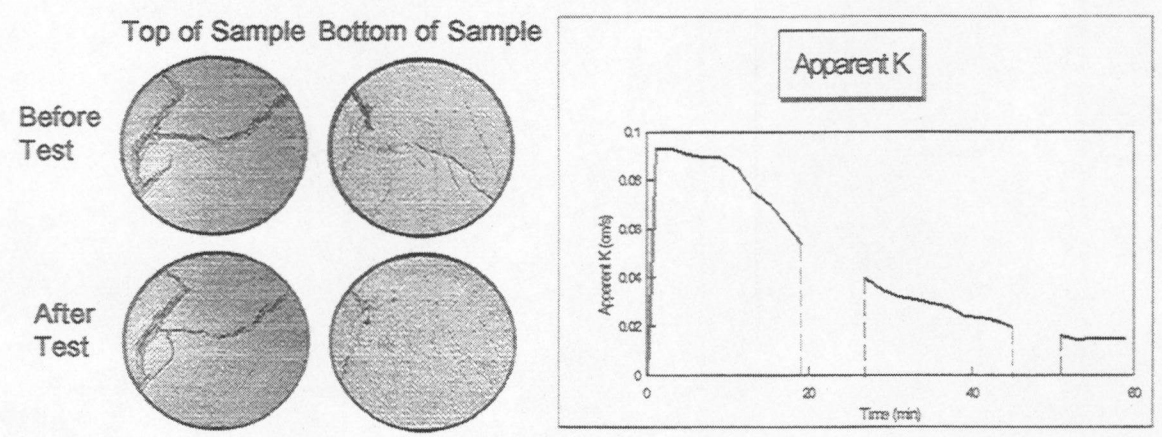
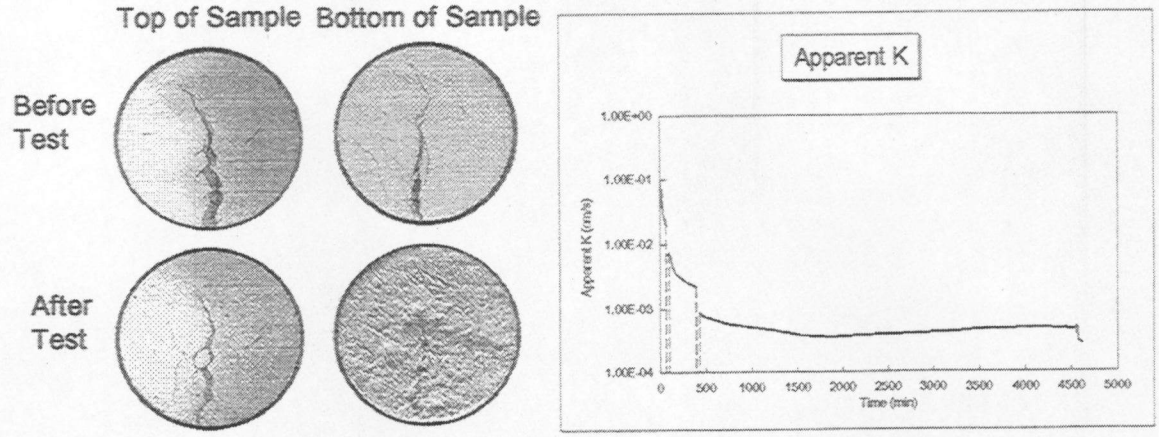
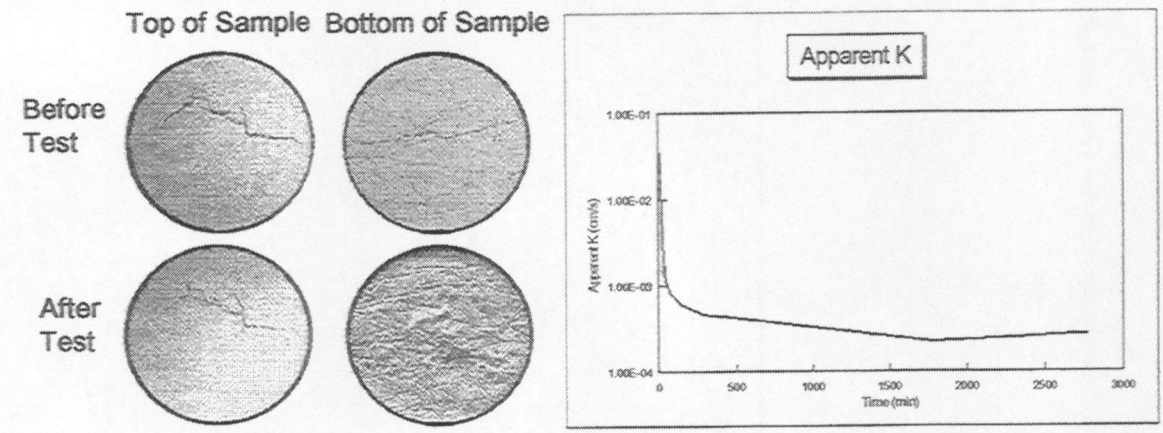


Fig. 3-6. Short Term Flow Tests

(a) Sample 5-4



(b) Sample 5-5



(c) Sample 8-2

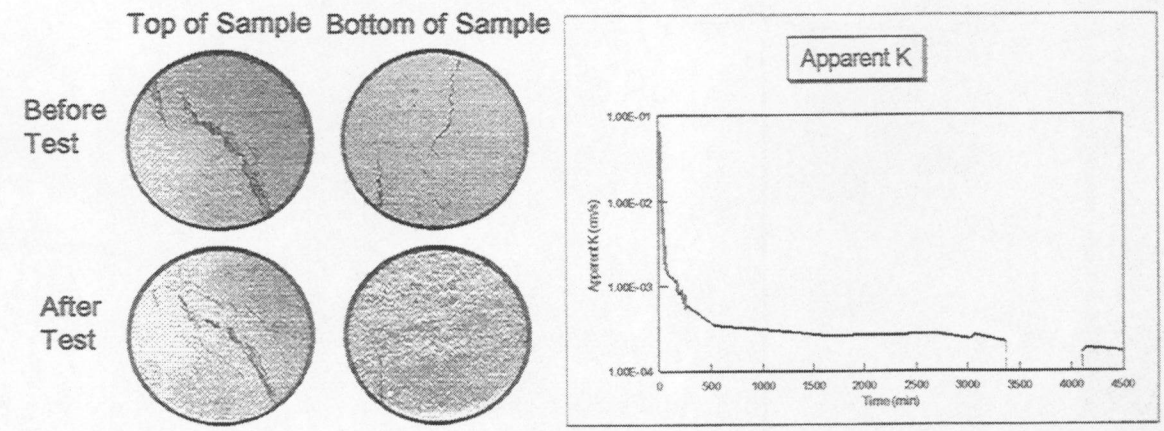


Fig. 3-7. Long Term Flow Tests

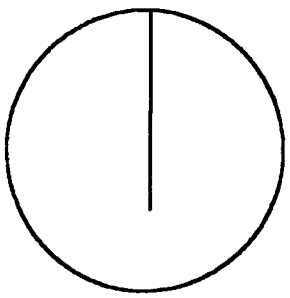
squares was placed over pictures of the samples and the area of the fracture estimated by the number of squares occupying the area. The fracture area of the top of the sample was important for it determines the amount of water that penetrates the surface and is available to the interior of the fracture. The fractures in all of the flow tests decreased in size with depth, as is the case for fractures in general. The fracture area of the bottom of the sample is important as it serves as the "bottleneck" which ultimately limits the outflow. The average of these two areas was used in the investigation.

Fracture Geometry

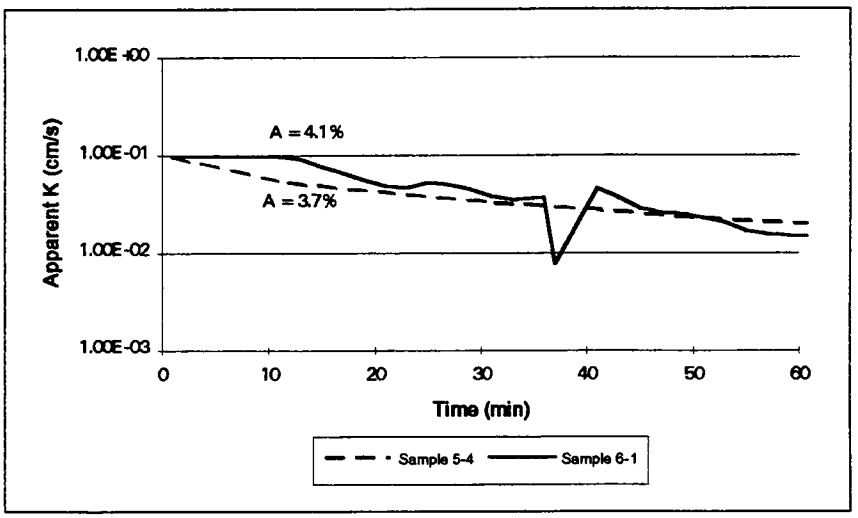
Another important consideration found in these flow tests was the geometry of the fractures. A general relationship between average fracture area and the apparent conductivity for all samples was wrought with inconsistencies. Although there seemed to be a tendency for apparent conductivity to increase with increasing fracture area, there were significant departures from this rule. Errors in measuring the average fracture area could contribute to this, but effects due to geometry are more likely. Specific geometrical configurations behave differently from others which can make comparisons difficult. These effects are especially important in relation to how the fractures close due to swelling. Five general fracture geometries were defined for the flow tests (Figure 3-8). As the flow behaviors for the samples are broken down into these groups, a very

(a)

Fracture Pattern

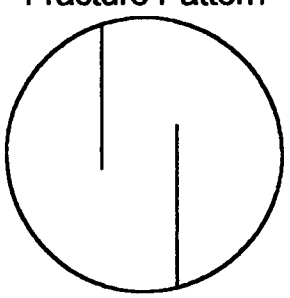


A = Average Fracture Area expressed as a percentage of the total area.



(b)

Fracture Pattern



A = Average Fracture Area expressed as a percentage of the total area.

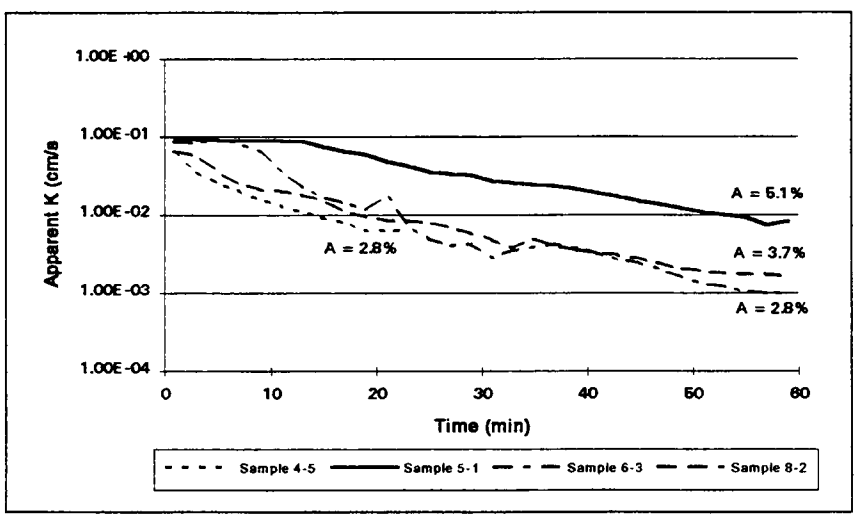
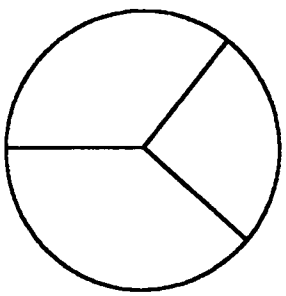


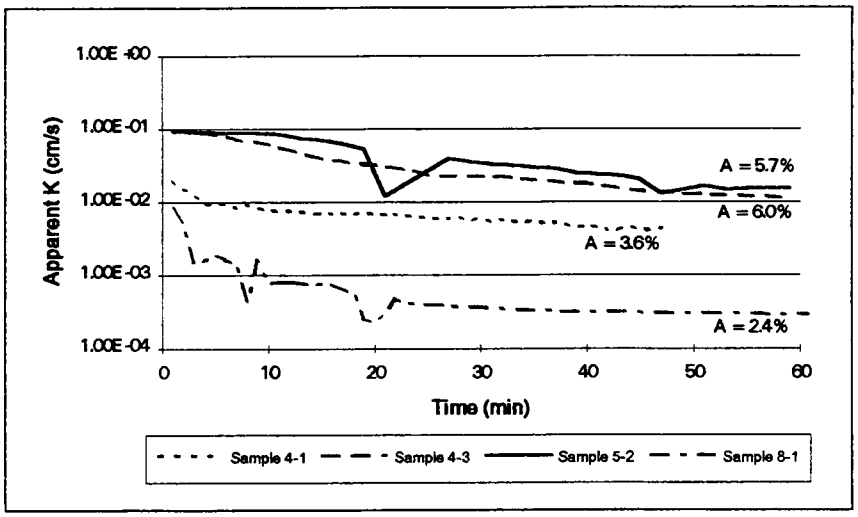
Fig. 3-8. Relationship Between Apparent Conductivity and Average Fracture Area

(c)

Fracture Pattern

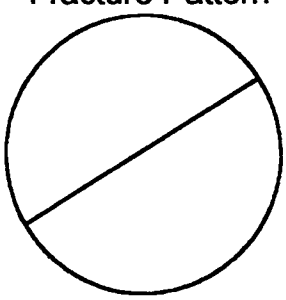


A = Average Fracture Area expressed as a percentage of the total area.



(d)

Fracture Pattern



A = Average Fracture Area expressed as a percentage of the total area.

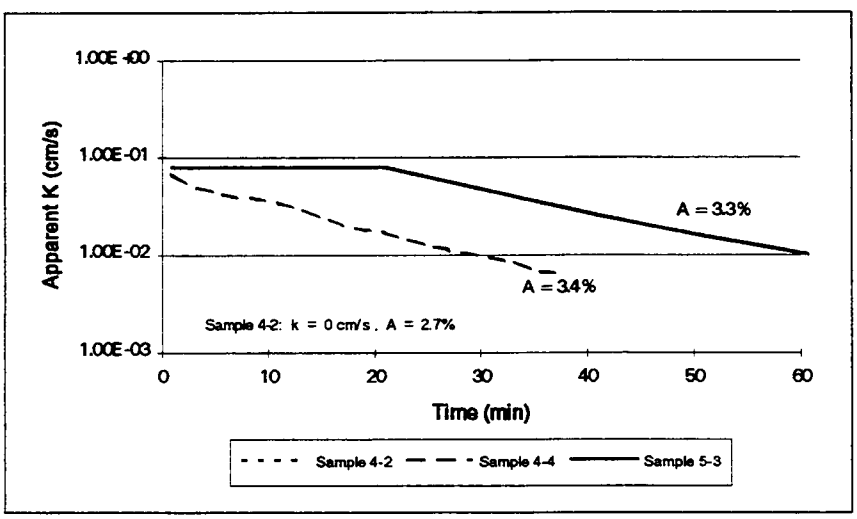


Fig. 3-8. (continued) Relationship Between Apparent Conductivity and Average Fracture Area

(e)

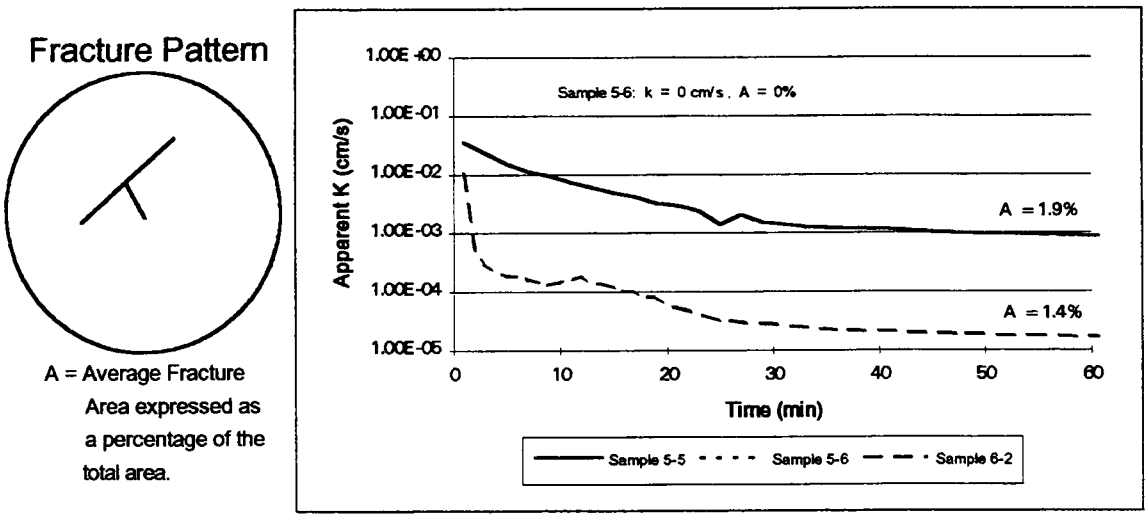


Fig. 3-8. (continued) Relationship Between Apparent Conductivity and Average Fracture Area

distinct relationship between average fracture area and apparent conductivity becomes clear. There were some slight inconsistencies, but these should be expected due to the nature of the tests and the uncertainties associated with estimating fracture area. Although this relationship may seem immediately intuitively obvious, it is nonetheless important in considering water and contaminant transport through preferential flow paths.

Closing of Fractures

In all of the flow tests, a general decease in apparent conductivity with time was found. This decrease was most likely related to swelling of the clay as more water was absorbed into the matrix. The sample responded to this swelling by expanding in directions of least resistance. For fractured media, the clay can heave, or expand upward, or it can expand inward closing the fracture void space. As this void space diminishes, the sample was unable the conduct the same amount of water. This was reflected by a measured decrease in the apparent conductivity. Estimates were made of the total fracture area on the top and bottom of the samples before and after the test. From this information, an estimate of the degree to which the fractures closed during the test were made, expressed as a percentage (Table 3-1). With respect to fracture closing, the most dynamic stage of the test was during the early stages.

Data from Table 3-1 show that samples that were saturated for extended periods of time only closed slightly more than samples saturated for one hour. This reinforces the point that flow during the early stages of saturation was the most important and the most difficult to capture. This rapid closing of fractures during early stages of the tests corresponded directly to the immediate decreases in measured apparent conductivity. The rate of closure slowed with time reaching an equilibrium condition just as the apparent conductivity decreased slowly to a steady state value.

Table 3-1. Estimated percent fracture closure

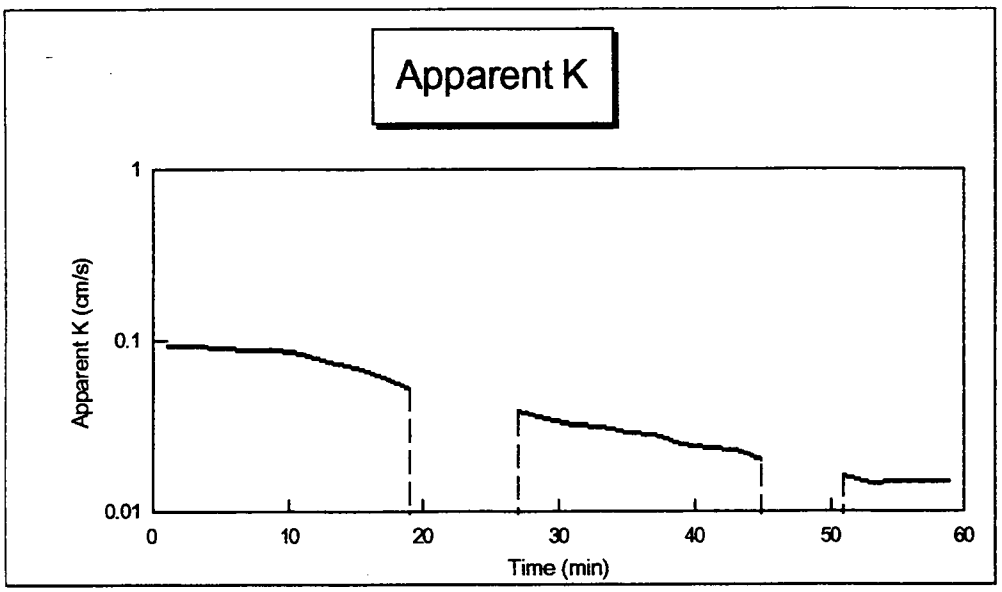
	Sample	Percent Fracture Closure	Duration of Test
Short Term Tests	4-3	47.8	60 min
	4-4	32.7	37 min
	4-5	22.9	23 min
	5-1	35.2	60 min
	5-2	31.4	60 min
Long Term Tests	5-4	50.6	4500 min
	5-5	35.3	2750 min
	6-1	39.8	3300 min
	6-2	61.0	1400 min
	6-3	33.8	1750 min
	8-1	51.8	4200 min
	8-2	59.6	4200 min

Effect of Head on Fracture Closure

The calculated value of apparent hydraulic conductivity (K) decreased in all the flow tests due to healing of the fractures as a result of swelling of the clay matrix. However, the rate and manner in which these fractures closed was in large part dependent upon the magnitude of the head of water applied and the degree of saturation of the clay matrix. Flow interruptions were used to examine these effects. A flow interruption simply involved shutting off the pump and allowing the water to drain through the sample. The pump was then turned back on and measurements made. These flow interruptions are denoted by a break in the apparent conductivity curves in Figure 3-9. From these flow interruptions, a theory was developed, which suggests that the rate of fracture closure may be dependent upon the head.

Near the beginning of the test, apparent K was unaffected by these flow interruptions as shown in Figures 3-9 (a) and (b). In these cases, the sample was only partially saturated and the applied heads were relatively small. Although there was swelling at this point, it was largely unimpeded by the developing head. The largest impact of head on apparent K was experienced at intermediate times as shown in Figures 3-9 (c) and 3-9 (d). The apparent K typically dropped one half an order of magnitude after the flow interruption. This suggests that the applied head before the flow interruption was actually serving to keep the fracture open. At this point, the sample was not fully saturated and

(a) Sample 5-2



(b) Sample 6-1

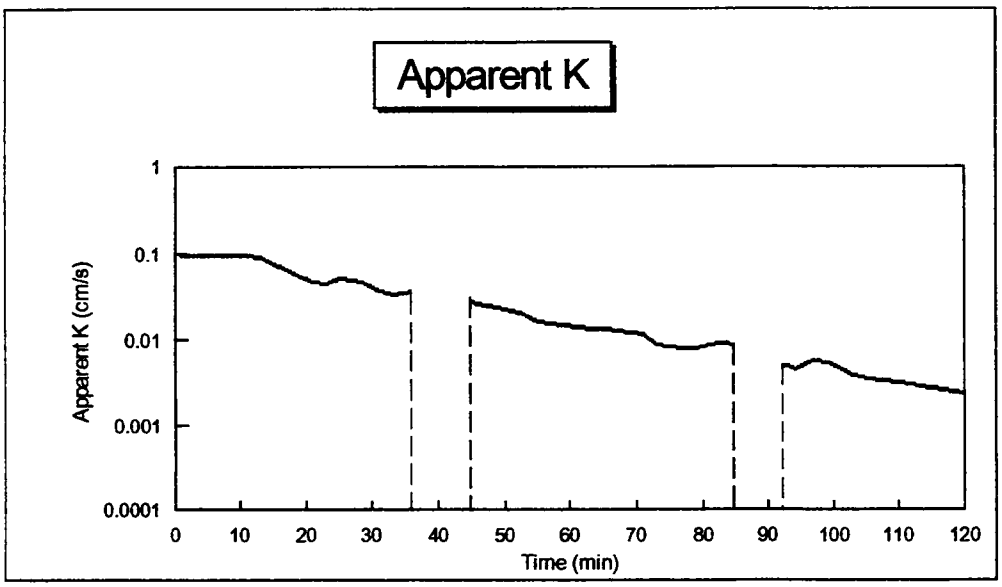
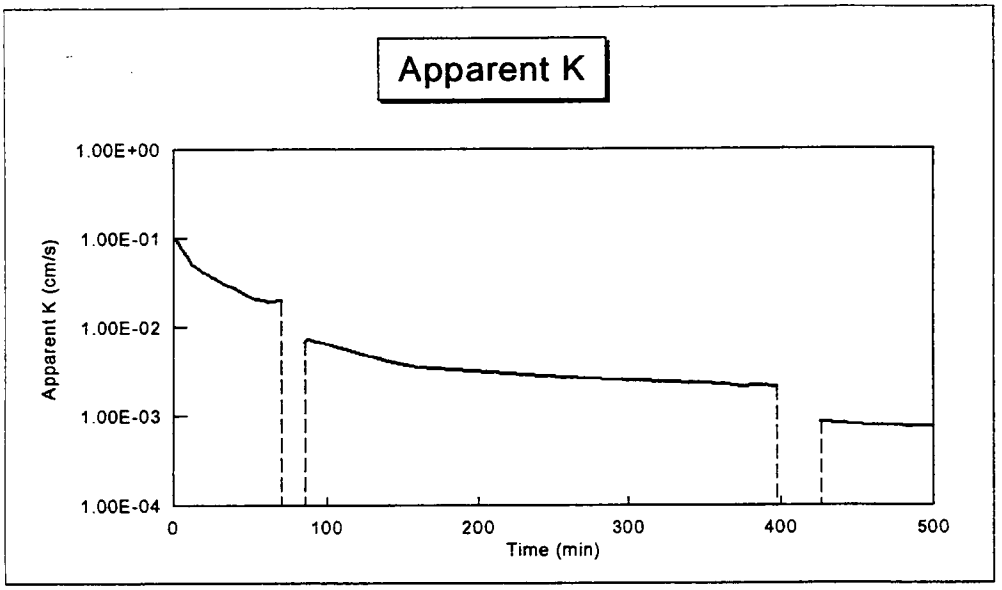


Fig. 3-9. Effect of head on fracture closure: Early times (a) sample 5-2, (b) sample 6-1

(c) Sample 5-4



(d) Sample 6-1

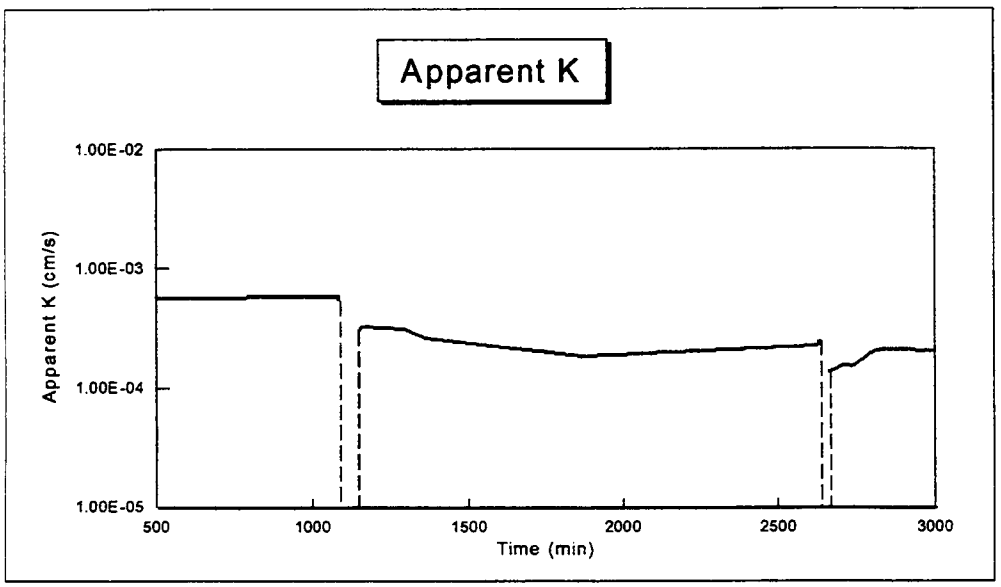


Fig. 3-9. (continued) Effect of head on fracture closure: Intermediate times (c) sample 5-4, (d) sample 6-1

(e) Sample 8-2

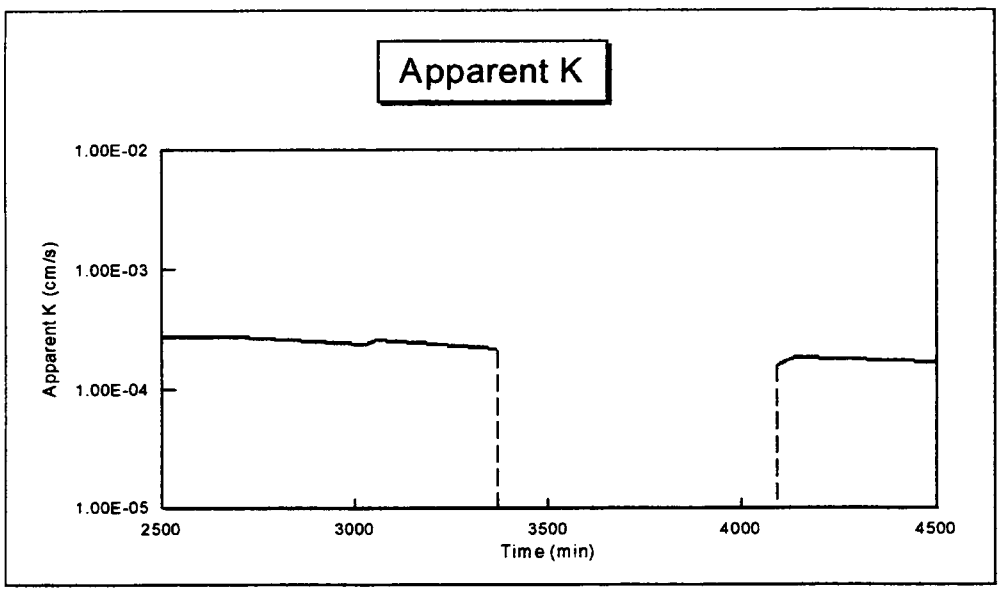


Fig. 3-9. (continued) Effect of head on fracture closure: Long times (e) sample 8-2

the effective stress on the outside of the fracture was greater than that in the matrix. Capillary forces exist in the dry matrix drawing water into the soil. The higher the column of water on the sample, the higher these forces are and the quicker water infiltrates into the matrix. It is this pressure and perhaps the kinetic energy of the water moving into the matrix that resists the forces developed by the swelling of the clay. When this force is removed during the flow interruption, the swelling forces which tend to close the fracture are unimpeded, resulting in a smaller fracture. As the flow test resumes, the calculated apparent conductivity jumps to a lower value, reflecting the smaller fracture volume.

At large times, the sample was saturated and the effective stress was constant across the fracture. This suggests that the head applied to the sample should no longer affect the dynamics of the fracture. Examples of this behavior are presented in Figure 3-9 (e). The apparent conductivity was relatively unaffected by the flow interruption at these larger times. It is interesting to note from Figure 3-9 how the impact of head on apparent conductivity increased to a maximum at intermediate times and faded to a minimum at larger times. Figure 3-10 illustrates and summarizes the conditions of the soil during these three phases.

This behavior is very important especially with regard to contaminant transport through a dry fractured clay. The flow interruptions presented here suggest that increasing head can lead to increased "short-circuiting" by combating the developing swelling pressures and keeping the fracture open. It

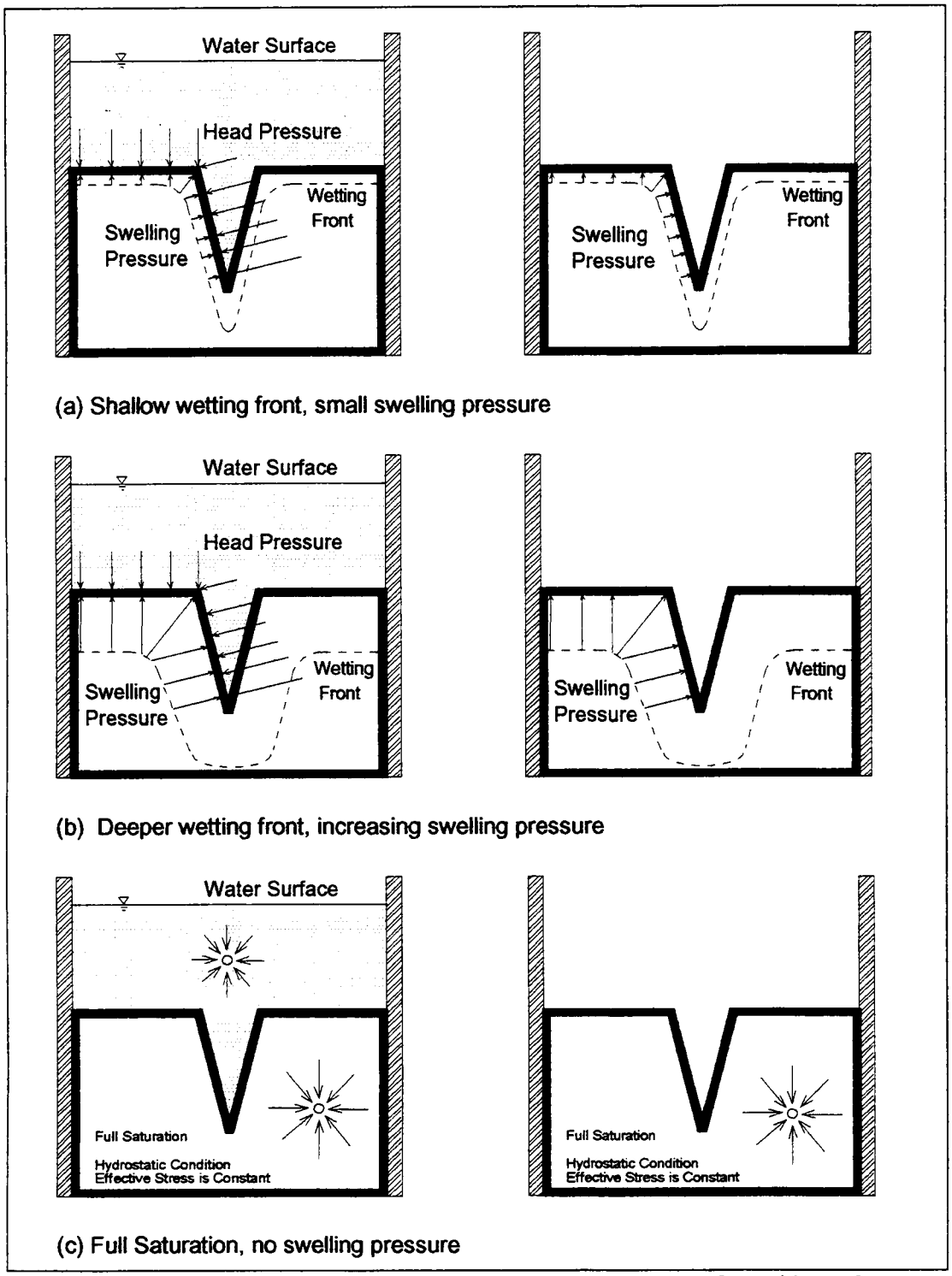


Fig. 3-10. Pressure equilibrium / disequilibrium at crack surface (the left column shows water head on the sample; the right column shows the sample response when head is removed)

should be recognized that the swelling pressure will eventually prevail as the matrix becomes saturated. This head pressure does not impact the degree and magnitude to which a fracture will close. The geometry of the fracture and the swelling potential of the matrix will ultimately determine that. The importance of this head pressure lies in the increased flow of water (or contaminants) during the interim phase.

PART 4

INFILTRATION TESTS IN FRACTURED CLAY

INFILTRATION

The true importance of preferential flow paths in fractured clay should be more fully captured during unsaturated infiltration. Infiltration is simply the entry of water into a soil surface. Matric potential gradients (negative water pressure gradients) control infiltration during early stages and gradually dissipate with time. The decreasing influence of the matric potential gradient as the wetting front deepens results in a decrease in the infiltration rate. Soil swelling and closing of any pore spaces can also contribute to this decrease. As more water infiltrates, the water content, pressure head, and hydraulic head increase while the hydraulic gradient decreases. The decrease in hydraulic gradient is not fully offset by the increase in hydraulic conductivity from the rising pressure head. The infiltration rate begins to decrease at a critical combination of these factors (Freeze and Cherry, 1979).

Beven and Germann (1981) conducted a series of infiltration tests to evaluate the influence of macropores. They found the macropores allowed deeper infiltration and a higher cumulative infiltration into the subsurface (see Figure 4-1). The influence of the macropores was greatest for an intermediate value of hydraulic conductivity. However, the nature of the macropore system is the most important variable, such as depth, magnitude, connectivity, and variability of the pore space.

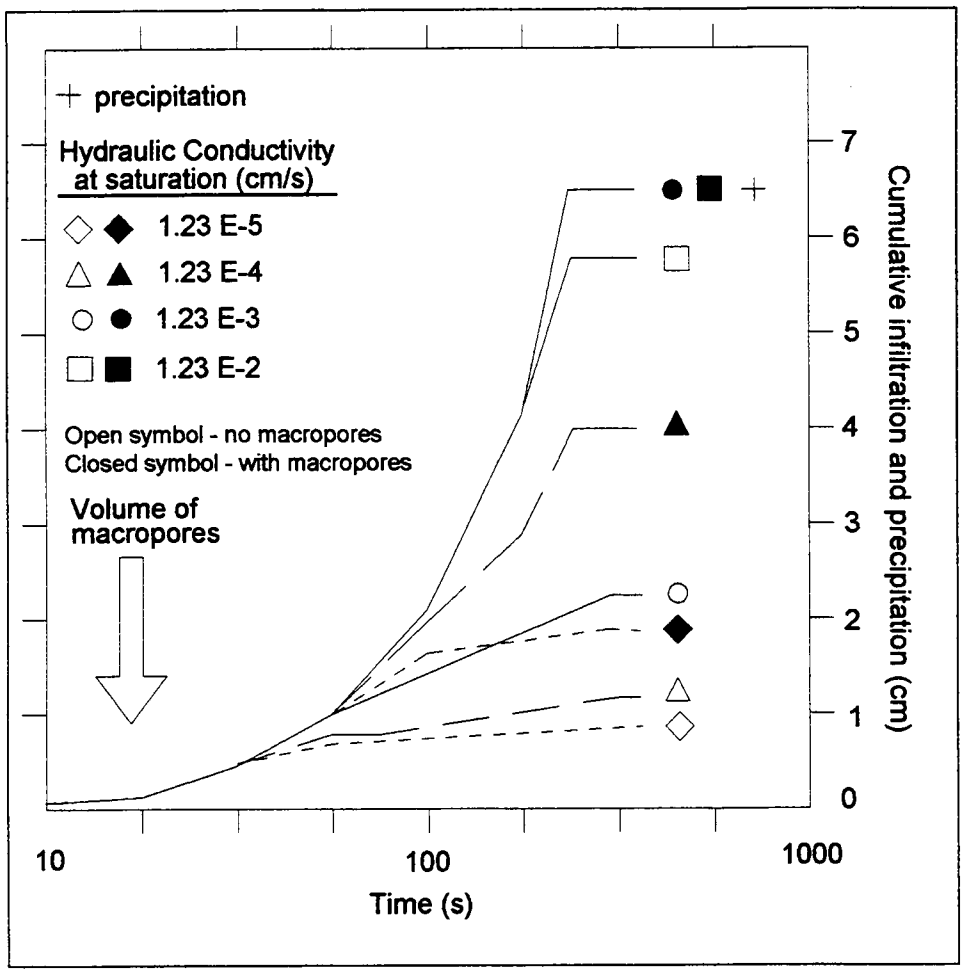


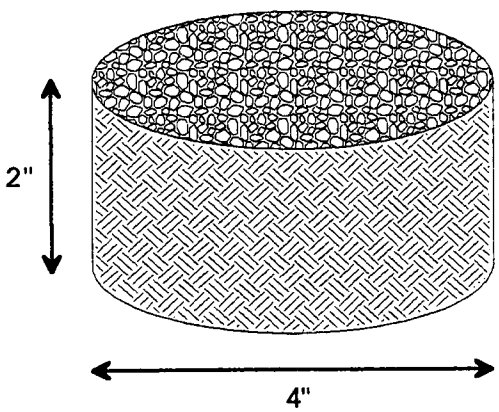
Fig. 4-1. Macropore effects on infiltration (Beven & Germann, 1981)

From the cracking tests discussed earlier, it was found that preferential flow paths can develop due to desiccation and freeze/thaw. Also, these pathways can close as the clay swells. The flow tests showed that flow of water through these pathways decreased as the fractures became smaller. The saturated hydraulic conductivity is found after these pathways can close, and thus gives little insight into the conductivity of these fractures during infiltration. For these reasons, a series of infiltration tests were performed to investigate the significance of initially unsaturated conditions on infiltration from a surface pond.

INFILTRATION TESTS

Samples used for the infiltration tests were compacted in PVC molds, extracted, and subjected to cycles of desiccation or freeze/thaw. The soil was mixed at optimum +3 water content and compacted to standard proctor energy. Figure 4-2 summarizes the infiltration testing procedure. A Mariotte device (see Figure 4-3) was set up to apply a constant head of about 5 cm on the sample. A scale was used to measure the amount of permeant lost from the reservoir, or the amount infiltrated into the sample. The reservoir was filled with 0.1% Rhodamine B red dye solution. After infiltration, the sample was allowed to dry at room temperature, and when it was strong enough, the sample was sliced into twelve approximately equal slices to expose the stains left by the dye. Digital images of these slices were taken to evaluate these stained pathways. Data

1. Clay Samples were compacted in a PVC mold and extracted.



2. The samples were placed in a flexible rubber membrane to help maintain their integrity throughout the testing. A piece of geotextile filter fabric was placed on the top and bottom of the samples and confined with rubber bands.

3. The samples were then subjected to cycles of desiccation or freeze/thaw.

4. After these cycles, the samples were allowed to dry completely. A ~5 cm head of dye was placed on the samples for 24 hours.

5. After the samples were dry, they were cut into approximately equal slices to expose the fracture stains on twelve cross-sections.

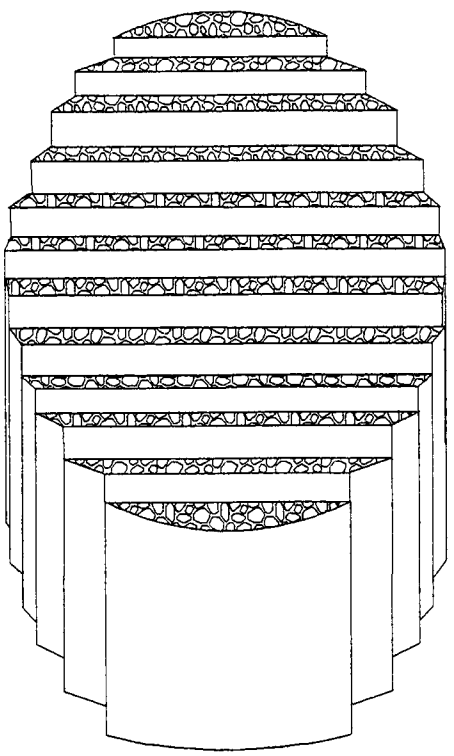


Fig. 4-2. Procedure for Exposing Fracture Stains

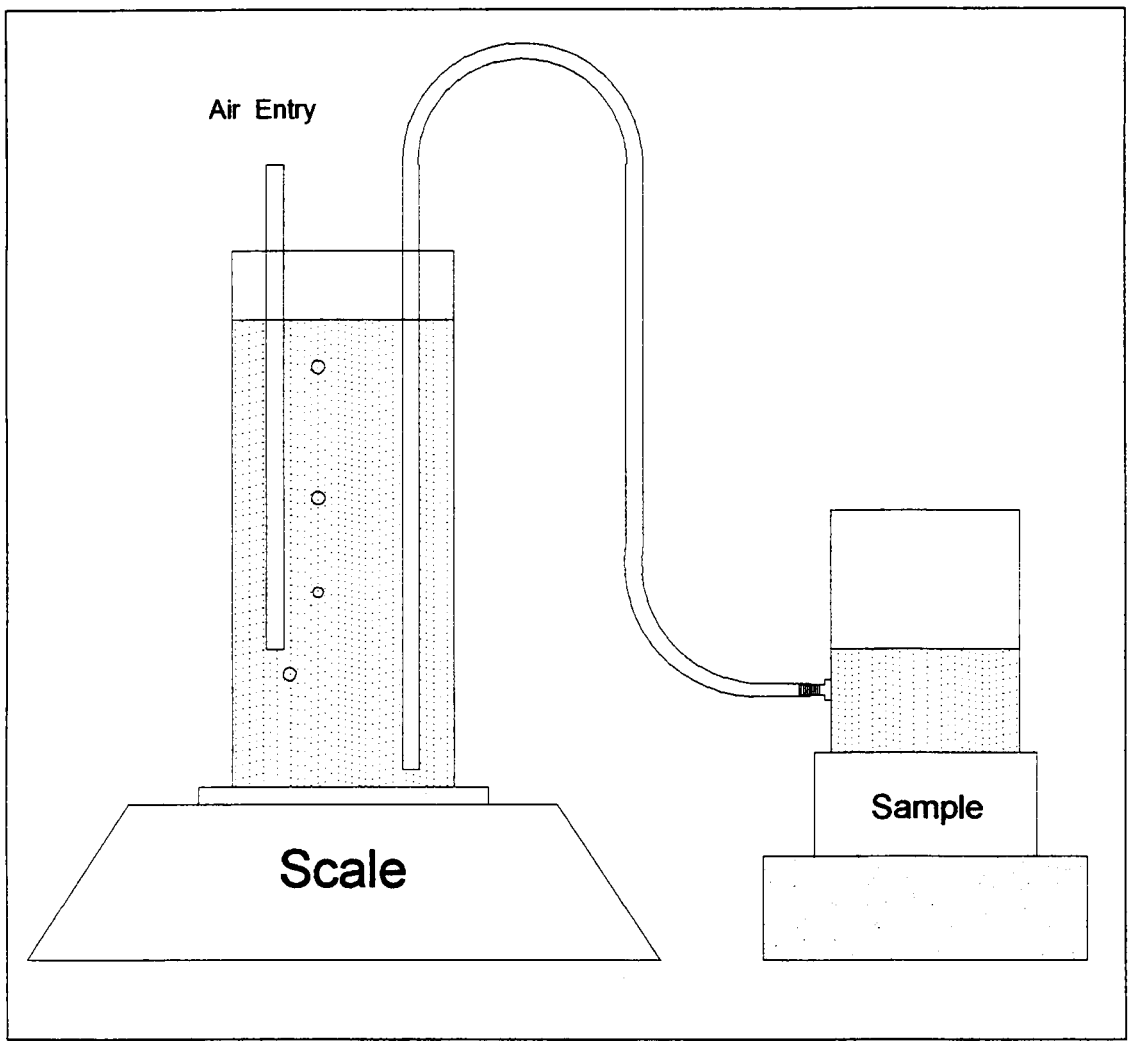
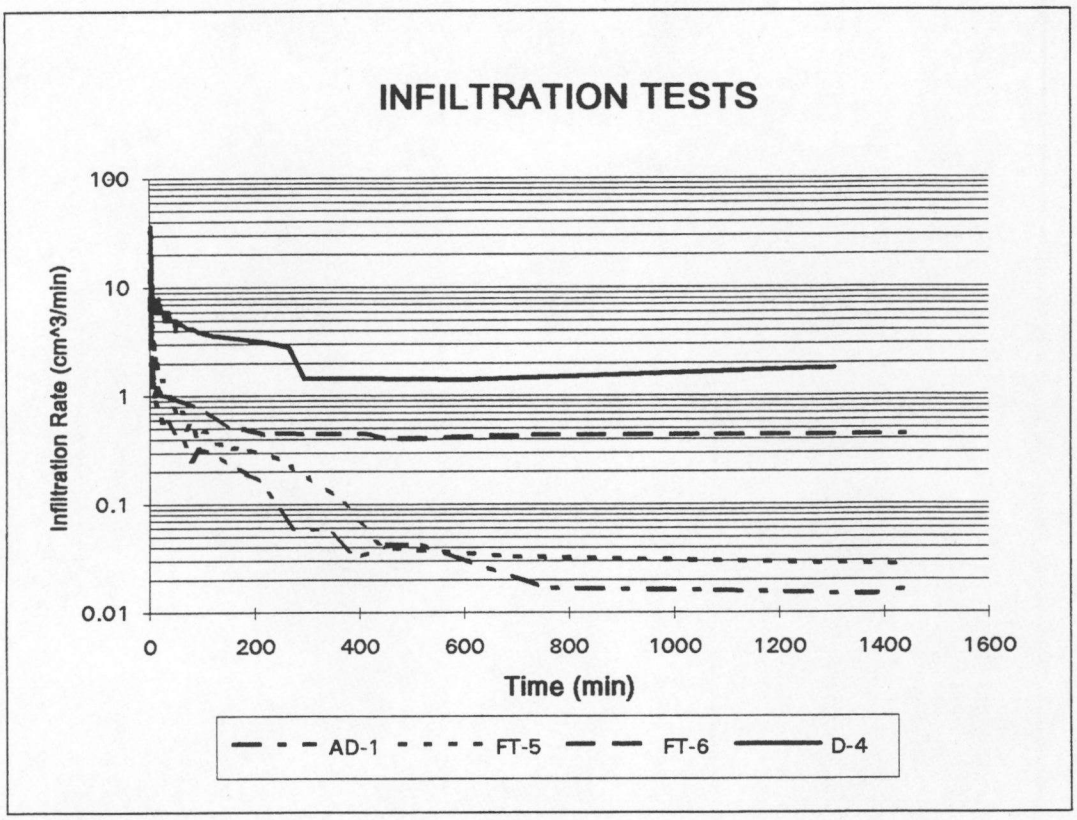


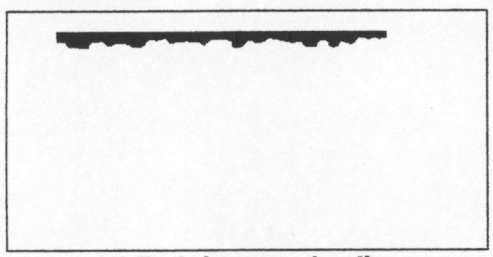
Fig. 4-3. Schematic of Infiltration system

from all of the infiltration tests are presented in Appendix 2. The discussion will include an evaluation of how fractures influence infiltration rate, the correlation between fracture stains and infiltration rate, the influence of clod size on infiltration, and closing of fractures during infiltration.

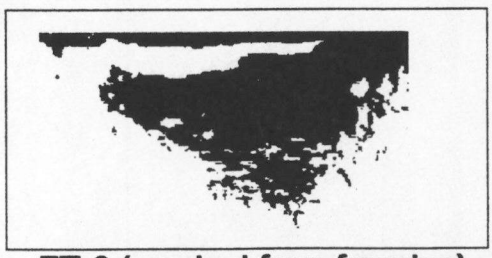
Influence of Fractures on Infiltration

The infiltration tests proved that fractures are indeed very important during transient infiltration. Not only do the presence of fractures cause an increase in infiltration rate, but they also generate great variability in infiltration (Figure 4-4). The uncracked sample showed the lowest infiltration rate as well as the shallowest penetration of the dye. The three samples that were cracked showed higher infiltration rates as well as deeper penetration of the dye. These fractured samples exhibited large variability due to differences in the fracture network. Sample D-4 contained a significant fracture that penetrated completely through the sample. As a result, the measured infiltration rate was the highest and the dye penetration was the most vast of all samples tested. Sample FT-6 had a horizontal fracture across the sample as indicated by the dye staining pattern. This pathway allowed additional infiltration into the sample as reflected from the measured infiltration rate. Sample FT-5 contained only small surface cracks as indicated by the dye pattern and the infiltration rate. The processes

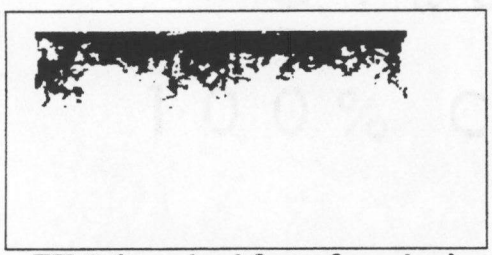




AD-1 (uncracked)



FT-6 (cracked from freezing)



FT-5 (cracked from freezing)



D-4 (cracked from desiccation)

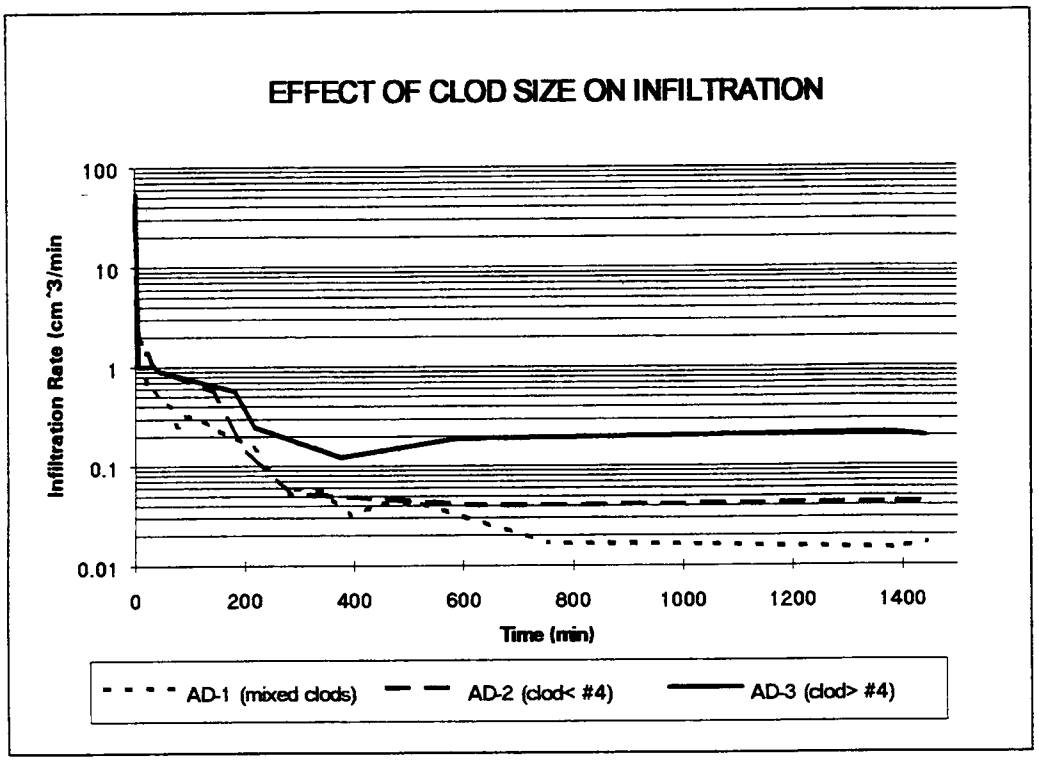
Fig. 4-4. Fracture effects on infiltration

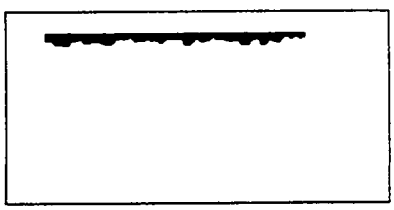
desiccation and freeze/thaw can lead to significant pathways through which water can flow.

Rhodamine B red dye was used for most of the infiltration tests to highlight the hydraulically active pathways. Methylene blue dye was used on two samples (D-2 and FT-2) but did not adequately highlight the fractures because it was readily absorbed by the soil. Methylene blue is a cationic dye, which forms cations upon hydrolysis. This cationic nature is the reason it is sorbed by the soil. Rhodamine B is not as reactive and is not sorbed by the soil as much. Because rhodamine B moves more closely with the wetting front, it was chosen as the permeant for the majority of the tests.

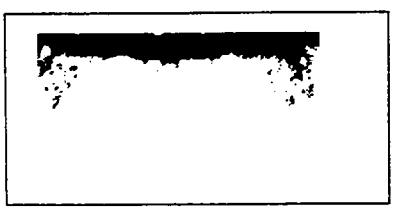
Influence of Clods on Infiltration

Benson and Daniel (1990) have shown how clod size can affect the hydraulic conductivity. The influence of clod size during infiltration should be even more dramatic. Three samples were compacted to investigate the role of clod size on infiltration (see Figure 4-5). Sample AD-3 was compacted with a large clod size, all of which were retained on the #4 sieve. The maximum clod size was about 1.3 cm. Sample AD-2 was compacted with a small clod size passing the #4 sieve, and sample AD-1 was compacted with a mixture of these two sizes. The mixed clod size provided the least pore space as reflected by the

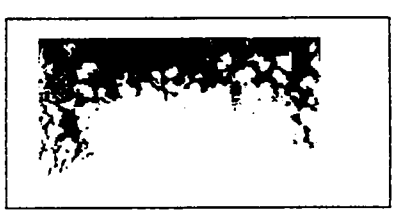




Mixed clod sizes provided the least pore space for preferential flow



A small clod size (< #4 sieve) gave intermediate preferential flow zones



A large clod size (> #4 sieve) led to significant preferential flow zones

Fig. 4-5. Clod size effects on infiltration

smallest infiltration rate and the shallowest dye penetration. The large clod size provided larger voids allowing increased infiltration and deeper penetration.

Closing of Fractures

As demonstrated before, fractures tend to close as the soil becomes saturated. The closing of fractures is one of the reasons the infiltration rate decreases with time. A ~5 cm head of water was applied to sample FT-6 for twenty minutes before the onset of infiltration to determine if the fractures would close. Upon first examination of the twelve cross-sections of the sample illustrated in Figure 4-6, it seems that the application of the water had no effect on infiltration of the red dye. However, more careful examination suggests that many of the fractures were closed during this time. The left and middle portion of all the cross-sections reveal dye stains very similar to uncracked samples with uniform wetting front and no preferential flow. Recall that a large horizontal fracture was noted in this sample after infiltration. Apparently, a large vertical crack on the right side of the cross-sections did not completely close and continued to feed this larger horizontal crack. This led to increased infiltration and deeper dye penetration. The process of "differential swelling" may be the reason some fractures will close and others remain open. Similarly, it could be argued that fractures smaller than a "critical aperture" will close upon saturation while apertures greater than this will remain open. Differential swelling can occur

Sample Info: Permeant - Rhodamine Red Dye
Size - 10.2 cm diameter; 5.1 cm thick
Soil - Compacted Kaolinite
Sample state - 3 freeze/thaw cycles

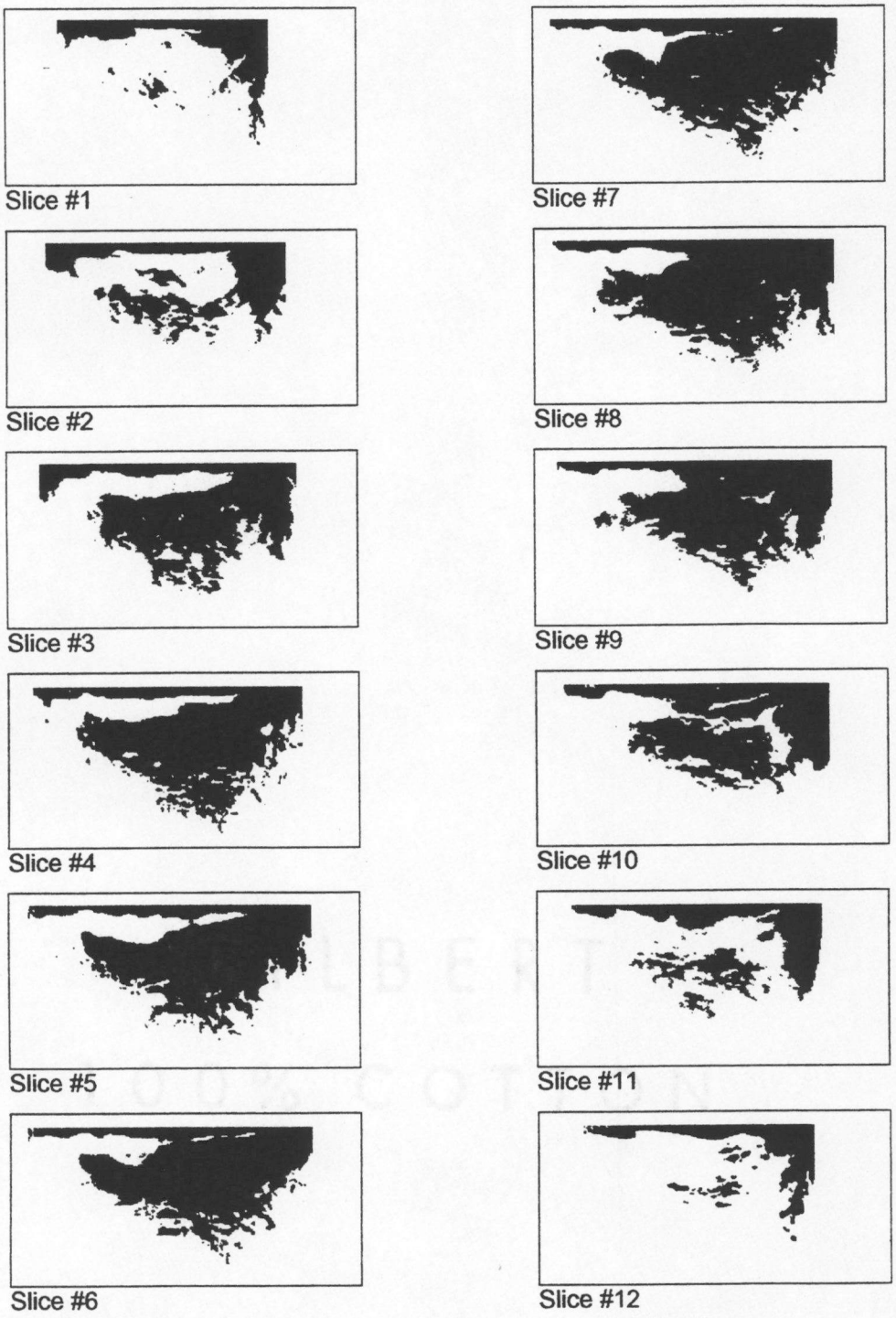


Fig. 4-6. Fracture stains: Sample FT-6

when some areas swell more than others leaving some fractures open. Differential swelling is far more critical for larger samples. This is why increases in hydraulic conductivity due to fractures are more likely for larger samples. Fractures close more completely in smaller samples.

PART 5

DEVELOPMENTAL STUDY IN USING ELECTRICAL RESISTIVITY TO PREDICT SUBSURFACE CRACKING

INTRODUCTION

Preferential flow paths can impair the effectiveness of clay liners in solid waste landfills. These pathways can allow rapid migration of contaminants into the subsurface where they may enter the groundwater. Such parameters as fracture aperture, spacing, orientation, and, most importantly, the inter-connectedness of fractures are important in determining the hydraulic behavior of the soil. However, determining these properties can be quite difficult. Several techniques are currently being developed to determine this information.

The use of geophysical surveys has increased greatly over the past several decades. One of the advantages geophysical methods have is that they are non-destructive. This is particularly important for investigating such sites as a solid waste landfills where destructive testing can damage the integrity of the landfill. One geophysical method that may prove very useful for determining the influence of fractures on the hydraulic conductivity is electrical resistivity surveys. Water, seeking the shortest route through a mass via interconnected fractures, is analogous to a current passing through the mass along the path of least resistance. Though several factors affect the electrical conductivity of earth materials, attempts were made to isolate the influence of fractures. Ideally, a new approach can eventually be developed using electrical resistivity surveys to determine the presence, magnitude, and interconnectedness of fractures in clay barriers.

THEORY OF ELECTRICAL RESISTIVITY SURVEYS

The usefulness of electrical methods depends on the fact that any subsurface variation in electrical conductivity alters the form of the current flow within the earth and this affects the distribution of electric potential. The degree to which this potential is affected depends on the size, shape, location, and electrical resistivity of the subsurface masses (Griffiths, 1965). It is therefore possible to gather information about the subsurface from electrical resistivity measurements at the surface. The resistivity of a material is simply a measure of the difficulty with which a current flows through it. Another useful term is electrical conductivity which is defined as the reciprocal of electrical resistivity.

The resistivity of a medium can best be understood by considering the following illustration. Consider a square element with four insulated sides and two sides with conductive end plates (See Figure 5-1). A battery is connected to

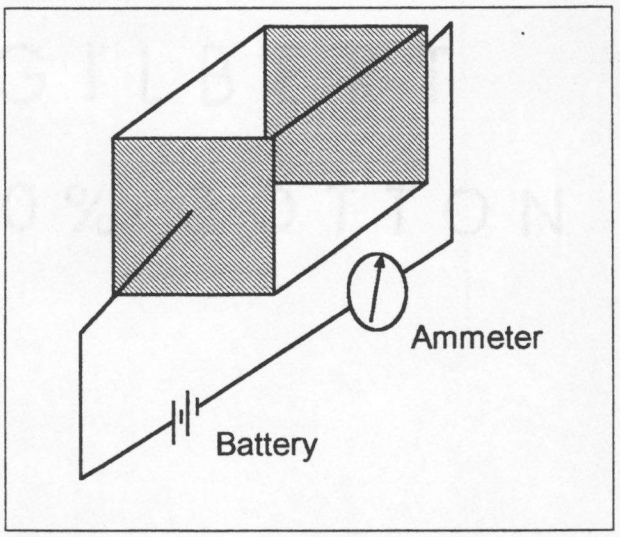


Fig. 5-1. Measuring Resistivity

the end plates through an ammeter to measure the current flow through the element. When a voltage is applied across the two plates, an electric field is established in the element. Positively charged ions are attracted to the negative plate and the negatively charged ions are attracted to the positive plate (McNeill, 1980). If the element is air, no current can flow between the two end plates and the ammeter will read zero. If the element is clay or rock, the ammeter will measure a current whose magnitude depends on the properties of the geologic medium. The measured resistance is proportional to the length between the two plates and is inversely proportional to their area according to the equation:

$$R = \frac{\rho L}{A} \qquad (5\text{-}1)$$

where R = resistance (ohms) - $R = \frac{V}{I}$

ρ = electrical resistivity (ohm-meters)

A = area (m^2)

L = length (m)

The constant of proportionality is called the electrical resistivity (ρ), which is a property of the medium and is independent of the plate dimensions. The electrical conductivity is the inverse of the electrical resistivity with units $\frac{\text{mhos}}{\text{meter}}$ (where mhos = $\frac{1}{\text{ohms}}$). Because the measured values are very low, it is often more convenient to express the conductivity in millimhos per meter.

THE ELECTRICAL RESISTIVITY OF EARTH MATERIALS

The passage of electricity through geologic materials takes place by way of the water contained in the pores and fissures, with the matrix being relatively non-conducting. Thus, electrical conduction in the majority of rocks is essentially electrolytic. An increase in the concentration of dissolved salts in the groundwater leads to a decrease in resistivity. Hence the resistivity of a formation generally depends on the resistivity of the contained electrolyte and is inversely related to the effective porosity and the degree of saturation. In crystalline rocks with low porosity, conduction takes place along cracks and fissures. In fact, unless the pore water is saline, the degree of fracturing is the most important factor controlling resistivity.

As far as soils are concerned, sand and silt particles are electrically neutral, whereas clay particles carry a negative charge. The conductivity of sand is essentially through the pore water. The sand grains serve to make the current path more tortuous thus reducing the conductivity. The situation for clay is a bit more complicated because the clay particles carry a negative charge. This means that cations are attracted to the surface of individual clay particles, and exchange can occur between different cations. The extent to which this occurs defines the cation exchange capacity (CEC) for the clay. This can be large in clays due to their large surface area, by which many ions may be supplied for

electrical conductivity. Therefore, a small amount of clay can substantially increase the electrical conductivity.

Resistivities can vary widely from formation to formation, but as a rule of thumb, the order of increasing resistivity is clay, sand and gravel, limestone, and crystalline rocks (depending of degree of fissuring). Figure 5-2 gives an approximate range of resistivities of soils and rocks (Griffiths, 1981).

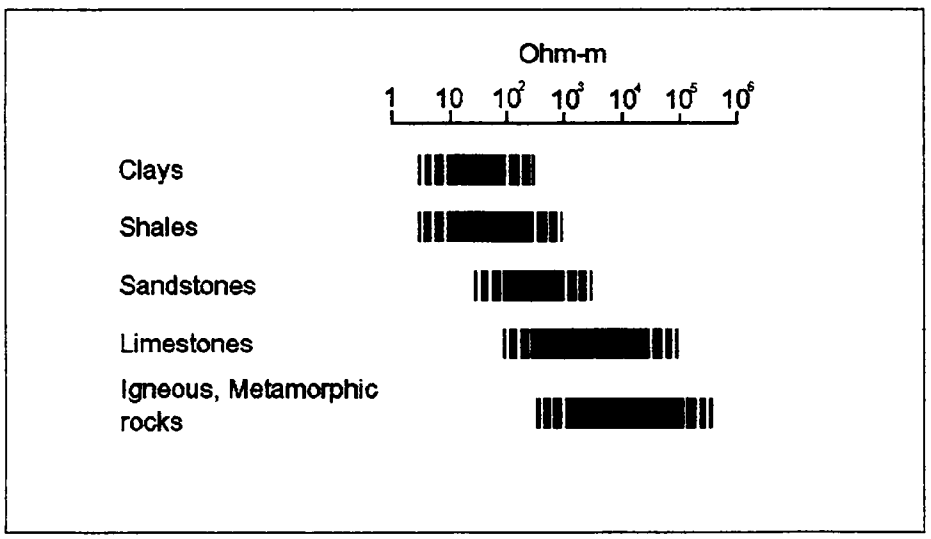


Fig. 5-2. The Electrical Resistivity of Earth Materials

McNeill (1980) gives five factors which affect the conductivity in soils and rocks:

(1) porosity; shape and size of pores, number, size and shape of interconnected passages

(2) the extent to which pores are filled by water (water content)

(3) the concentration of dissolved electrolytes in the pore water

(4) temperature and phase state of the pore water

(5) amount and composition of colloids

The water content plays a significant role in the resistivity of soils and rocks. Studies by McCollum and Logan (1930) and Higgs (1930) showed that at low water contents resistivity decreased rapidly with increasing water content. (see Figure 5-3). The rate of decrease reduces considerably at water contents in excess of 15%, and to a minimum for water contents in excess of 20%. The degree of saturation is also an important parameter. At a particular water content, an increase in the degree of saturation (or a decrease in the air-void ratio) will mean a decrease in resistivity (McCarter, 1984). In the field, these values can vary depending on the compactive effort. Resistivity measurements on the surface perhaps can estimate the soil's state.

The Effect of Fractures on Electrical Resistivity

As discussed before, the electrical conductivity of soils and rocks take place primarily through the pore water. In general, the presence of the soil grains tends to reduce the electrical conductivity. There are two reasons for this; first, electrical conductivity is proportional to the area available for current flow, which is reduced by the soil matrix, and second, electrical conductivity is inversely proportional to the length of the current path which is effectively increased by the soil. The current path becomes more tortuous and reduces the overall electrical

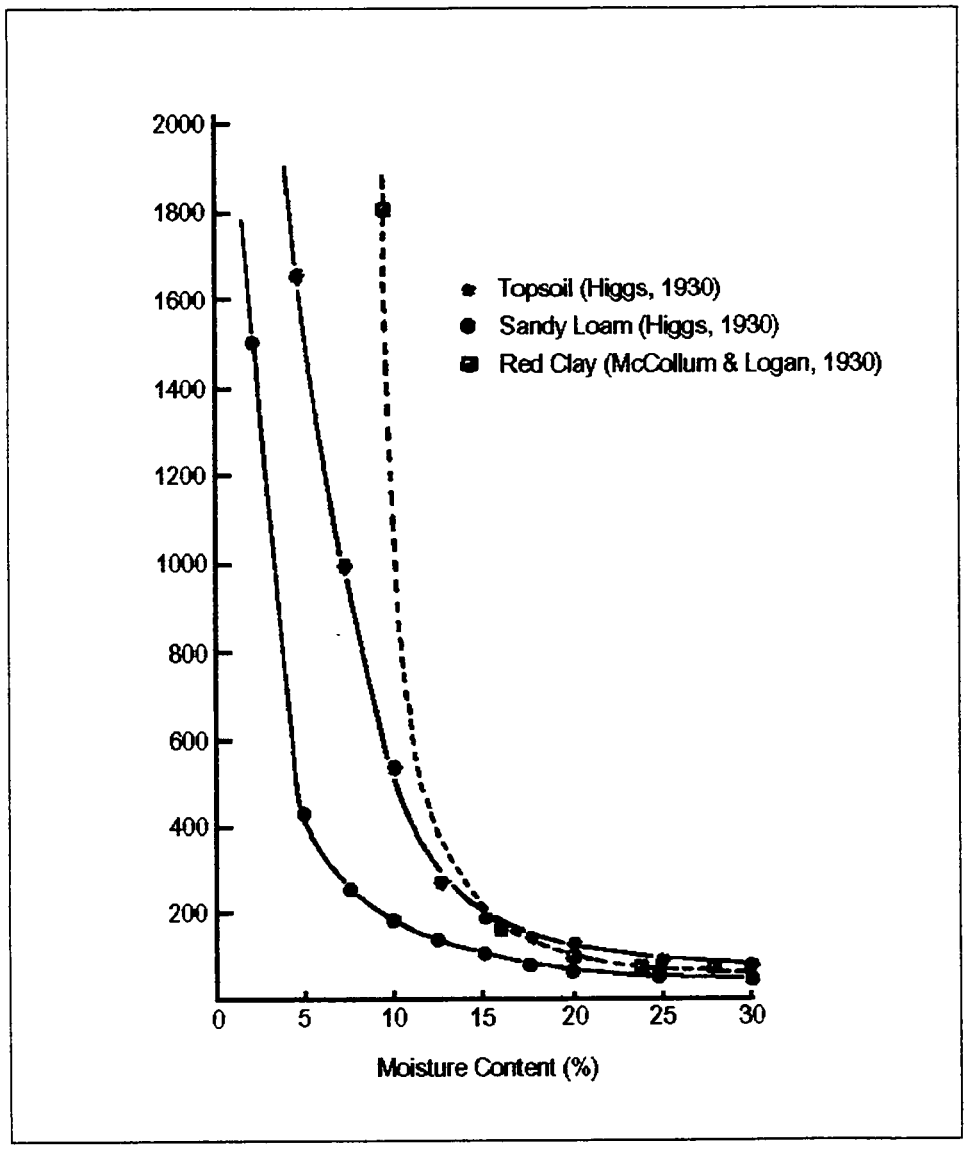


Fig. 5-3. Variation in Soil Resistivity with Moisture Content (McCarter, 1984)

conductivity. However, the presence of wet fractures can increase the electrical conductivity. Two reasons for this include:

1) the fractures provide more pore space for water to conduct electric current

2) the fractures can provide a less tortuous path through the sample

However, if the fractures are not filled with water, they can actually impede current flow. As indicated before, high resistivities can be expected for soils compacted with low water content and/or high air-filled porosity (Kalinski, 1994). Comparatively, soils compacted with less than optimum water content can have large air-filled porosities resulting in high hydraulic conductivity (Benson and Daniel, 1990). As for clay liners, high resistivity can also be indicative of a higher than desired sand or gravel content. In any event, field measurement of resistivity is a promising method for revealing areas of high fracture porosity.

Resistivity Studies in Compacted Clay Barriers

A number of investigations have been carried using electrical resistivity surveys to evaluate landfill structures (Klefstad et al., 1975; Carpenter et al., 1990; Kalinski and Kelly, 1994; and Carpenter et al., 1994). Each of these studies show great promise for the use electrical resistivity in determining landfill conditions. High resistivity measurements over a landfill is a potential indicator of subsurface preferential flow zones. As noted before, these preferential flow

zones can destroy the integrity of compacted clay barriers. Azimuthal resistivity surveys may also prove useful in evaluating preferred orientations or connectivity in subsurface fracture networks. Taylor and Fleming (1988) found a strong relationship between resistivity measurements and fracture geometry.

DESIGN OF A LABORATORY RESISTIVITY SURVEY

A laboratory resistivity test was designed to investigate its potential for detecting subsurface defects in clay. Resistivity in the field is typically performed with the four-probed Wenner electrode configuration, as illustrated in Figure 5-4. The Wenner array consists of four aligned, evenly spaced electrodes in which current in passes between the outer electrodes and the voltage drop is measured between the inner electrodes. If lateral variations in resistivity exist with the ground, a measurement from a given position of the array is designated as the apparent resistivity. The apparent resistivity equals the true resistivity as defined in equation 5-1 if the medium is infinitely homogeneous.

A special Wenner type array was designed and built to use for laboratory samples. The resistivity was calculated by dividing the measured voltage difference by the current times a factor for the geometry of the electrode configuration. For the Wenner configuration, the resistivity is given by:

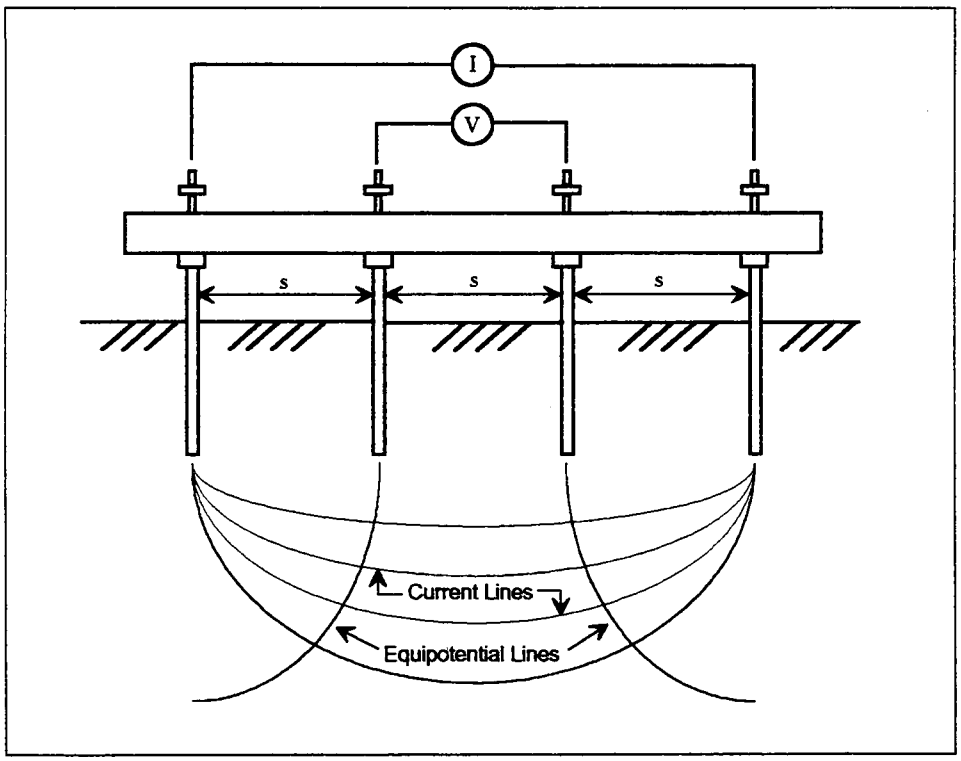


Fig. 5-4. Four-probed Wenner array

$$\rho = 2 \pi a \frac{V}{I} \qquad (5\text{-}2)$$

where a is the distance between electrodes, V is the potential difference, and I is the current (Todd, 1980). The array consisted of 48 electrodes evenly spaced 1 cm apart. The electrodes penetrated into the soil to a 1 cm depth. A control panel was built and wired to the array to allow easy measurement of resistivity. A kaolinite clay slurry was used for the investigation and was placed in 50 cm diameter lysimeter. The lysimeter provided no drainage and was simply used to hold a large clay sample. To simulate subsurface cracks, a 10 x 10 cm plate was inserted into the soil and locked into position. A copper plate was used to simulate "conductive" fractures, and a plexiglass plate was used to simulate "non-conductive" fractures. The electrode array was placed at various orientations with respect to the plates to investigate the utility of azimuthal resistivity surveys. Probes were placed on the control panel such that measurements were taken at every possible position from a spacing of 1 cm to 15 cm. Studies have shown that about 90% of the applied current flows through depths less than the electrode spacing (Kalinski and Kelly, 1994). Thus varying the spacing may determine properties at various depths. A schematic of the whole system is shown in Figure 5-5.

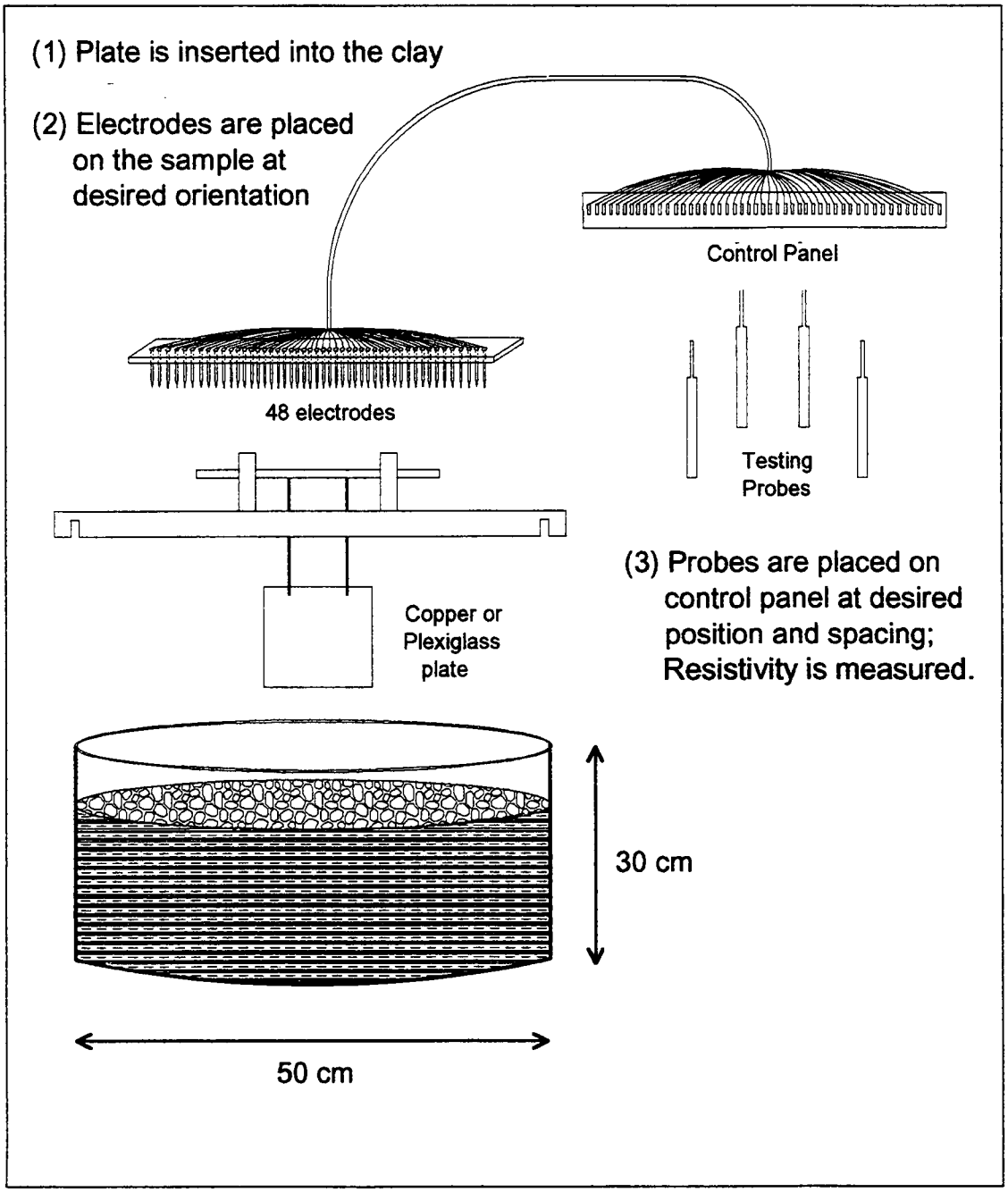


Fig. 5-5. Design of Electrical Resistivity Test

Resistivity Test Results

Although a full evaluation of the test results was incomplete as of this writing, preliminary results were promising for the resistivity method. The presence of the copper and plexiglass plates were detected as areas of low and high resistivity, respectively. Measurements without either of the plates showed a relatively homogeneous material. It is yet to be determined if azimuthal measurements were useful in determining the orientation of the plates. In any event, the use of electrical resistivity surveys may prove very informative in locating and characterizing subsurface cracking in and beneath landfills.

A similar type testing apparatus was constructed for use on small laboratory compacted clay samples. The unit consisted of four equally spaced electrodes along four different orientations. A similar control panel was wired to the electrodes for easy application. Although testing using this device has not begun as of this writing, hopefully it will prove useful in detecting fractures in compacted clay on small scale laboratory samples. Many thanks are extended to Dr. Richard Williams and John Hanson of the Department of Geology at the University of Tennessee for their input and assistance with the electrical resistivity experiment.

PART 6

SUMMARY

INTRODUCTION

Compacted clay barriers are used in solid waste landfills to isolate the waste from infiltrating water and to minimize the flow of leachate from the waste. The effectiveness of these barriers depends on their ability to limit the movement of these contaminants. The saturated hydraulic conductivity (K_s) of the clay is used to quantify this. The hydraulic conductivity is given by Darcy's Law which describes the rate water flows through soil. The U.S. Environmental Protection Agency (EPA) requires liner material to achieve a K_s of less than $1x10^{-7}$ cm/sec (EPA, 1989). Many factors affect the hydraulic conductivity such as compactive effort and water content. However, the development of preferential flow paths may be of greater importance especially in considering the long term integrity of a compacted clay liner.

Preferential flow paths can allow contaminants to migrate and spread rapidly, sometimes referred to as "short-circuiting." Bouma and Dekker (1978) define "short-circuiting" as the "rapid downward movement of water through initially air-filled large, vertical pores, thereby bypassing dry or moist soil inside peds." This water can carry contaminants during dry periods in which there is little adsorption to the soil resulting pollution of the groundwater. Although clay compacted wet of optimum can initially serve well as a barrier to contaminant transport, it is also susceptible to post compaction structure changes that can alter the integrity of the liner. Kleppe (1981) showed that high plasticity clays

placed wet of optimum have the highest potential to crack due to the high shrink-swell characteristics. It has generally been assumed that covering or burying these liners will prevent these cracks from developing. The rationale for this is that the liner will be protected from atmospheric attack and that the overburden pressures will tend to keep cracks from opening at depth. However, Corser and Cranston (1991) have shown that desiccation can occur even with a protective soil cover and/or geomembrane. The liner section with a HDPE (high density polyethylene) cover and vegetative soil cover performed the best regarding desiccation. The section with only the vegetative cover was found to crack significantly over the course of a summer. This suggests that simply burying a liner does not necessarily protect it from desiccation.

Saturated hydraulic conductivity is the parameter used to judge the quality and integrity of compacted clay liners. Hydraulic conductivity is given by Darcy's law, which was originally applied for saturated flow only, but was extended by Richards (1931) to unsaturated flow. Hydraulic conductivity is typically a maximum at saturation so that the saturated hydraulic conductivity is generally believed to be a conservative parameter for barrier evaluation. This would be true of course except that the formation and closure of fractures in clay media is highly dynamic. Preferential flow paths tend to open during unsaturated conditions and close following saturation. There have been numerous studies that show an increase in saturated hydraulic conductivity due to the presence of preferential flow paths. Bowders et al. (1994) report an increase in hydraulic

conductivity after the development of fractures due to freeze/thaw cycles. However, the measured increase was not as great as expected given the observed severity of the cracks. They comment, "given the appearance of the specimens one might have anticipated much larger increases in permeability than were measured." The most likely reason for this is that cracks begin to close upon permeation, and were likely closed by the time K_s was determined. Bowders et al. (1994) also report that as the effective confining stress increased, the ratios of permeability after freeze/thaw to that before decreased . This suggests that the confining stress plays a large role in the degree to which the fractures will close. At higher confining stresses, the fractures close more completely resulting in a lower impact on the saturated hydraulic conductivity.

Anderson and Bouma (1973) showed that very small variations in pore size have a significant impact on the amount of water that can be conducted at a given hydraulic gradient. Shrinking and swelling of clays can contribute greatly to this variation in pore size. Although there are many studies that show an increase in hydraulic conductivity due to preferential flow, they still do not fully capture the impact of these flow paths. The pathways contribute most at the initiation of saturation, but before crack closure. The saturated hydraulic conductivity at best underestimates the role of these pathways during transport.

Preferential flow paths may develop in compacted clay barriers through a number of different mechanisms. Some of these include damage incurred by chemical attack from retained fluids, fractures developed due to differential

settlement, macropores caused by plant roots and animals, desiccation, and freeze/thaw cycles. The size of clods used for compaction can also lead to preferential flow zones. Flow between poorly bonded lifts of a compacted liner provides further means of preferential transport. Preferential flow paths through any of these processes can impair the ability of a liner to prevent the migration of contaminants into the subsurface.

Of particular interest here are the processes of desiccation and freeze/thaw. Desiccation cracking can occur when soil is exposed to drying resulting in shrinkage. The tensile stresses that cause cracking are produced by negative pore water pressures that develop as water evaporates from the soil. These negative pore water pressures lead to an increase in effective stress resulting in a volume reduction. As a result, cracking occurs to accommodate this shrinkage. When water is added, hydration of the clay particles begins closing the cracks. However, significant preferential flow may occur through these cracks before complete closure is obtained. Cracking resulting from freeze/thaw cycles can also lead to significant preferential flow paths. The freezing of soil is accompanied by the formation of ice crystals or lenses. The volume of a soil can increase about 10% due to the volumetric expansion of water upon freezing (Holtz & Kovacs, 1981). Thermodynamic processes produce hydraulic gradients as more water migrates to these lenses. These lenses can range from a millimeter to several centimeters in thickness (Holtz & Kovacs,

1981). When these lenses melt, a void or preferential flow path is left through which contaminants may travel.

OBJECTIVES

This paper describes a laboratory investigation of the development of hydraulic defects and preferential flow paths in clay, and their resulting influence on the flow of water. Our objective in this research was three-fold:

(1) Examine the initiation and development of preferential flow paths after a series of desiccation and freeze/thaw cycles

(2) Investigate the response of clay fractures during a series of flow tests.

(3) Capture preferential flow before the fractures close from swelling during unsaturated infiltration tests.

MATERIALS AND METHODS

A kaolinite was utilized in all of the tests, which was produced by the J.M. Huber Corporation under the trade name Barden AG-1. Pertinent material properties are given by Phifer (1994).

Crack Development Tests

Samples were subjected to cycles of desiccation or freeze/thaw to investigate the formation of preferential flow paths. Samples were prepared at optimum +3 water content and compacted to standard proctor energy. Desiccated samples were compacted in 15.2 cm diameter PVC molds with a thickness of 5.1 cm. Freeze/thaw samples were compacted in 10.2 cm diameter PVC molds with a thickness of 5.1 cm. Each 24 hour desiccation cycle consisted of 12 hours under a heat lamp and 12 hours saturating in a water bath. The temperature under the heat lamp averaged about 150° F. Each 24 hour freeze/thaw cycle consisted of 12 hours of three-dimensional freezing and 12 hours of thawing. Othman et al. (1994) concluded that three-dimensional freezing, as used for these samples, gives similar results as one-dimensional freezing.

Flow Tests

The kaolinite was mixed to the desired water content in 0.5 cubic yard concrete mixer until the slurry was smooth and uniform. The slurry was then spread into a 30 cm x 60 cm pan lined with wax paper to a uniform thickness of about 3.2 cm. The pan was then placed in an oven at a specific temperature until significant desiccation occurred (Figure 6-1 (a)). The specimens were retrieved by cutting out a portion of the sample using a steel cylinder with a beveled edge much like a cookie cutter (Figure 6-2 (b)). Because the sample was fairly moist,

a good cohesion was established with the wall of the cylinder. Experiments on uncracked sections indicated that side-wall leakage was negligible.

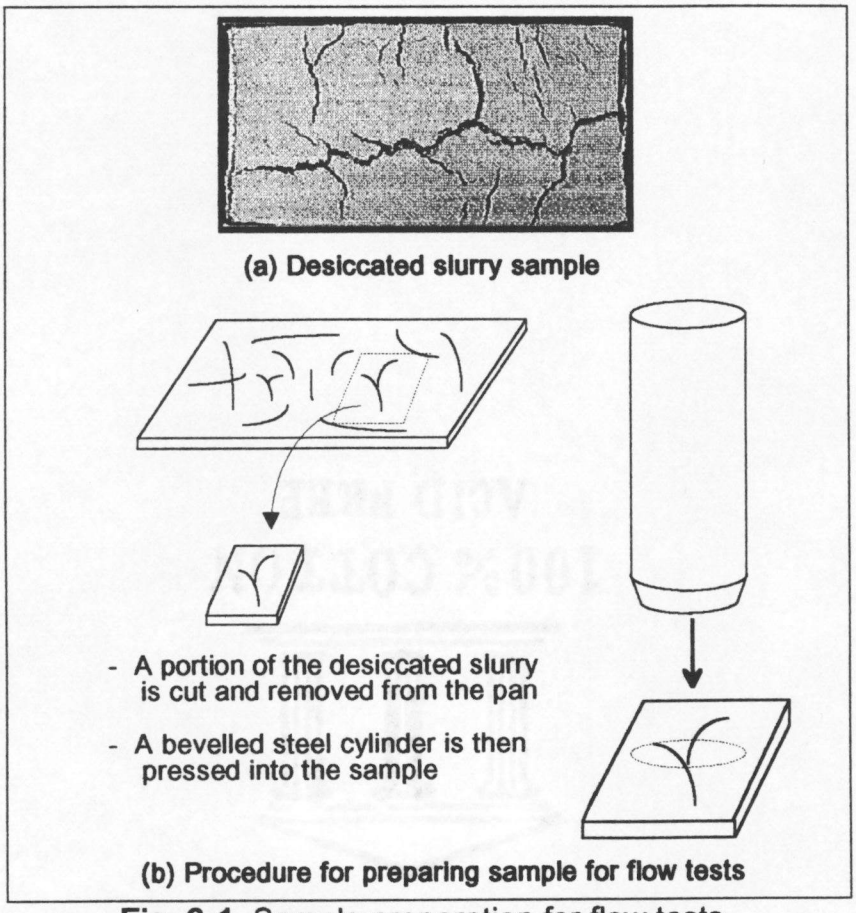


Fig. 6-1. Sample preparation for flow tests

A flow pump was used to supply water to the sample at a constant flow rate. The system, illustrated in Figure 6-2, eventually reaches a point at which the fracture network is unable to conduct flow at the rate at which water is being applied. This can occur immediately or with time as the fractures close depending on the flow rate and the fracture system. At this point, the system will begin to "back up" and the height of water on the sample increases. A floating

depth meter was used to measure the depth of water at any given time on the sample. The water can rise to the top of the cylinder where additional water will be diverted such that constant head conditions can be maintained. An electronic scale was used to measure the outflow.

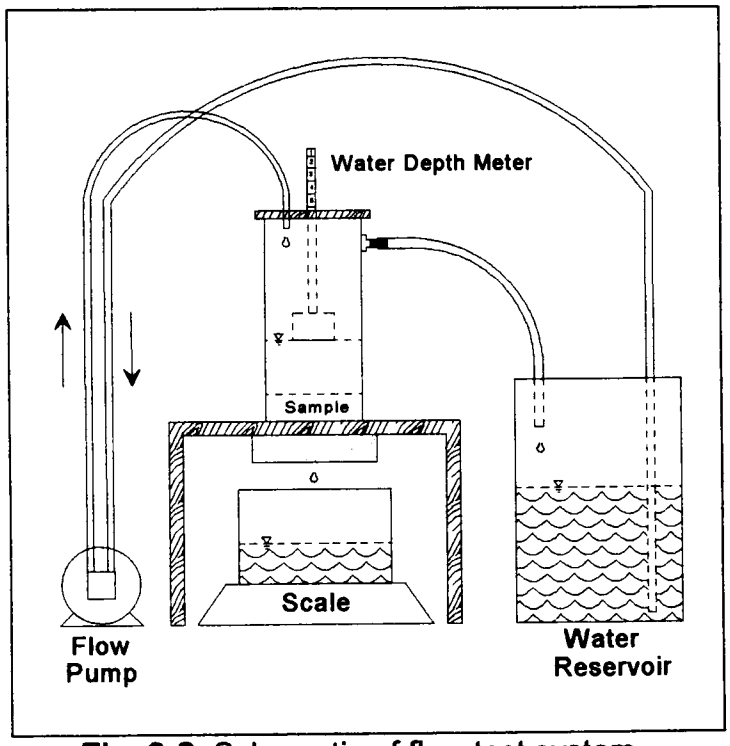


Fig. 6-2. Schematic of flow test system

An apparent conductivity was defined from these flow tests. The term 'apparent' is used to distinguish this conductivity from that obtained in a true Darcy experiment. The apparent conductivity was defined for three cases: rising head, constant head, and falling head (Figure 6-3). Due to the short time intervals, an approximate solution was used for the rising and falling head conditions for simplicity and consistency.

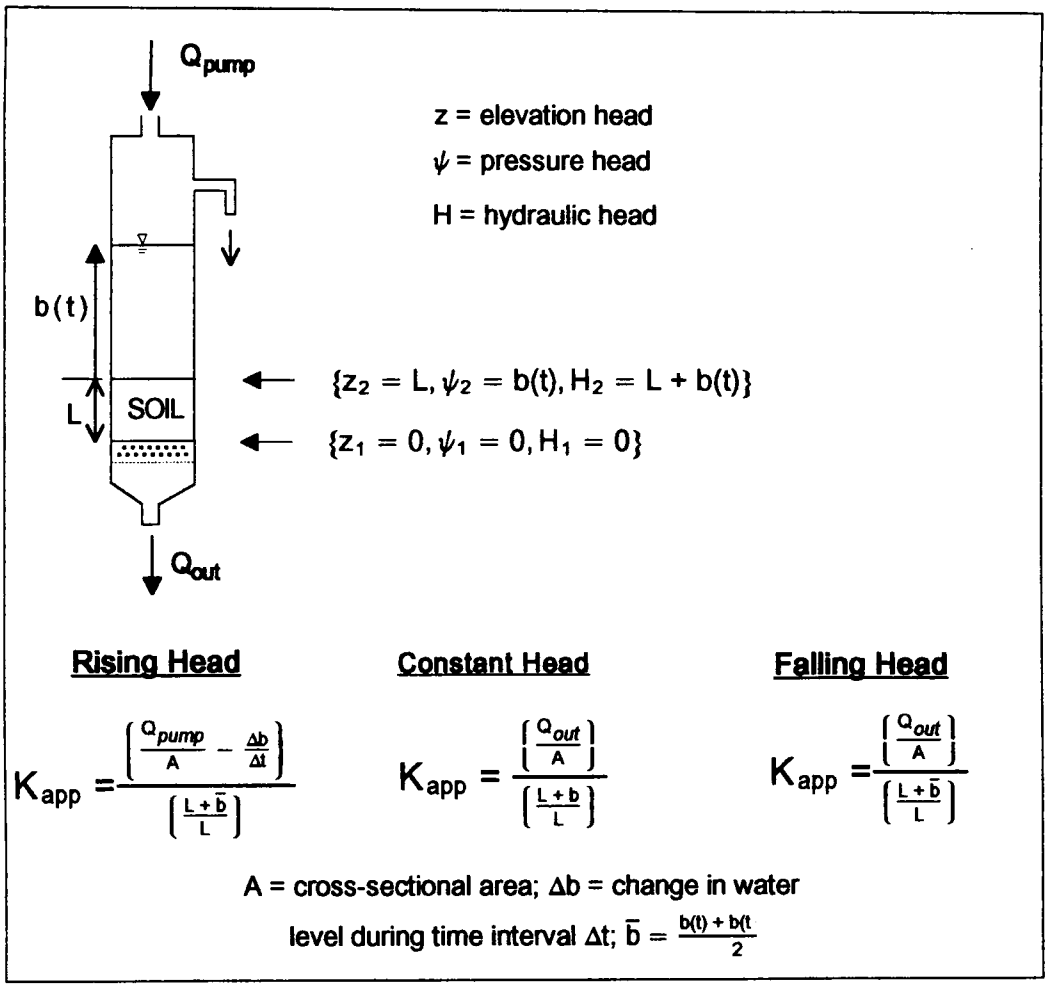


Fig. 6-3. Apparent Conductivity

Infiltration Tests

A series of infiltration tests were performed to investigate the significance of initially unsaturated conditions on infiltration from a surface pond (Figure 6-4). Samples were compacted in 10.2 cm diameter PVC molds, extracted, and subjected to cycles of desiccation or freeze/thaw. The soil was mixed at optimum +3 water content and compacted to standard proctor energy. A Mariotte device was set up to apply a constant head of about 5 cm on the sample. An electronic

scale was used to measure the amount of permeant lost from the reservoir, or the amount infiltrated into the sample. The reservoir was filled with 0.1% Rhodamine B red dye solution. After infiltration, when the sample was dry and strong enough, the sample was sliced into twelve approximately equal slices to expose the stains left by the dye. Digital images of these slices were taken to evaluate these stained pathways.

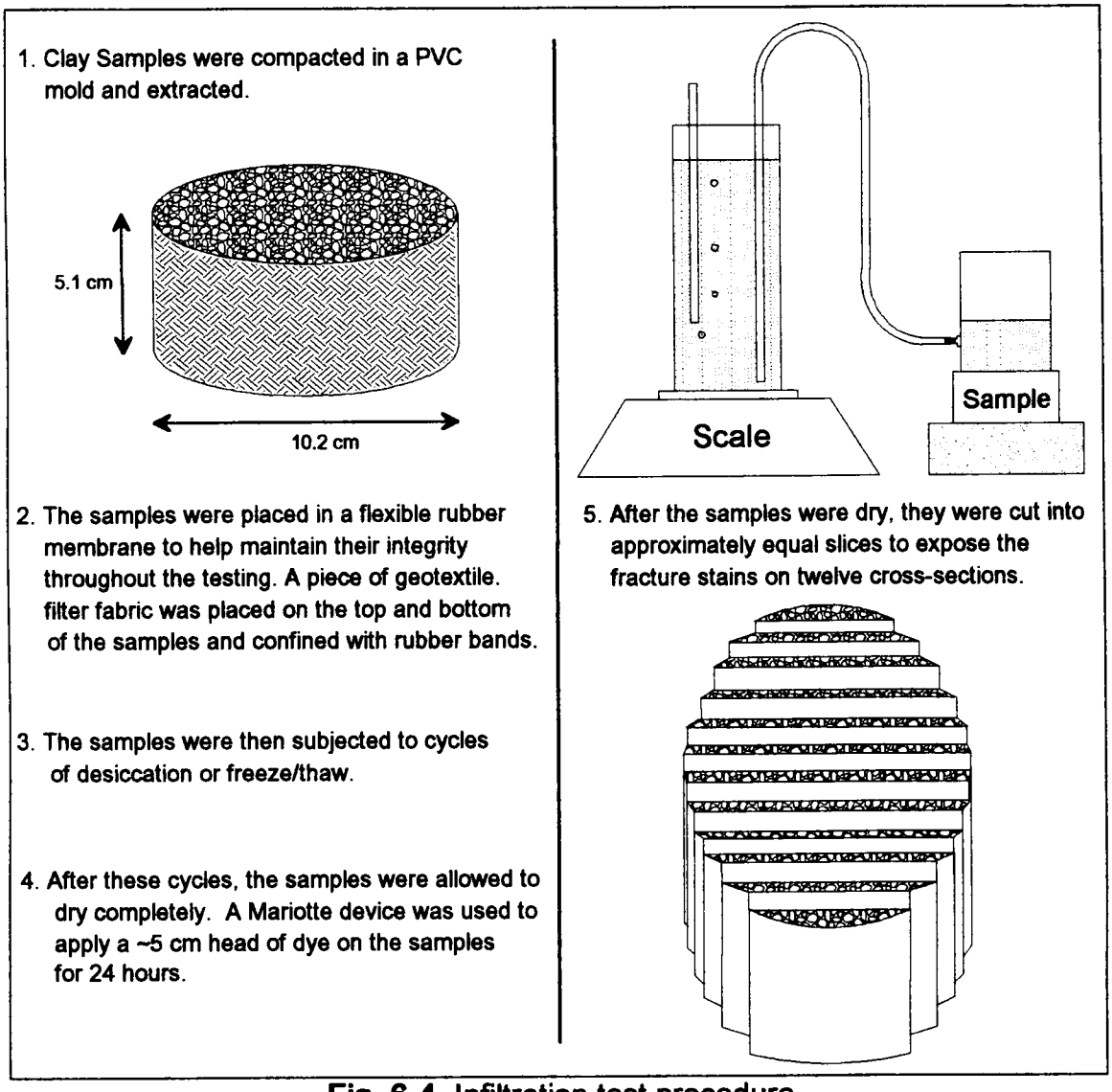


Fig. 6-4. Infiltration test procedure

RESULTS AND DISCUSSION

Crack Development Tests

Images of the surface of typical samples subjected to cycles of desiccation and freeze/thaw are shown in Figure 6-5. Both samples were compacted with a clod size passing the #4 sieve, and experienced extensive cracking due to these cycles. The most significant characteristic for the desiccated sample was the healing of the cracks after saturation. As the sample absorbed more water and increased in volume, the interior cracks and perimeter voids closed. These same cracks opened up again to greater lengths and wider apertures during the next cycle. New cracks were also created during succeeding cycles. It is reasonable to conclude that more energy is necessary to create a crack than it is to open a previously existing one. For this reason, the first cycle of desiccation is the most important to the structure of a clay soil. As for freeze/thaw, the most significant change in the sample also occurred after the first cycle. Othman et al. (1994) support this when they stated, "the network of cracks formed during the first cycle of freeze-thaw causes the greatest change in a soil's fabric." The surface of the sample appeared as if it had been sliced with a sharp object. The formation of ice lenses in the sample was concluded to be the cause. As these lenses melted during the thaw cycle, a fracture or preferential flow path was left. With respect to clay barriers, it is very important to protect them from desiccation and freeze/thaw, or any other process leading to cracking, during and immediately after construction. If they become damaged during

construction, or early in their design life, it will be increasingly more difficult to maintain their function.

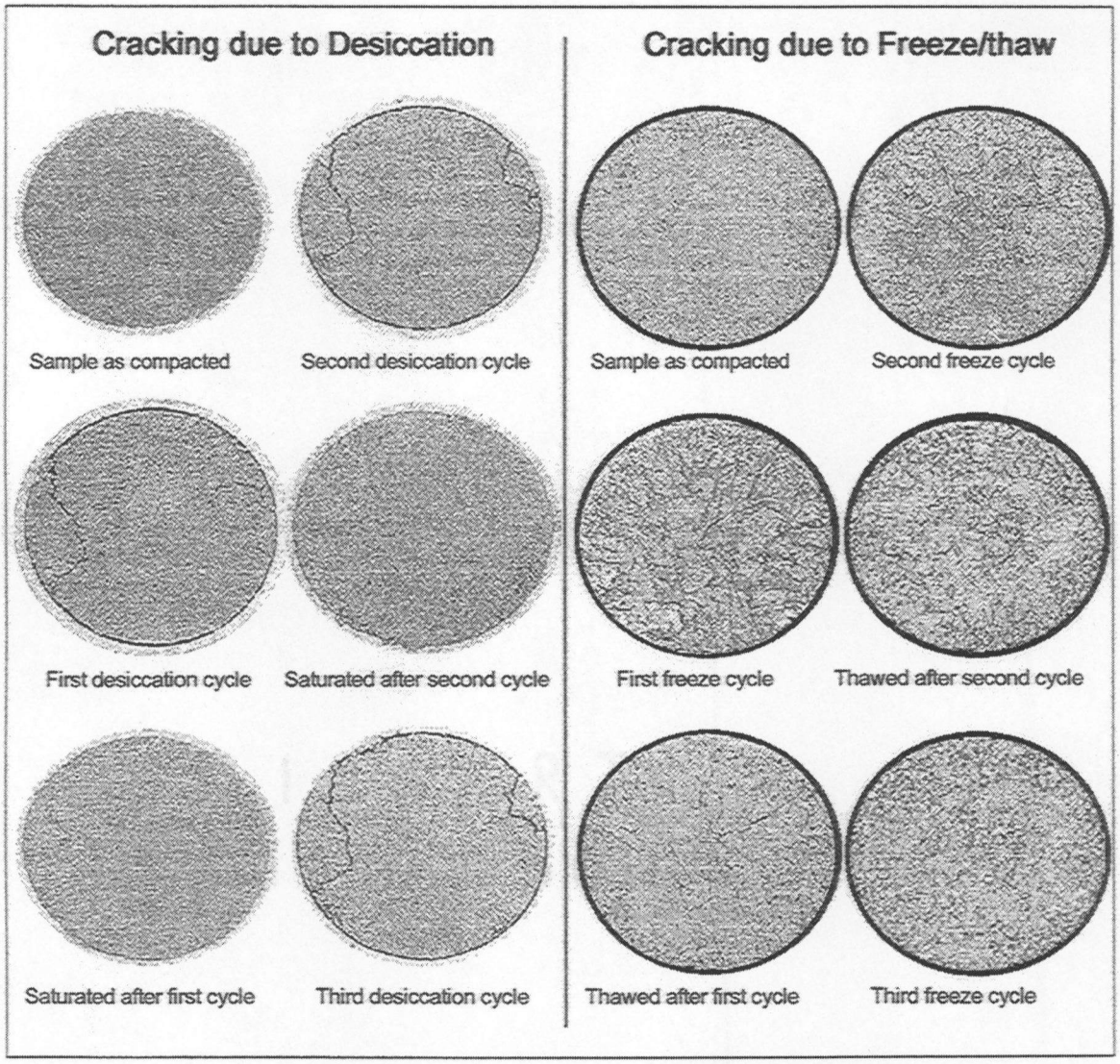


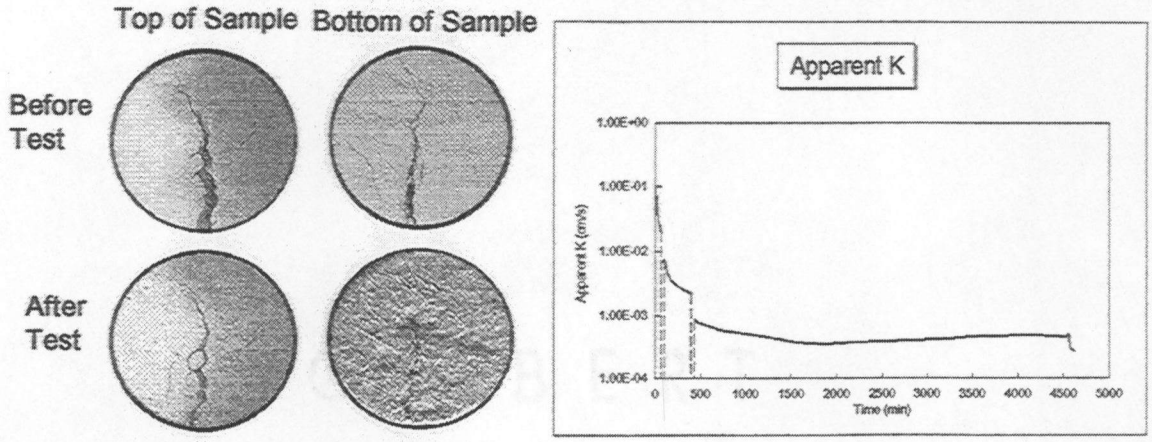
Fig. 6-5. Cracking due to desiccation and freeze/thaw

Flow Tests

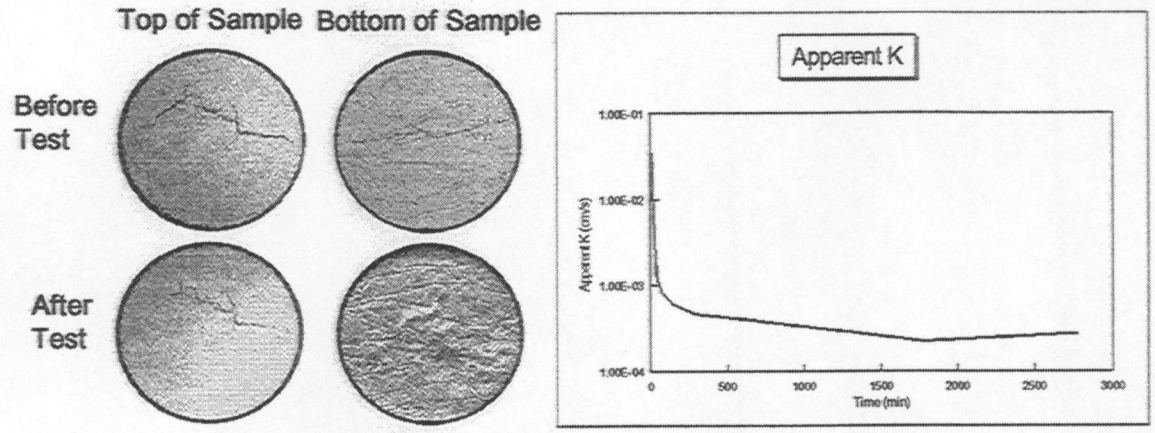
As discussed before, fractures tend to close as the soil expands due to water being absorbed into the matrix. A testing plan was formulated to evaluate the response of fractures in partially saturated clay after the application of water. In all of the flow tests, a general decease in measured apparent conductivity with time was found (Figure 6-6). Images of the samples before and after the tests showed the closing of the fractures, which likely led to the decrease in apparent conductivity. The apparent conductivity decreased rapidly during the early stages of the test and slowly reached a steady value. The decrease in each of these examples was almost three orders of magnitude, and is likely related to swelling of the clay as more water was absorbed into the matrix. The sample responds to this swelling by expanding in directions of least resistance. For fractured media, the clay can heave, or expand upward, or it can expand inward closing the fracture void space. As this void space diminishes, the conductivity decreases. This was reflected by a measured decrease in the apparent conductivity. Also, larger fracture void spaces allowed increased flow and led to larger apparent conductivities.

In these flow tests, the fractures were relatively large and rarely closed completely upon saturation. There probably exists a critical aperture of fractures below which the fracture will close, and above which will remain open. Also, larger samples are more susceptible to "differential swelling" in which some

(a) Sample 5-4



(b) Sample 5-5



(c) Sample 8-2

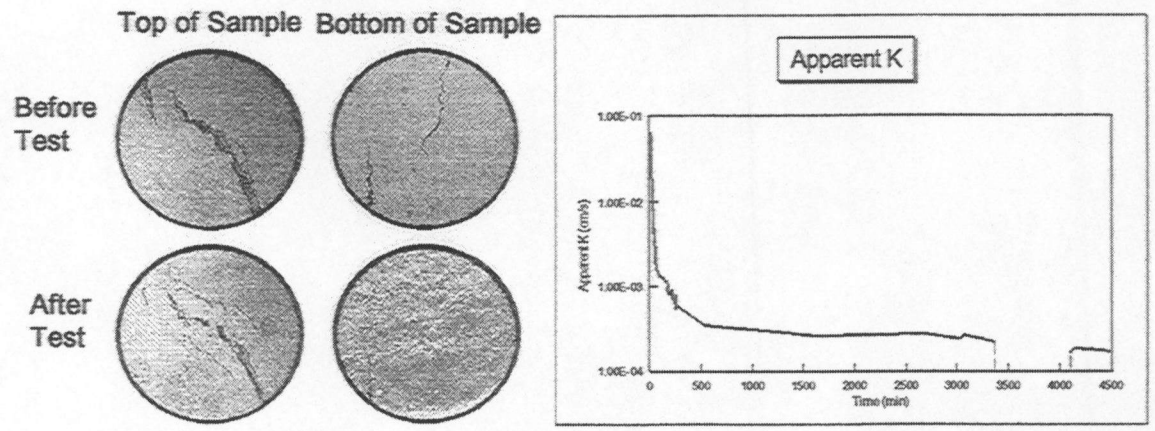


Fig. 6-6. Flow test results

areas may swell more than others leaving some fractures open. This is one reason why field measurements of hydraulic conductivity are generally higher than laboratory measurements. Smaller laboratory samples swell more uniformly, thereby closing open fractures leading to a lower hydraulic conductivity.

In all the flow tests, healing of the fractures led to decreased values of apparent conductivity. However, the rate and manner in which these fractures closed was in large part dependent upon the magnitude of the head of water applied and the degree of saturation of the clay matrix. Flow interruptions were used to examine these effects. A flow interruption simply involved shutting off the pump and allowing the water to drain through the sample. The pump was then turned back on and measurements made. These flow interruptions are denoted by a break in the apparent conductivity curve in Figure 6-7. From these flow interruptions, a theory was developed, which suggests that the rate of fracture closure may be dependent upon the head.

Near the beginning of the test, apparent K was unaffected by these flow interruptions. In this case, the sample was only partially saturated and the applied heads were relatively small. Although there was swelling at this point, it was largely unimpeded by the developing head. The largest impact of head on apparent K was experienced at intermediate times. The apparent K dropped typically one half an order of magnitude after the flow interruption. This suggests

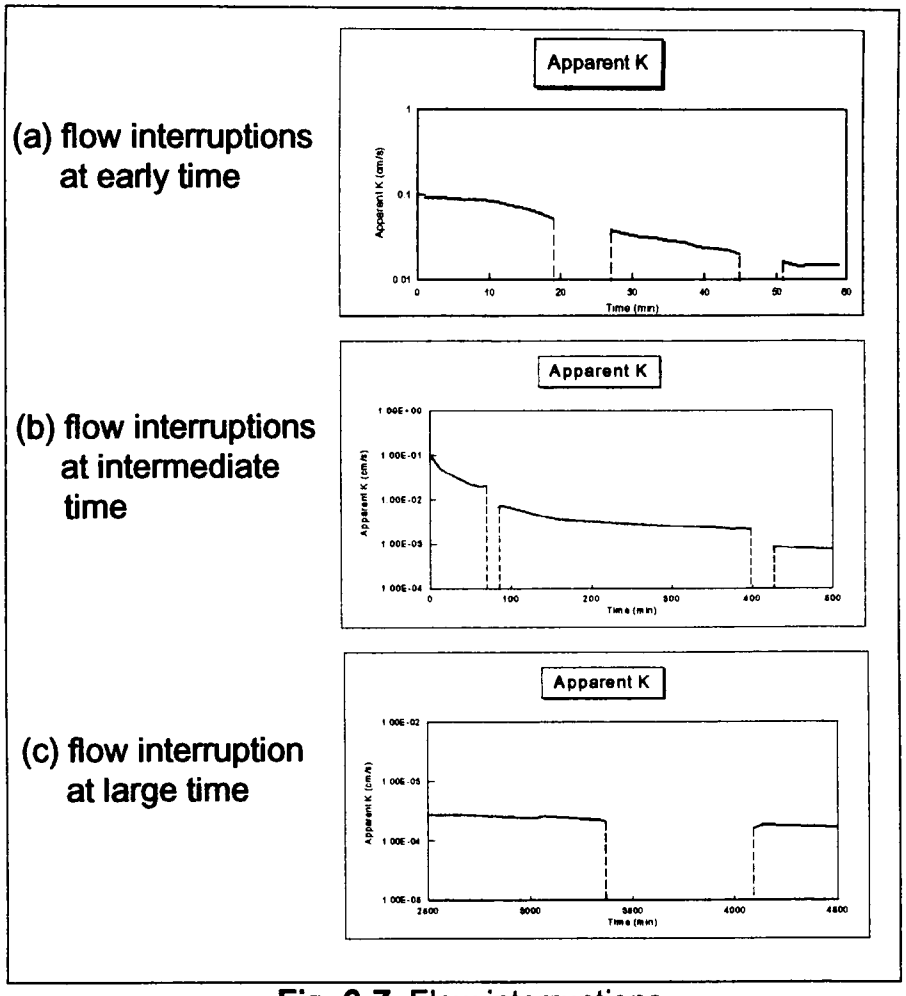


Fig. 6-7. Flow interruptions

that the applied head before the flow interruption was actually serving to keep the fracture open. At this point, the sample was not fully saturated and the effective stress on the outside of the fracture is greater than that in the matrix. Capillary forces exist in the dry matrix drawing water into the soil. The higher the column of water on the sample, the higher these forces are and the quicker water infiltrates into the matrix. It is this water pressure gradient that resists the forces developed by the swelling of the clay. When this pressure gradient is

removed during the flow interruption, the swelling forces which tend to close the fracture are unimpeded, resulting in a smaller fracture. As the flow test resumes, the calculated apparent conductivity jumps to a lower value, reflecting the smaller fracture volume. At large times, the sample was saturated and the effective stress was constant across the fracture. This suggests that the head applied to the sample should no longer affect the dynamics of the fracture. The measured apparent conductivity was relatively unaffected by the flow interruption at these larger times. The condition of the soil during each of these three phases are summarized in Figure 6-8.

This behavior is very important especially with regard to contaminant transport through a dry fractured clay. The flow interruptions presented here suggest that increasing head can lead to increased "short-circuiting" by combating the developing swelling pressures and keeping the fracture open. It should be recognized that the swelling pressure will eventually prevail as the matrix becomes saturated. This head pressure does not impact the degree and magnitude to which a fracture will close, but only the rate at which will close. The geometry of the fracture and the swelling potential of the matrix will ultimately determine the magnitude of closure. The importance of this head pressure lies in the increased flow of water (or contaminants) during the interim phase. The effect of this head pressure reinforces the common design philosophy whereby barriers are constructed with slopes to minimize the head build up.

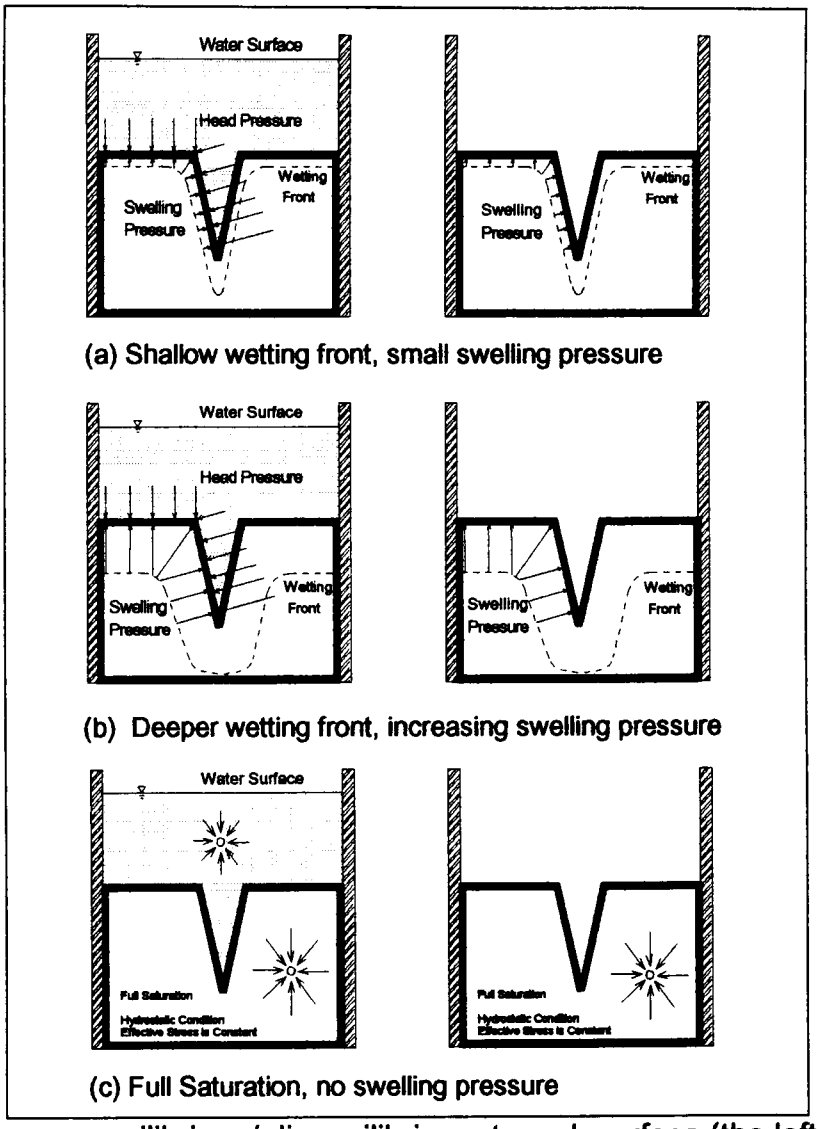


Fig. 6-8. Pressure equilibrium / disequilibrium at crack surface (the left column shows water head on the sample; the right column shows the sample response when head is removed)

Infiltration Tests

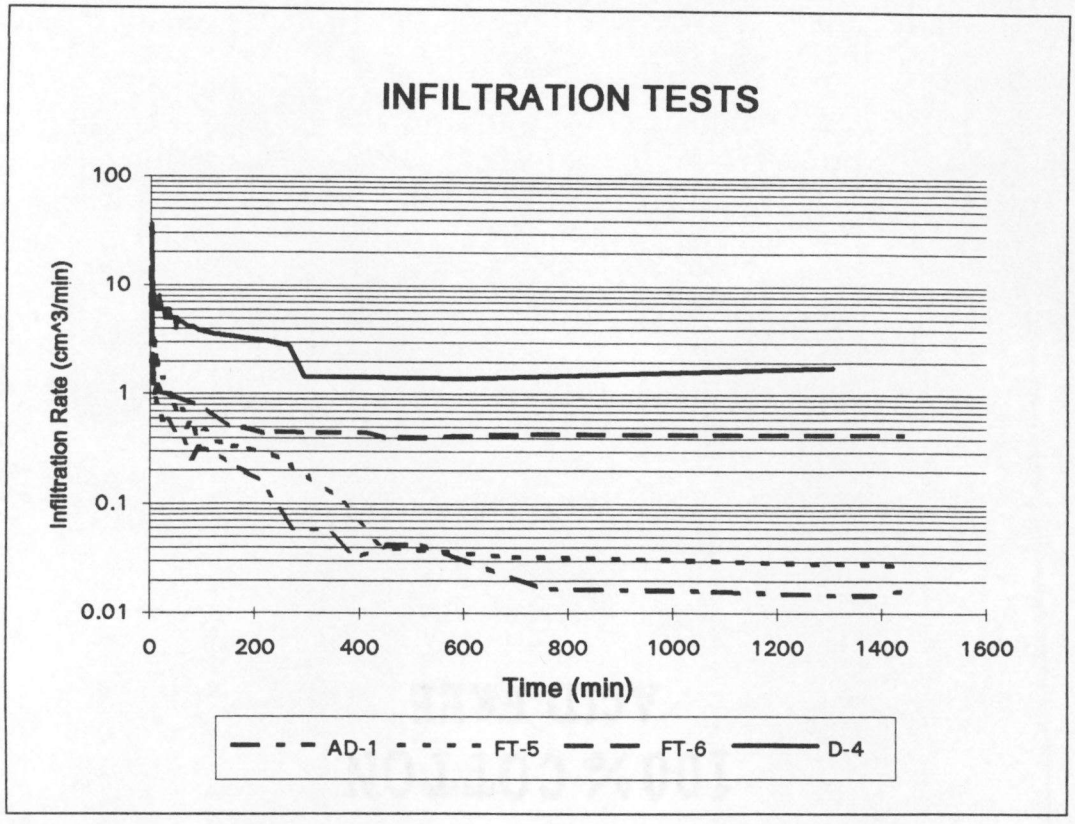
The true importance of preferential flow paths in fractured clay should be more fully captured during unsaturated infiltration. Infiltration is simply the entry of water into the soil surface. Matric potential gradients (negative water pressure

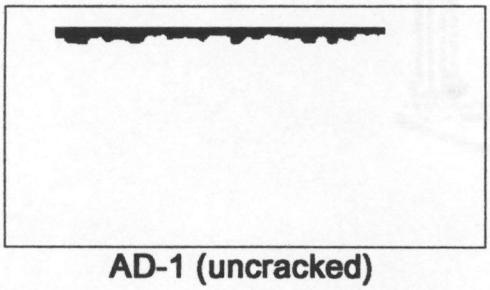
gradients) control infiltration during early stages and gradually dissipate with time. The decreasing influence of the matric potential gradient as the wetting front deepens results in a decrease in the infiltration rate. Soil swelling and closing of any pore spaces can also contribute to this decrease. As more water infiltrates, the water content, pressure head, and hydraulic head increase while the hydraulic gradient decreases. The decrease in hydraulic gradient is not fully offset by the increase in hydraulic conductivity from the rising pressure head. The infiltration rate begins to decrease at a critical combination of these factors (Freeze and Cherry, 1979). The flow of water in a fracture can greatly increase the surface area available for infiltration into the soil matrix. In this way, the infiltration capacity of a soil can increase significantly with the presence of preferential flow paths. These processes also may not be adequately described by Darcy's Law since the hydraulic properties of a typical soil are not homogeneous over some representative cross-sectional area. Water fluxes can vary significantly over small distances, and the hydraulic gradient may not be properly defined for the soil due to turbulence in the preferential flow paths. Swelling may ultimately close some of the preferential flow paths forcing water to flow through the matrix and restoring the integrity of a clay barrier. In any event, although preferential flow paths may make up only a small portion of the total soil voids, they can dominate vertical flow during infiltration.

Recall that often no significant differences in traditional saturated hydraulic conductivity have been found due to fractures on small laboratory

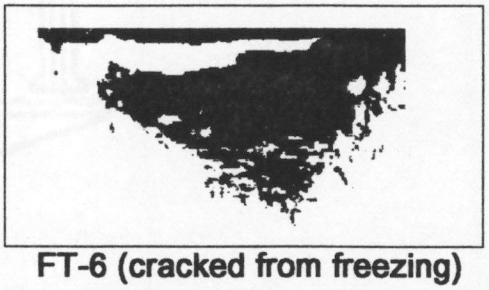
samples. It was suggested that these pathways were more hydraulically active during the dynamic stage of infiltration during which fractures are closing. The infiltration tests described here were performed on similar samples to verify or nullify this assumption. These tests proved that fractures are indeed very important during transient infiltration. Not only do the presence of fractures cause an increase in infiltration rate, they also generate great variability in infiltration (Figure 6-9). The uncracked sample showed the lowest infiltration rate as well as the shallowest penetration of the dye. The three samples that were cracked showed higher infiltration rates as well as deeper penetration of the dye. These fractured samples exhibited large variability due to differences in the fracture network. Sample D-4 contained a significant fracture that penetrated completely through the sample. As a result, the measured infiltration rate was the highest and the dye penetration was the most vast of all the samples tested. Sample FT-6 had a horizontal fracture across the sample as indicated by the dye staining pattern. This pathway allowed additional infiltration into the sample as reflected by the measured infiltration rate. Sample FT-5 contained only small surface cracks as indicated by the dye pattern and the infiltration rate. The processes of desiccation and freeze/thaw can lead to significant pathways for water.

Benson and Daniel (1990) have shown how clod size can affect the hydraulic conductivity. The influence of clod size during infiltration should be even more dramatic. Three samples were compacted to investigate the role of

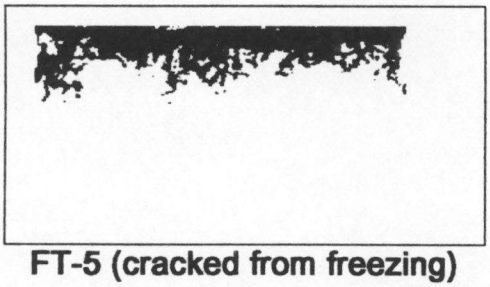




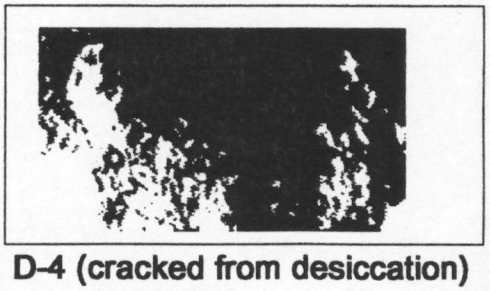
AD-1 (uncracked)



FT-6 (cracked from freezing)



FT-5 (cracked from freezing)

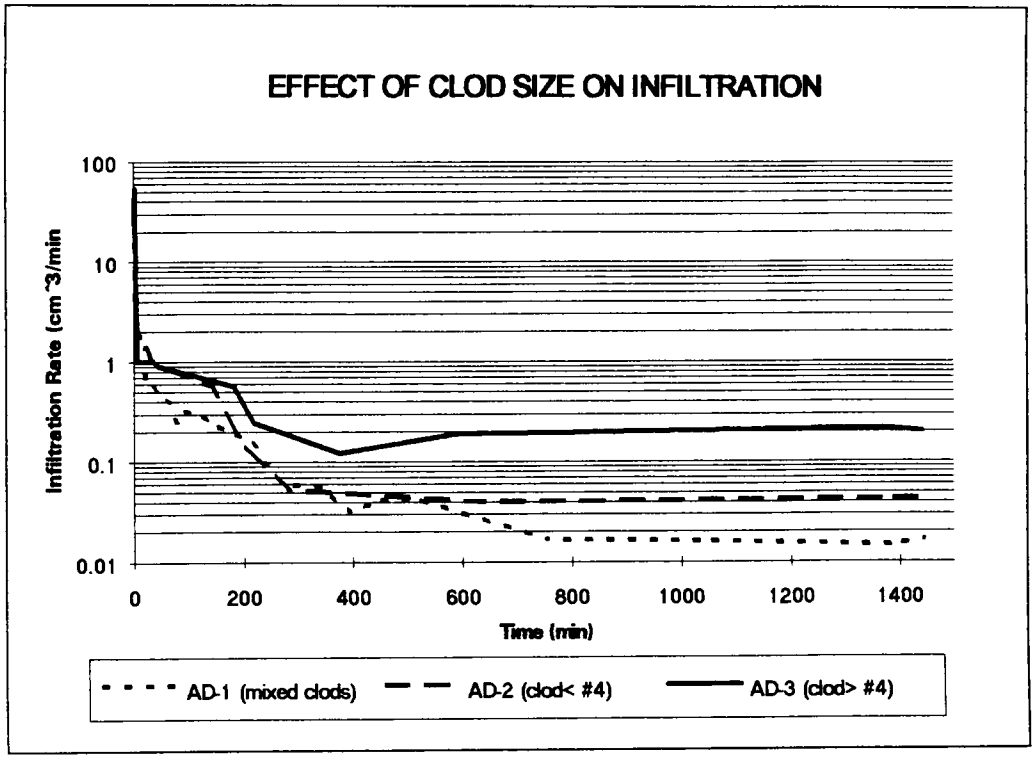


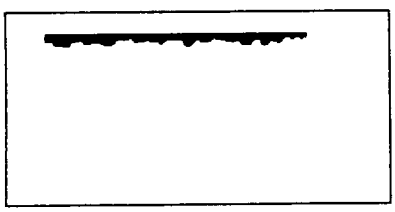
D-4 (cracked from desiccation)

Fig. 6-9. Fracture effects on infiltration

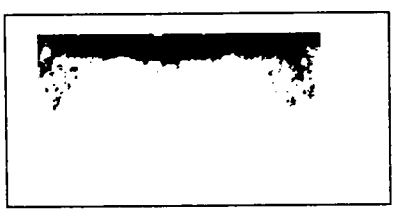
clod size on infiltration (Figure 6-10). Sample AD-3 was compacted with a large clod size, all of which were retained on the #4 sieve. The maximum clod size was about 1.3 cm. Sample AD-2 was compacted with a small clod size, all of which passed the #4 sieve, and sample AD-1 was compacted with a mixture of these two sizes. The mixed clod size sample provided the least pore space as reflected by the smallest infiltration rate and the shallowest dye penetration. The large clod size sample possessed larger voids allowing increased infiltration and deeper penetration.

As demonstrated before, fractures tend to close as the soil becomes saturated. The closing of fractures is one of the reasons the infiltration rate decreases with time. A 5 cm head of water was applied to sample FT-6 for twenty minutes before application of the dye to determine if the fractures would close. Upon first examination of the twelve cross-sections of the sample illustrated in Figure 6-11, it seems that the application of the water had no effect on infiltration of the red dye. However, more careful examination suggests that many of the fractures were closed during this time. The left and middle portion of all the cross-sections reveal dye stains very similar to uncracked samples with uniform wetting front and no preferential flow. Recall that a large horizontal fracture was noted in this sample after infiltration. Apparently, a large vertical crack on the right side of the cross-sections did not completely close and continued to feed this larger horizontal crack. This led to increased infiltration and deeper dye penetration. The process of "differential swelling" may be the

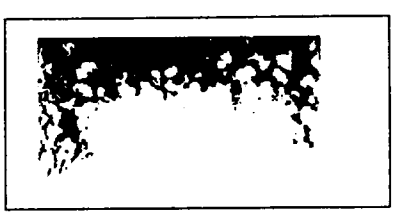




Mixed clod sizes provided the least pore space for preferential flow



A small clod size (< #4 sieve) gave intermediate preferential flow zones



A large clod size (> #4 sieve) led to significant preferential flow zones

Fig. 6-10. Clod size effects on infiltration

reason some fractures will close and others remain open. Differential swelling, however, should be far more critical for larger samples. This is why increases in hydraulic conductivity due to fractures are more likely for larger samples. Fractures close more completely in smaller samples.

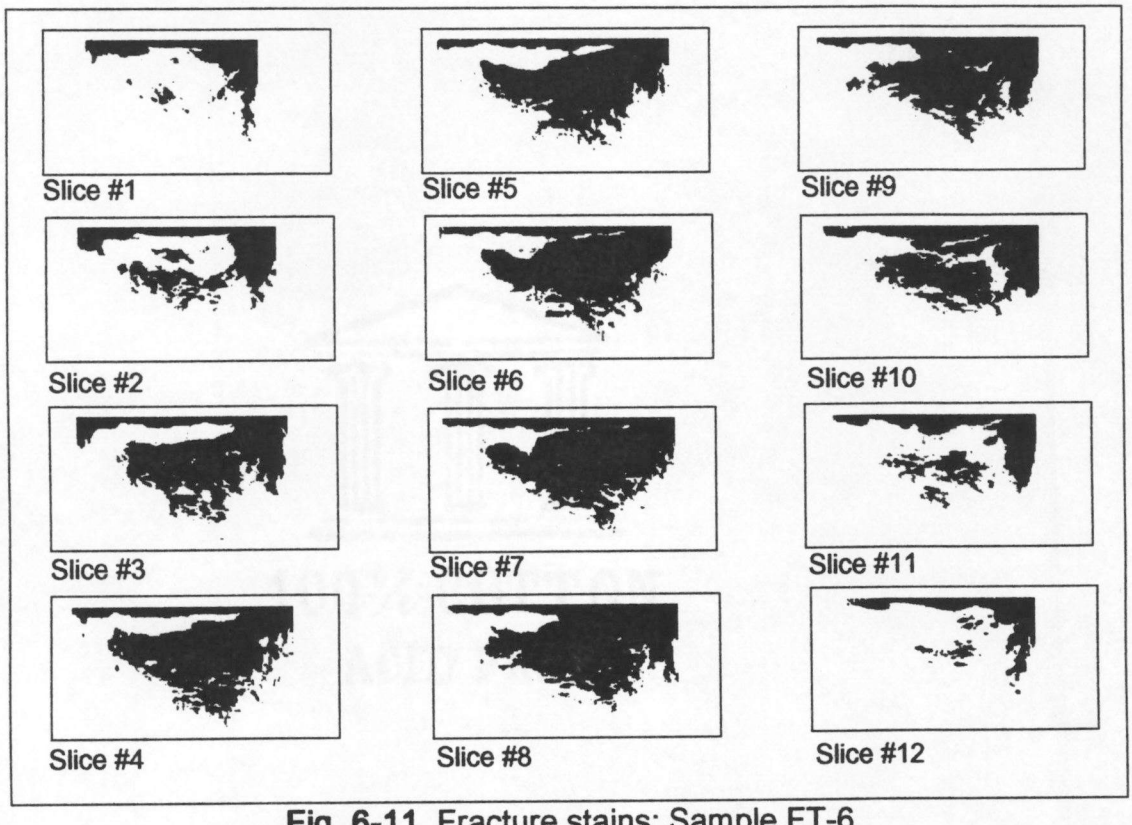


Fig. 6-11. Fracture stains: Sample FT-6

CONCLUSIONS

This study showed that post-compaction changes can lead to the development of preferential flow paths which will be of great importance in determining the long term integrity of these barriers. Changes observed in this study included fractures developed due to desiccation cycles and freeze/thaw

cycles. The size of clods used for compaction can also influence preferential flow zones. Preferential flow paths can impair the ability of a liner to prevent the migration of contaminants into the subsurface. The environmental impact of such a process can prove critically important.

Saturated hydraulic conductivity is the parameter used to judge the quality and integrity of compacted clay barriers. Due to clay swelling and closing of fractures, flow calculations based on hydraulic conductivity may underestimate flow during the dynamic stage of infiltration. The tests performed in this study revealed: (1) Desiccation and freeze/thaw cycles can lead to significant flow paths in clay, (2) Preferential flow paths may completely close due to swelling, (3) These pathways can re-open and grow in size, (3) Apparent conductivity can be reduced by three orders of magnitude due to swelling, (4) Preferential flow paths are far more hydraulically active during the dynamic stage of infiltration, (5) Saturated hydraulic conductivity may not be the best parameter to evaluate the performance of clay barriers.

The most important function of a compacted clay barrier in a landfill is to limit the migration of contaminants into the subsurface. A liner meeting the minimum hydraulic conductivity at compaction does not guarantee it can meet the long-term purpose of limiting contaminant transport. The development of post-compaction preferential flow paths can destroy the integrity of these barriers. Once the importance of preferential flow is fully recognized, steps can then be taken to eliminate or minimize their impact. The most obvious way to

achieve this is to prevent the development of preferential flow paths. At a minimum, barrier design should ensure that such pathways will not penetrate the depth of the liner.

PART 7

CONCLUSIONS AND RECOMMENDATIONS

CONCLUSIONS

Compacted clay barriers are used in solid waste landfills to protect the waste from infiltrating water and to minimize the flow of leachate from the waste. Much care is taken in controlling the condition of the soil used in landfill barriers at compaction. However, post-compaction changes leading to the development of preferential flow paths may be of greater importance in determining the long term integrity of these barriers. Such changes may include: ① damage incurred by chemical attack from retained fluids, ② fractures due to differential settlement, ③ macropores caused by plant roots and animals, ④ desiccation cycles, and ⑤ freeze/thaw cycles. The size of clods used for compaction can also influence preferential flow zones. Flow between poorly bonded lifts of a compacted liner provide further means of preferential transport. Preferential flow paths can impair the ability of a liner to prevent the migration of contaminants into the subsurface. The environmental impact of such a process can prove critically important. Groundwater contamination by dense, non-aqueous phase liquids (DNAPLs) through preferential flow paths can be very important as they are very mobile in saturated and unsaturated media due to their high densities and low viscosities. They also may not be readily absorbed by the soil matrix leaving more available for transport through the void space. Water flow is much more critical under transient conditions than saturated conditions (Brusseau and Rao, 1990). In contaminant transport, the breakthrough curve may be shifted leftward under

unsaturated conditions in comparison to curves obtained under saturated conditions. This quicker breakthrough again reinforces the importance of unsaturated transport. The presence of more open pathways during unsaturated conditions will serve to shift the breakthrough curve even more to earlier breakthrough.

Saturated hydraulic conductivity is the parameter used to judge the quality and integrity of compacted clay barriers. Some studies have found an increase in hydraulic conductivity due to fractures, but the increase did not meet expectations given the magnitude of the cracking. Other tests found no difference in hydraulic conductivity between cracked and uncracked samples. Due to clay swelling and closing of fractures, flow calculations based on saturated hydraulic conductivity may underestimate flow during unsaturated conditions. Three series of tests were carried out for this investigation: ① experimentally induced desiccation cracks, ② flow tests on desiccated kaolin slurry samples, and ③ infiltration tests on compacted kaolin samples

From these tests, a number of conclusions can be drawn:

- Desiccation and freeze/thaw cycles can lead to significant flow paths in clay
- Preferential flow paths may completely close due to swelling
- These pathways can re-open and grow in size
- Apparent conductivity can be reduced by three orders of magnitude due to swelling

- Preferential flow paths are far more hydraulically active during the dynamic stage of infiltration
- Saturated hydraulic conductivity may not be the best parameter to evaluate the performance of clay barriers

The hydraulic conductivity not only does not fully capture fracture flow, but it is an as-compacted criterion. Albrecht and Cartwright (1989) discuss this further, stating that

> "The hydraulic conductivity criterion is a construction quality assurance measure which must be met for earthen liners. Implicitly, it suggests that the liner should also meet some minimum long-term performance expectation. However, criteria which are more appropriate for evaluating the long-term effectiveness of a liner generally include one or more of the following: a specified seepage flux or contaminant flux for a particular leachate component at the liner bottom, time taken to reach a specified flux or leachate chemical flux at the liner bottom, or time taken for the concentration of a specific leachate component to reach a specified value at the liner bottom (USEPA, 1986)."

The most important function of a compacted clay barrier in a landfill is to limit the migration of contaminants into the subsurface. A liner meeting the minimum hydraulic conductivity at compaction does not guarantee it can meet the long-term purpose of limiting contaminant transport. The development of post-compaction preferential flow paths can destroy the integrity of these barriers. The best solution to this problem is to limit the development of these

pathways. However, this may prove very difficult to accomplish and impossible to verify. Perhaps electrical resistivity studies will prove useful in determining subsurface cracking.

RECOMMENDATIONS FOR FURTHER RESEARCH

In order to better evaluate hydraulic defects and preferential flowpaths in compacted clay barriers, the following recommendations are suggested for future research.

- Evaluation of the development and closing of clay fractures on large scale samples employing infiltration of a dye permeant.
- Determination of "critical apertures" above which fractures will not fully close. Develop a method to characterize fracture networks and how they change with saturation.
- Expand the use of electrical resistivity surveys to detect subsurface cracking.
- Develop a mathematical model to characterize and predict contaminant transport through compacted clay barriers.
- Develop methods to prevent or minimize the development of preferential flow paths to preserve the long term integrity of compacted clay barriers.

REFERENCES

Albrecht, K.A., Herzog, B.L., Follmer, L.R., Krapac, I.G., Griffin, R.A., and Cartwright, K., (1989) "Excavation of an Instrumented Earthen Liner: Inspection of Dyed Flow Paths and Morphology," *Hazardous Waste & Hazardous Materials,* Vol. 6, No. 3, pp. 269-279.

Albrecht, K.A., and Cartwright, K., (1989) "Infiltration and Hydraulic Conductivity of a Compacted Earthen Liner," *Ground Water,* Vol. 27, No. 1, pp. 14-19.

Anderson, J.C., and Bouma, J., (1973) "Relationships between saturated hydraulic conductivity and morphometric data of an argillic horizon," *Soil Sci. Soc. Am. Proc.*, Vol. 37, pp. 408-413.

Benson, C.B., and Daniel, D.E., (1990) "Influence of Clods on Hydraulic Conductivity of Compacted Clay," *Journal of Geotechnical Engineering,* Vol. 116, No. 8, pp. 1231-1248.

Benson, C.H. and Daniel, D.E., (1994) "Minimum thickness of Compacted Soil Liners: II. Analysis and Case Histories," *Journal of Geotechnical Engineering,* ASCE, Vol. 120, No. 1, pp. 153-172.

Benson, C.H., and Othman, M.S., (1993) "Hydraulic Conductivity of Compacted Clay Frozen and Thawed In Situ," *Journal of Geotechnical Engineering,* Vol. 119, No. 2, pp. 276-294.

Beven, K., and P. Germann, (1981) "Water flow in soil macropores, II. A combined flow model," *Journal of Soil Science,* 32, pp.15-29.

Beven, K., and Germann, P., (1982) "Macropores and Water Flow in Soils," *Water Resources Research,* Vol. 18, No. 5, pp. 1311-1325.

Boles, D.R., (1994) "The Effects of Water Content Variation on Laboratory Samples Simulating Low Permeable Clay Barriers," thesis presented to The University of Tennessee, Knoxville in partial fulfillment of the requirements for the degree of Master of Science.

Bouma, J., and Dekker, L.W., (1978) "A Case Study on Infiltration Into Dry Clay Soil, I. Morphological Observations," *Geoderma,* 20, pp. 27-40.

Bouma, J., Dekker, L.W., and Wosten, J.H.M., (1978) "A Case Study on Infiltration Into Dry Clay Soil, II. Physical Observations," *Geoderma,* 20, pp. 41-51.

Bowders, J.J., Jr., and McClelland, S., (1994) "The Effects of Freeze/Thaw Cycles on the Permeability of Three Compacted Soils," *Hydraulic Conductivity and Waste Contaminant Transport in Soil, ASTM STP 1142*, David E. Daniel and Stephen J. Trautwein, Eds., American Society for Testing and Materials, Philadelphia.

Brusseau, M.L., and Rao, P.S.C., (1990) "Modeling Solute Transport in Structured Soils: A Review," *Geoderma*, Vol. 46, pp. 169-192.

Carpenter, P.J., Kaufmann, R.S., and Price, B., (1990) "Use of Resistivity Soundings to Determine Landfill Structure," *Ground Water*, Vol. 28, No. 4, pp. 569-575.

Carpenter, P.J., Keeley, M.C., and Kaufmann, R.S., (1994) "Azimuthal Resistivity Surveys Over a Fractured Landfill Cover," *Bulletin of the Association of Engineering Geologists*, Vol. XXXI, No. 1, pp. 123-131.

Cheng, S.C., Larralde, J.L. and Martin, J.P., (1994) "Hydraulic Conductivity of Compacted Clayey Soils Under Distortion or Elongation Conditions," *Hydraulic Conductivity and Waste Contaminant Transport in Soil, ASTM STP 1142*, David E. Daniel and Stephen J. Trautwein, Eds., American Society for Testing and Materials, Philadelphia, pp. 266-283.

Corser, P., and Cranston, M., (1991) "Observations on Long-Term Performance of Composite Clay Liners and Covers," *Geosynthetics: Design and Performance*, 6th Annual Symposium, Vancouver Geotechnical Society, Vancouver, B.C., 16 p.

Corte, Arturo and Higashi, Akira, (1964) "Experimental Research on Desiccation Cracks in Soil," Cold Regions Research & Engineering Laboratory, Hanover, N.H., no. 66, 72 p.

Daniel, D.E., (1984) "Predicting Hydraulic Conductivity of Clay Liners," *Journal of Geotechnical Engineering*, ASCE, Vol. 110, No.2, pp. 285-300.

Daniel, D.E., and Benson, C.H., (1990) "Water Content-Density Criteria for Compacted Soil Liners," *Journal of Geotechnical Engineering*, ASCE, Vol. 116, No. 12, pp. 1811-1830.

Environmental Protection Agency (EPA, 1989), Technical Guidance Document: Final Covers on Hazardous Waste Landfills and Surface Impoundments, EPA/530-SW-89-047, Office of Solid Waste and Emergency Response, U.S. EPA, Washington, DC.

Freeze, R.A., and Cherry, J.A., (1979) *Groundwater*, Prentice-Hall, Inc., Englewoods Cliffs, New Jersey, 604 p.

Griffiths, D.H., and King, R.F., (1965) *Applied Geophysics for Engineers and Geologists*, Pergamon Press, London, 223 p.

Haines, W.B., (1923) "The volume change associated with variations of water content in soil," *Journal of Agricultural Science*, Vol. 13, pp. 296-310.

Higgs, P.J., (1930) "An investigation of earthing resistances," *J. Instn Electr. Engrs*, Vol. 68, pp. 736-750.

Holtz, R.D., and Kovacs, W.D., (1981) *An Introduction to Geotechnical Engineering,* Prentice-Hall, Inc., Englewoods Cliffs, New Jersey, 733 p.

Kalinski, R.J., and Kelly, W.E., (1994) "Electrical-Resistivity Measurements for Evaluating Compacted-Soil Liners," *Journal of Geotechnical Engineering*, Vol. 120, No. 2, pp. 451-457.

Kim, W.H., and Daniel, D.E., (1992) "Effects of Freezing on Hydraulic Conductivity of Compacted Clay," *Journal of Geotechnical Engineering,* Vol. 118, No. 7, pp. 1083-1097.

Klefstad, G., Sendlein, L.V.A., and Palmquist, R.C., (1975) "Limitations of the Electrical Resistivity Method in Landfill Investigations," *Ground Water*, Vol. 13, No. 5, pp. 418-427.

Kleppe, J.H., (1981) "Desiccation Cracking of Cohesive Soils," M.S. thesis, University of Texas, Austin.

Kleppe, J.H. and Olson, R.E., (1985) "Desiccation Cracking of Soil Barriers," *Hydraulic Barriers in Soil and Rock*, ASTM STP 874, A.I. Johnson, R.K. Frobel, N.J. Cavalli, and C.B. Pettersson, Eds., American Society for Testing and Materials, Philadelphia, pp. 263-275.

Lachenbruch, A.H., (1962) *Mechanics of Thermal Contraction Cracks and Ice-Wedge Polygons in Permafrost*, Special GSA Papers No. 70., New York, 65 p.

Leeds-Harrison, Shipway, C.J.P., Jarvis, N.J., and Youngs, E.G., (1986) "The influence of soil macroporosity on water retention, transmission and drainage in a clay soil," *Soil Use and Management*, Vol. 2, No. 2, pp. 47-50.

Leonards, G.A., and Narain, J., (1963) *Journal of the Soil Mechanics and Foundations Division*, American Society of Civil Engineers, Vol. 89, No. SM2, pp. 47-98.

Lima, L.A. and Grismer, M.E., (1992) "Soil Crack Morphology and Soil Salinity," *Soil Science*, Vol. 153, No. 2, pp. 149-153.

McCarter, W.J., (1984) "The electrical resistivity characteristics of compacted clays," *Geotechnique*, Vol. 34, No. 2, pp. 263-267.

McCollum, B., and Logan, K.H., (1930) *Electrolytic corrosion of iron in soils*, Bureau of Standards Technologic, Paper No. 25.

McKay, L.D., Cherry, J.A., and Gillham, R.W., (1993) "Field Experiments in a Fractured Clay Till, I. Hydraulic Conductivity and Fracture Aperture," *Water Resources Research,* Vol. 29, No. 4, pp. 1149-1162.

McNeill, J.D., (1980) "Electrical Conductivity of Soils and Rocks," Goenics Limited, Technical Note TN-5, Mississauga, Ontario, Canada, 22 p.

Miller, R.J., and Low, P.F., (1963) "Threshold gradient for water flow in clay systems," *Soil Sci. Soc. Amer. Proc.*, Vol. 27, pp. 605-609.

Mitchell, J.K., (1976) *Fundamentals of Soil Behavior,* John Wiley & Sons, New York, 422 p.

Mundell, J.A., and Bailey, B., (1985) "The Design and Testing of a Compacted Clay Barrier Layer to Limit Percolation Through Landfill Covers," *Hydraulic Barriers in Soil and Rock*, ASTM STP 874, A.I. Johnson, R.K. Frobel, N.J. Cavalli, and C.B. Pettersson, Eds., American Society for Testing and Materials, Philadelphia, pp. 246-262.

Nerpin, S., Pashkina, S., and Bondarenko, N., (1966) "The evaporation from bare soil and the way of its reduction," Symp. Water in the Unsaturated Zone, Wageningen.

Othman, M.A., Benson, C.H., Chamberlain, E.J., and Zimmie, T.F., (1994) "Laboratory Testing to Evaluate Changes in Hydraulic Conductivity of Compacted Clays Caused by Freeze-Thaw: State-of-the-Art," *Hydraulic Conductivity and Waste Contaminant Transport in Soil, ASTM STP 1142*, David E. Daniel and Stephen J. Trautwein, Eds., American Society for Testing and Materials, Philadelphia, pp. 227-254.

Phifer, M.A., Drumm, E.C., and Wilson, G.V., (1994) "Effects of Post Compaction Water Content Variation on Saturated Conductivity," *Hydraulic Conductivity and Waste Contaminant Transport in Soil, ASTM STP 1142*, David E. Daniel and Stephen J. Trautwein, Eds., American Society for Testing and Materials, Philadelphia, pp. 319-334.

Pyrak-Nolte, L.J., and Montemagno, C.D., (1994) "The effect of the critical path on fluid flow through a fracture," *Rock Mechanics*, Nelson and Laubach, Eds., pp. 81-88.

Richards, L.A., (1931) "Capillary conduction of liquids in porous medium," *Physics*, Vol. 1, pp 318-333.

Shackelford, C.D., (1994) "Waste-Soil Interactions that Alter Hydraulic Conductivity," *Hydraulic Conductivity and Waste Contaminant Transport in Soil, ASTM STP 1142*, David E. Daniel and Stephen J. Trautwein, Eds., American Society for Testing and Materials, Philadelphia.

Schumacher, W., (1864) *Die Physik des Bodens*, Berlin.

Snow, D.T., (1968) "Rock Fracture Spacings, Openings, and Porosities," *Journal of the Soil Mechanics and Foundations Division*, Proceedings of the American Society of Civil Engineers , Vol. 94, No. SM1, pp. 73-91.

Stirk, G.B., (1954) "Some Aspects of Soil Shrinkage and the Effect of Cracking Upon Water Entry Into the Soil," *Australian Journal of Agricultural Research,* Vol. 5, pp. 279-290.

Swartzendruber, D., (1962) "Non Darcy behavior in liquid saturated porous media," *J. Geophys. Res.*, Vol. 67, pp. 5205-5213.

Taylor, R.W., and Fleming, A.H., (1989) "Characterizing Jointed Systems by Azimuthal Resistivity Surveys," *Ground Water*, Vol. 26, No. 4, pp. 464-474.

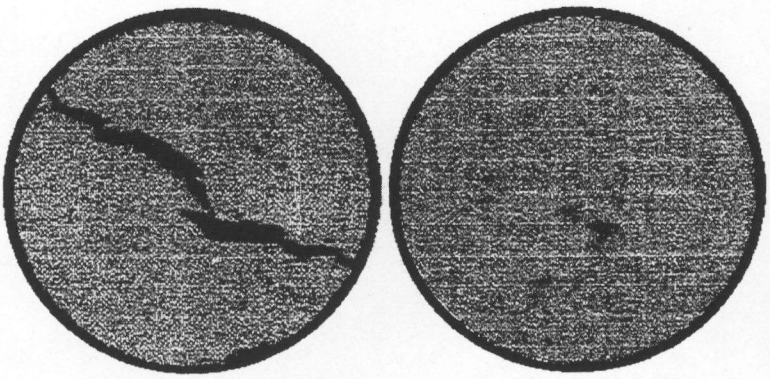
Tchobanoglous, G., (1993) *Integrated Solid Waste Management: Engineering Principles and Management Issues*, McGraw-Hill, New York, 978 p.

Todd, D.K., (1980) *Groundwater Hydrology*, John Wiley and Sons Inc.

APPENDIX 1

FLOW TEST RESULTS

Flow Test: Batch #1, Sample #2



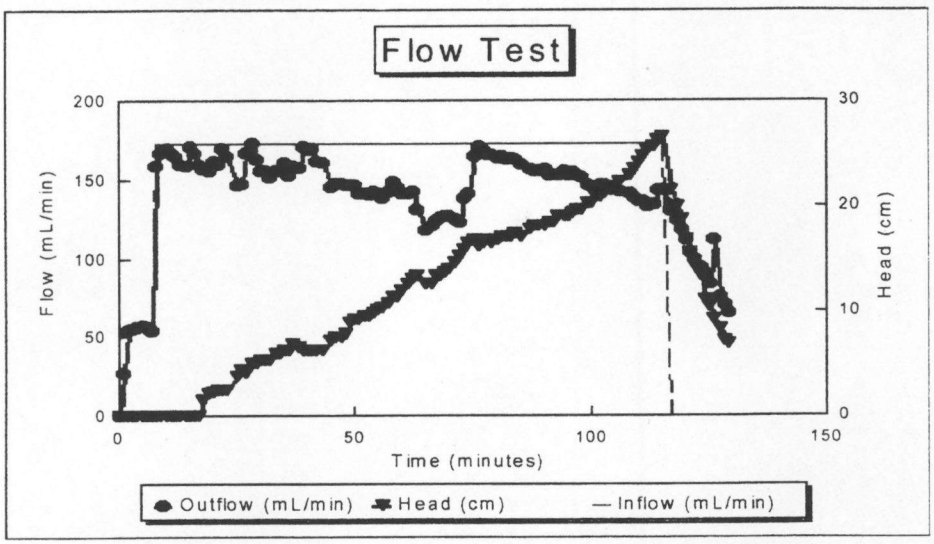
Top of Sample Bottom of Sample

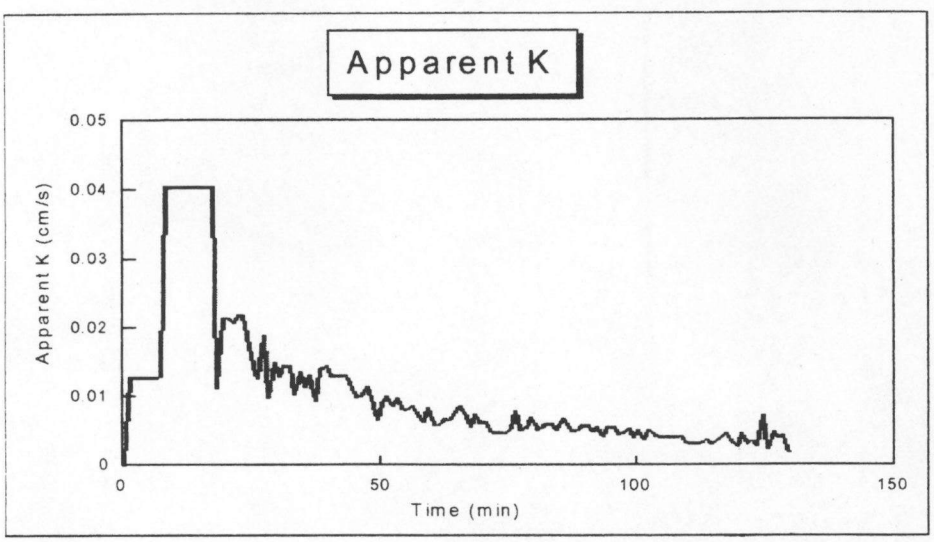
Initial Batch w%= 69.5%
Initial Sample w%= 51.3%

Thickness = 3.0 cm
Diameter = 9.5 cm

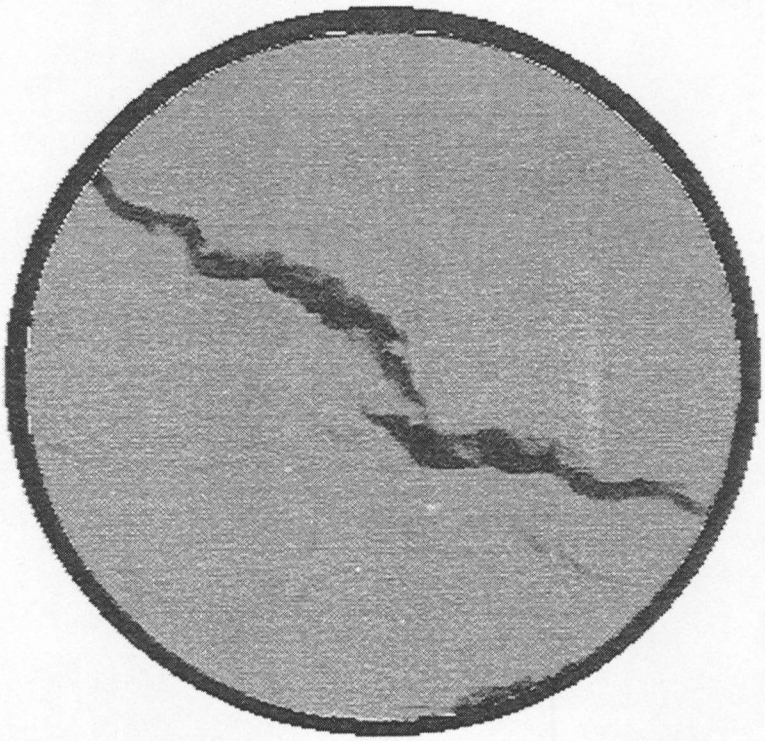
Maximum Aperture = 4.5 mm

Fracture Area Percentage
Top of Sample = 4.31%
Bottom of Sample = 0.58%

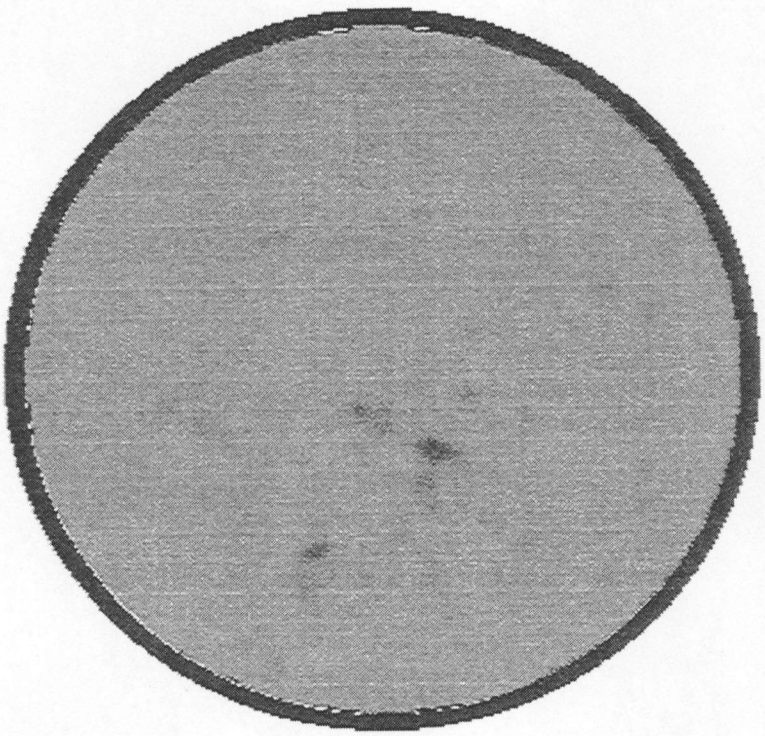




Batch #1 - Sample #2

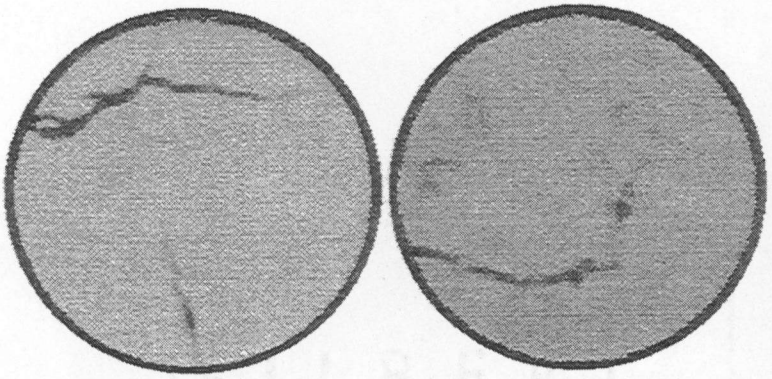


Top of Sample



Bottom of Sample

Flow Test: Batch #1, Sample #3



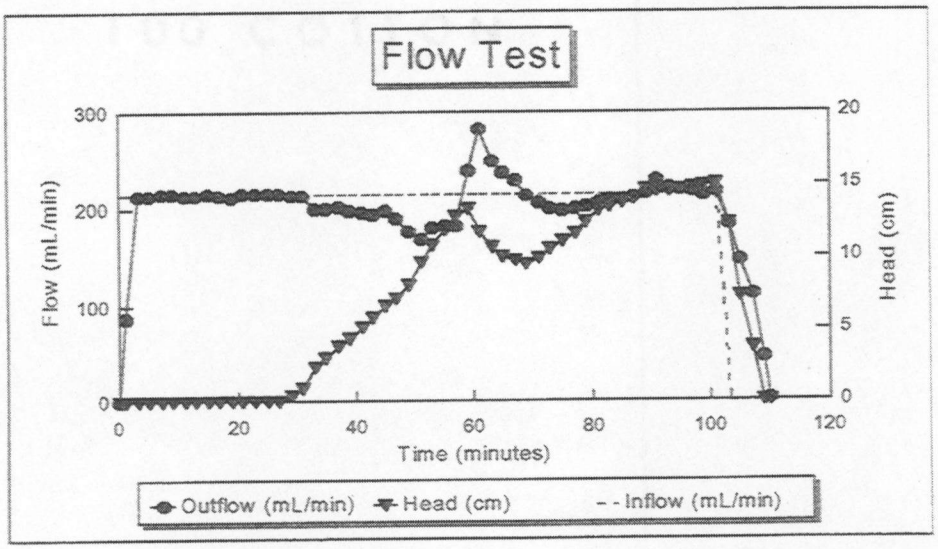
Top of Sample Bottom of Sample

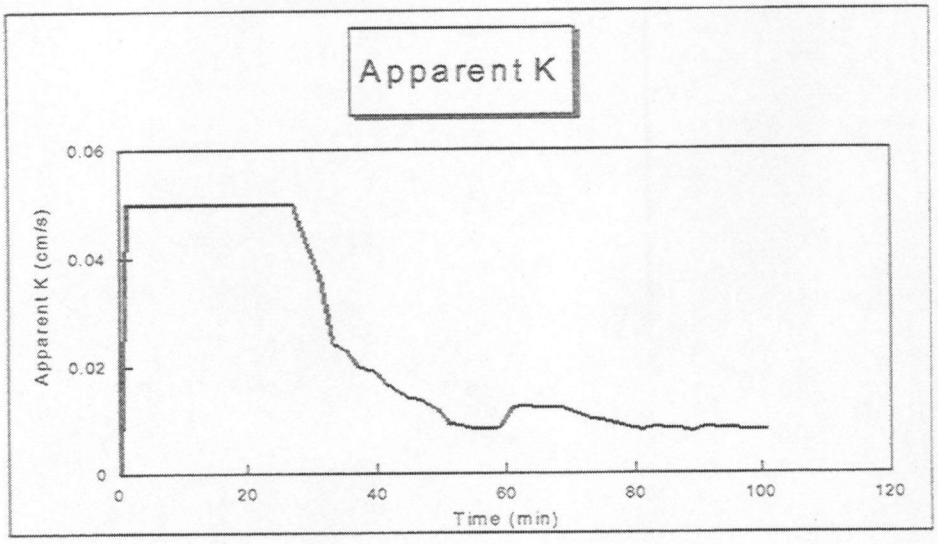
Initial Batch w%= 69.5%
Initial Sample w%= 49.0%

Thickness = 3.0 cm
Diameter = 9.5 cm

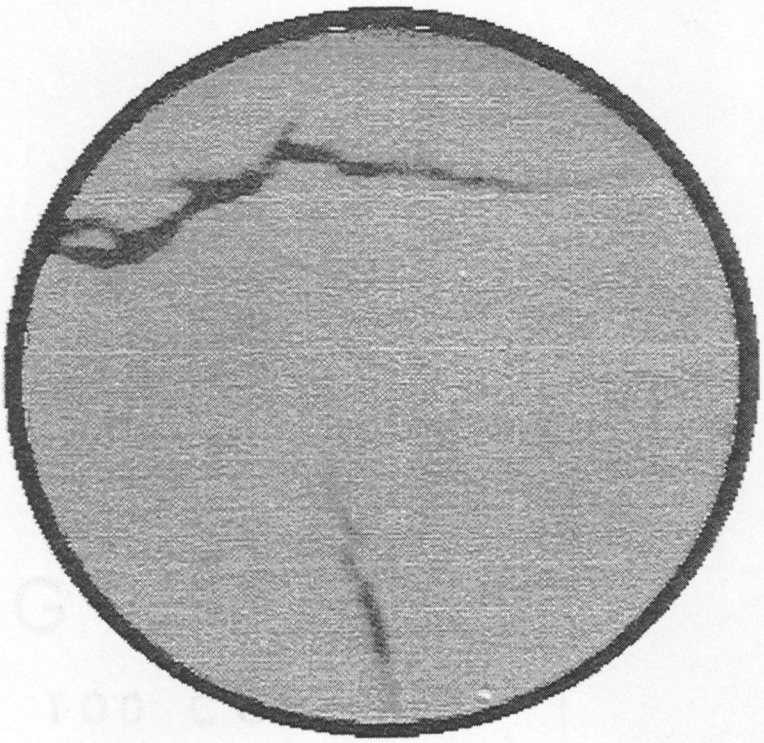
Maximum Aperture = 4.3 mm

Fracture Area Percentage
Top of Sample = 3.1%
Bottom of Sample = 2.2%

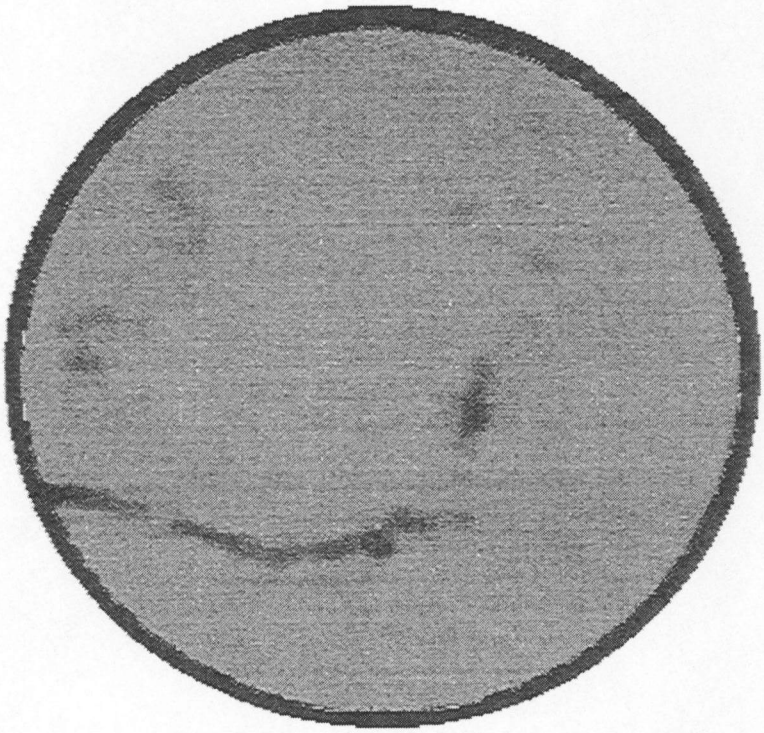




Batch #1 - Sample #3

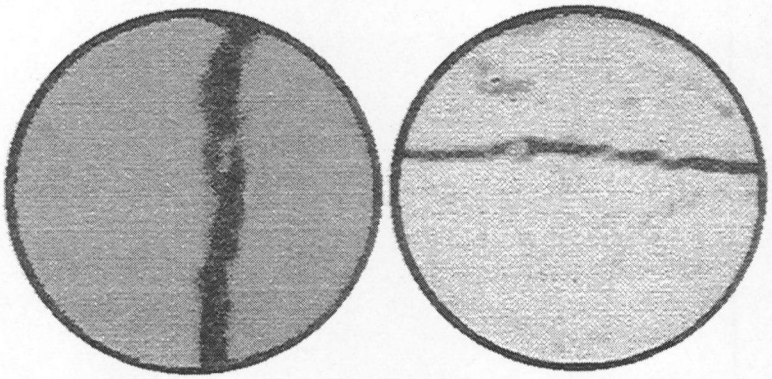


Top of Sample



Bottom of Sample

Flow Test: Batch #3, Sample #1



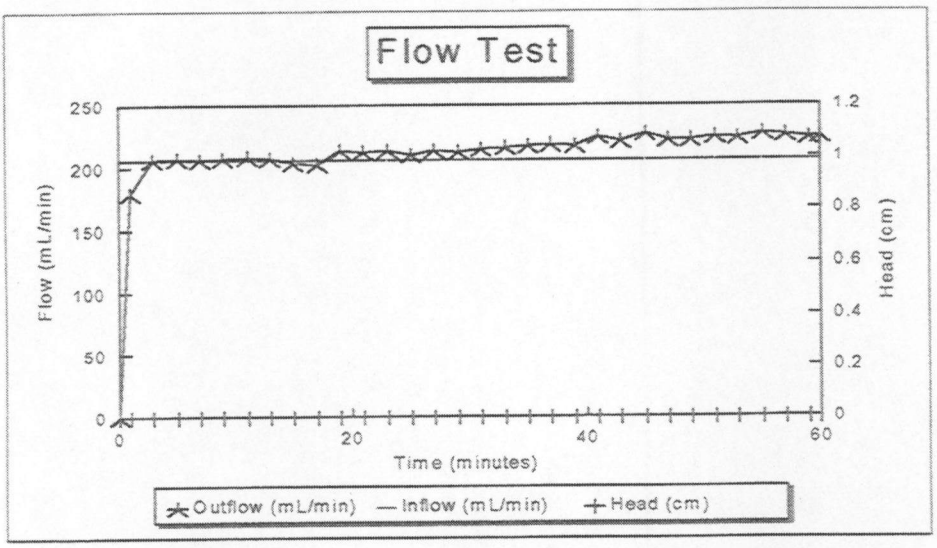
Top of Sample Bottom of Sample

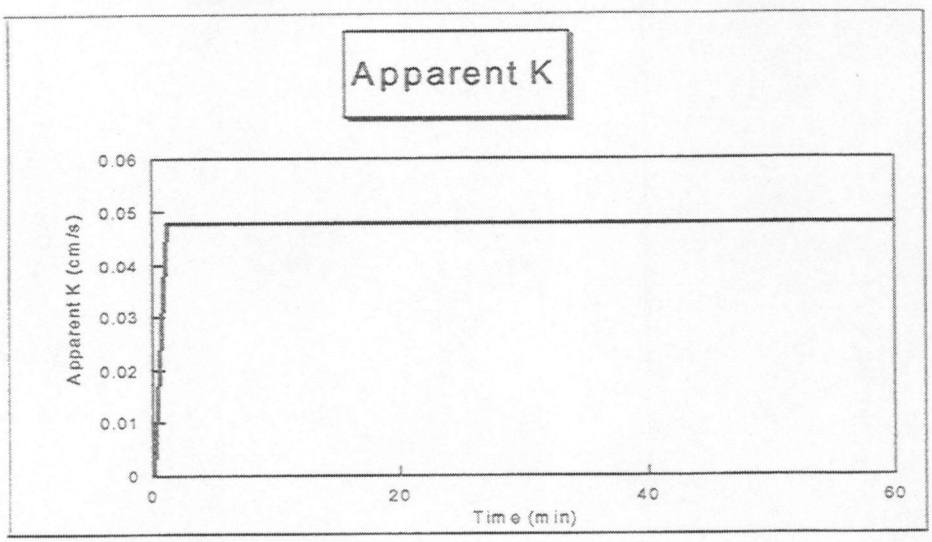
Initial Batch w%= 73.1%
Initial Sample w%= 54.6%

Thickness = 2.9 cm
Diameter = 9.5 cm

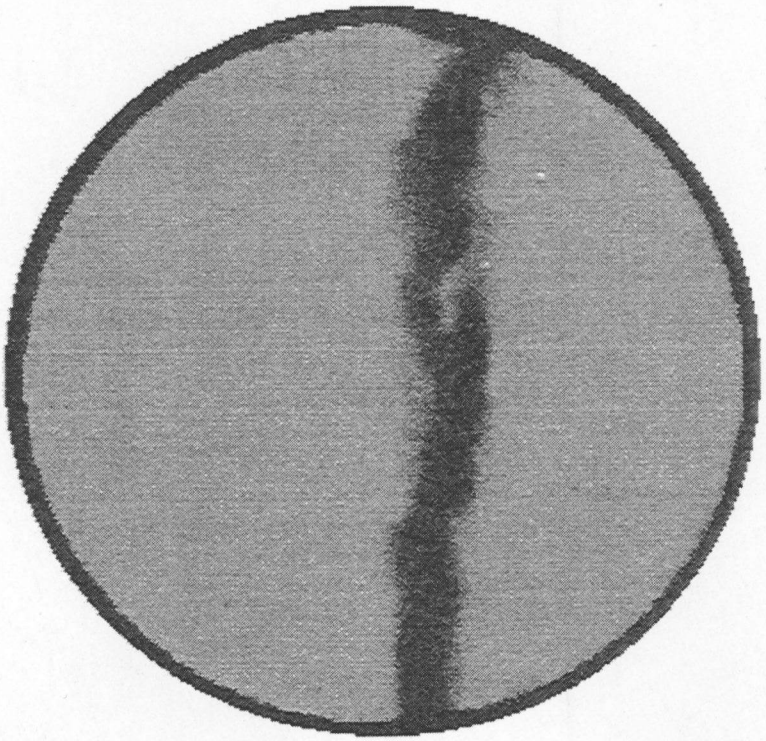
Maximum Aperture = 9.0 mm

Fracture Area Percentage
Top of Sample = 9.4%
Bottom of Sample = 3.6%

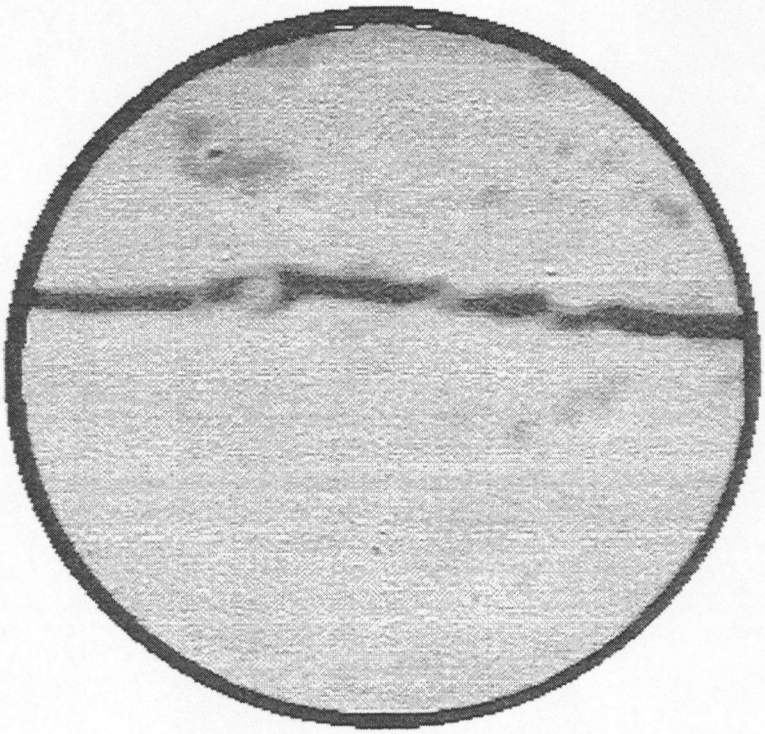




Batch #3 - Sample #1



Top of Sample



Bottom of Sample

Flow Test: Batch #4, Sample #1



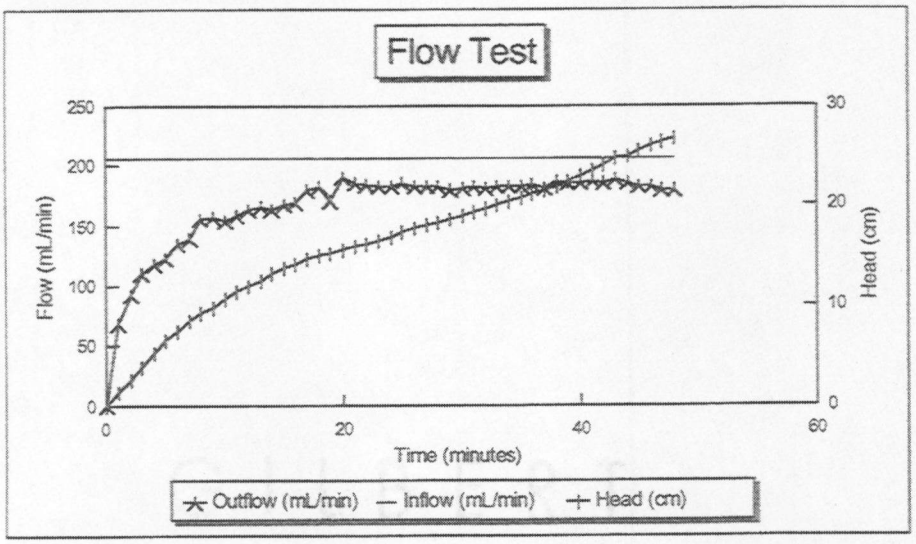
Top of Sample Bottom of Sample

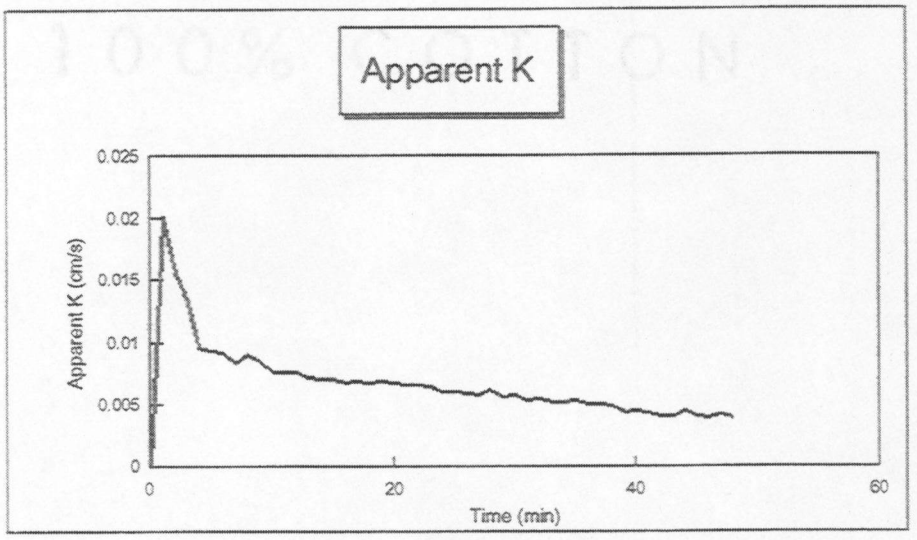
Initial Batch w%= 64.3%
Initial Sample w%= 50%

Thickness = 2.9 cm
Diameter = 9.5 cm

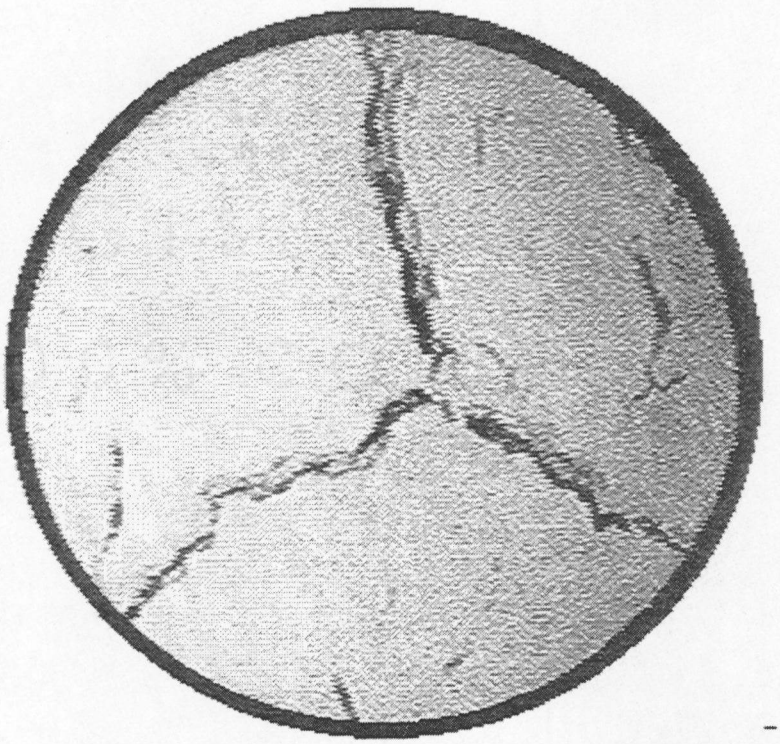
Maximum Aperture = 3.0 mm

Fracture Area Percentage
Top of Sample = 4.7%
Bottom of Sample = 2.4%





Batch #4 - Sample #1

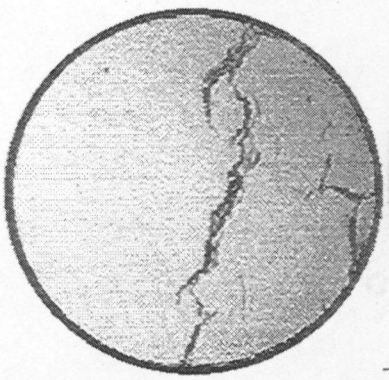


Top of Sample

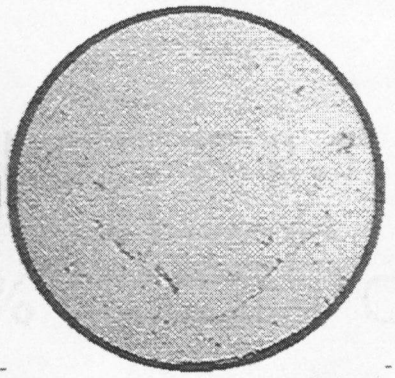


Bottom of Sample

Flow Test: Batch #4, Sample #2



Top of Sample



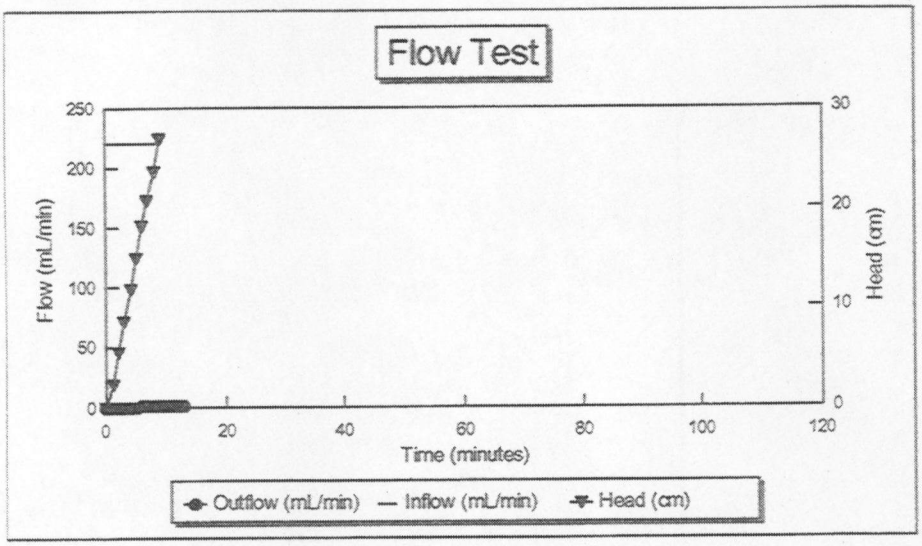
Bottom of Sample

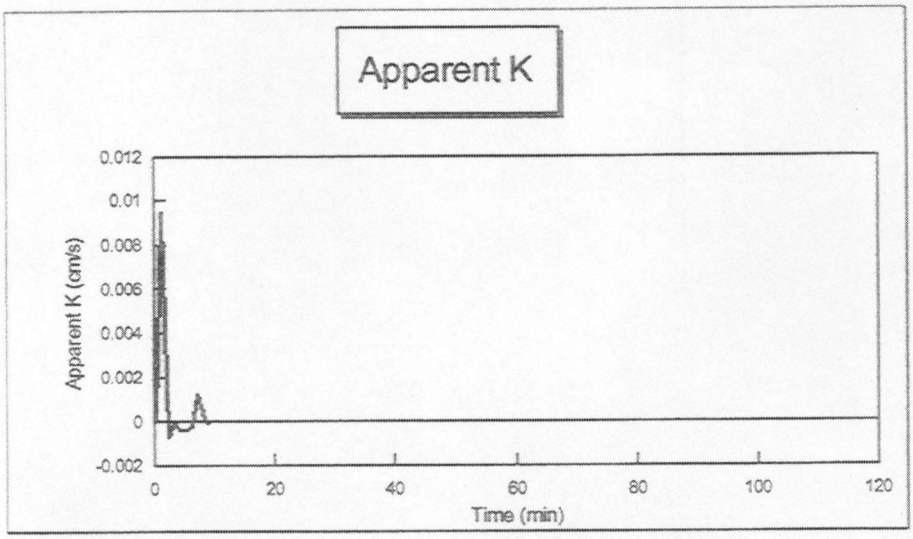
Initial Batch w%= 64.3%
Initial Sample w%= 53.4%

Thickness = 2.9 cm
Diameter = 9.5 cm

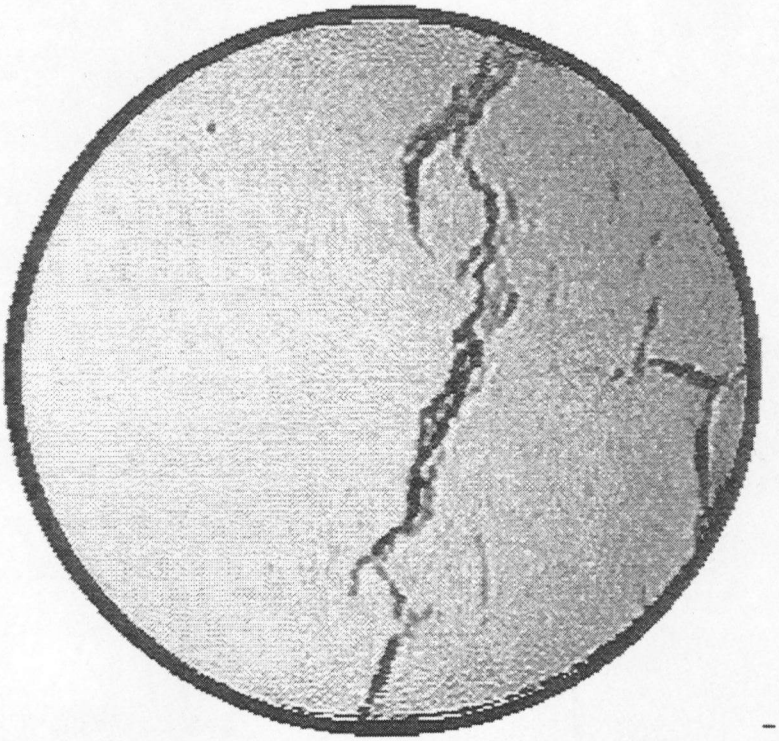
Maximum Aperture = 4.3 mm

Fracture Area Percentage
Top of Sample = 4.7%
Bottom of Sample = 0.7%

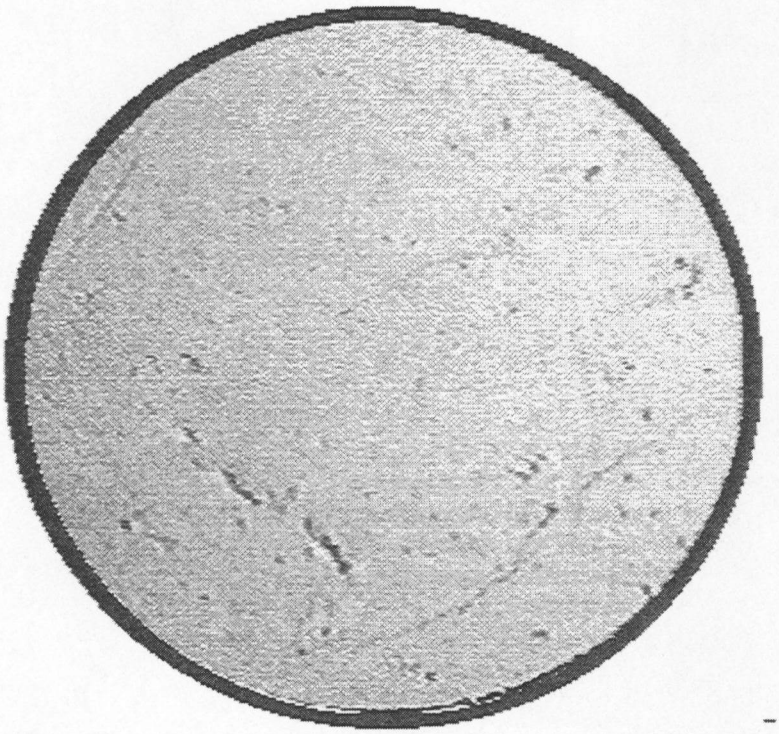




Batch #4 - Sample #2

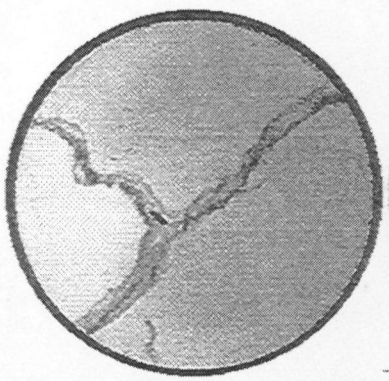


Top of Sample



Bottom of Sample

Flow Test: Batch #4, Sample #3



Top of Sample



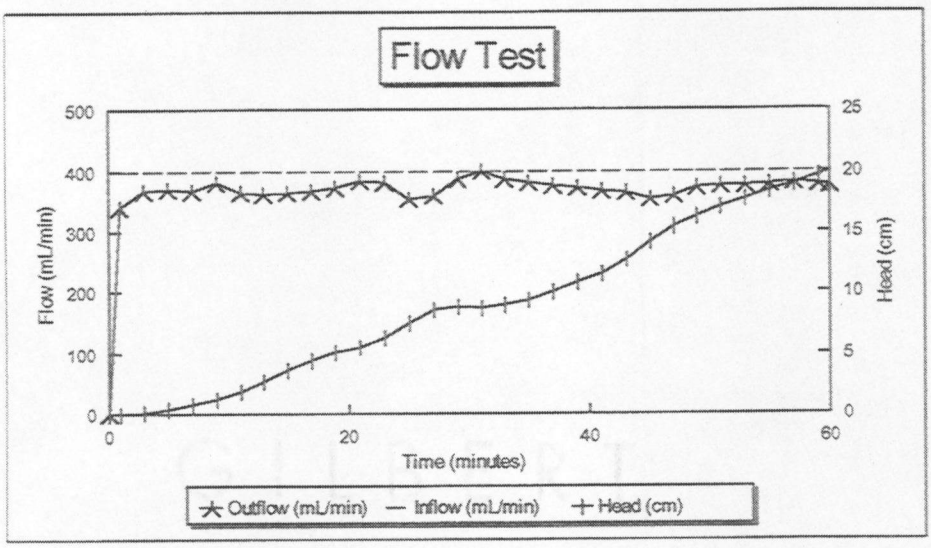
Bottom of Sample

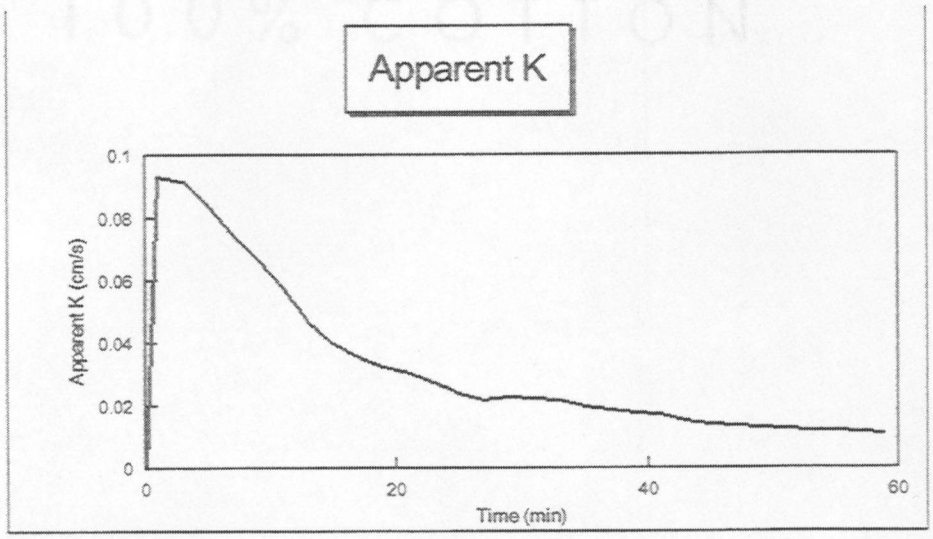
Initial Batch w%= 64.3%
Initial Sample w%= 47.9%

Thickness = 2.8 cm
Diameter = 9.5 cm

Maximum Aperture = 7.5 mm

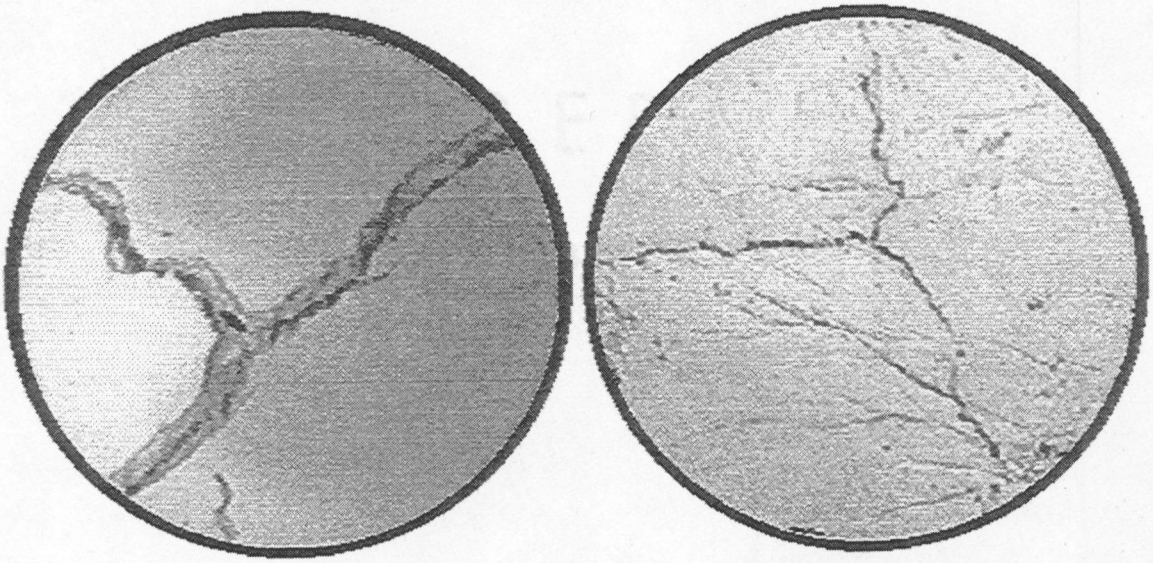
Fracture Area Percentage
Top of Sample = 9.2%
Bottom of Sample = 2.9%





Batch #4 - Sample #3

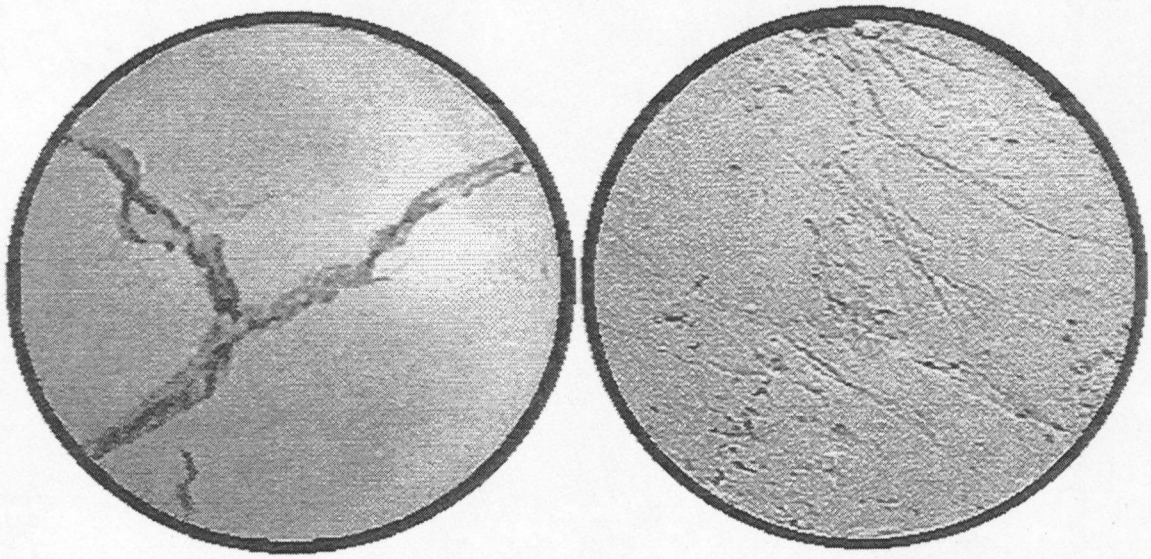
Before Testing



Top of Sample

Bottom of Sample

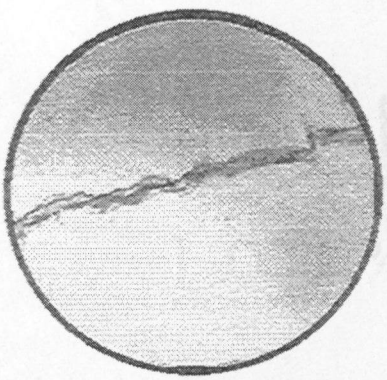
After Testing



Top of Sample

Bottom of Sample

Flow Test: Batch #4, Sample #4



Top of Sample



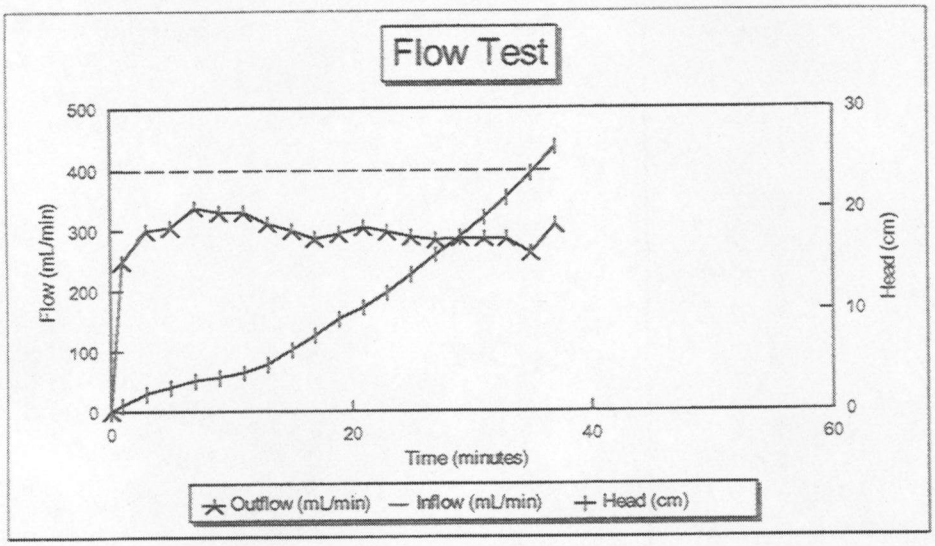
Bottom of Sample

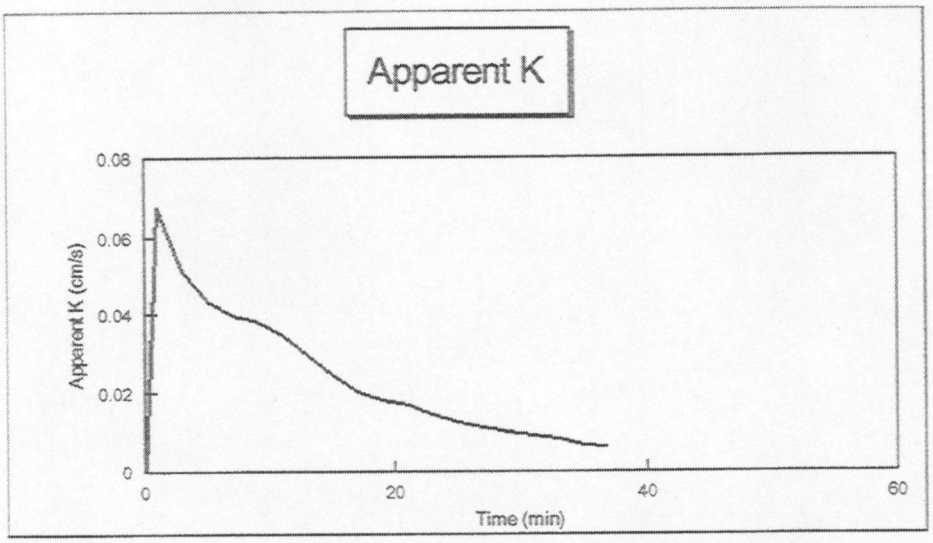
Initial Batch w%= 64.3%
Initial Sample w%= 49.0%

Thickness = 3.2 cm
Diameter = 9.5 cm

Maximum Aperture = 4.1 mm

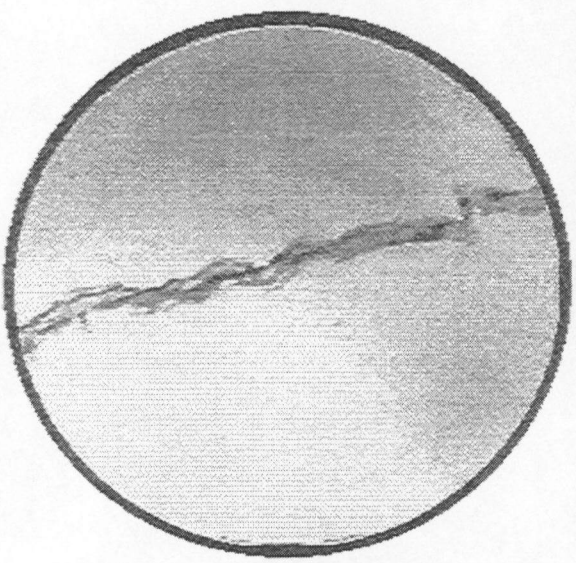
Fracture Area Percentage
Top of Sample = 4.8%
Bottom of Sample = 2.1%



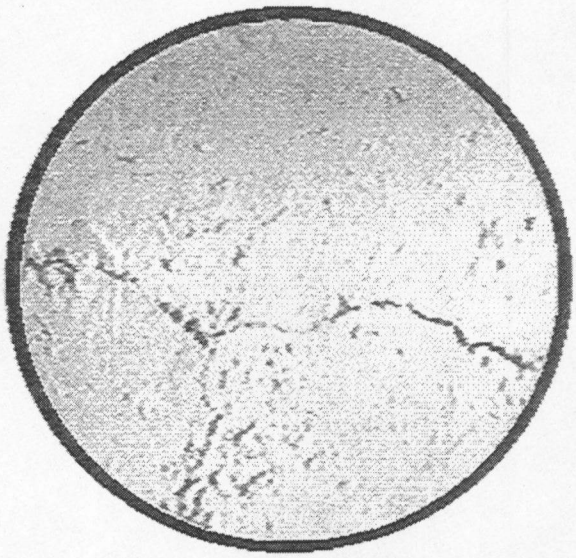


Batch #4 - Sample #4

Before Testing

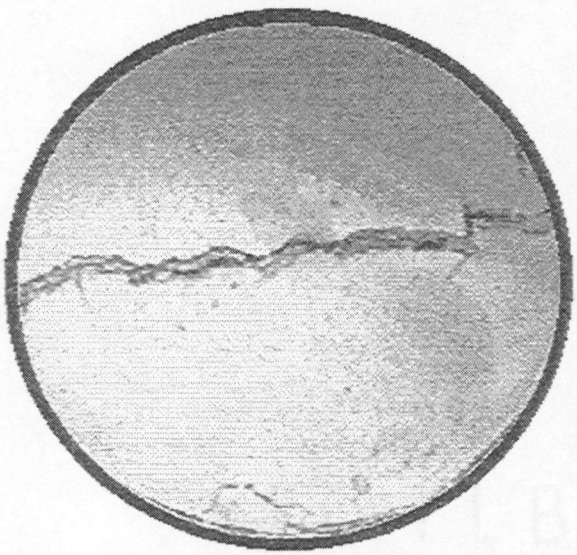


Top of Sample

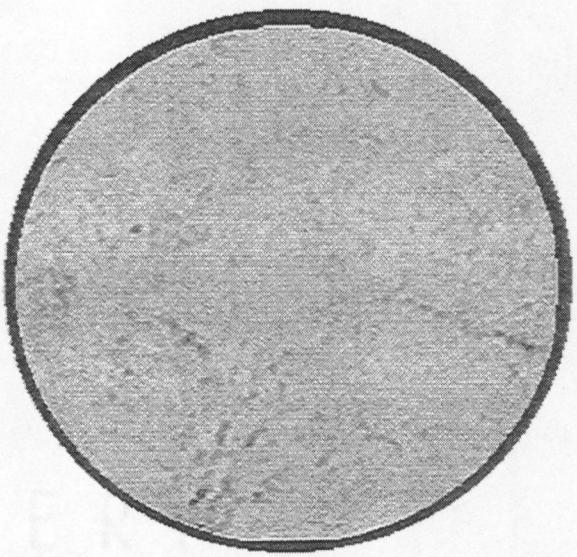


Bottom of Sample

After Testing

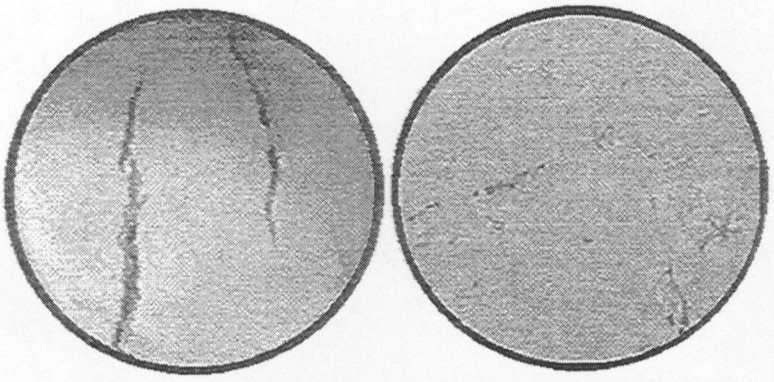


Top of Sample



Bottom of Sample

Flow Test: Batch #4, Sample #5



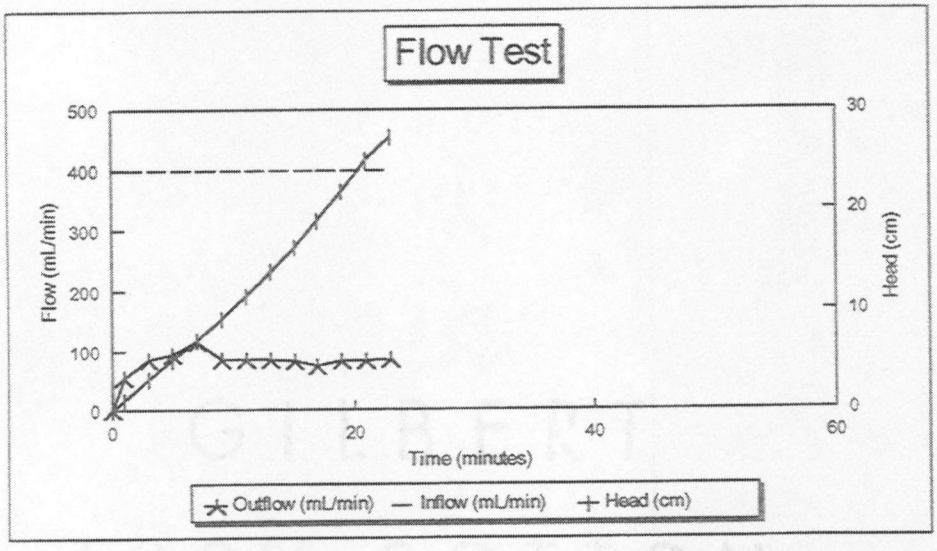
Top of Sample Bottom of Sample

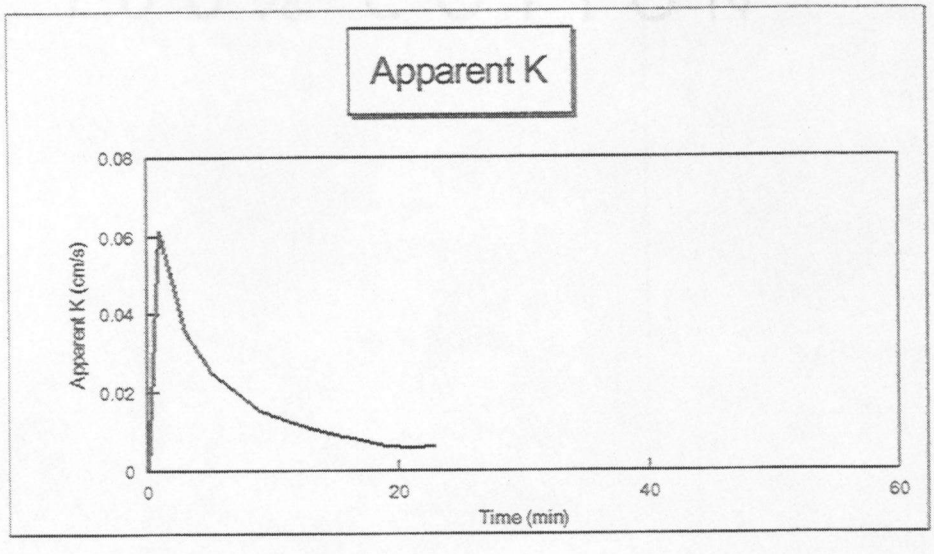
Initial Batch w%= 64.3%
Initial Sample w%= 48.8%

Thickness = 2.9 cm
Diameter = 9.5 cm

Maximum Aperture = 4.3 mm

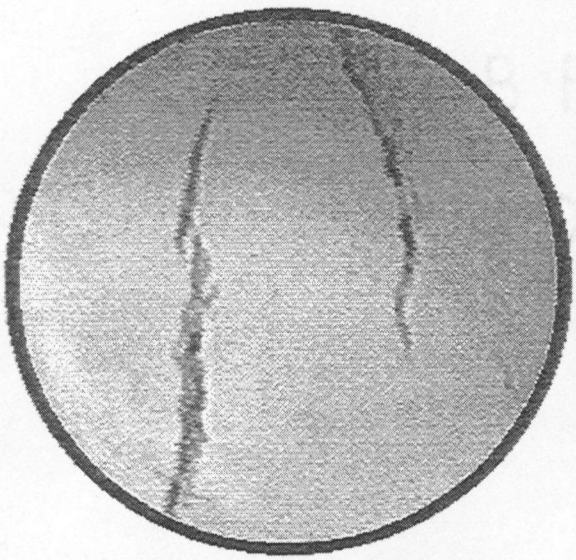
Fracture Area Percentage
Top of Sample = 4.4%
Bottom of Sample = 1.3%



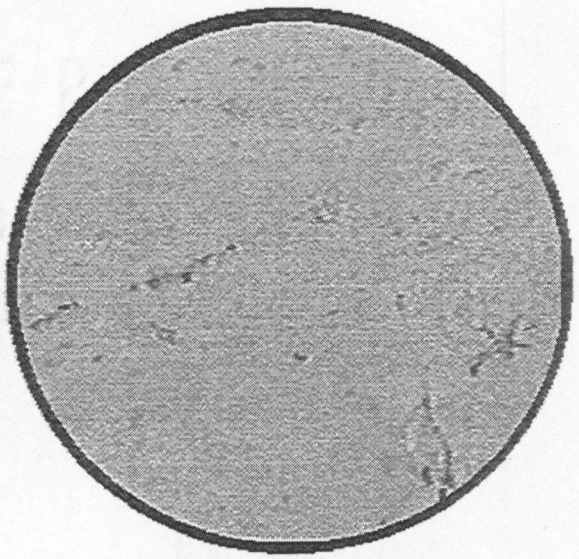


Batch #4 - Sample #5

Before Testing

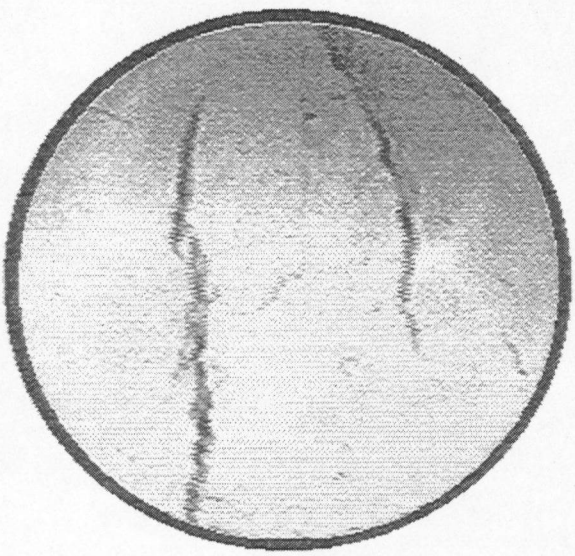


Top of Sample

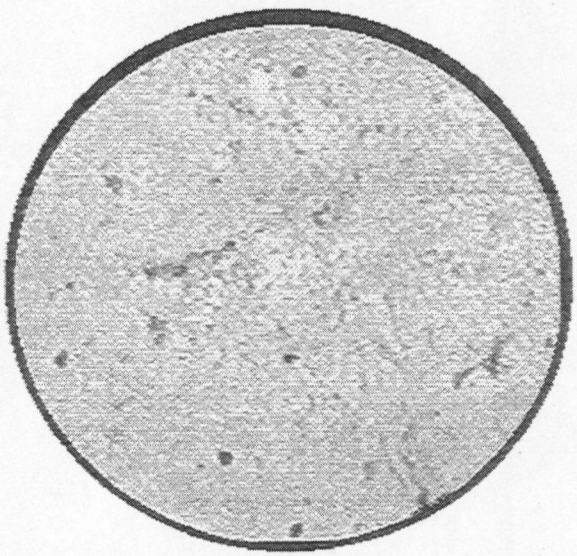


Bottom of Sample

After Testing



Top of Sample

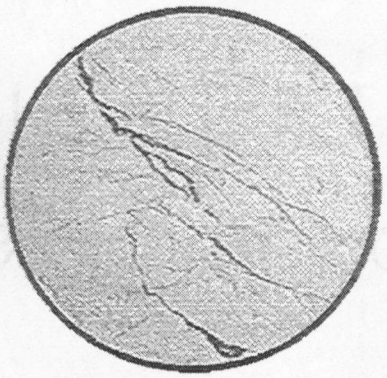


Bottom of Sample

Flow Test: Batch #5, Sample #1



Top of Sample



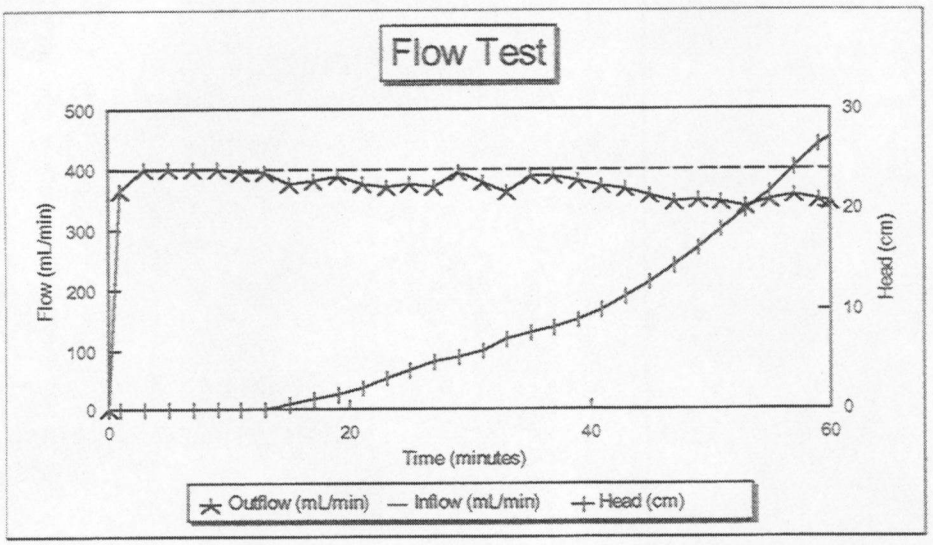
Bottom of Sample

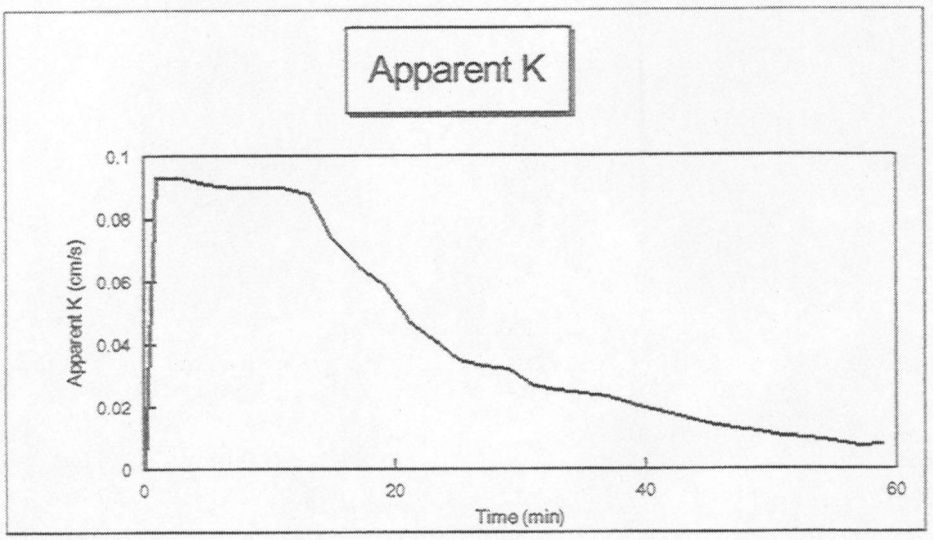
Initial Batch w%= 71.9%
Initial Sample w%= 56.0%

Thickness = 2.9 cm
Diameter = 9.5 cm

Maximum Aperture = 6.5 mm

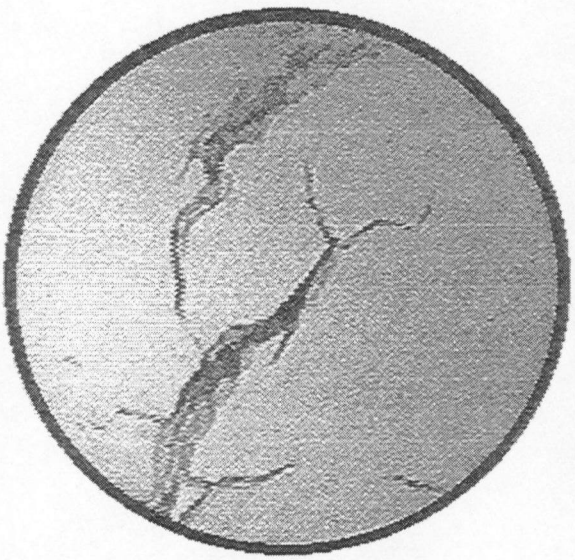
Fracture Area Percentage
Top of Sample = 7.7%
Bottom of Sample = 2.5%



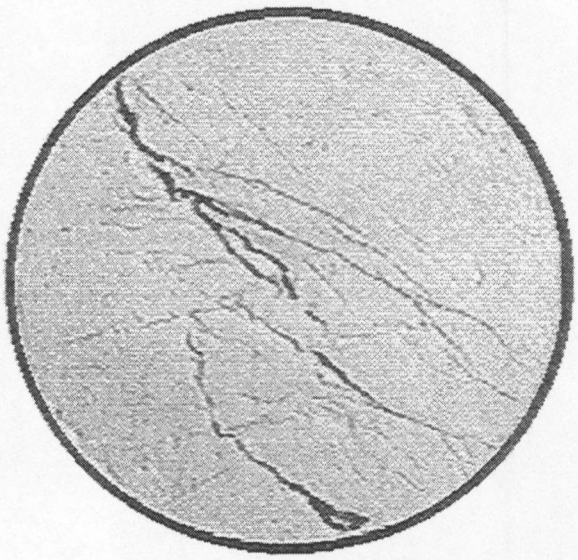


Batch #5 - Sample #1

Before Testing

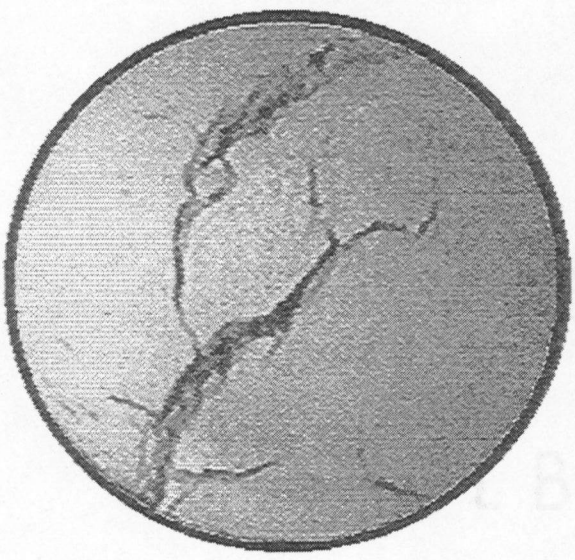


Top of Sample

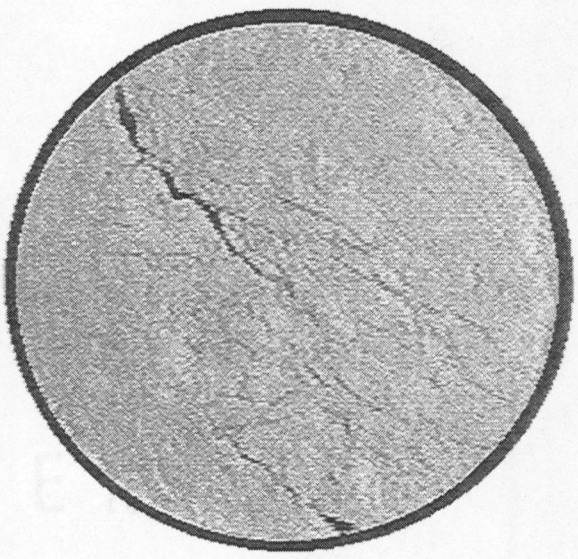


Bottom of Sample

After Testing

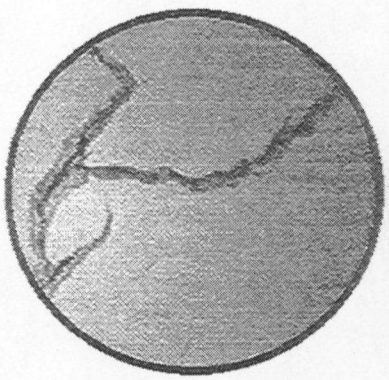


Top of Sample

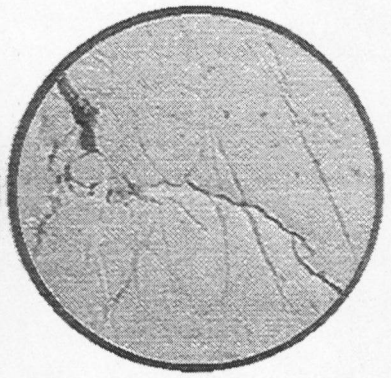


Bottom of Sample

Flow Test: Batch #5, Sample #2



Top of Sample



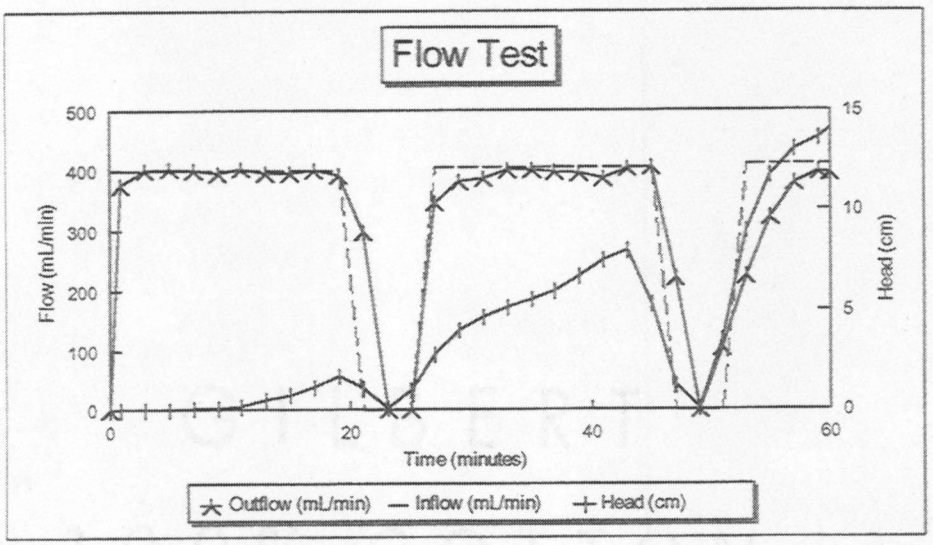
Bottom of Sample

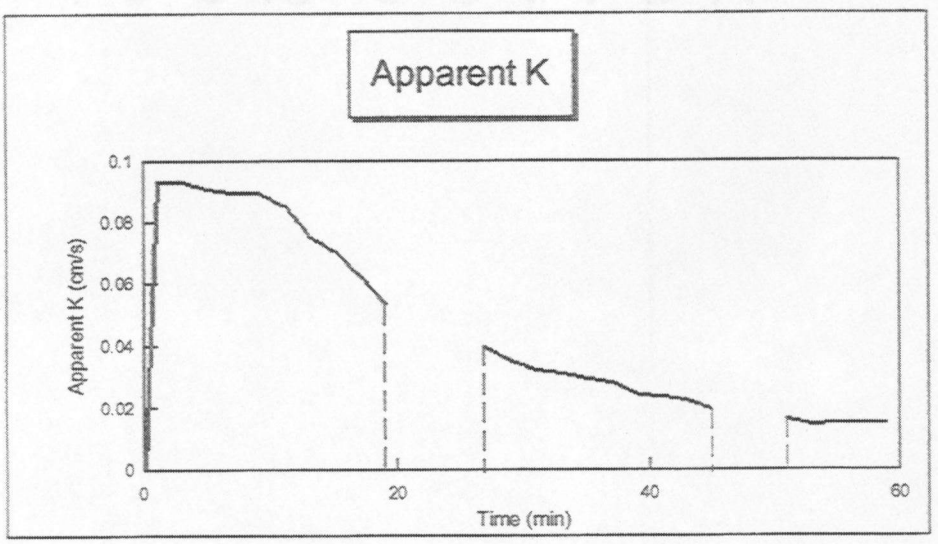
Initial Batch w%= 71.9%
Initial Sample w%= 51.1%

Thickness = 2.65 cm
Diameter = 9.5 cm

Maximum Aperture = 6.4 mm

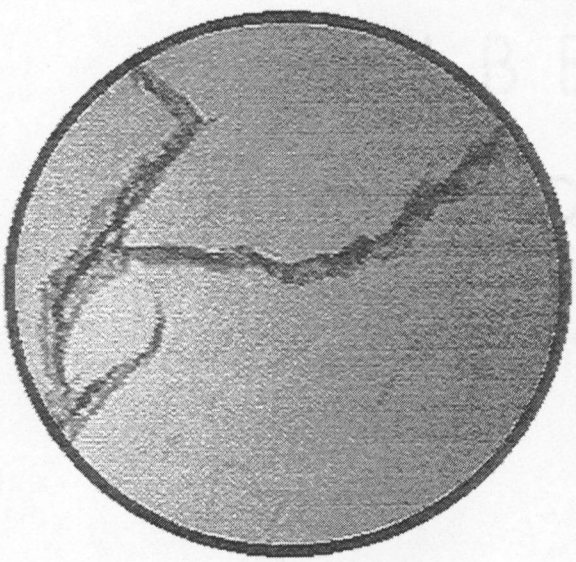
Fracture Area Percentage
Top of Sample = 8.6%
Bottom of Sample = 2.8%



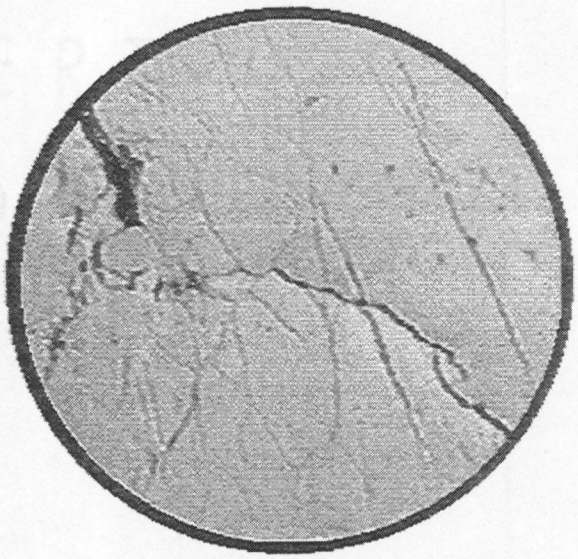


Batch #5 - Sample #2

Before Testing

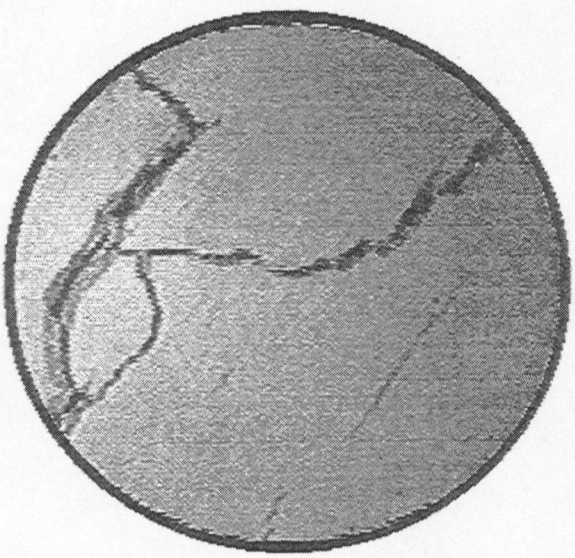


Top of Sample

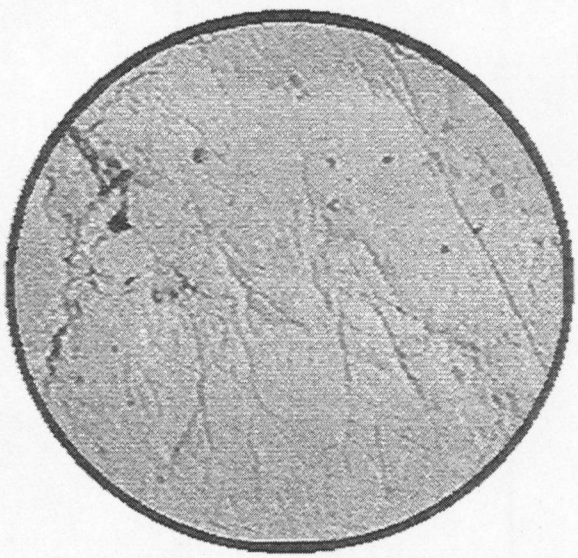


Bottom of Sample

After Testing

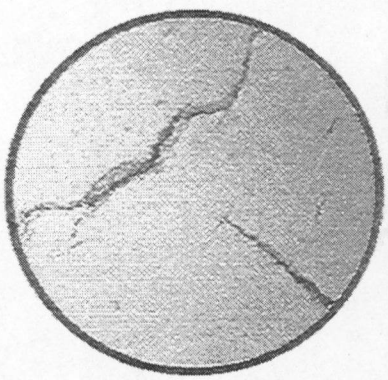


Top of Sample

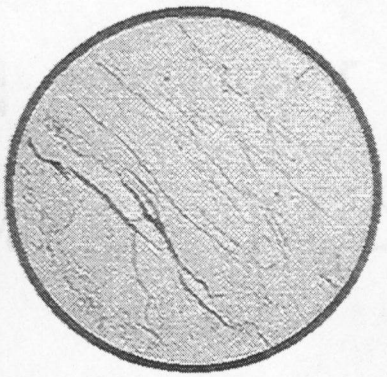


Bottom of Sample

Flow Test: Batch #5, Sample #3



Top of Sample



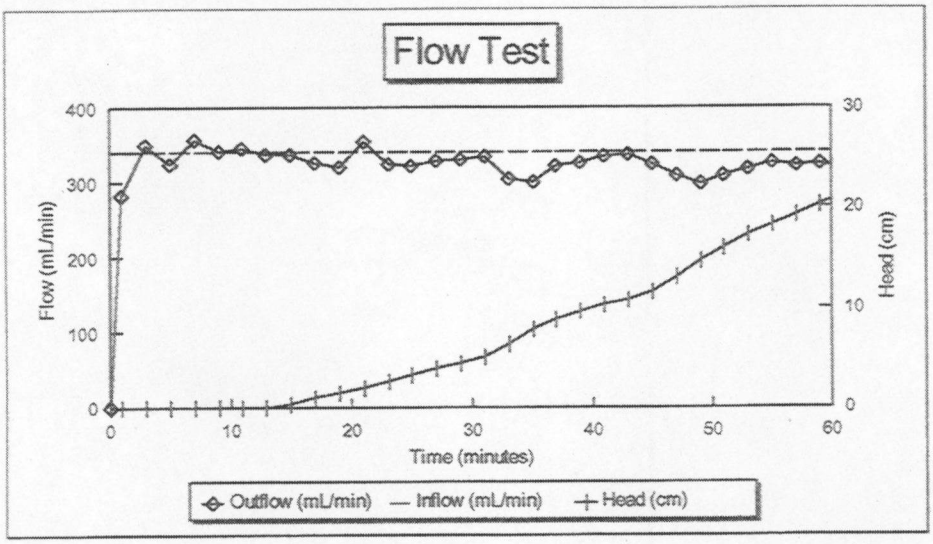
Bottom of Sample

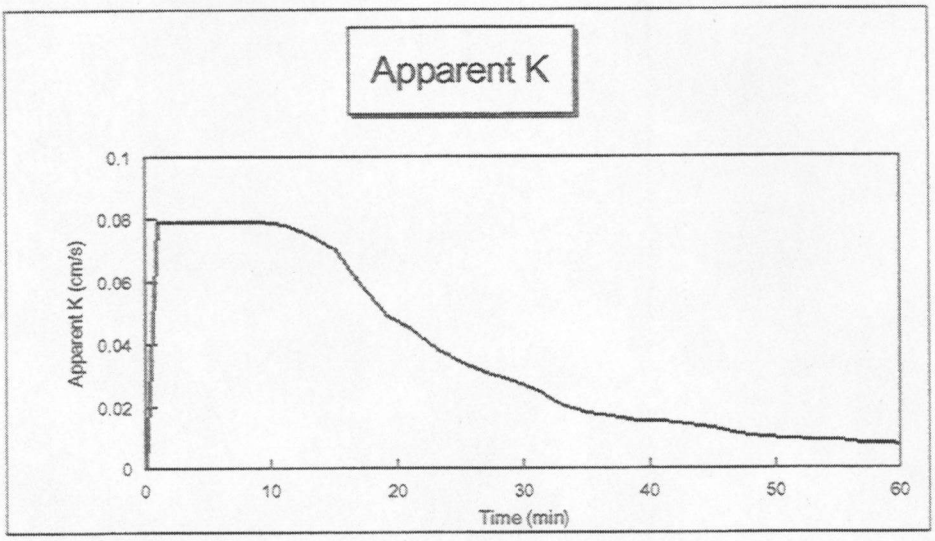
Initial Batch w%= 71.9%
Initial Sample w%= 50.3%

Thickness = 2.55 cm
Diameter = 9.5 cm

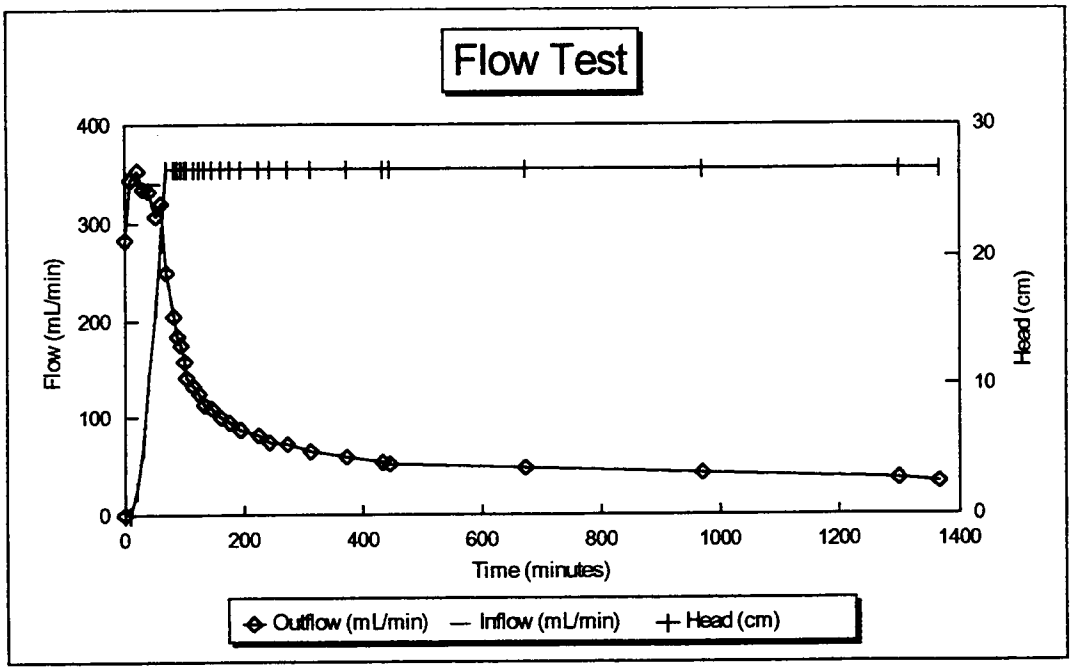
Maximum Aperture = 5.3 mm

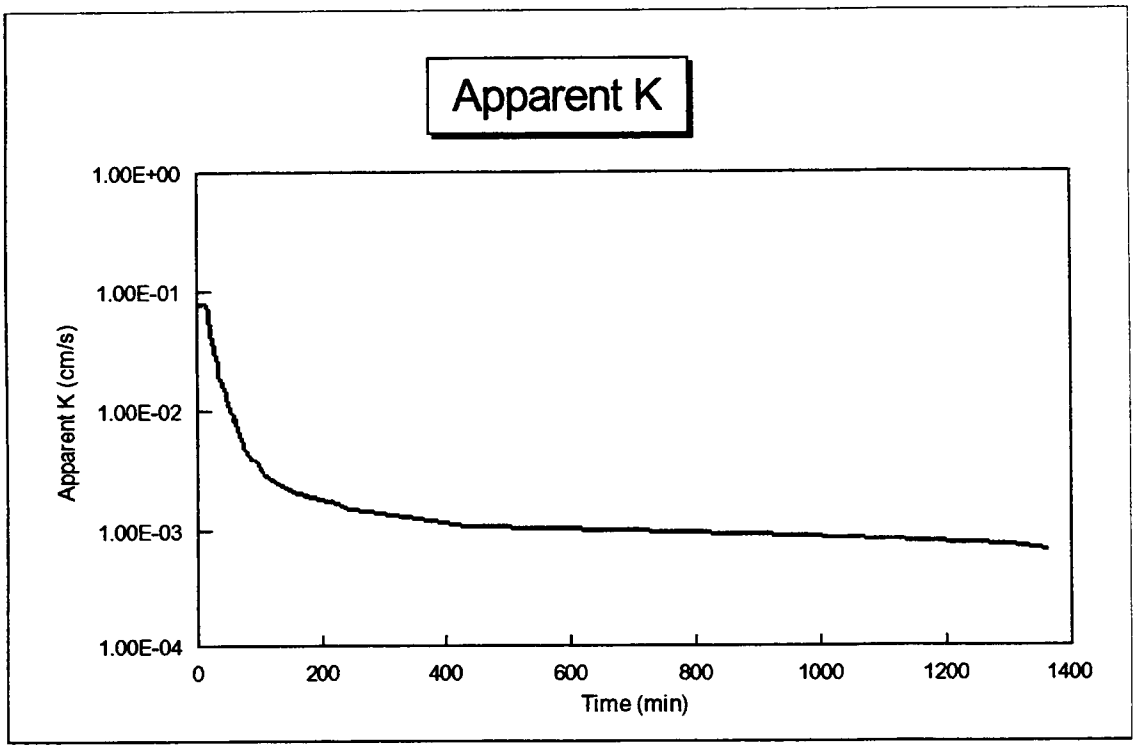
Fracture Area Percentage
Top of Sample = 4.5%
Bottom of Sample = 2.0%





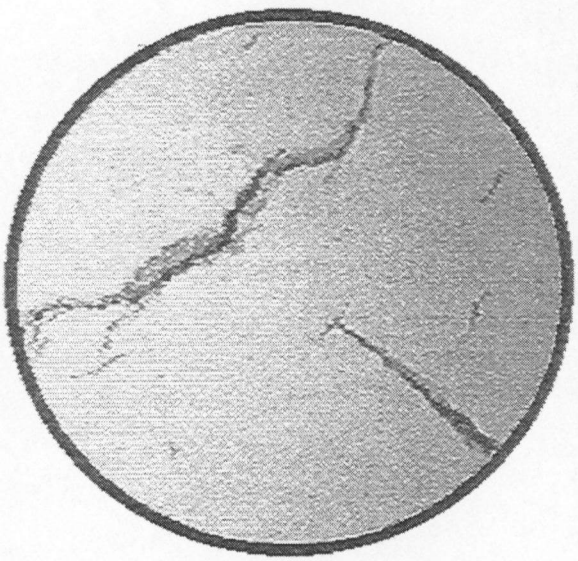
Long Term Test: Batch 5 - Sample 3



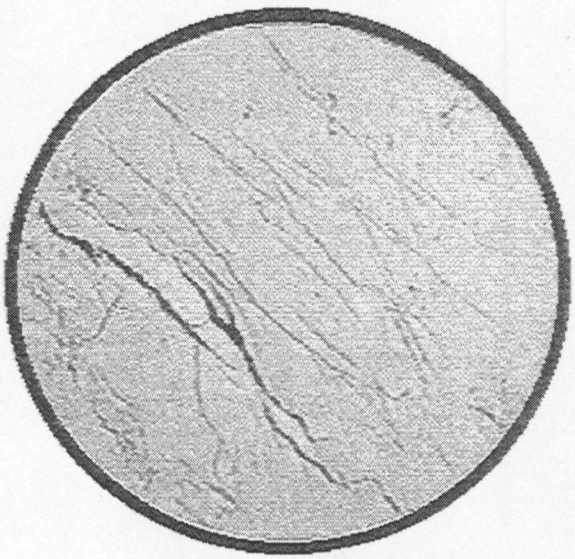


Batch #5 - Sample #3

Before Testing



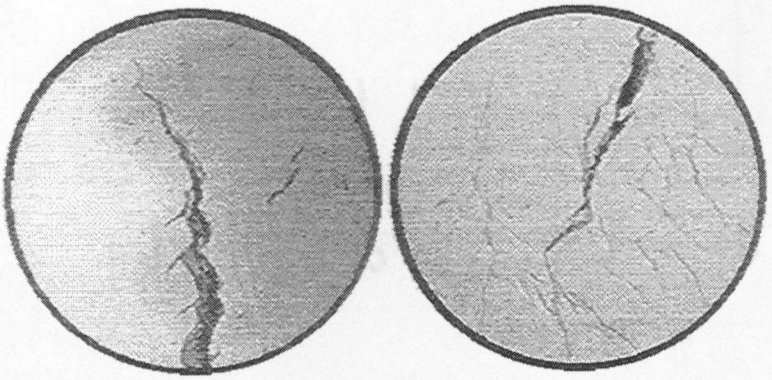
Top of Sample



Bottom of Sample

GILBERT
100% COTTON

Flow Test: Batch #5, Sample #4



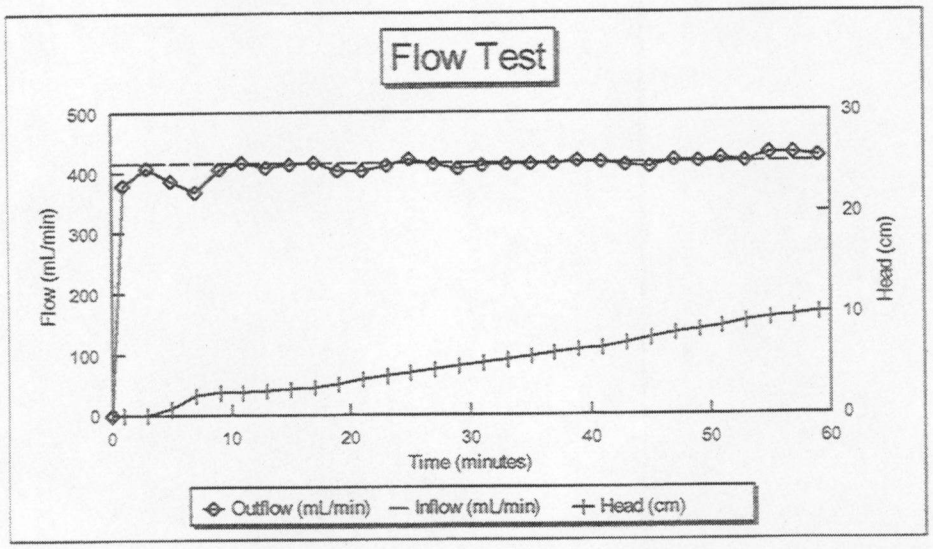
Top of Sample Bottom of Sample

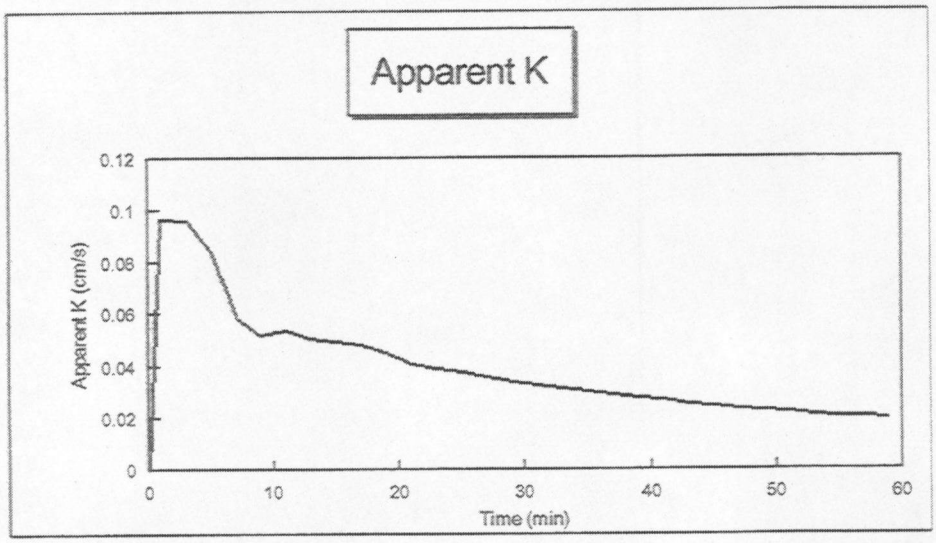
Initial Batch w%= 71.9%
Initial Sample w%= 50.0%

Thickness = 2.65 cm
Diameter = 9.5 cm

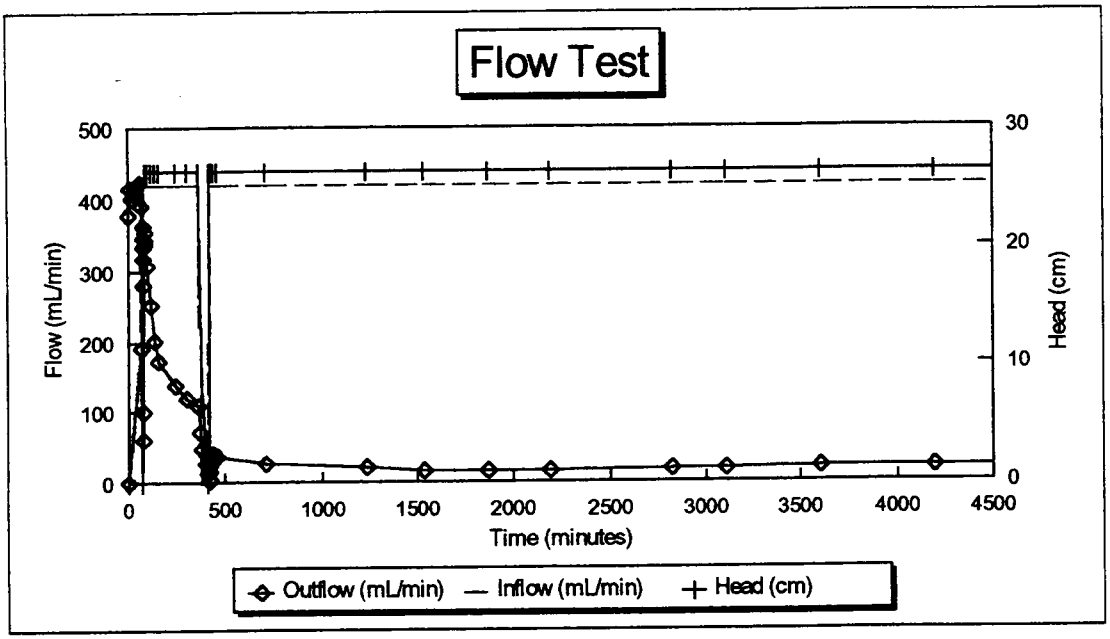
Maximum Aperture = 7.2 mm

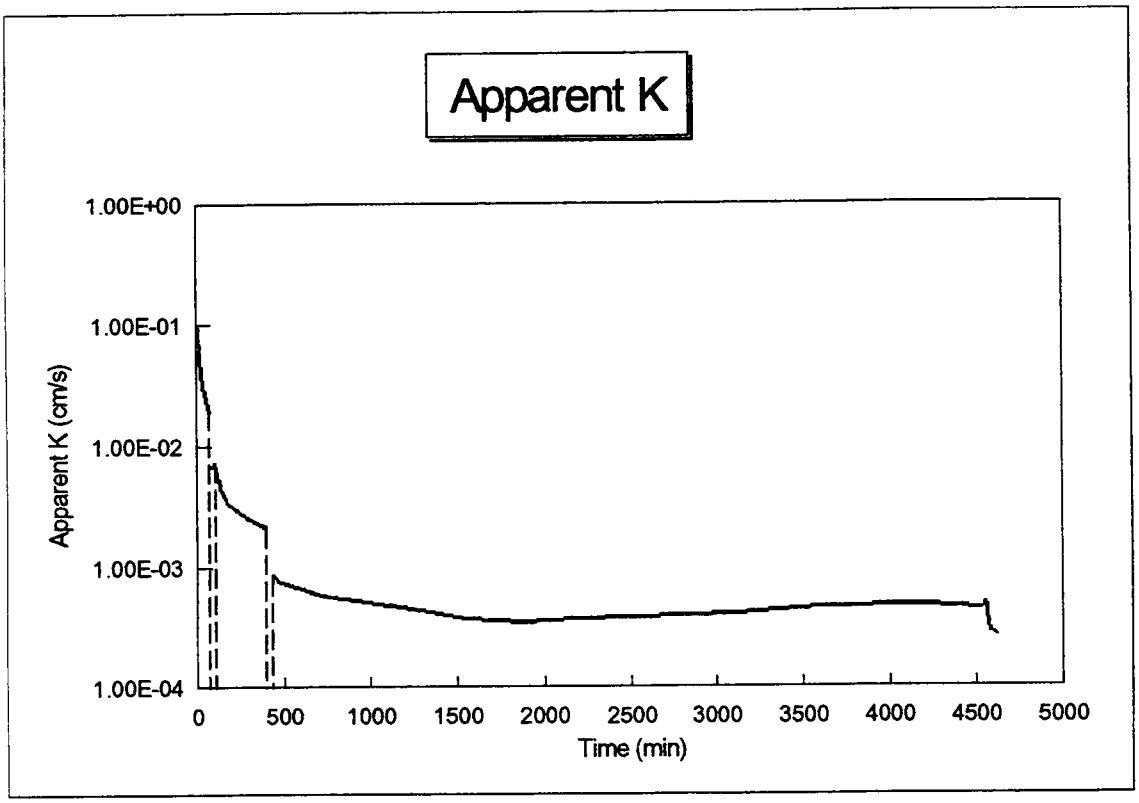
Fracture Area Percentage
Top of Sample = 4.9%
Bottom of Sample = 2.5%





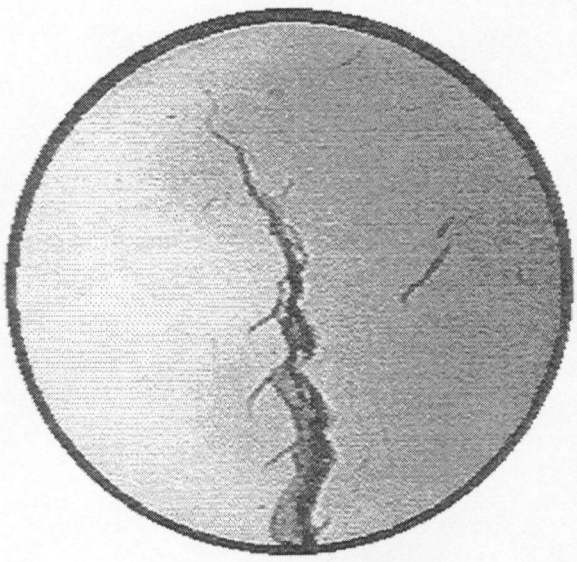
Long Term Test: Batch 5 - Sample 4



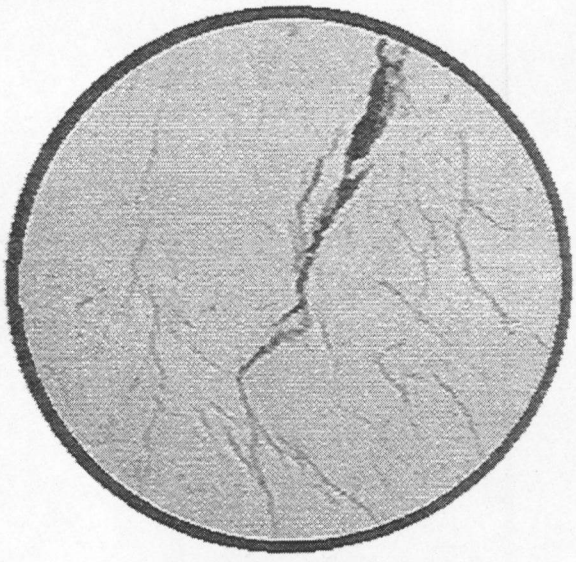


Batch #5 - Sample #4

Before Testing

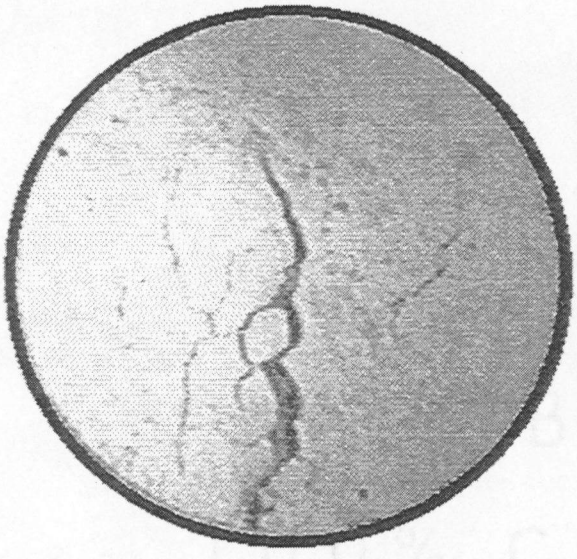


Top of Sample

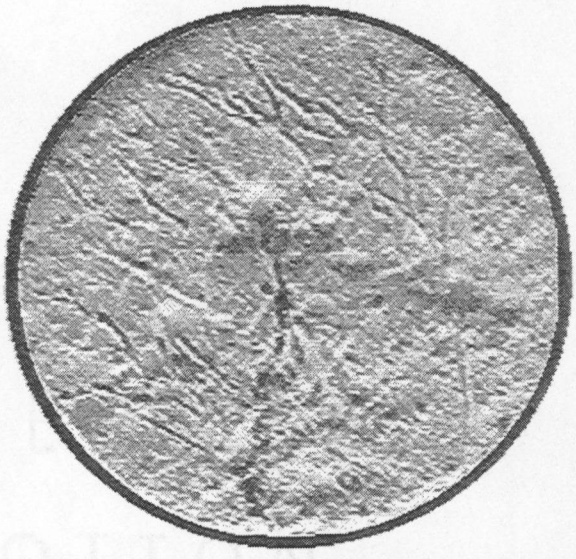


Bottom of Sample

After Testing



Top of Sample (12 hrs after test)



Bottom of Sample (12 hrs after test)

Flow Test: Batch #5, Sample #5



Top of Sample



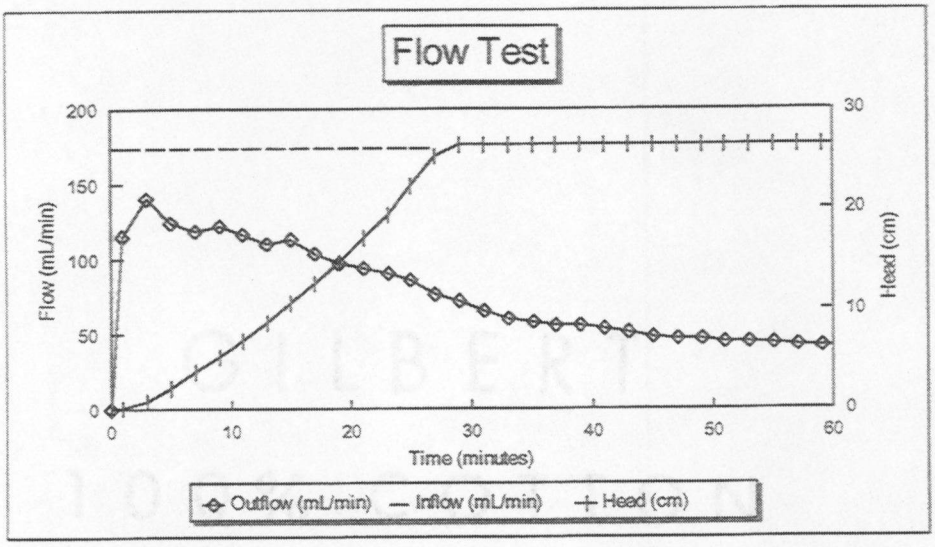
Bottom of Sample

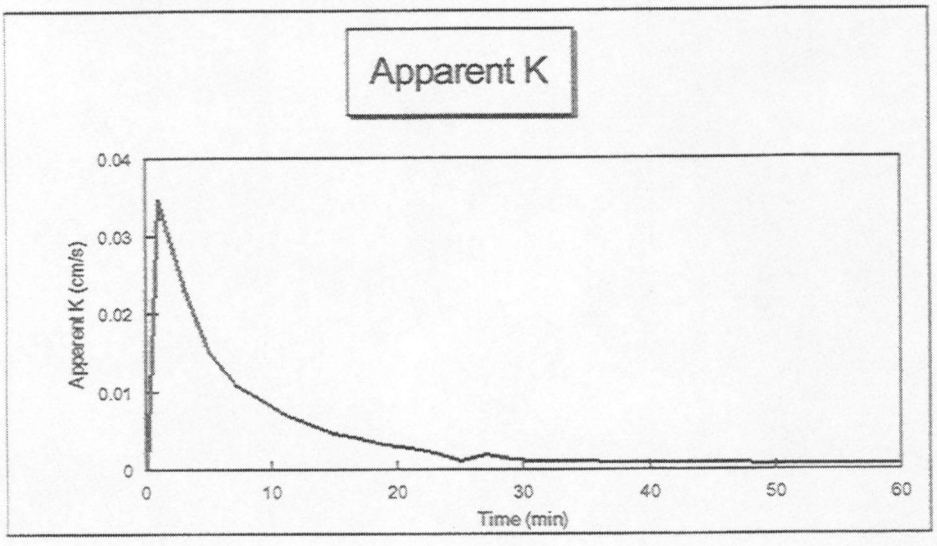
Initial Batch w%= 71.9%
Initial Sample w%= 47.2%

Thickness = 2.65 cm
Diameter = 9.5 cm

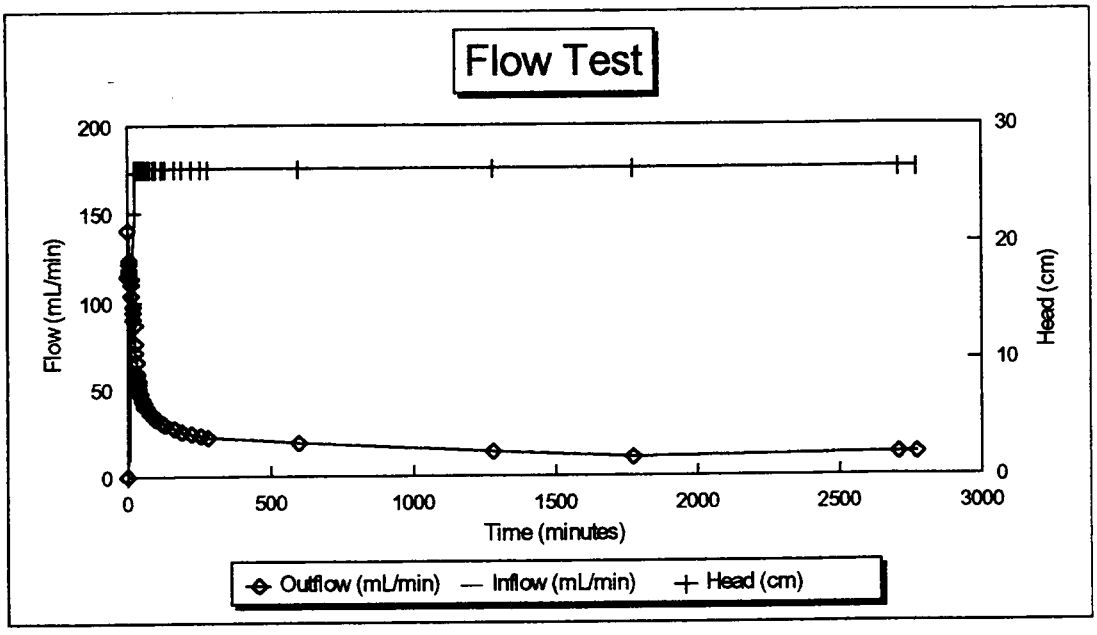
Maximum Aperture = 1.8 mm

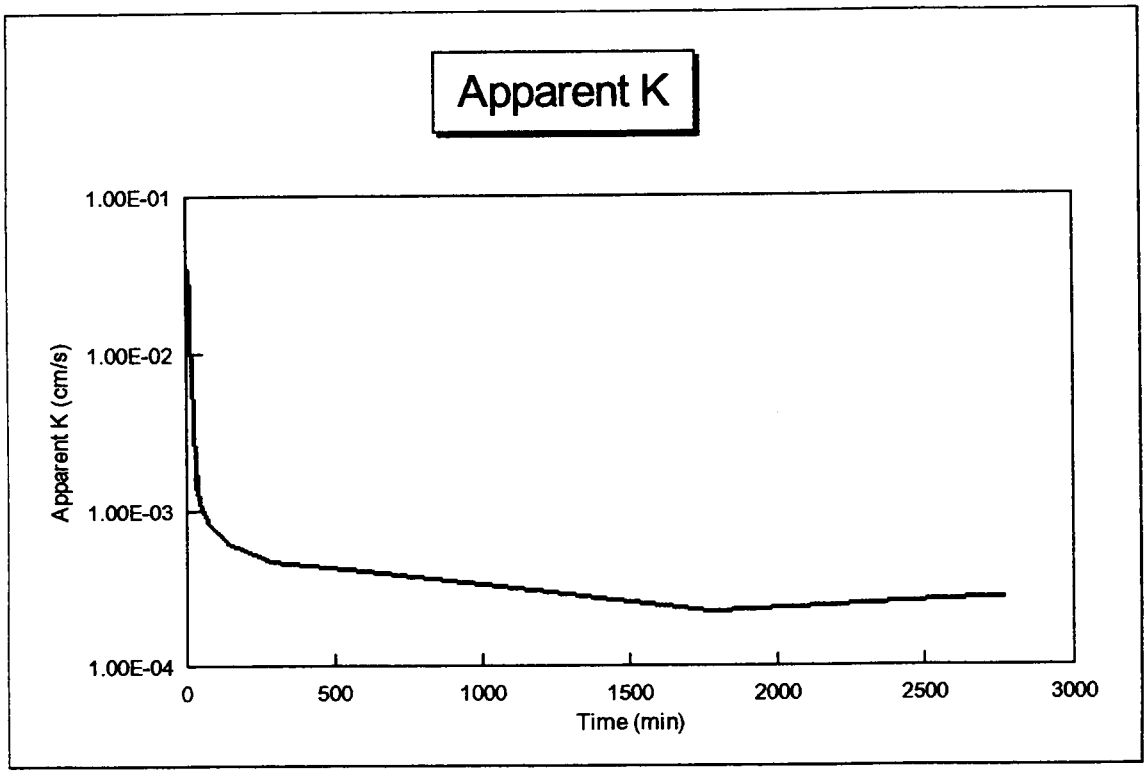
Fracture Area Percentage
Top of Sample = 2.8%
Bottom of Sample = 0.99%





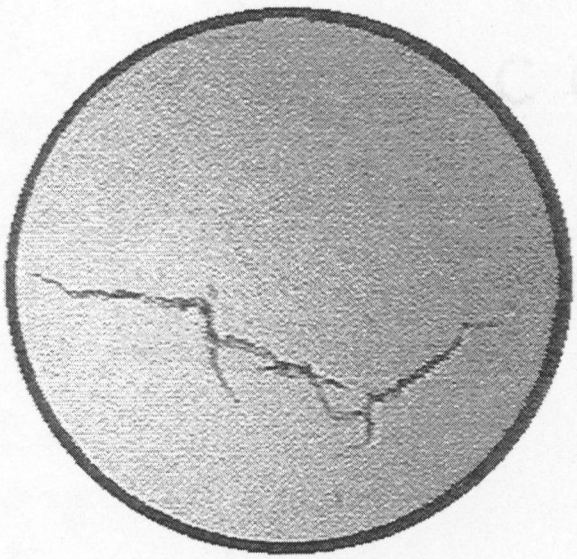
Long Term Test: Batch 5 - Sample 5



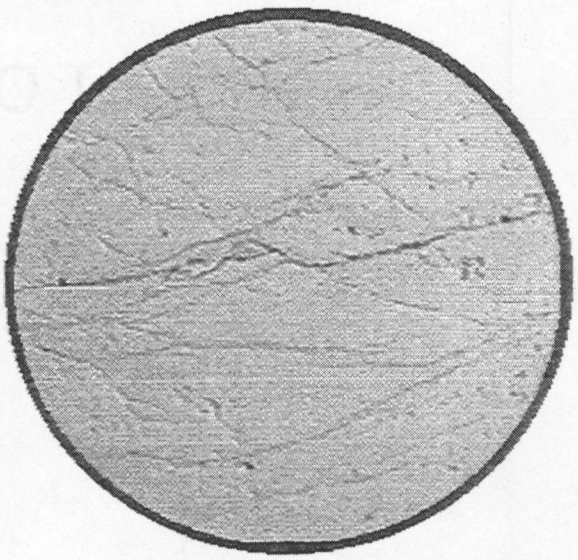


Batch #5 - Sample #5

Before Testing

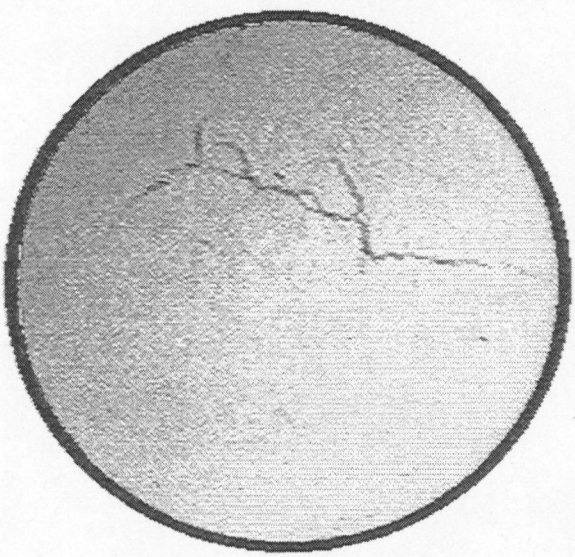


Top of Sample



Bottom of Sample

After Testing

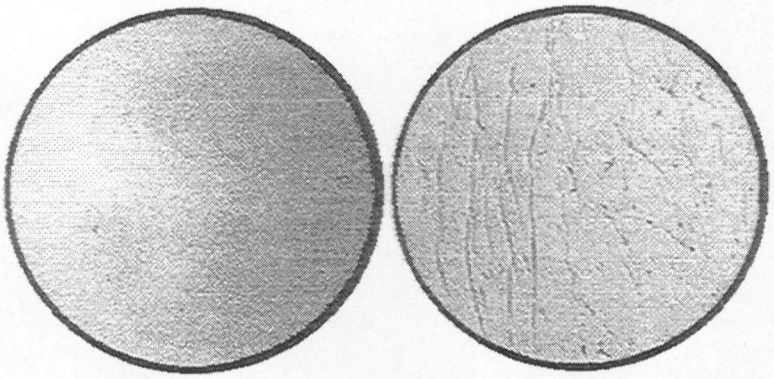


Top of Sample



Bottom of Sample

Flow Test: Batch #5, Sample #6



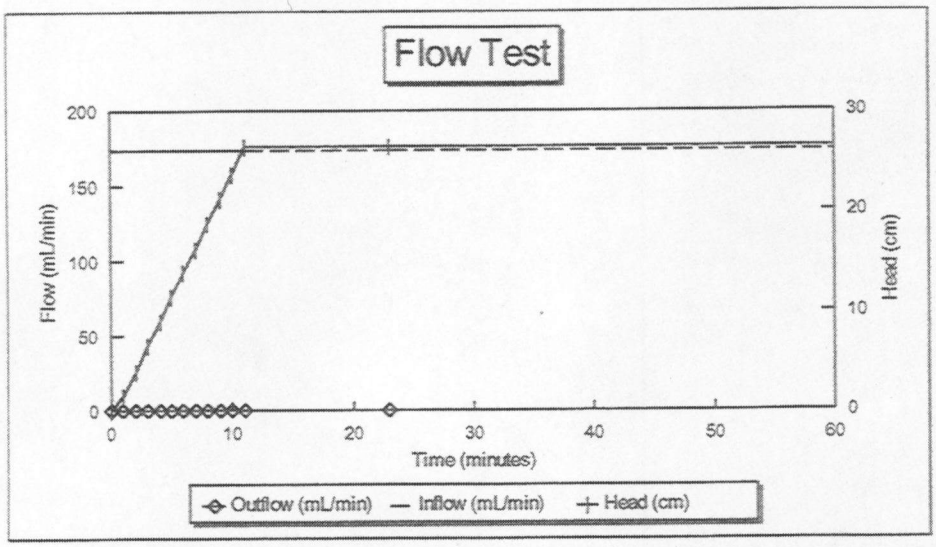
Top of Sample Bottom of Sample

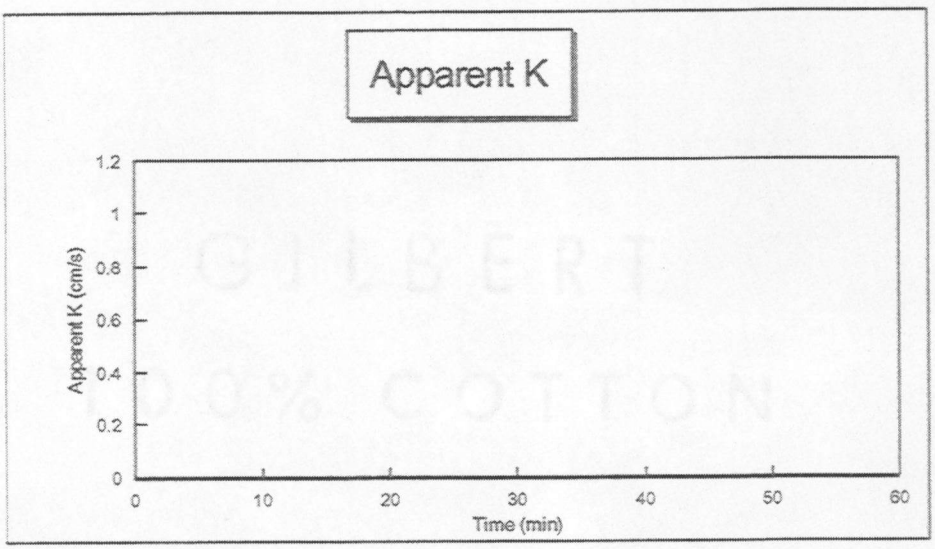
Initial Batch w%= 71.9%
Initial Sample w%= 45.3%

Thickness = 2.5 cm
Diameter = 9.5 cm

Maximum Aperture = 0.0 mm

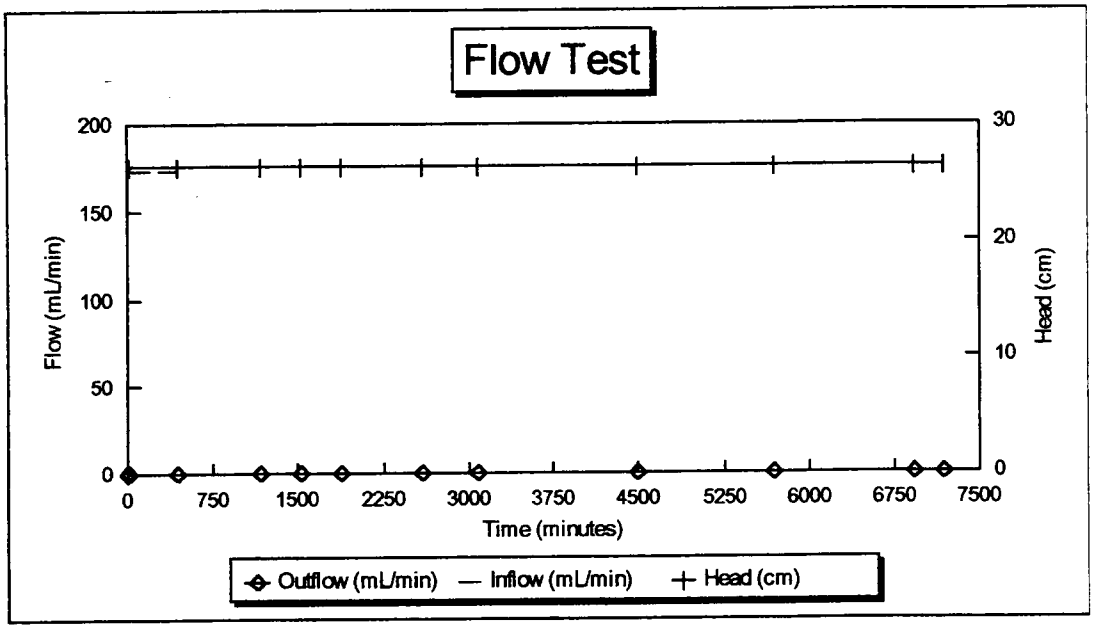
Fracture Area Percentage
Top of Sample = 0.0%
Bottom of Sample = 0.0%

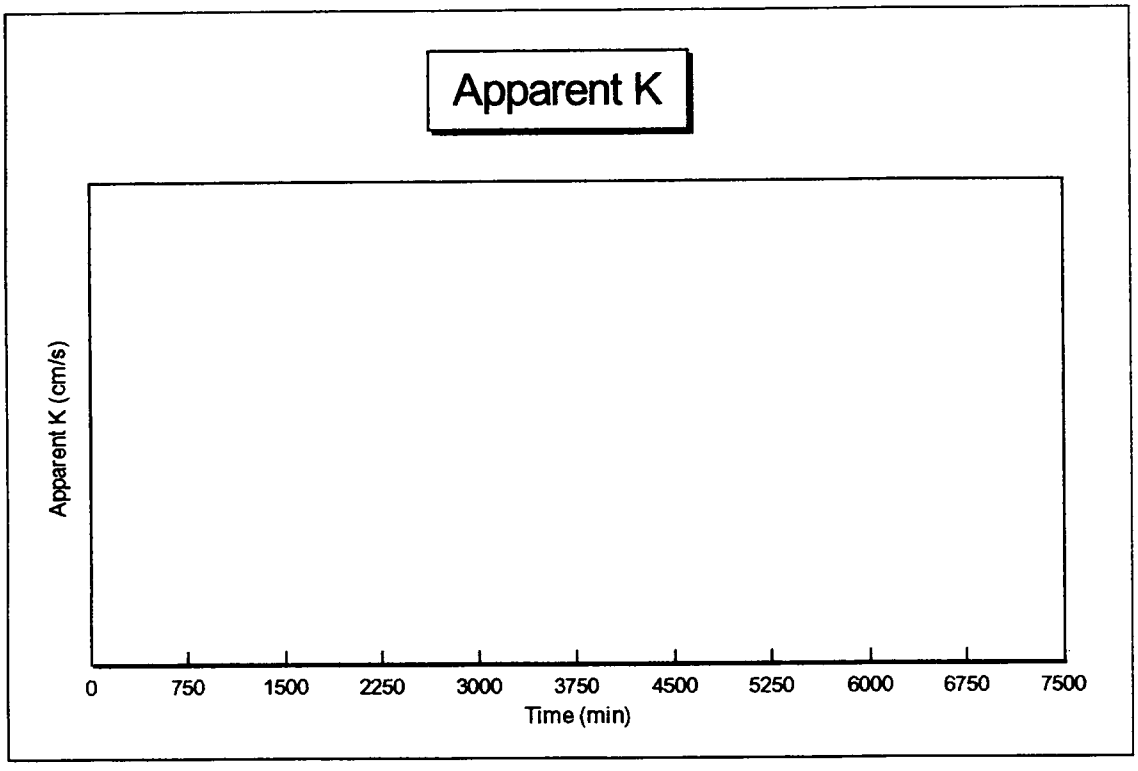




GILBERT
100% COTTON

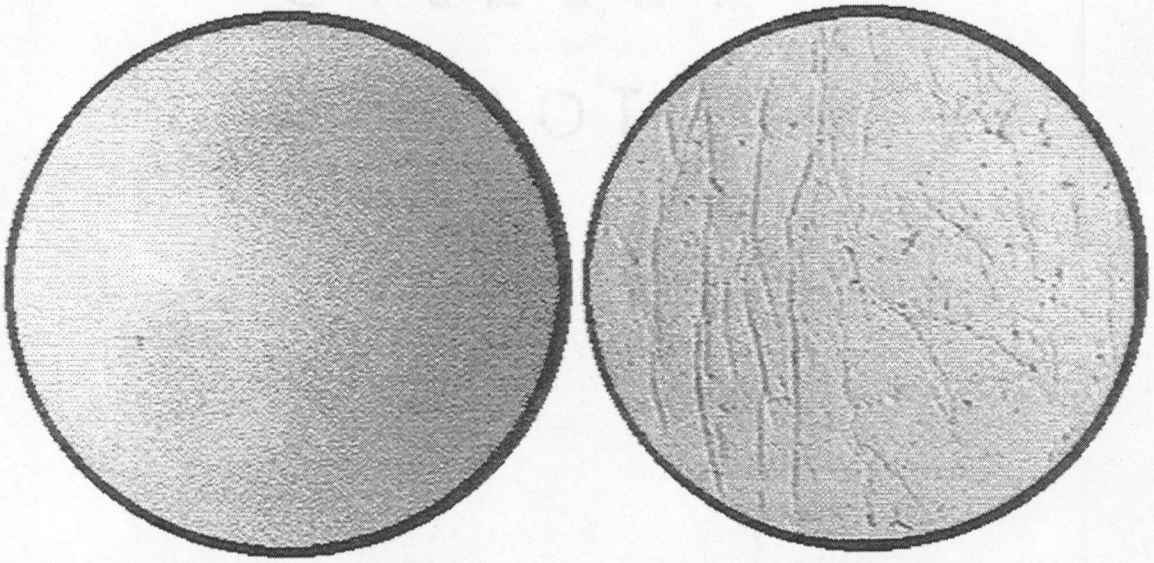
Long Term Test: Batch 5 - Sample 6





Batch #5 - Sample #6

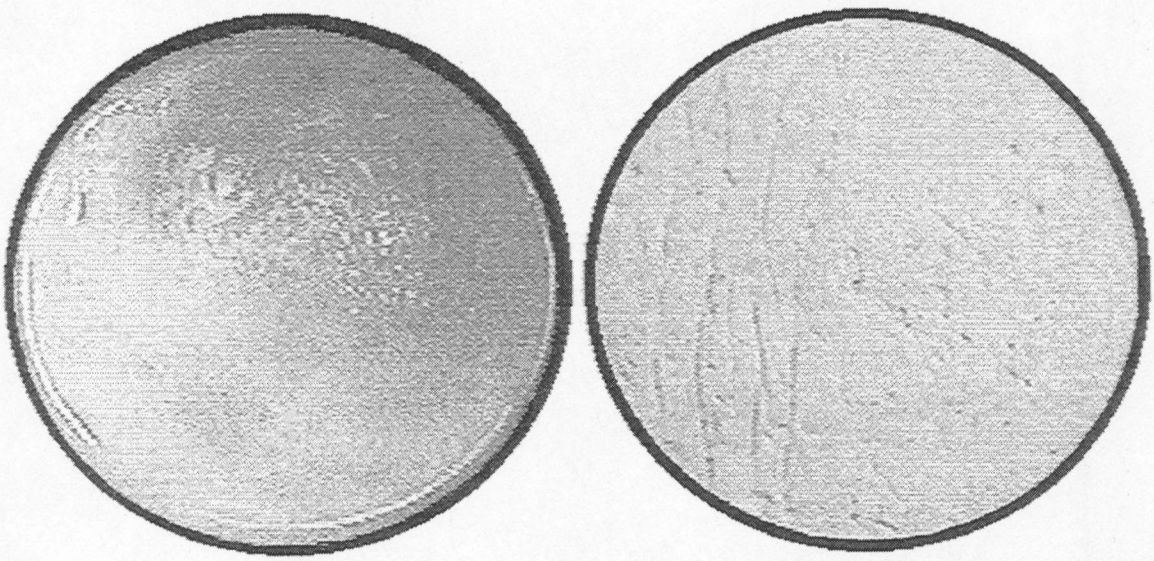
Before Testing



Top of Sample

Bottom of Sample

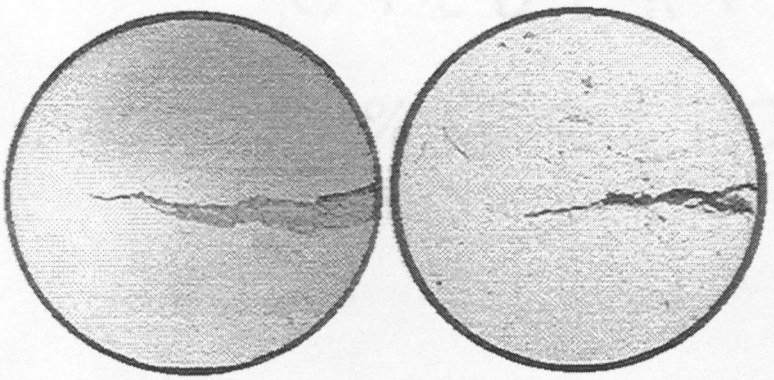
After Testing



Top of Sample

Bottom of Sample

Flow Test: Batch #6, Sample #1



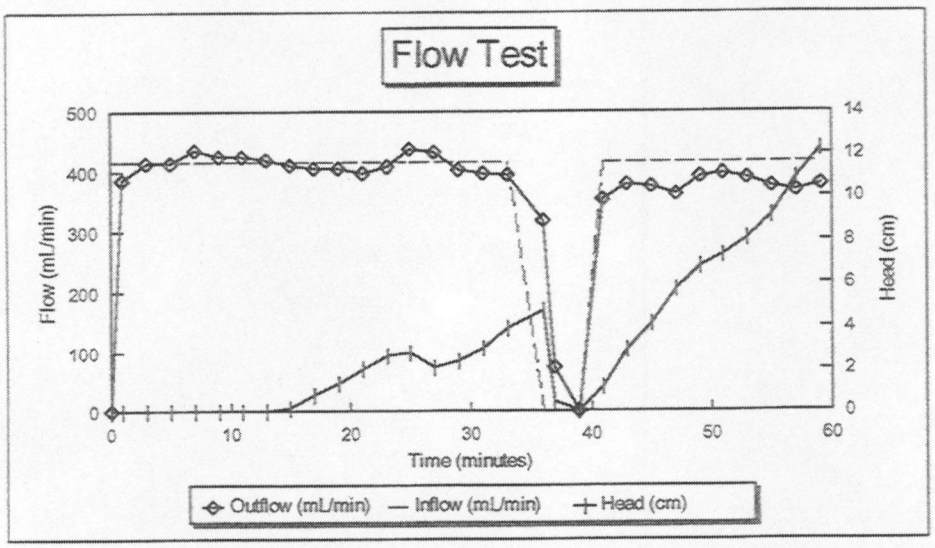
Top of Sample Bottom of Sample

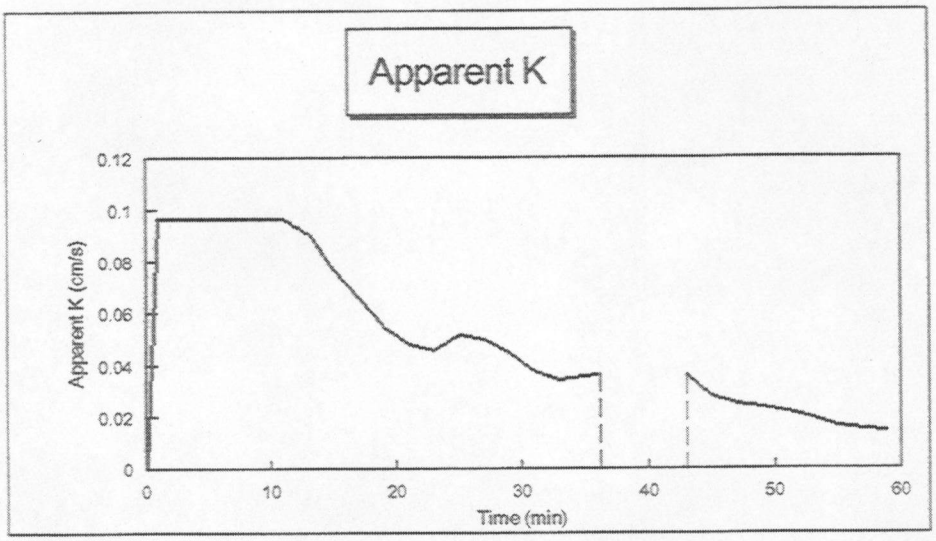
Initial Batch w%= 71.4%
Initial Sample w%= 48.0%

Thickness = 2.5 cm
Diameter = 9.5 cm

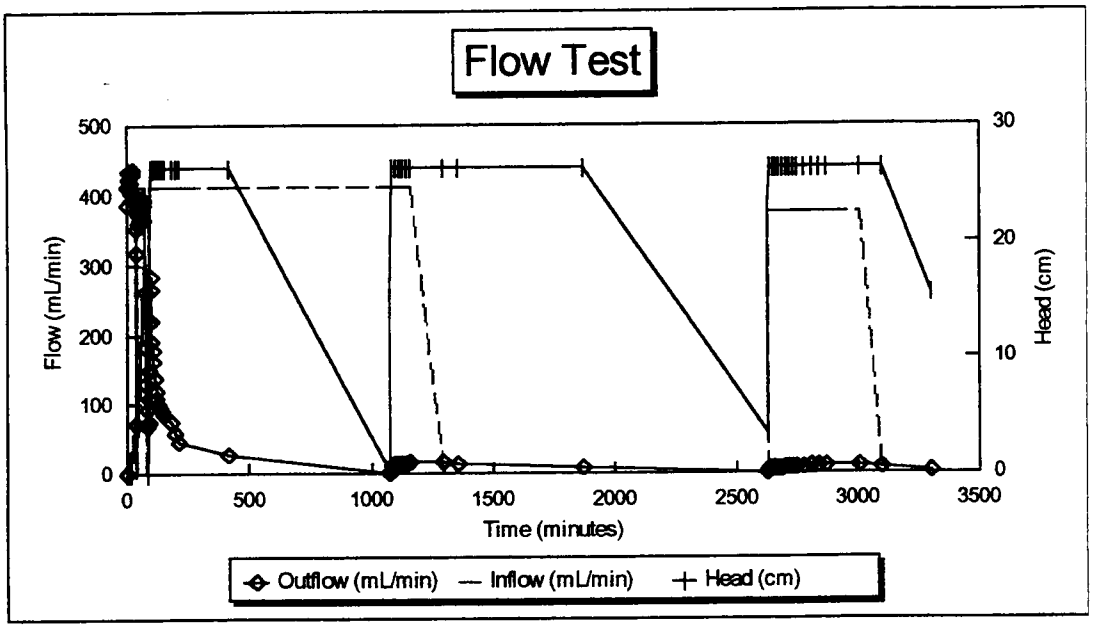
Maximum Aperture = 9.4 mm

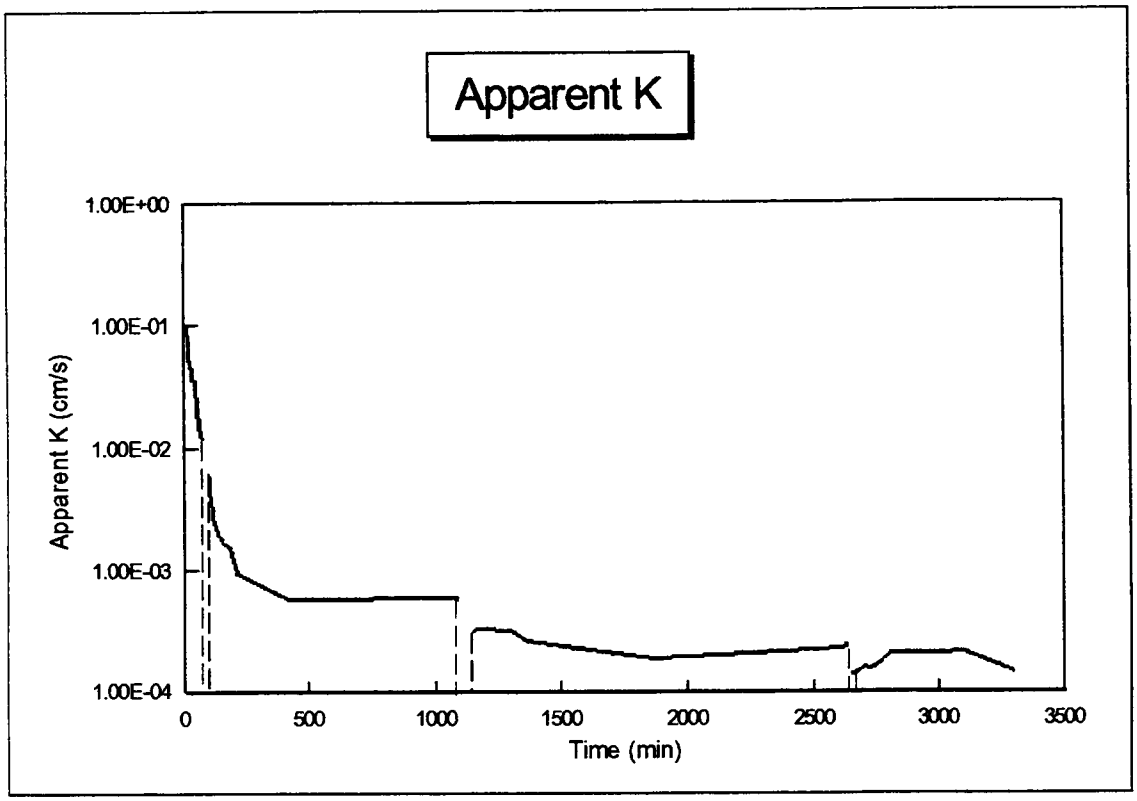
Fracture Area Percentage
Top of Sample = 5.7%
Bottom of Sample = 2.5%





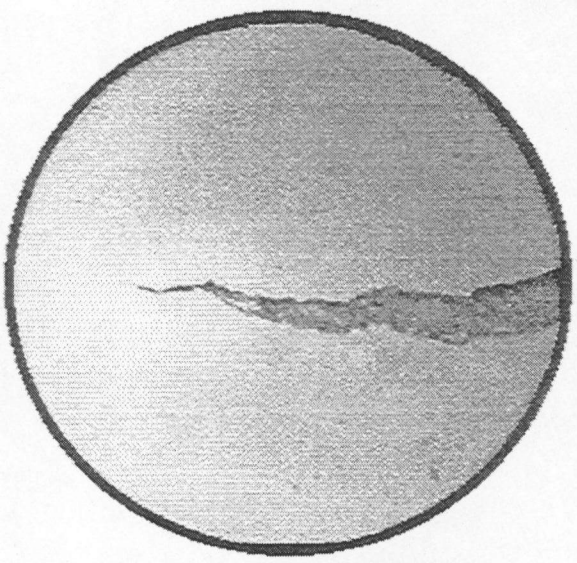
Long Term Test: Batch 6 - Sample 1



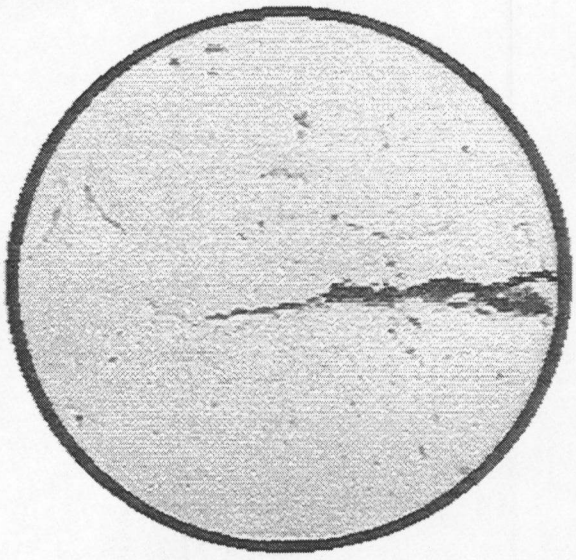


Batch #6 - Sample #1

Before Testing

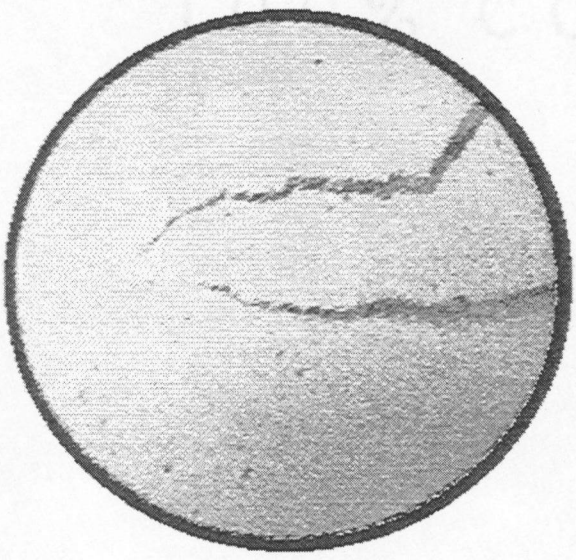


Top of Sample

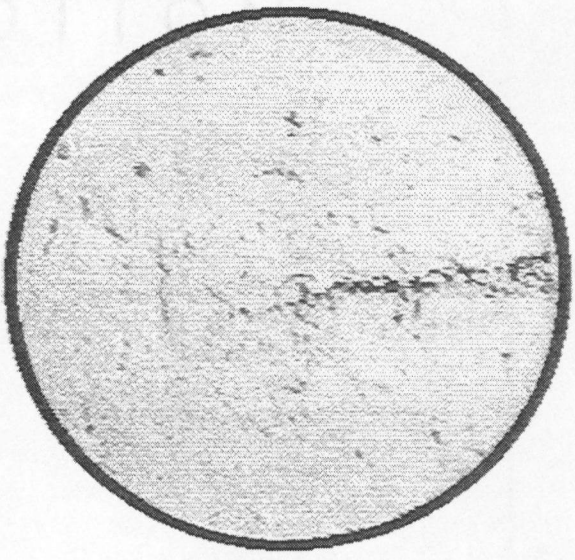


Bottom of Sample

After Testing

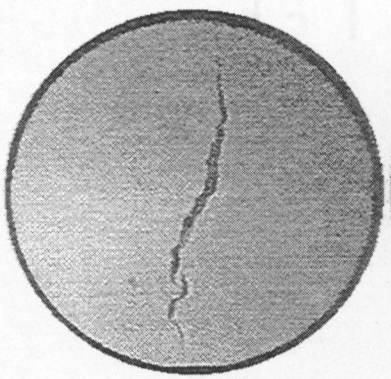


Top of Sample

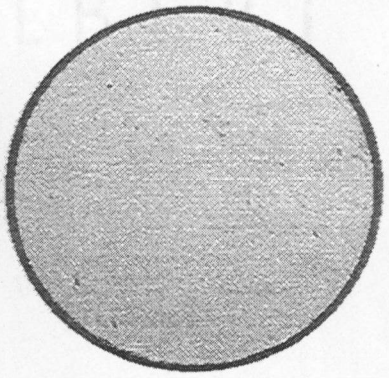


Bottom of Sample

Flow Test: Batch #6, Sample #2



Top of Sample



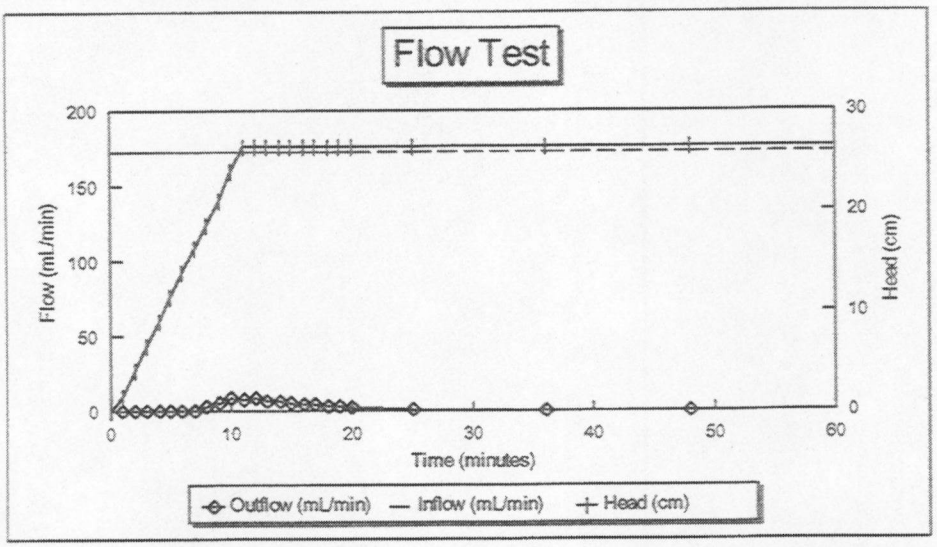
Bottom of Sample

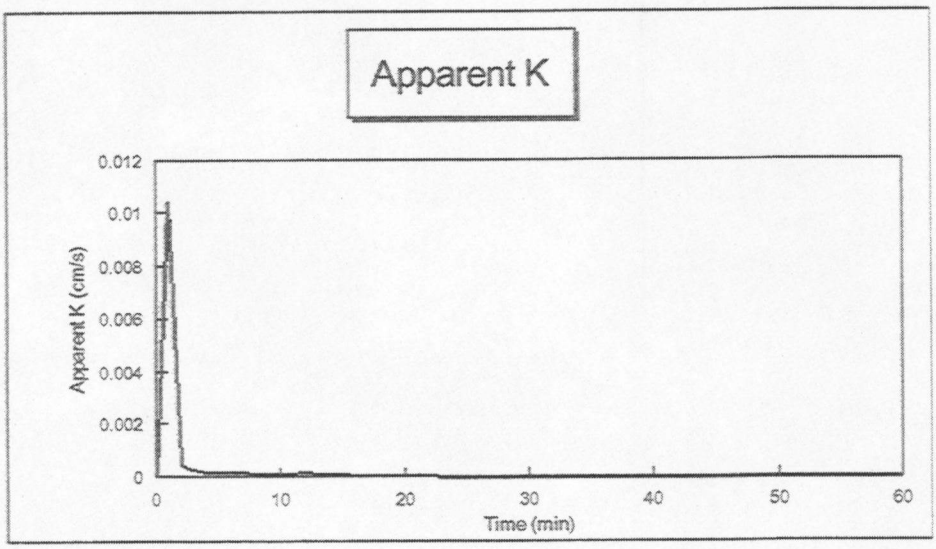
Initial Batch w%= 71.4%
Initial Sample w%= 45.2%

Thickness = 2.5 cm
Diameter = 9.5 cm

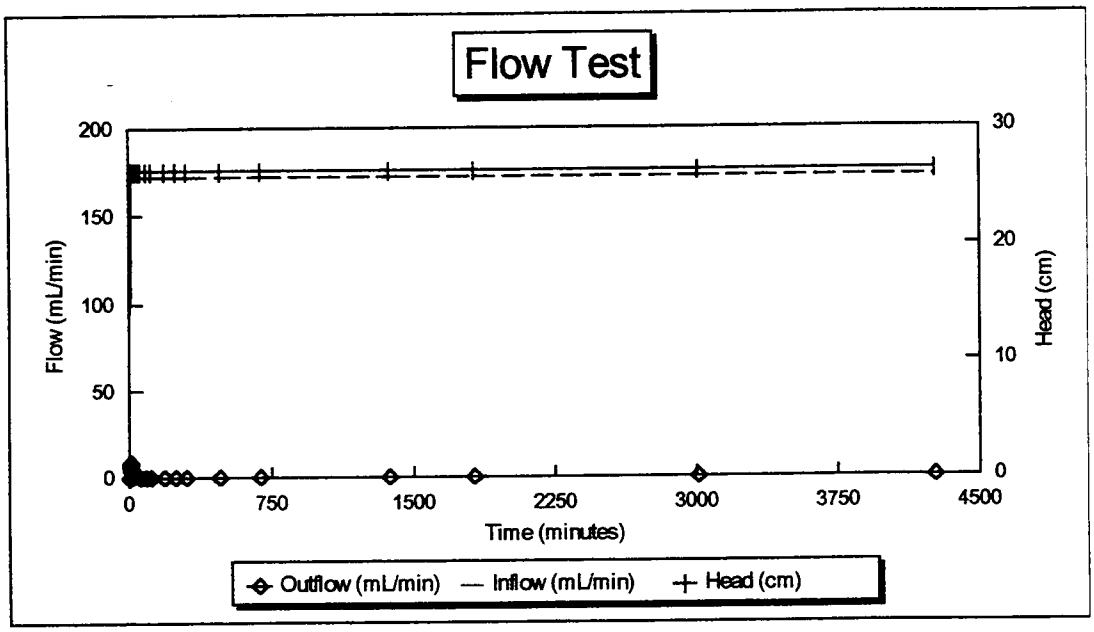
Maximum Aperture = 2.8 mm

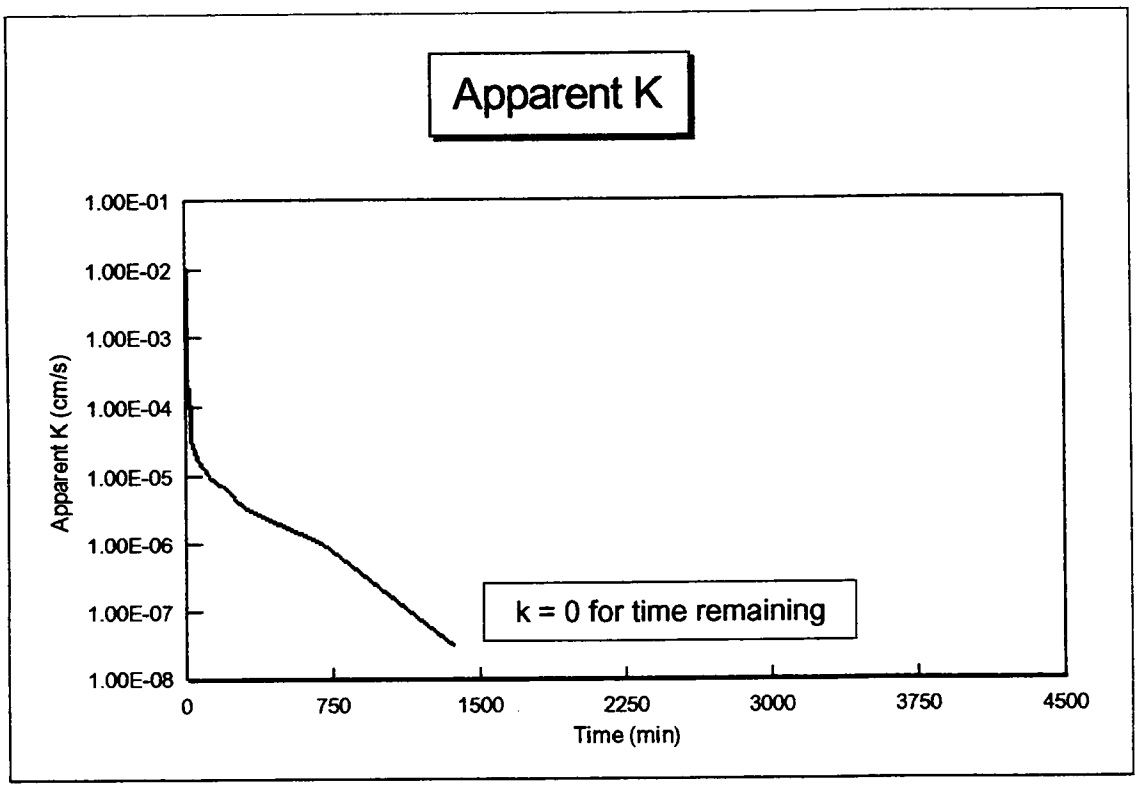
Fracture Area Percentage
Top of Sample = 2.4%
Bottom of Sample = 0.31%





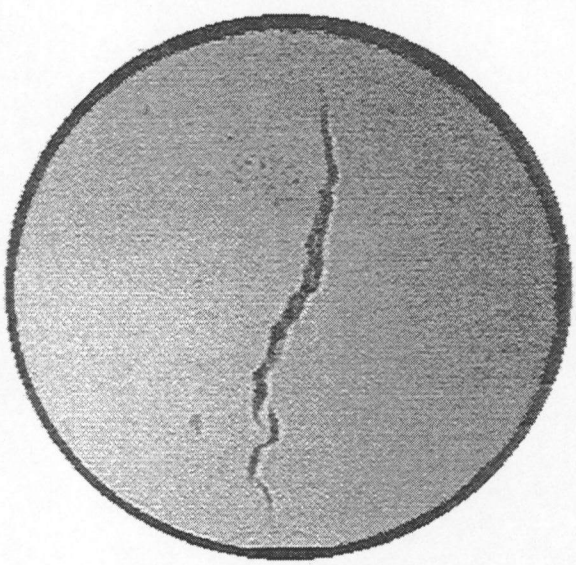
Long Term Test: Batch 6 - Sample 2



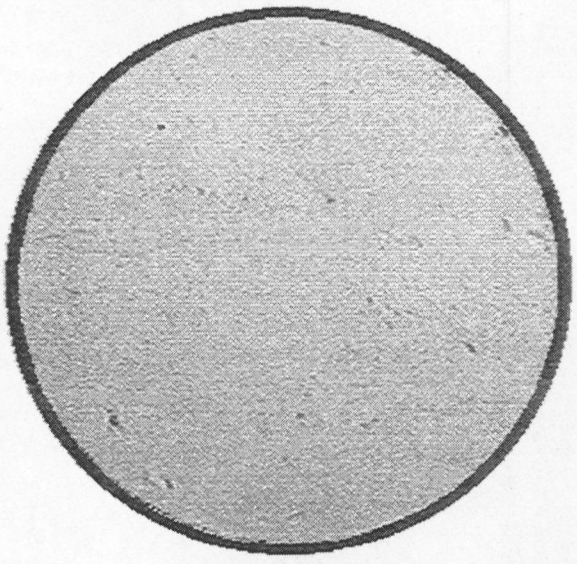


Batch #6 - Sample #2

Before Testing

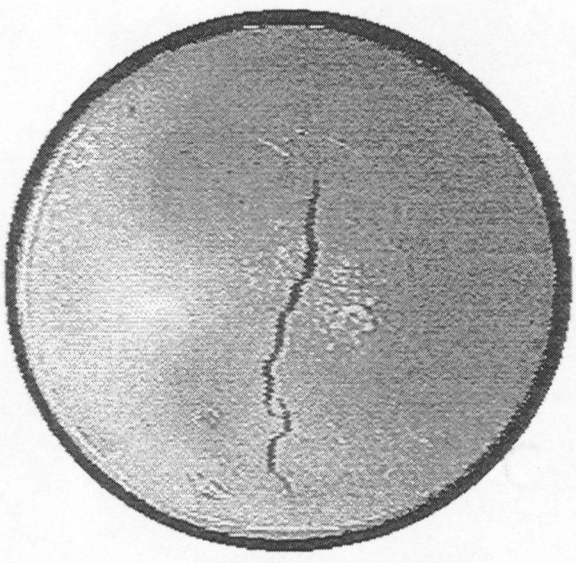


Top of Sample

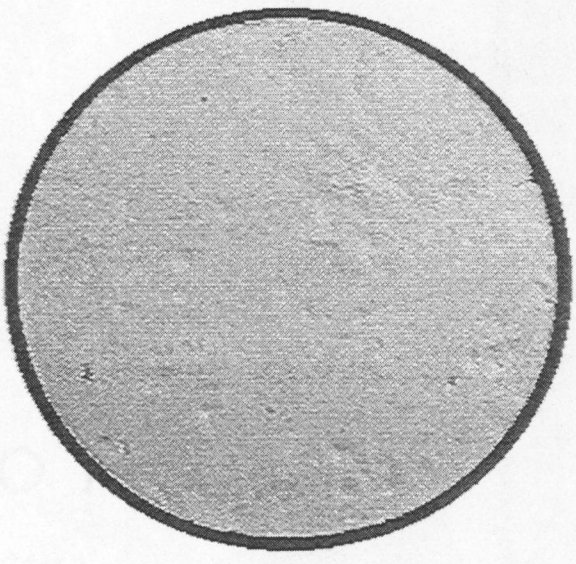


Bottom of Sample

After Testing

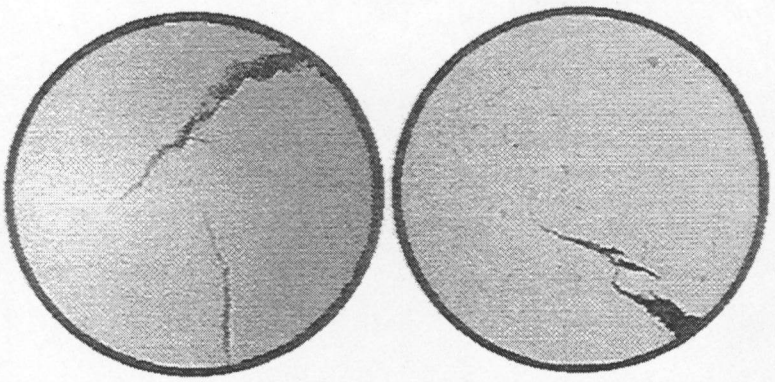


Top of Sample



Bottom of Sample

Flow Test: Batch #6, Sample #3



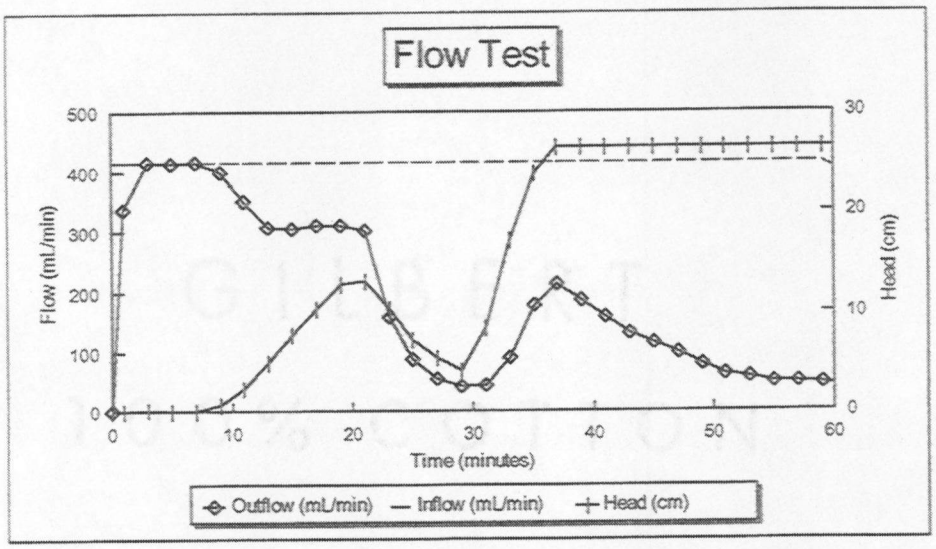
Top of Sample Bottom of Sample

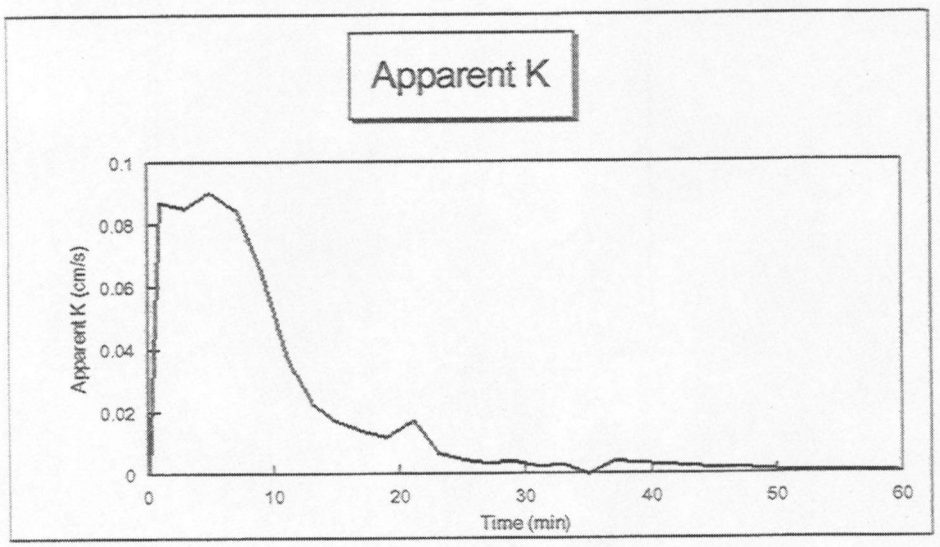
Initial Batch w%= 71.4%
Initial Sample w%= 45.9%

Thickness = 2.5 cm
Diameter = 9.5 cm

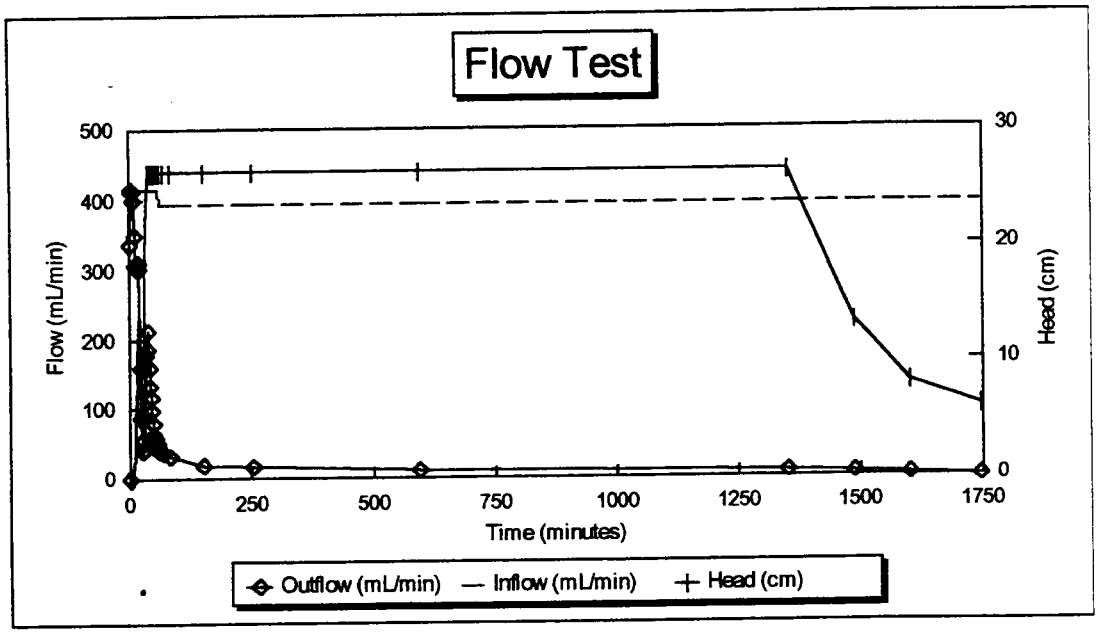
Maximum Aperture = 6.1 mm

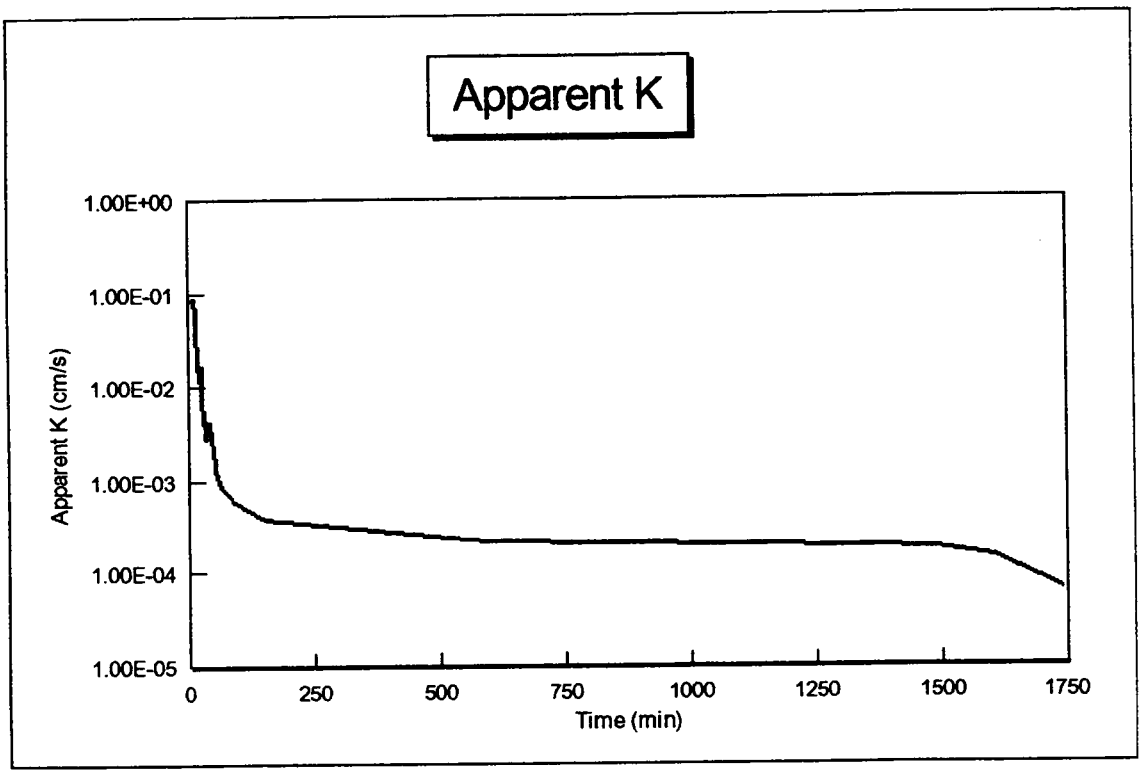
Fracture Area Percentage
Top of Sample = 3.8%
Bottom of Sample = 1.8%





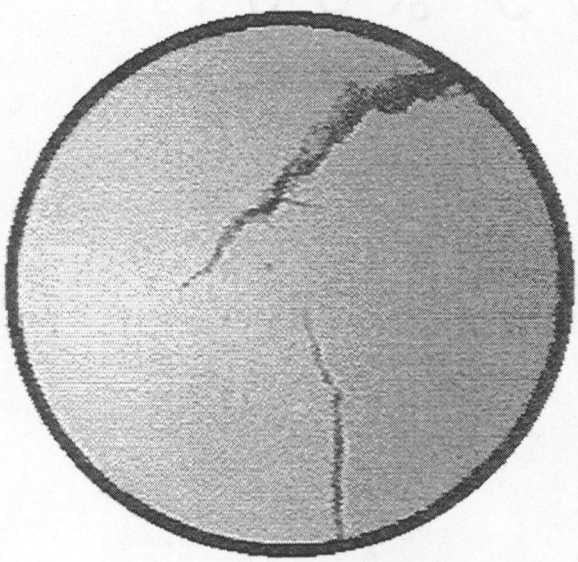
Long Term Test: Batch 6 - Sample 3



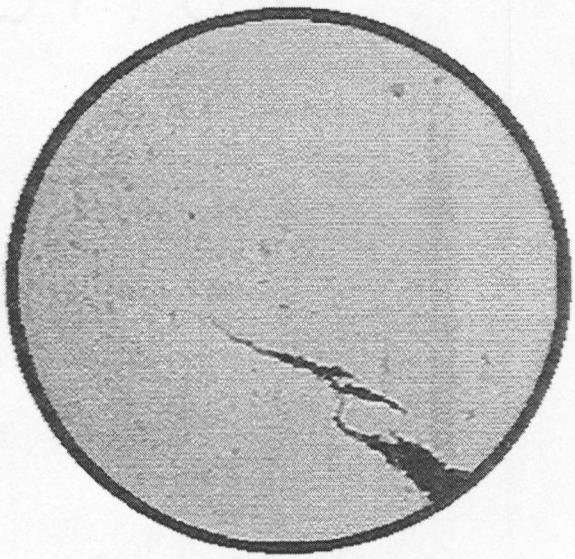


Batch #6 - Sample #3

Before Testing

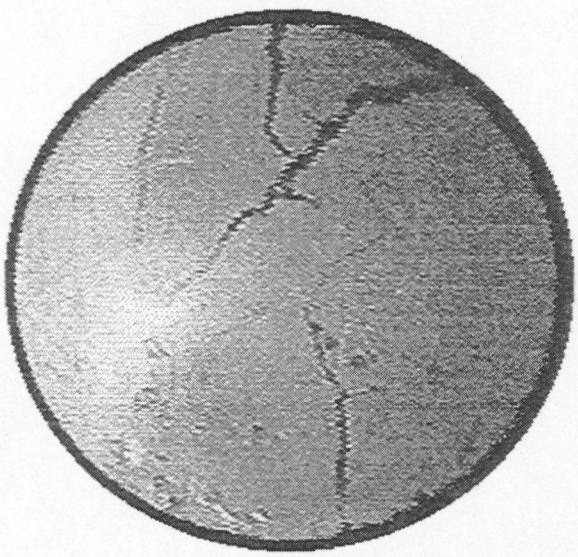


Top of Sample



Bottom of Sample

After Testing

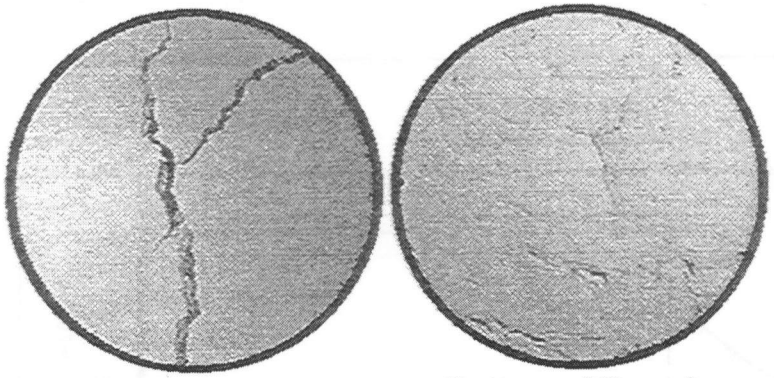


Top of Sample



Bottom of Sample

Flow Test: Batch #8, Sample #1



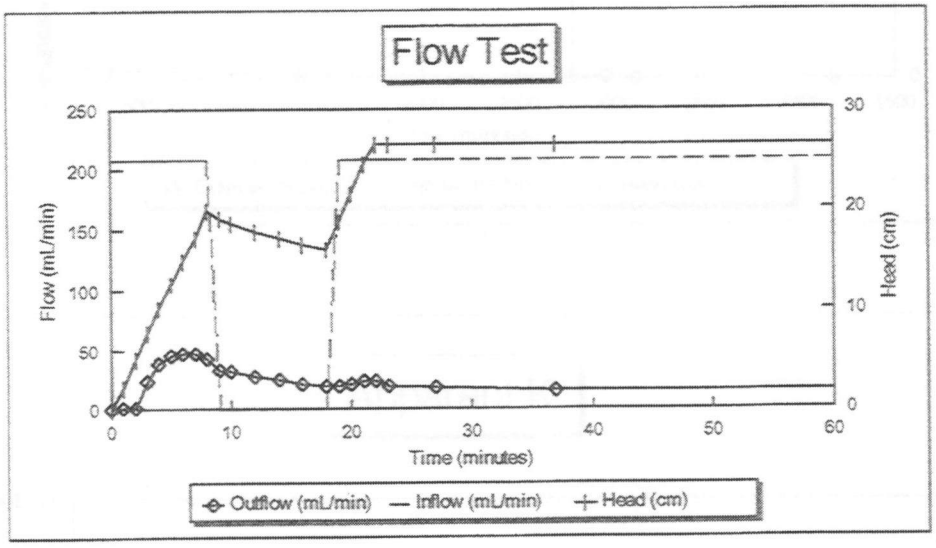
Top of Sample Bottom of Sample

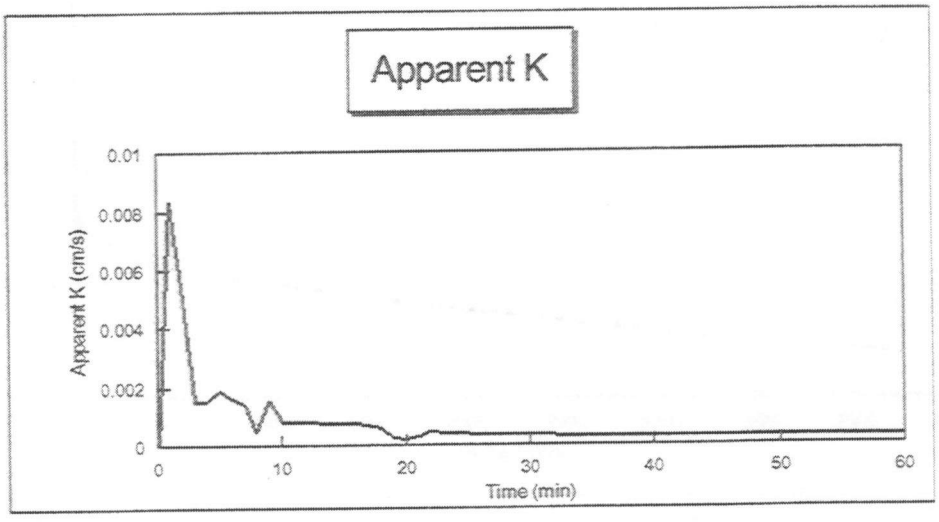
Initial Batch w%= 70.4%
Initial Sample w%= 41.6%

Thickness = 2.5 cm
Diameter = 9.5 cm

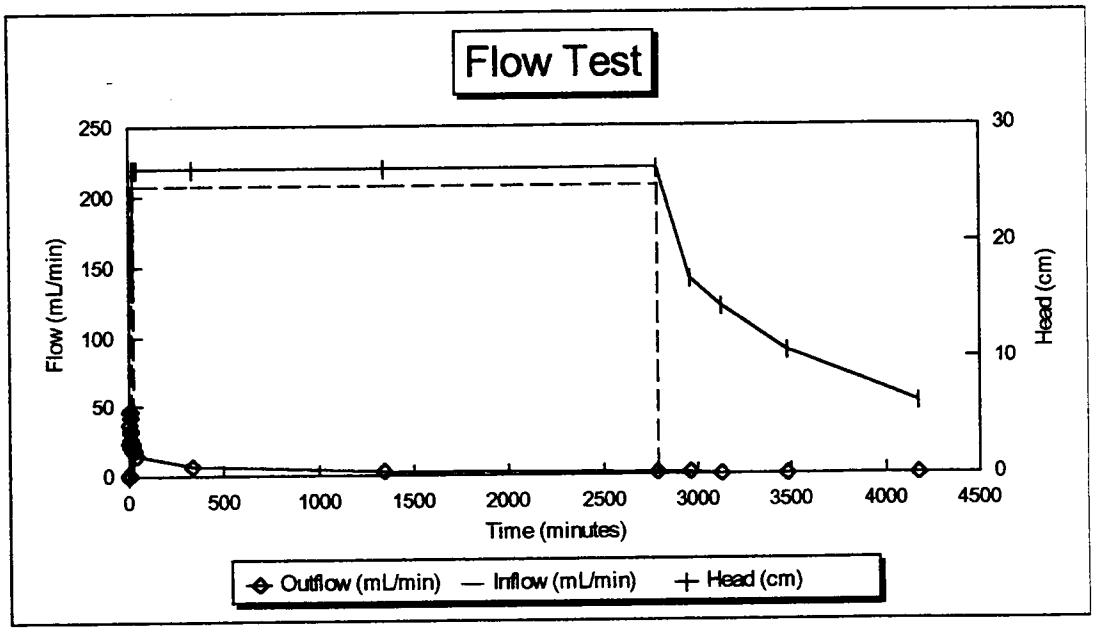
Maximum Aperture = 3.0 mm

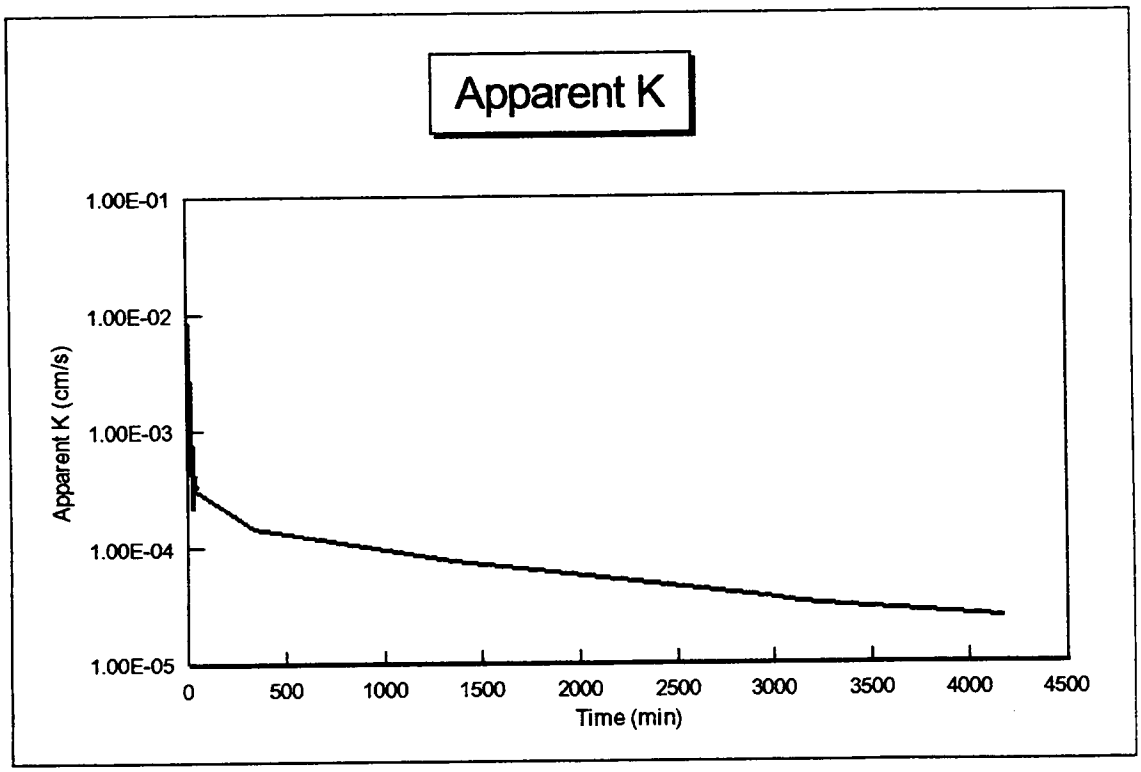
Fracture Area Percentage
Top of Sample = 4.2%
Bottom of Sample = 0.57%





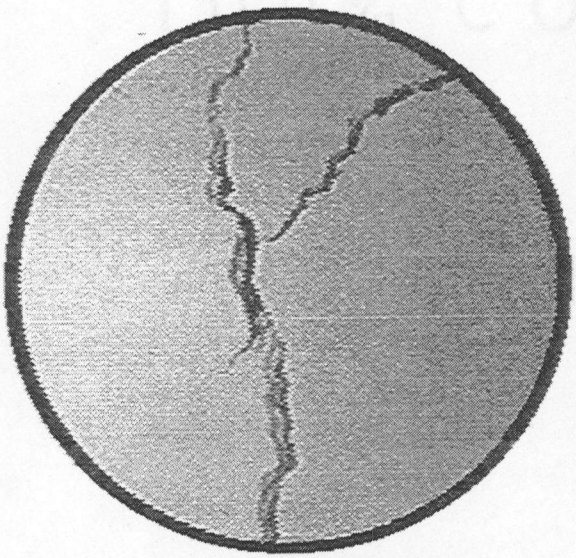
Long Term Test: Batch 8 - Sample 1



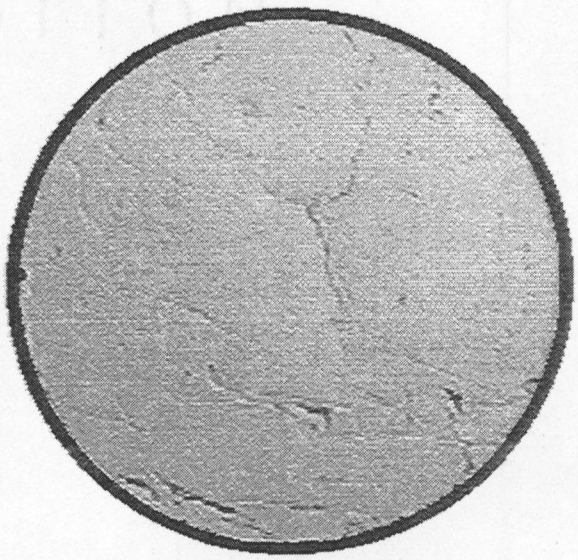


Batch #8 - Sample #1

Before Testing

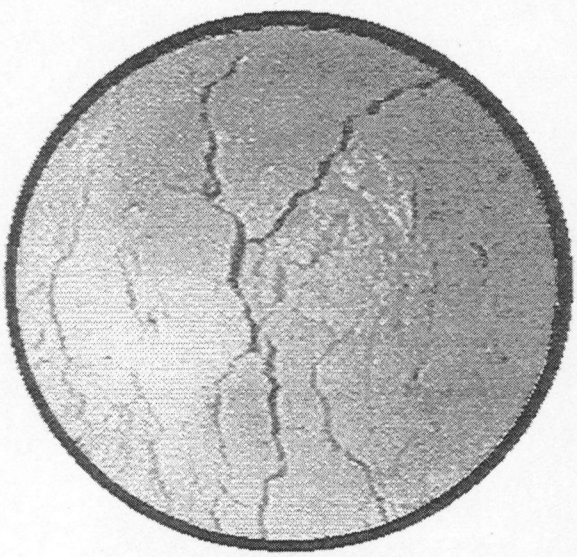


Top of Sample

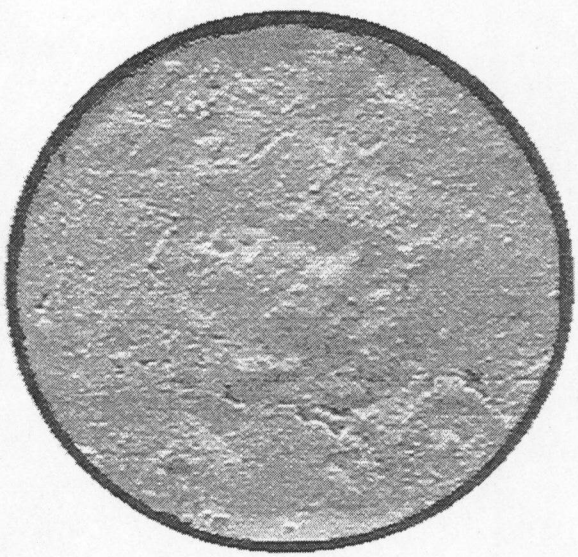


Bottom of Sample

After Testing

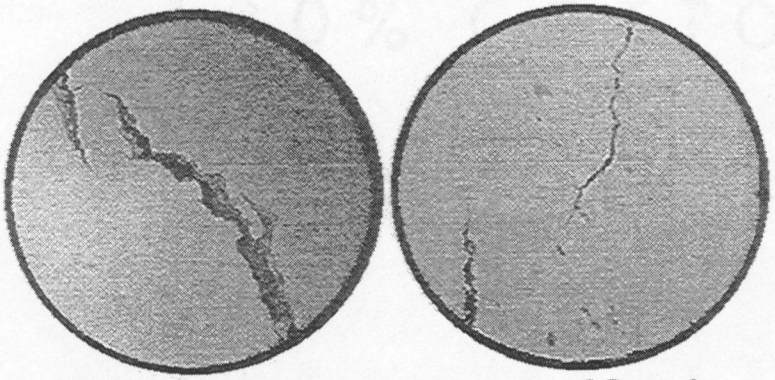


Top of Sample



Bottom of Sample

Flow Test: Batch #8, Sample #2



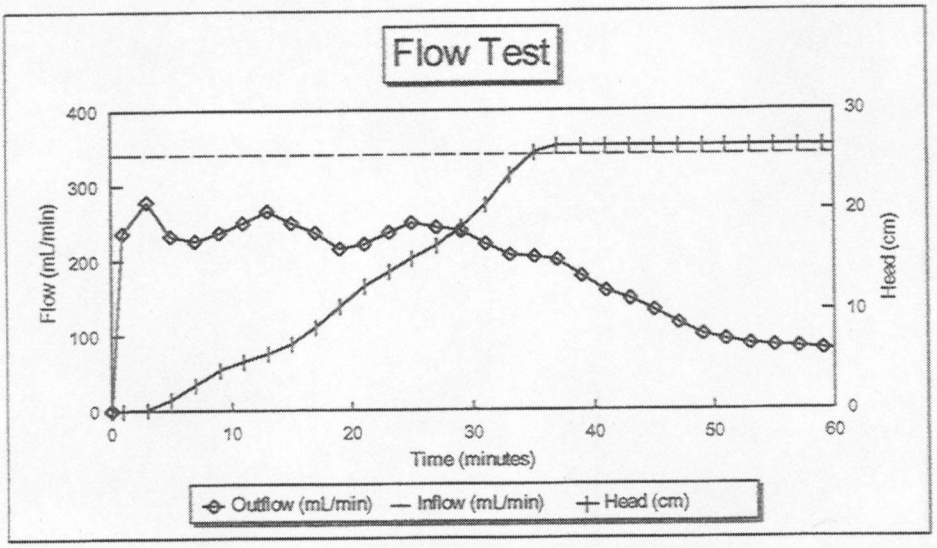
Top of Sample Bottom of Sample

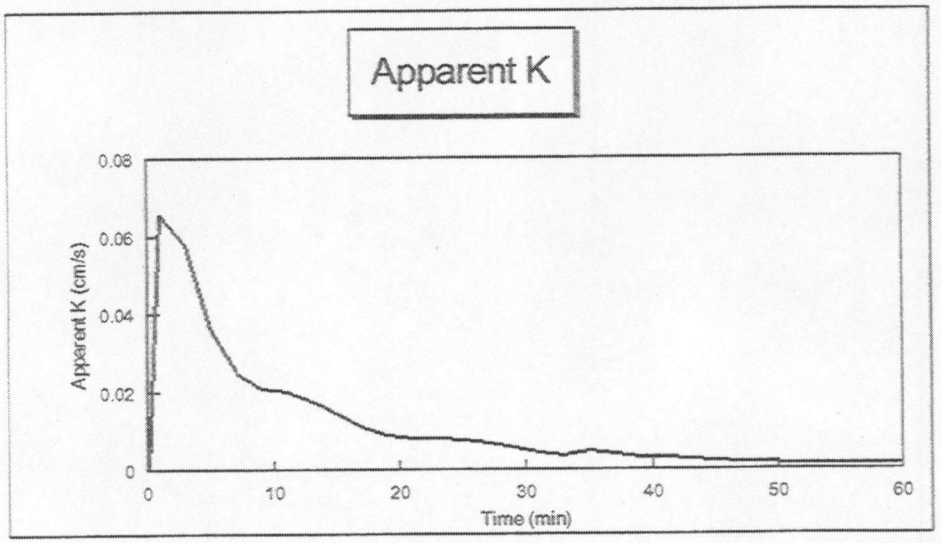
Initial Batch w%= 70.4%
Initial Sample w%= 42.9%

Thickness = 2.5 cm
Diameter = 9.5 cm

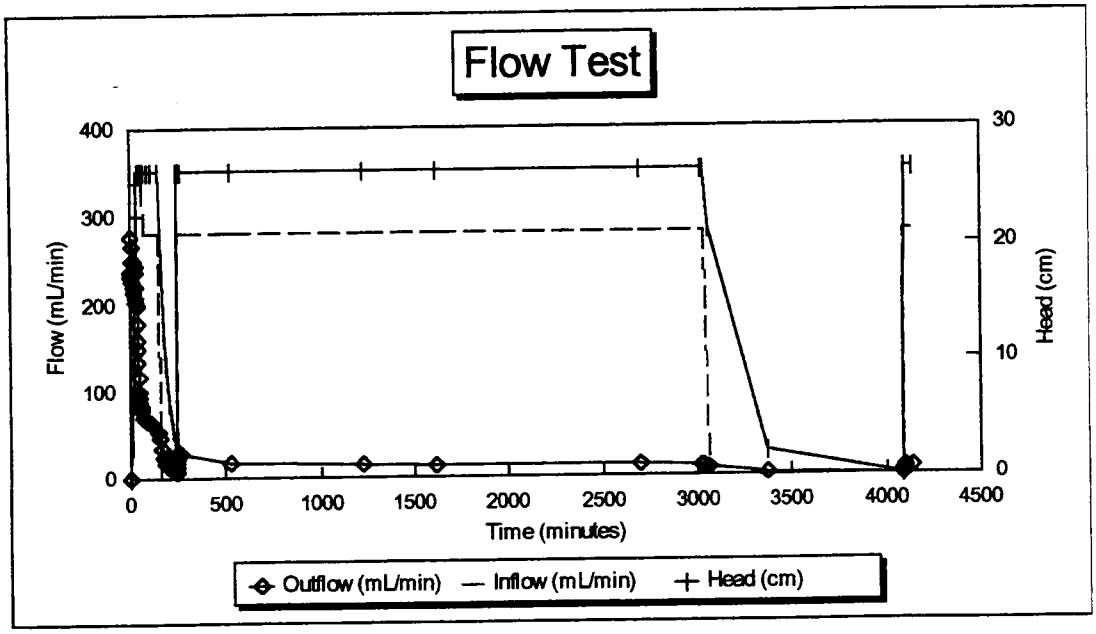
Maximum Aperture = 7.5 mm

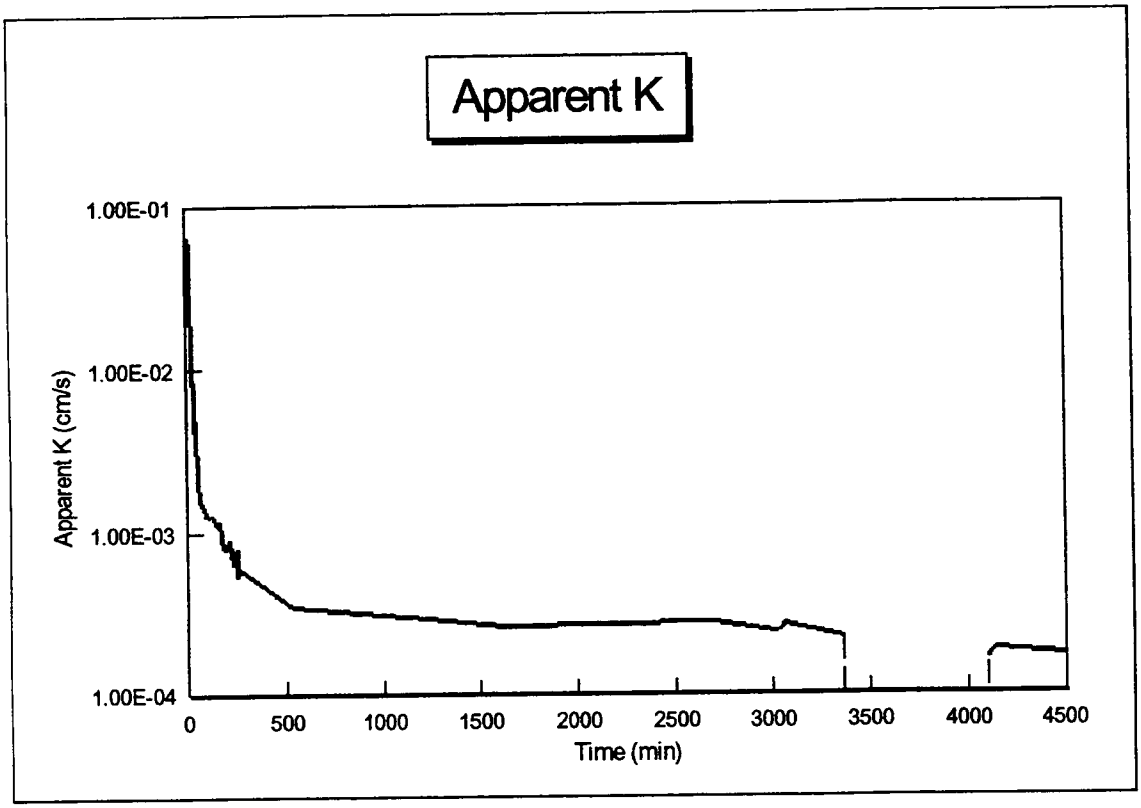
Fracture Area Percentage
Top of Sample = 5.7%
Bottom of Sample = 1.7%





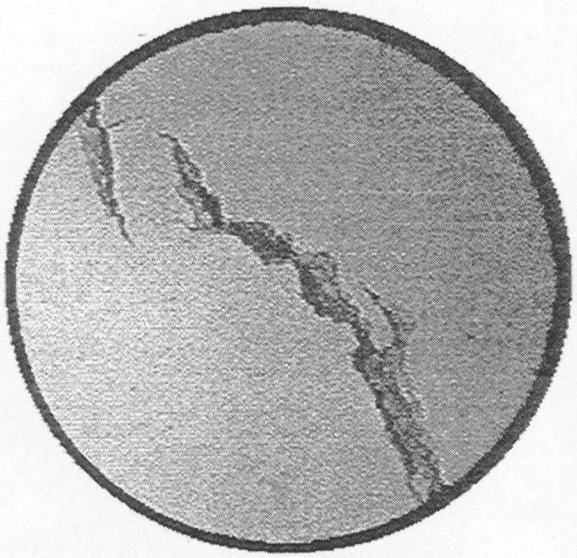
Long Term Test: Batch 8 - Sample 2



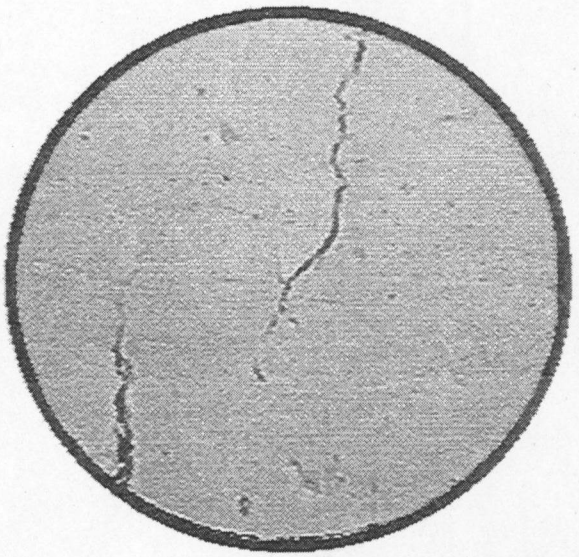


Batch #8 - Sample #2

Before Testing

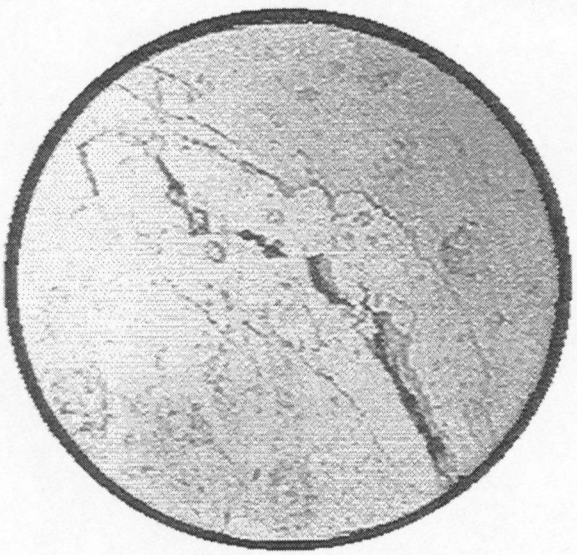


Top of Sample

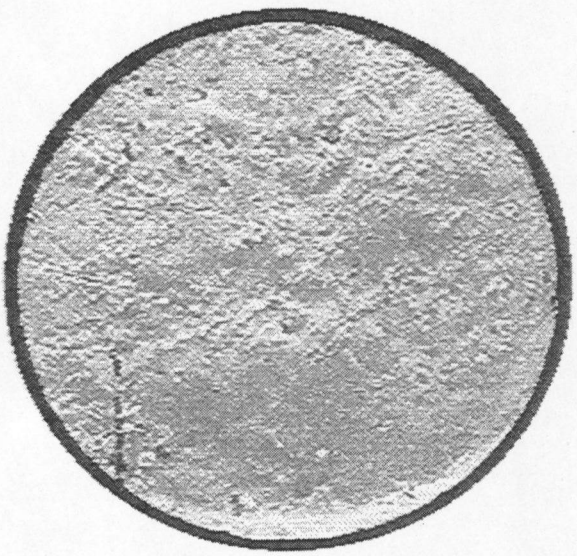


Bottom of Sample

After Testing



Top of Sample

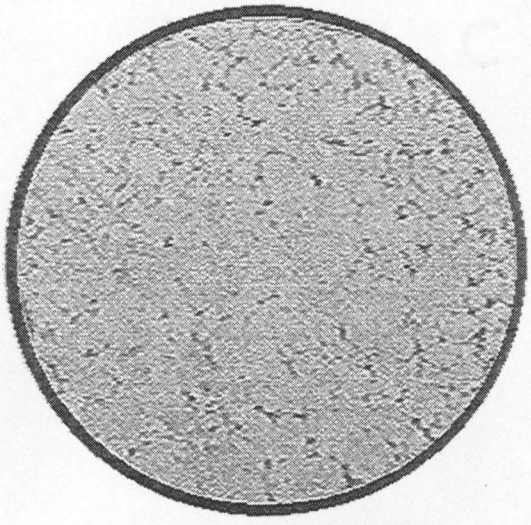


Bottom of Sample

APPENDIX 2

INFILTRATION TEST RESULTS

Infiltration Test: Sample AD-1



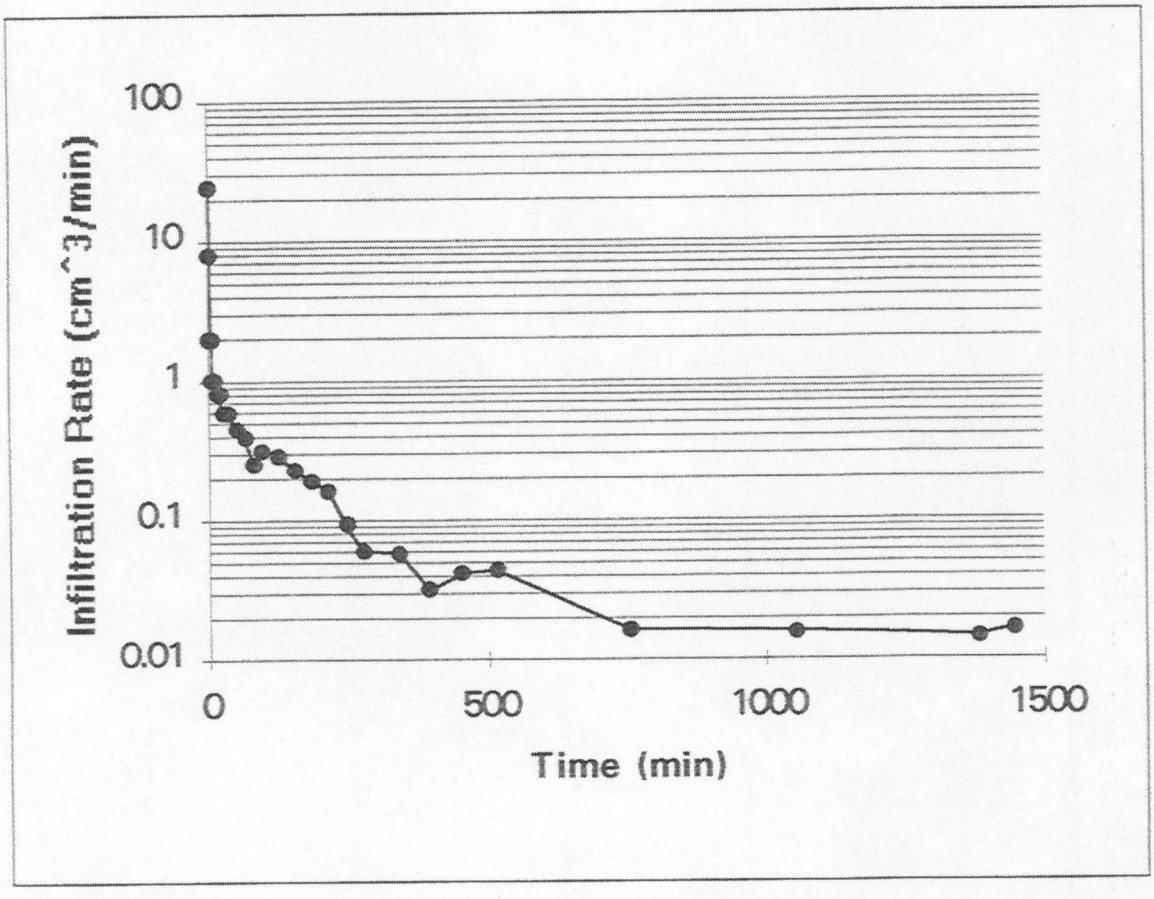
Sample just before test

Sample Information

Compacted Water Content = 35.9%
Compacted Dry Density = 1.36 g/cm^3

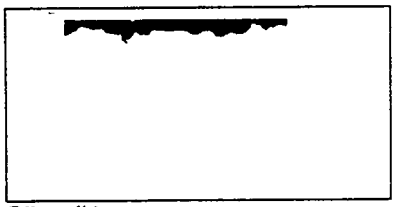
Sample History

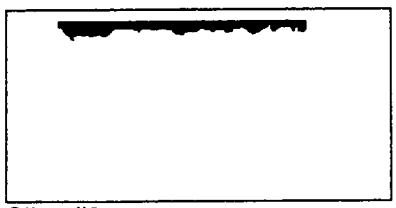
The sample was air dried at ambient temperature until dry. It was uncracked upon infiltration.

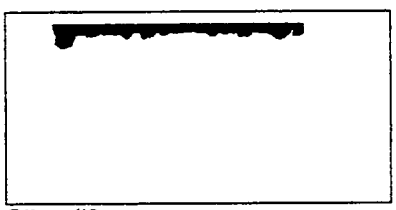


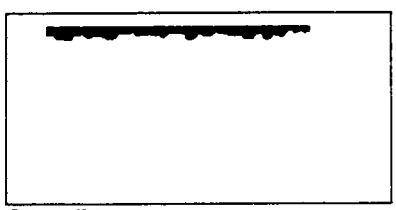
Fracture Stains: Sample AD-1

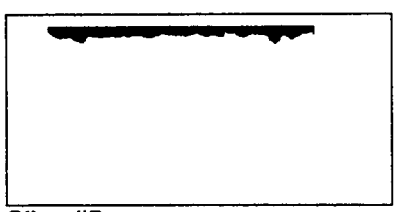
Sample Info: Permeant - Rhodamine Red Dye
Size - 4" diameter; 2" thick
Soil - Compacted Kaolinite
Sample state - Air dried; uncracked

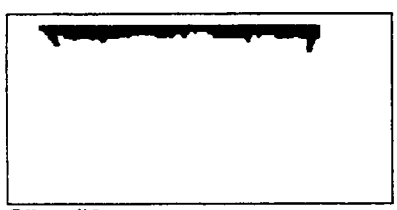

Slice #1

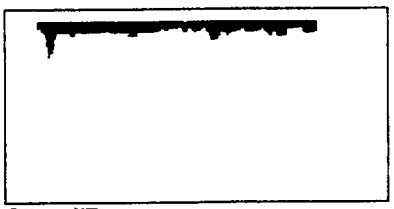

Slice #2

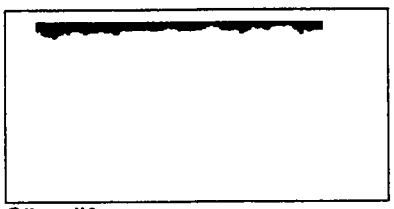

Slice #3

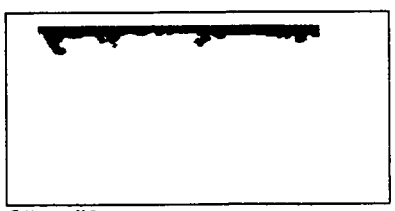

Slice #4

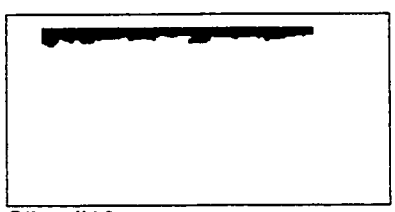

Slice #5

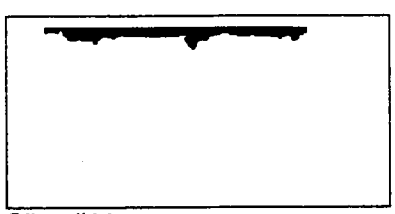

Slice #6

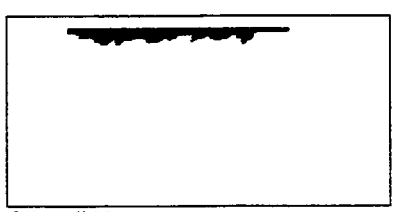

Slice #7


Slice #8

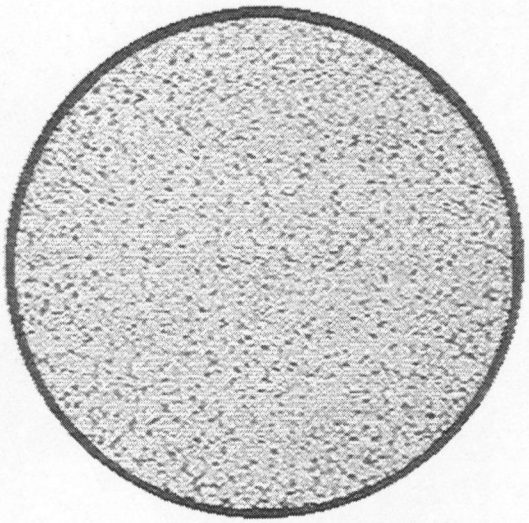

Slice #9


Slice #10


Slice #11


Slice #12

Infiltration Test: Sample AD-2



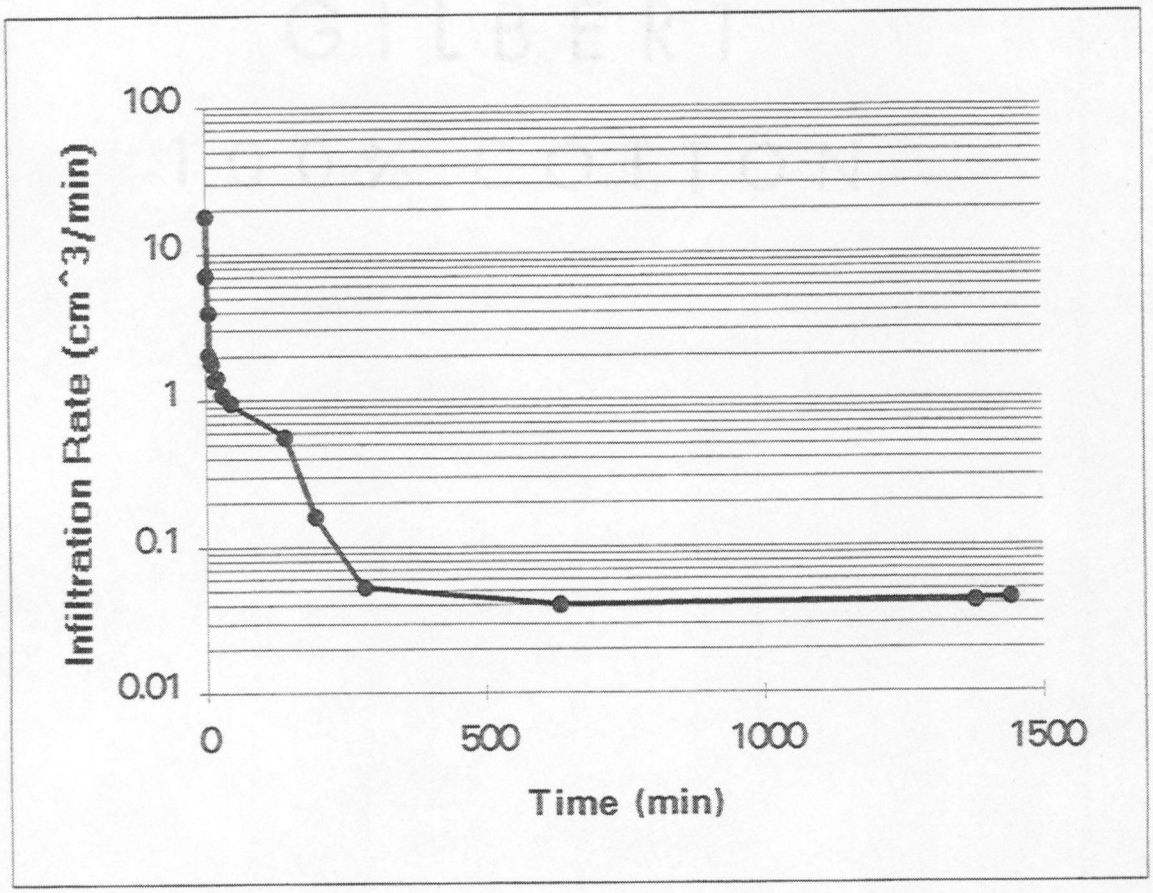
Sample just before test

Sample Information

Compacted Water Content = 34.9%
Compacted Dry Density = 1.34 g/cm^3

Sample History

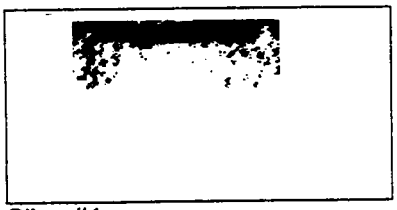
The sample was air dried at ambient temperature until dry..
It was uncracked upon infiltration.
(Clod size < #4 sieve)

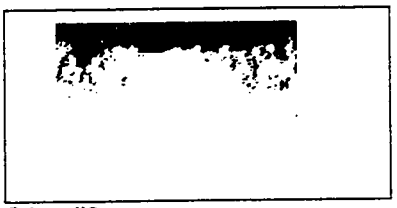


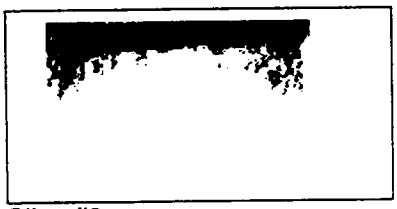
Fracture Stains: Sample AD-2

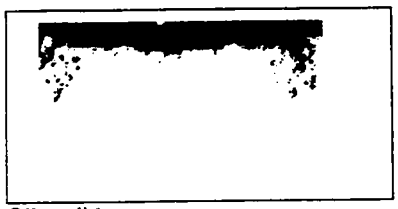
Sample Info: Permeant - Rhodamine Red Dye
Size - 4" diameter; 2" thick

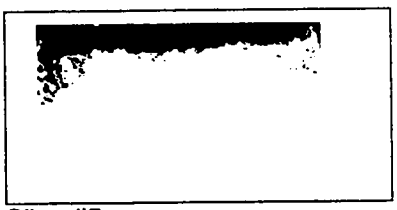
Soil - Compacted Kaolinite
Sample state - 3 desiccation cycles

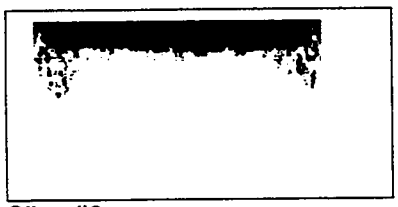

Slice #1

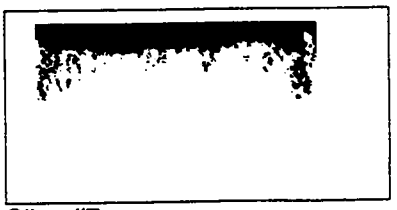

Slice #2

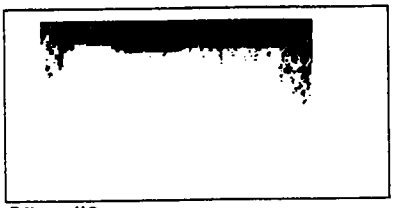

Slice #3

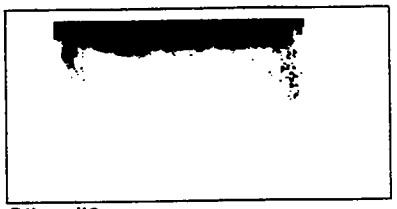

Slice #4

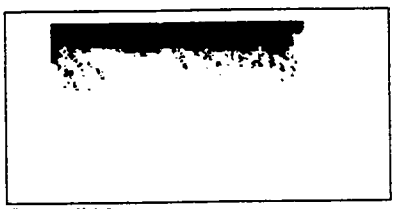

Slice #5

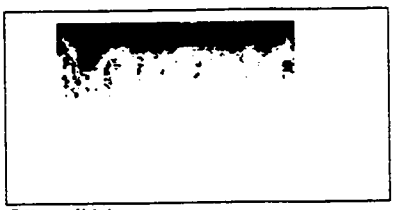

Slice #6

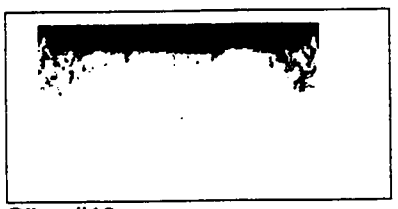

Slice #7


Slice #8

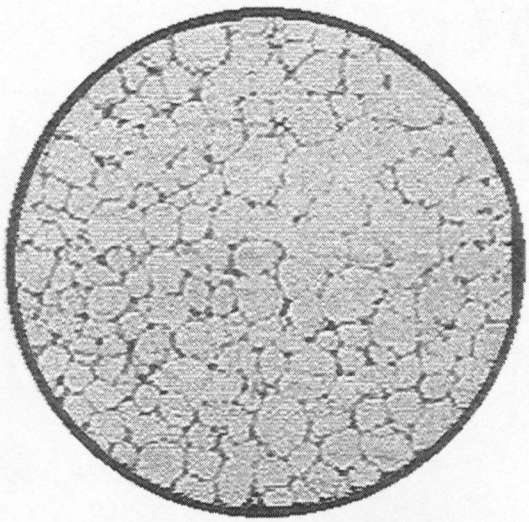

Slice #9


Slice #10


Slice #11


Slice #12

Infiltration Test: Sample AD-3



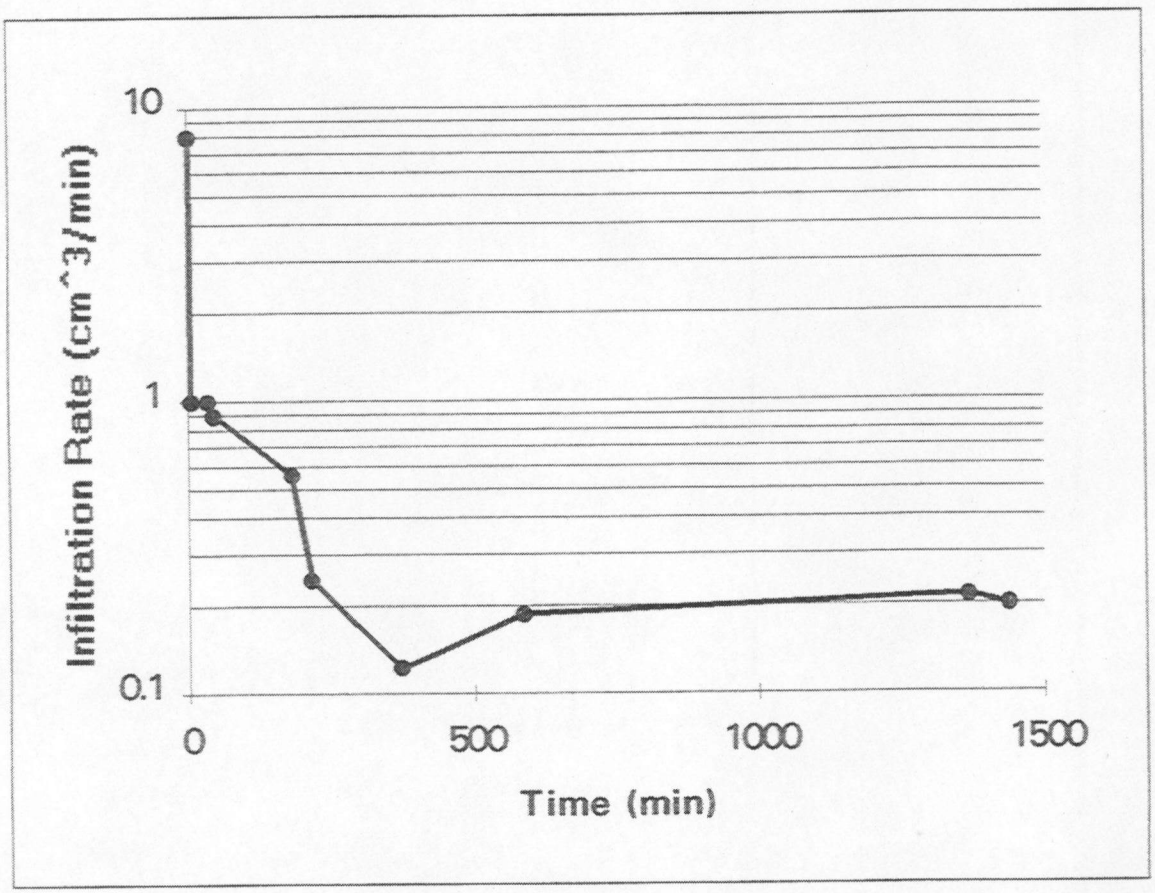
Sample just before test

Sample Information

Compacted Water Content = 34.9%
Compacted Dry Density = 1.35 g/cm^3

Sample History

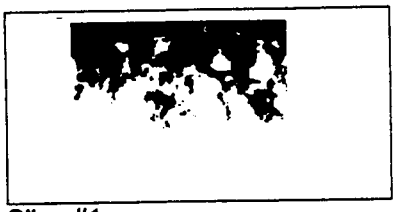
The sample was air dried at ambient temperature until dry. It was uncracked upon infiltration. (Clod size > #4 sieve)



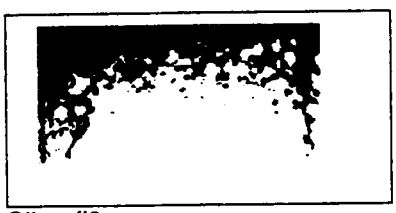
Fracture Stains: Sample AD-3

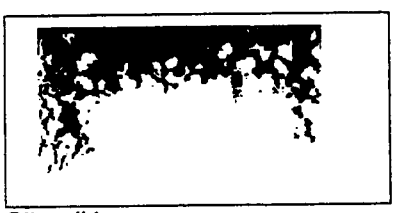
Sample Info: Permeant - Rhodamine Red Dye
Size - 4" diameter; 2" thick

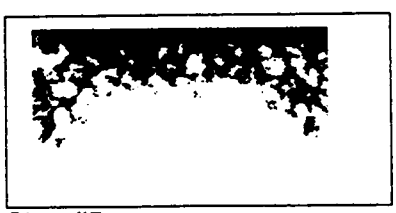
Soil - Compacted Kaolinite
Sample state - 3 desiccation cycles

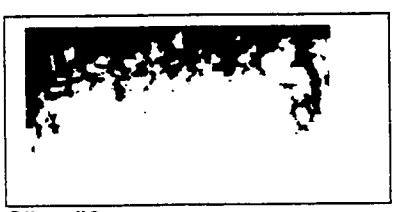

Slice #1

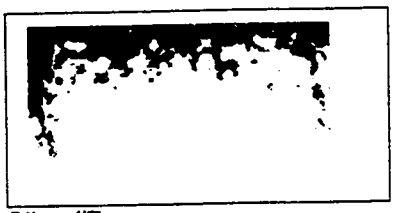

Slice #2

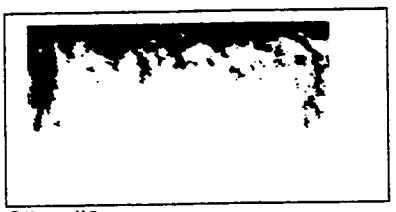

Slice #3

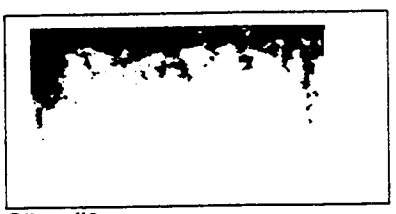

Slice #4

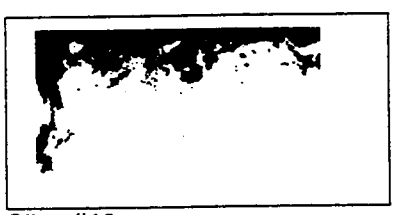

Slice #5

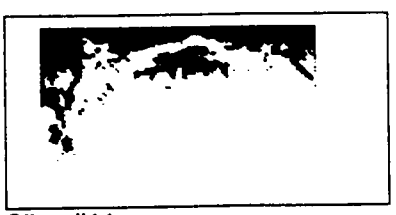

Slice #6

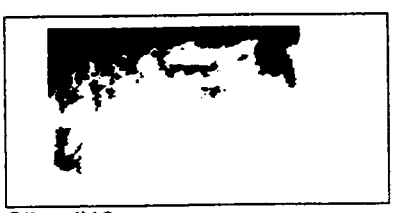

Slice #7


Slice #8


Slice #9


Slice #10


Slice #11

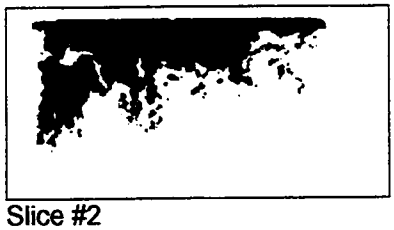

Slice #12

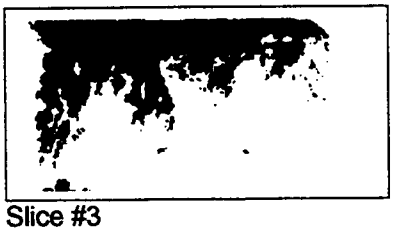
Fracture Stains: Sample D-1

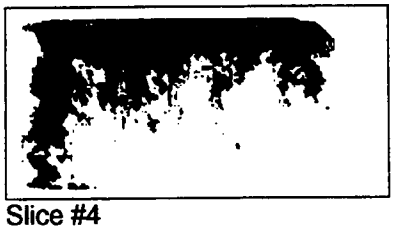
Sample Info: Permeant - Rhodamine Red Dye
Size - 4" diameter; 2" thick

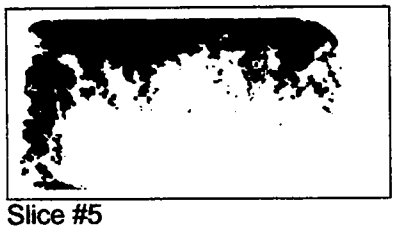
Soil - Compacted Kaolinite
Sample state - 3 desiccation cycles

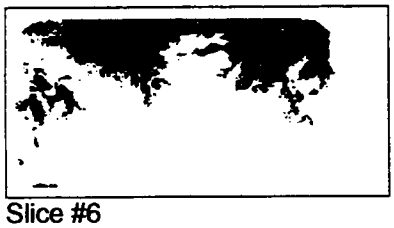

Slice #1

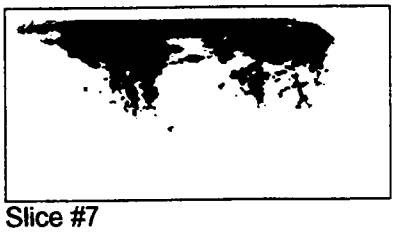

Slice #2

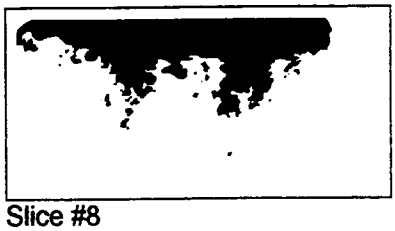

Slice #3

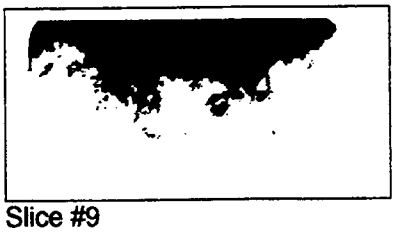

Slice #4

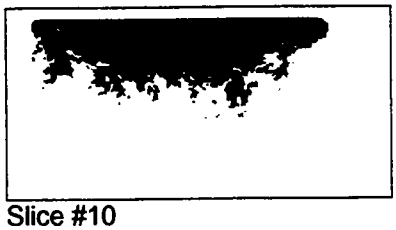

Slice #5

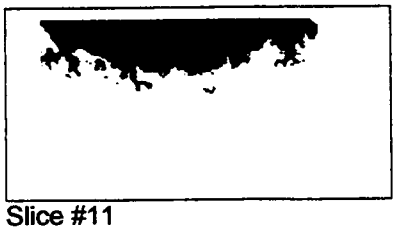

Slice #6

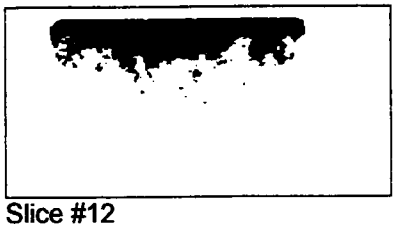

Slice #7


Slice #8


Slice #9


Slice #10

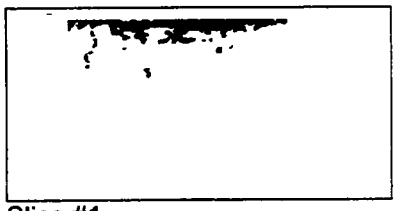

Slice #11

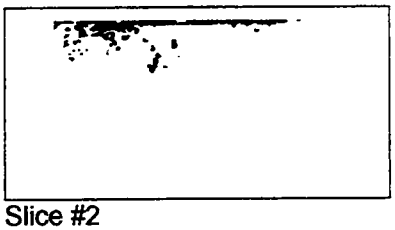

Slice #12

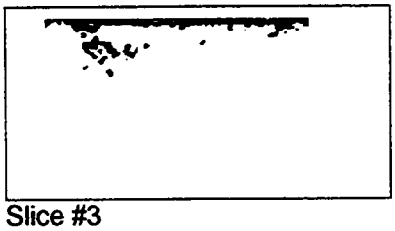
Fracture Stains: Sample D-2

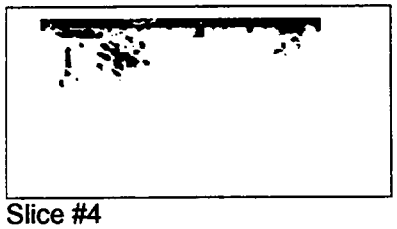
Sample Info: Permeant - Methylene Blue Dye
Size - 4" diameter; 2" thick

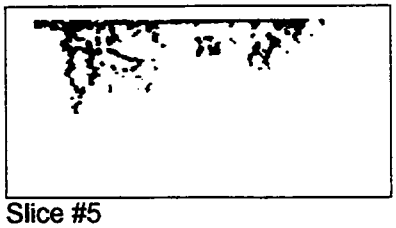
Soil - Compacted Kaolinite
Sample state - 3 desiccation cycles

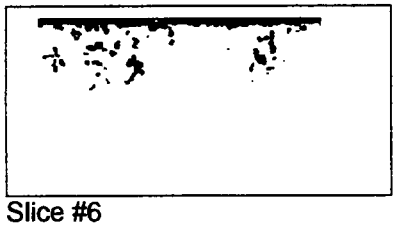

Slice #1

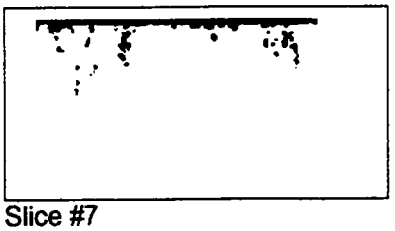

Slice #2

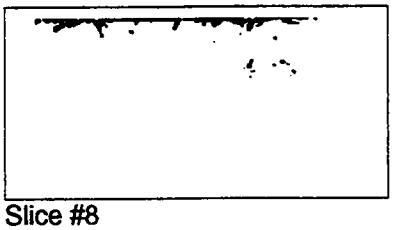

Slice #3

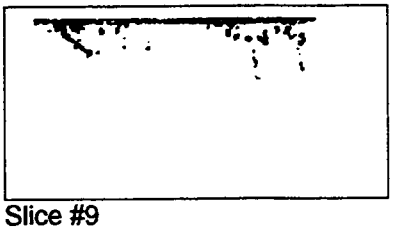

Slice #4

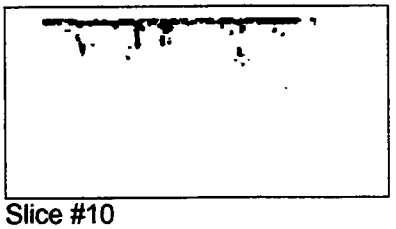

Slice #5

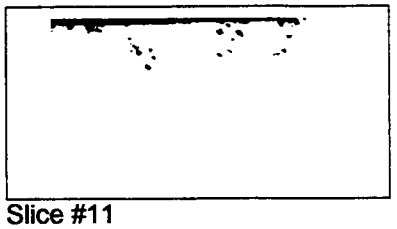

Slice #6

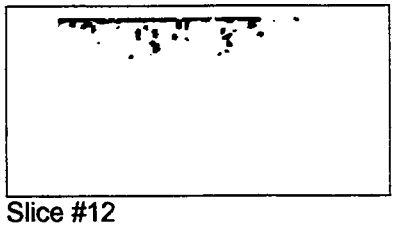

Slice #7


Slice #8


Slice #9


Slice #10

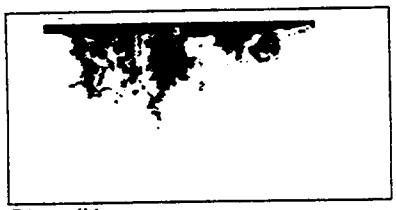

Slice #11

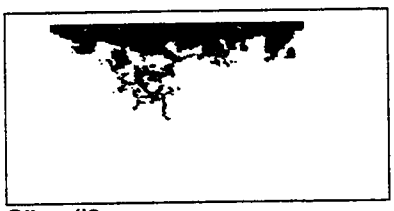

Slice #12

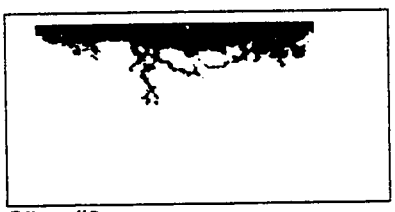
Fracture Stains: Sample D-3

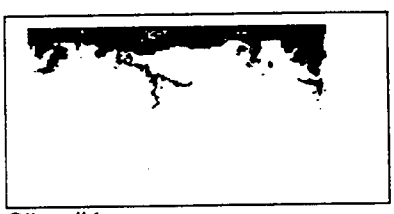
Sample Info: Permeant - Rhodamine Red Dye
Size - 4" diameter; 2" thick

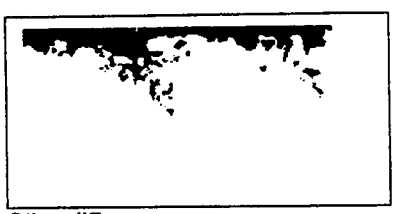
Soil - Compacted Kaolinite
Sample state - 3 desiccation cycles


Slice #1

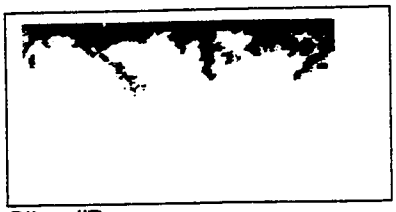

Slice #2


Slice #3

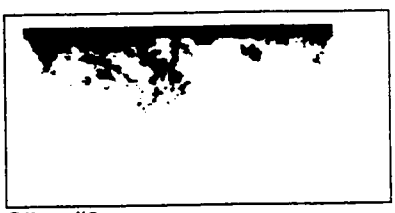

Slice #4

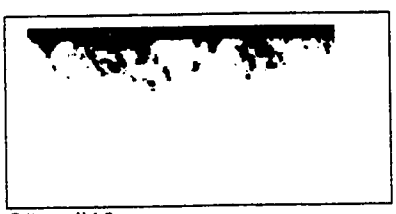

Slice #5

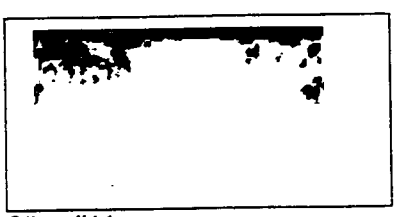

Slice #6

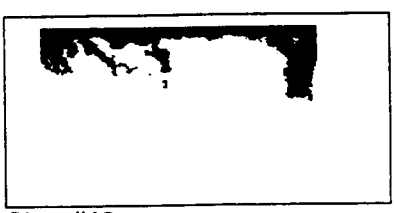

Slice #7


Slice #8

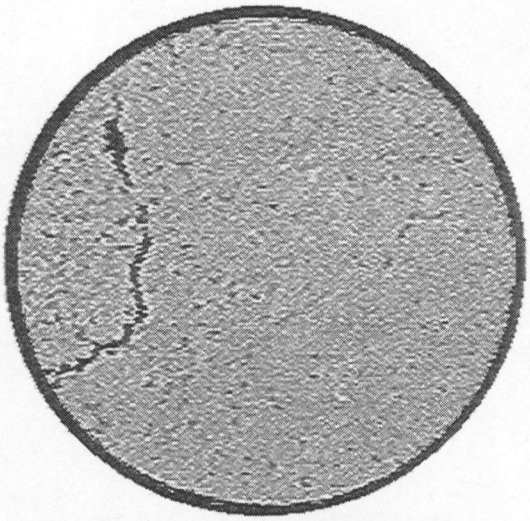

Slice #9


Slice #10


Slice #11


Slice #12

Infiltration Test: Sample D-4



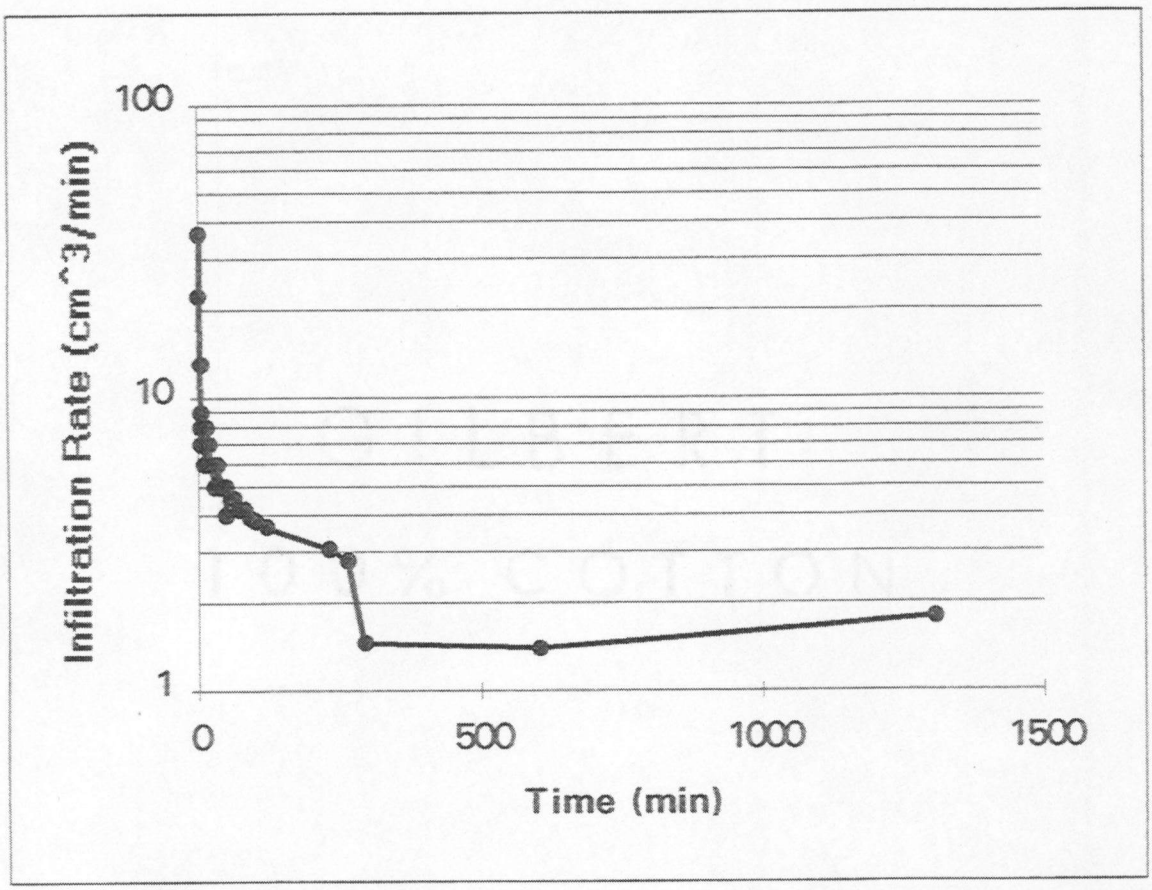
Sample just before test

Sample Information

Compacted Water Content = 34.9%
Compacted Dry Density = 1.28 g/cm^3

Sample History

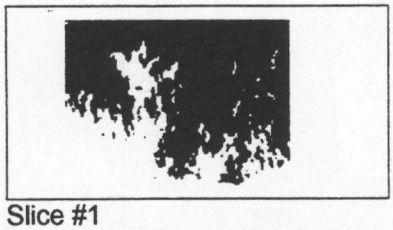
The sample was subjected to three wet-dry cycles. It was cracked upon infiltration.



Fracture Stains: Sample D-4

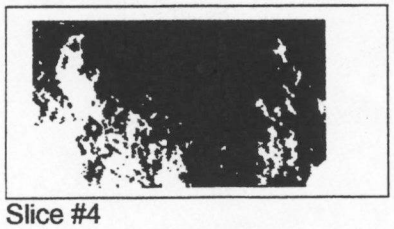
Sample Info: Permeant - Rhodamine Red Dye
Size - 4" diameter; 2" thick

Soil - Compacted Kaolinite
Sample state - 3 desiccation cycles

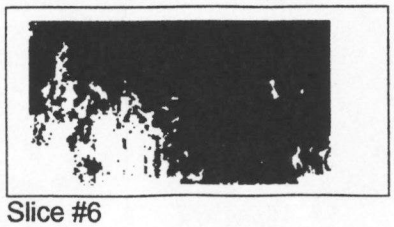

Slice #1


Slice #2

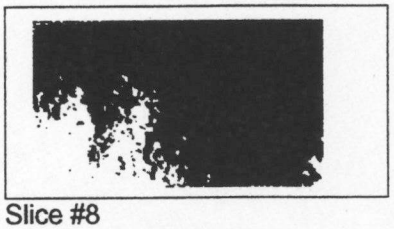

Slice #3

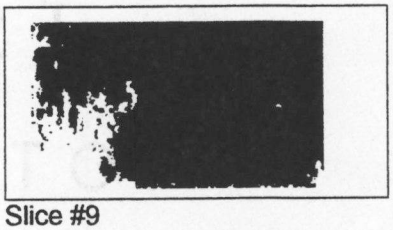

Slice #4

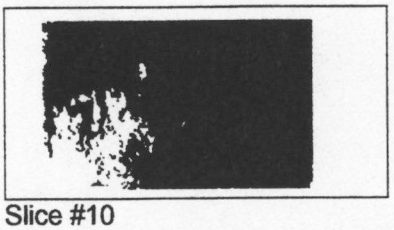

Slice #5

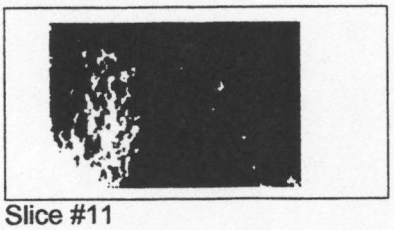

Slice #6

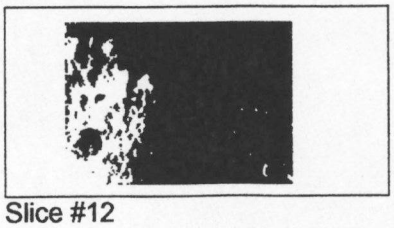

Slice #7


Slice #8

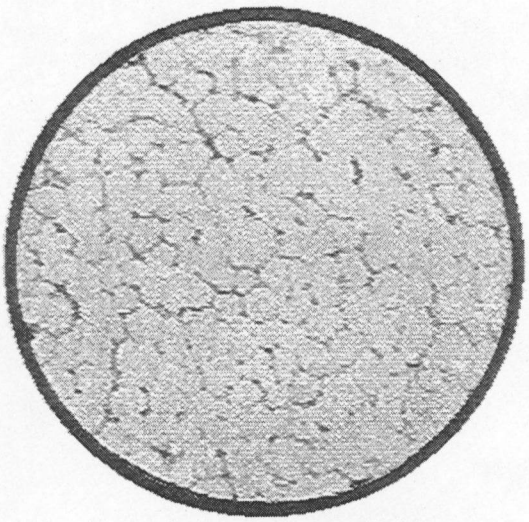

Slice #9


Slice #10


Slice #11


Slice #12

Infiltration Test: Sample D-5



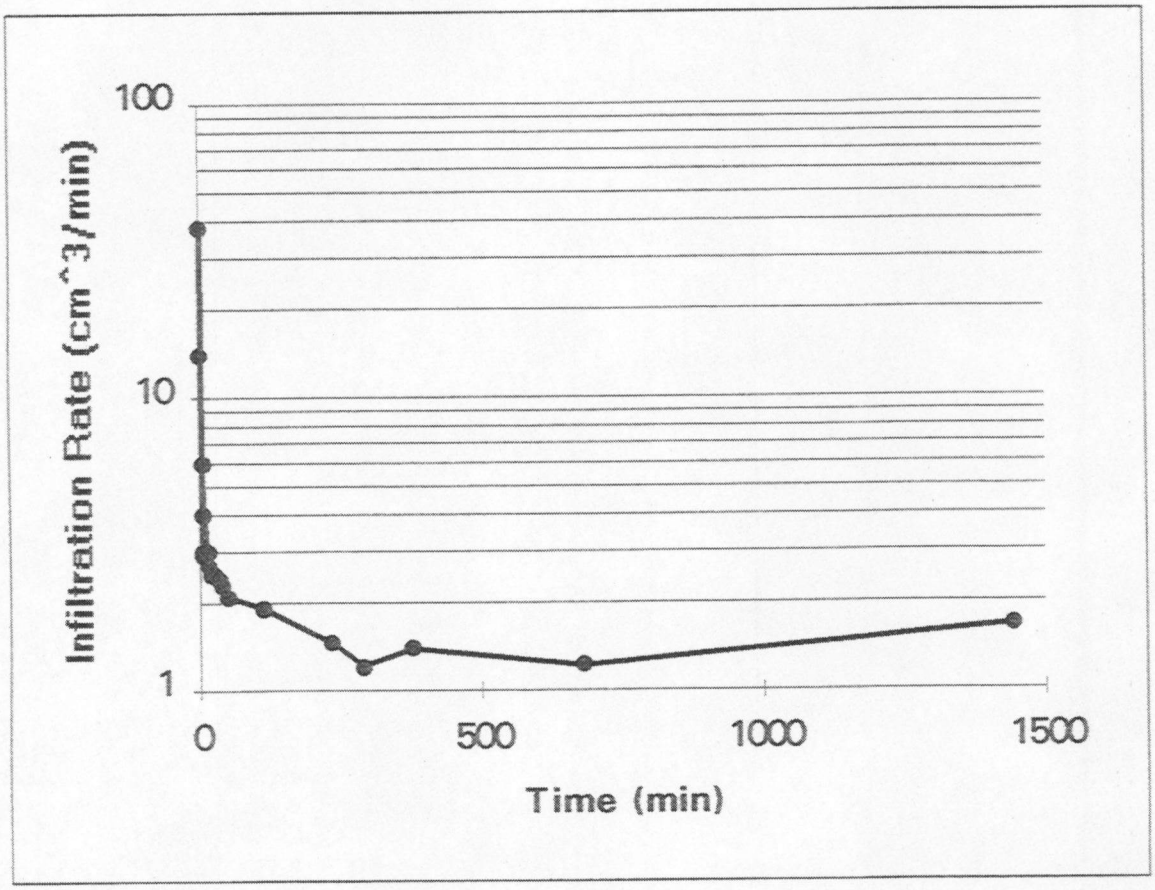
Sample just before test

Sample Information

Compacted Water Content = 34.9%
Compacted Dry Density = 1.36 g/cm^3

Sample History

The sample was subjected to three wet-dry cycles. It was cracked upon infiltration.

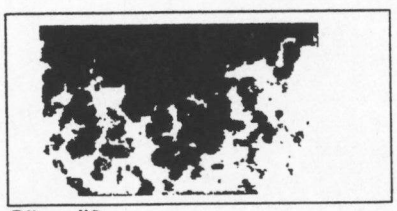


Fracture Stains: Sample D-5

Sample Info: Permeant - Rhodamine B Red Dye
Size - 10.2 cm diameter; 5.1 cm thick
Soil - Compacted Kaolinite
Sample state - 3 desiccation cycles


Slice #1


Slice #2


Slice #3


Slice #4


Slice #5


Slice #6


Slice #7


Slice #8


Slice #9


Slice #10

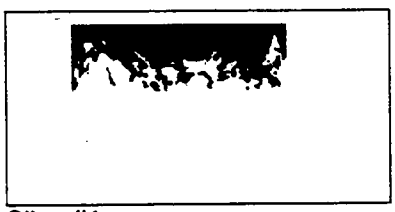

Slice #11

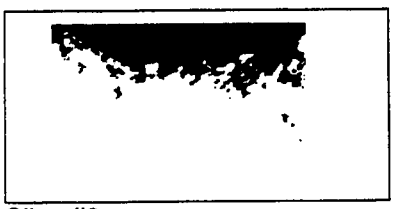

Slice #12

Fracture Stains: Sample FT-1

Sample Info: Permeant - Rhodamine Red Dye
Size - 4" diameter; 2" thick

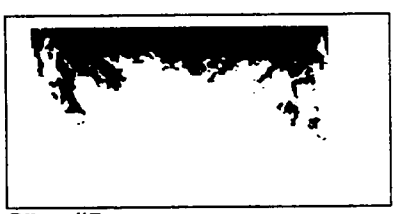
Soil - Compacted Kaolinite
Sample state - 3 freeze/thaw cycles

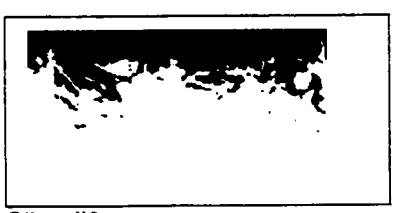

Slice #1


Slice #2


Slice #3

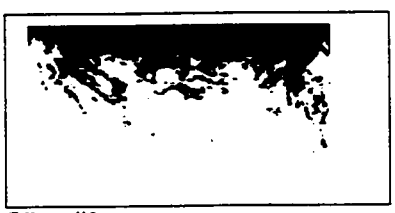

Slice #4

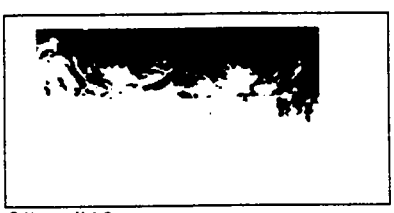

Slice #5

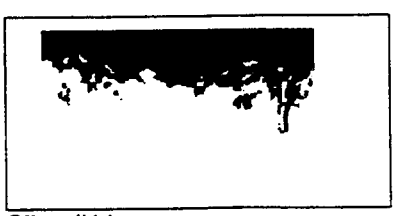

Slice #6

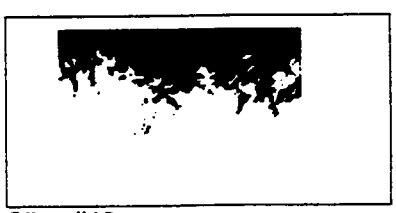

Slice #7


Slice #8


Slice #9


Slice #10

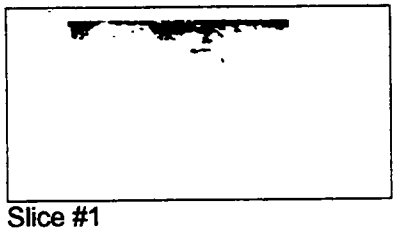

Slice #11

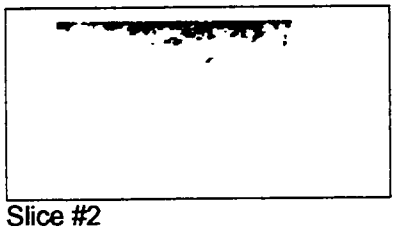

Slice #12

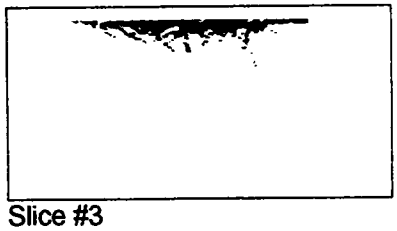
Fracture Stains: Sample FT-2

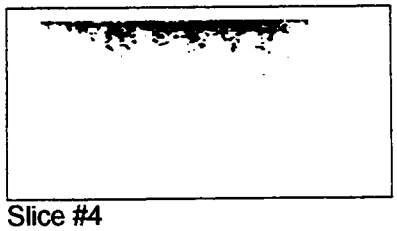
Sample Info: Permeant - Methylene Blue Dye
Size - 4" diameter; 2" thick

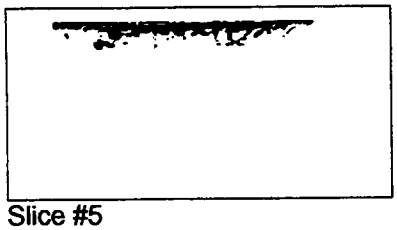
Soil - Compacted Kaolinite
Sample state - 3 freeze/thaw cycles

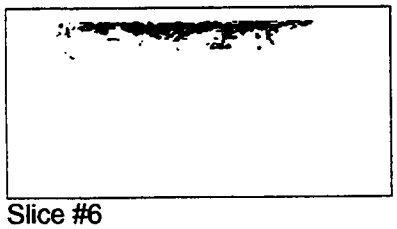

Slice #1

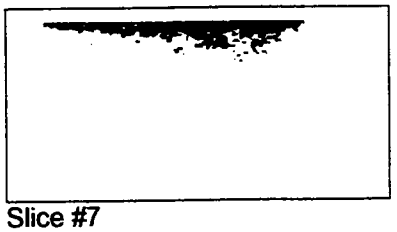

Slice #2

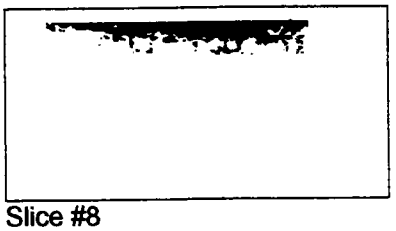

Slice #3

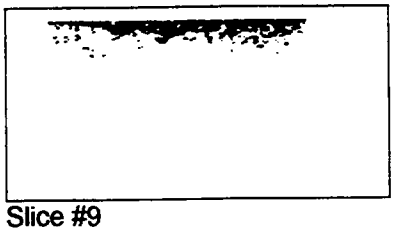

Slice #4

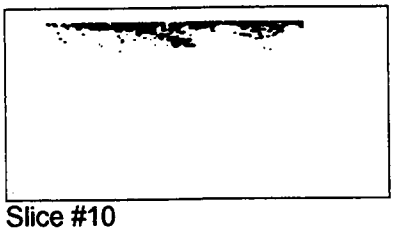

Slice #5

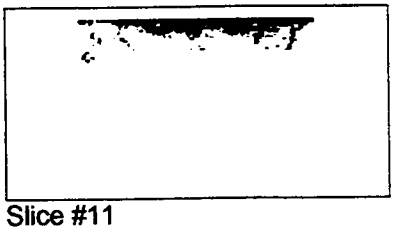

Slice #6

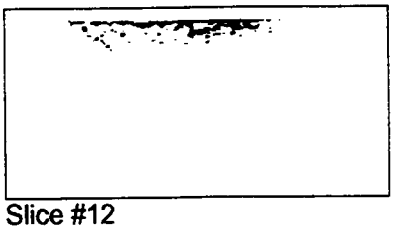

Slice #7


Slice #8

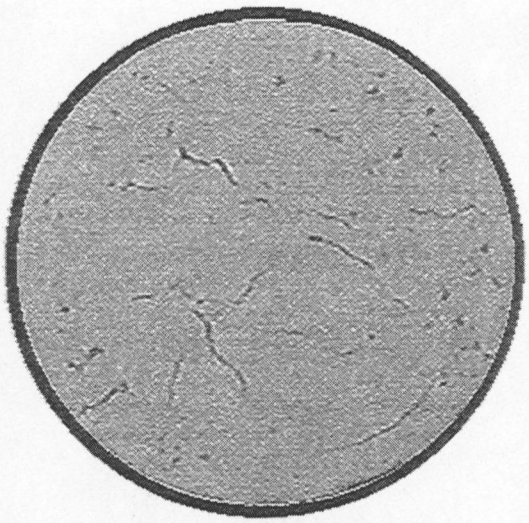

Slice #9


Slice #10


Slice #11


Slice #12

Infiltration Test: Sample FT-3



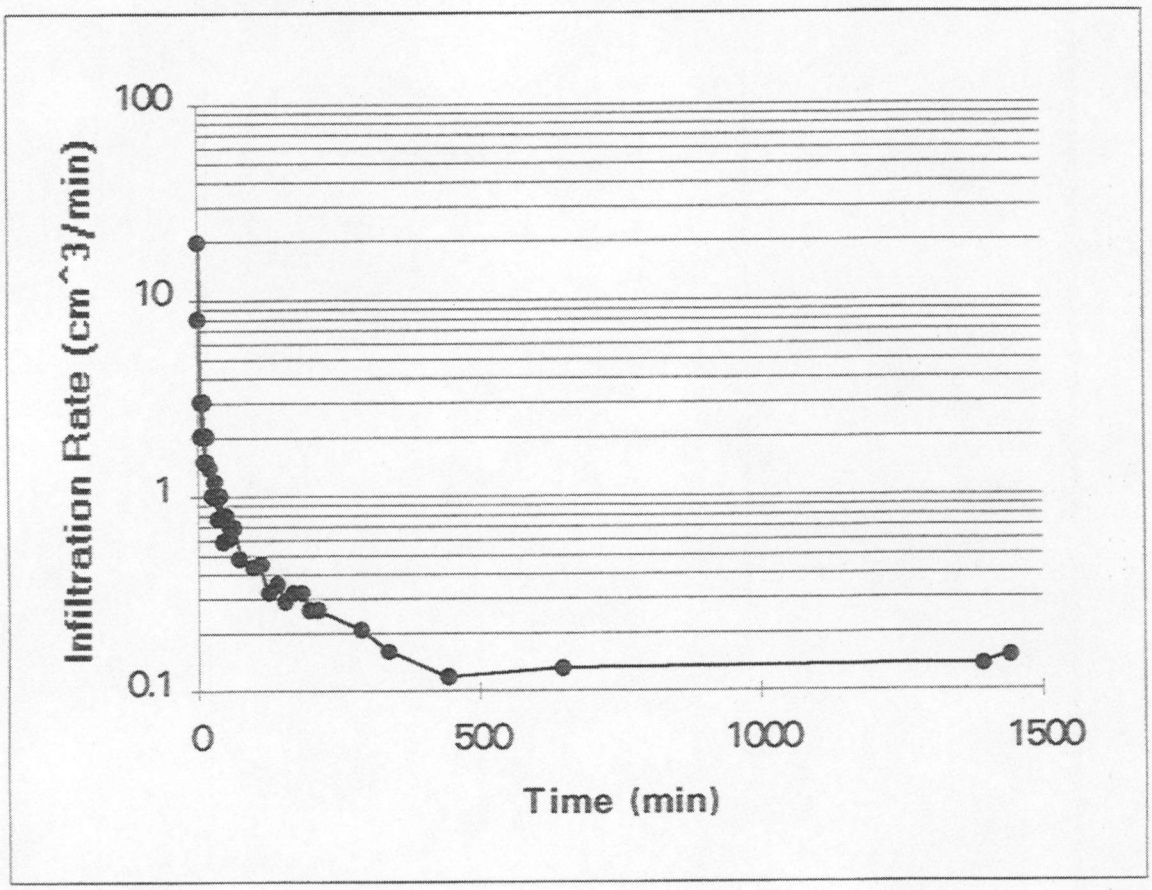
Sample just before test

Sample Information

Compacted Water Content = 36.9%
Compacted Dry Density = 1.34 g/cm^3

Sample History

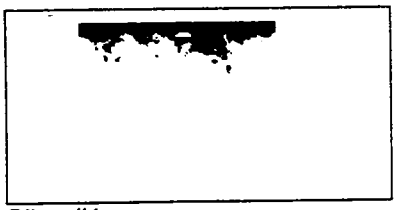
The sample was sujected to three freeze-thaw cycles. It was saturated before these cycles. It was cracked upon infiltration.

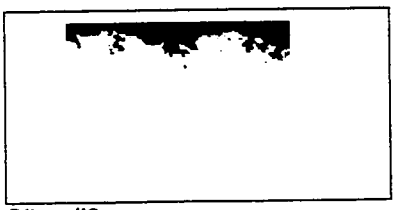


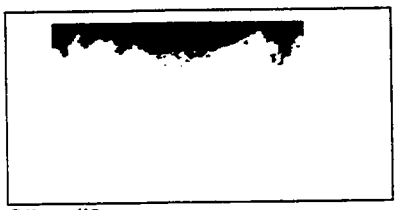
Fracture Stains: Sample FT-3

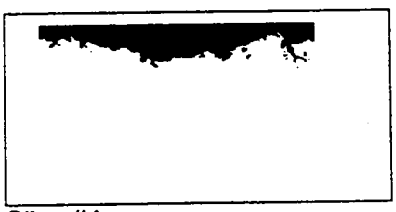
Sample Info: Permeant - Rhodamine Red Dye
Size - 4" diameter; 2" thick

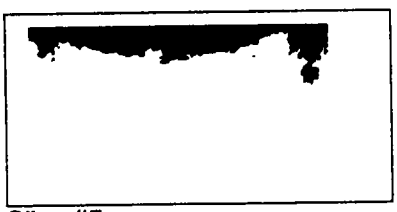
Soil - Compacted Kaolinite
Sample state - 3 freeze-thaw cycles

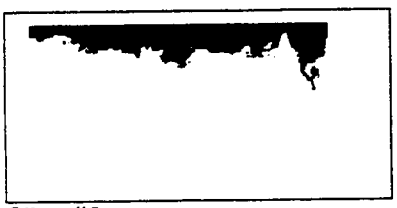

Slice #1

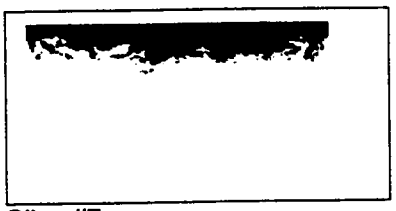

Slice #2

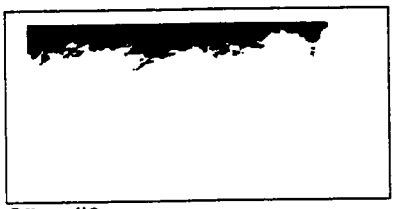

Slice #3

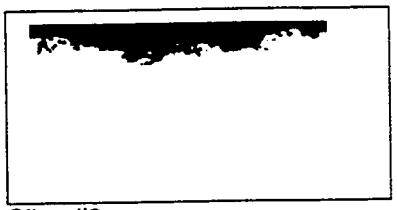

Slice #4

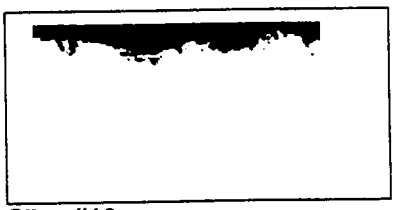

Slice #5

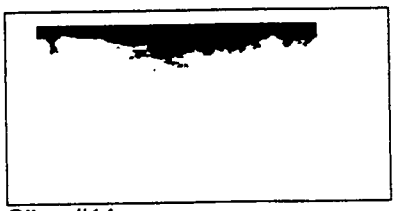

Slice #6

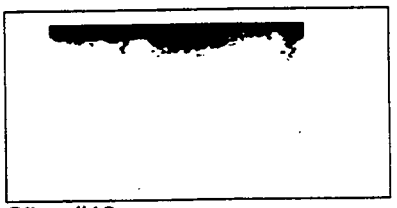

Slice #7


Slice #8

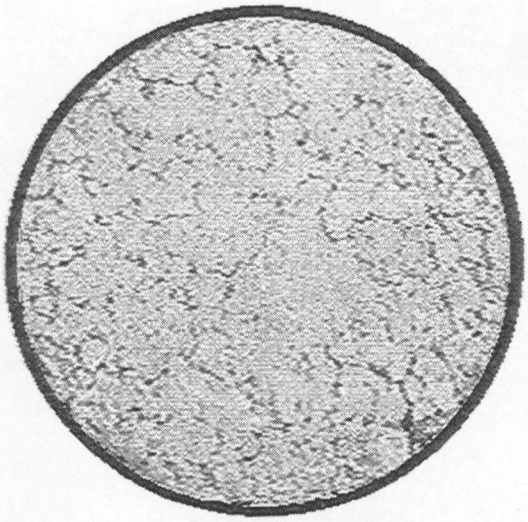

Slice #9


Slice #10


Slice #11


Slice #12

Infiltration Test: Sample FT-4



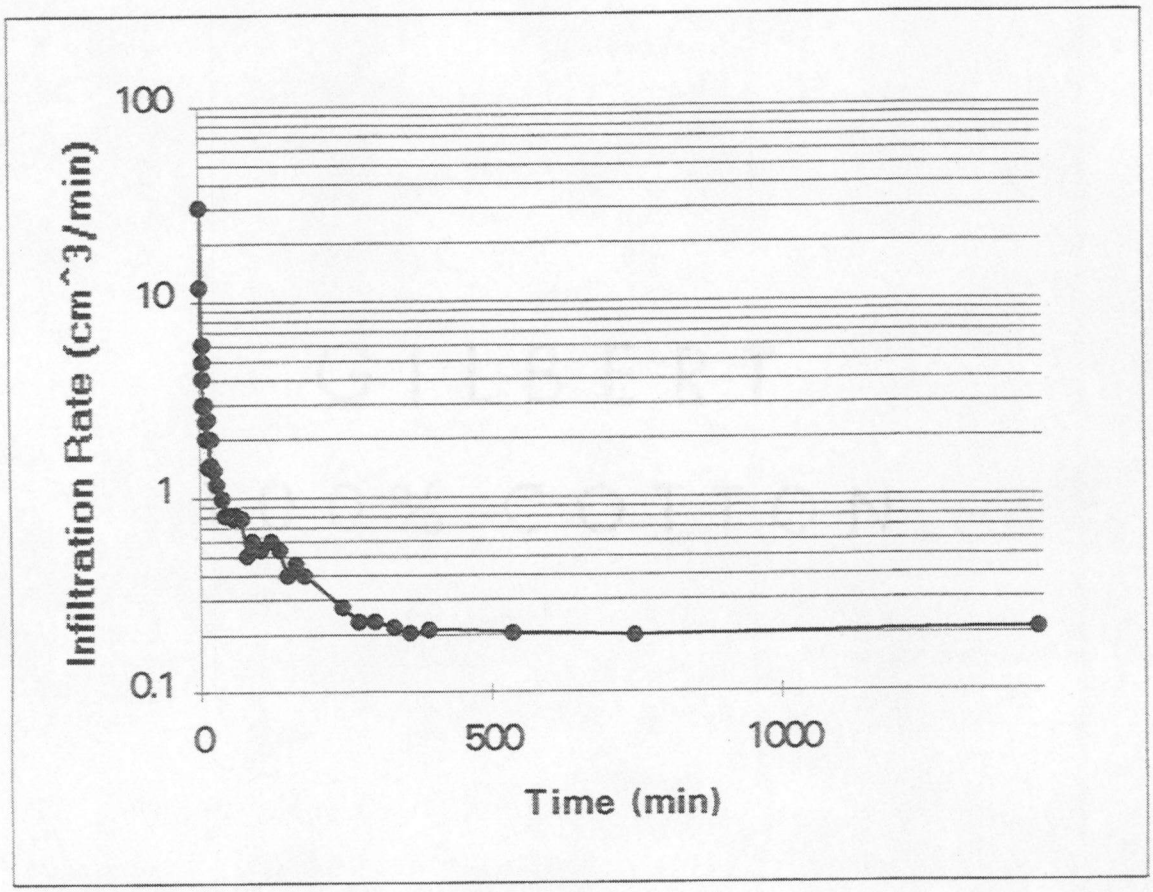
Sample just before test

Sample Information

Compacted Water Content = 36.9%
Compacted Dry Density = 1.33 g/cm^3

Sample History

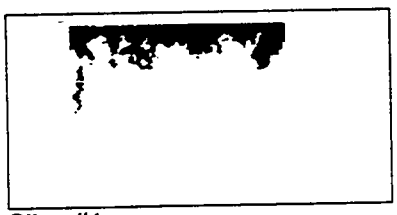
The sample was subjected to three freeze-thaw cycles. It was saturated before these cycles. It was cracked upon infiltration.

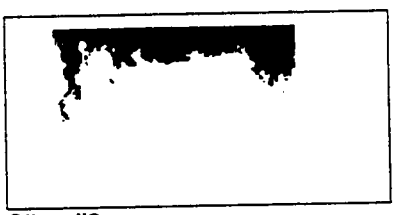


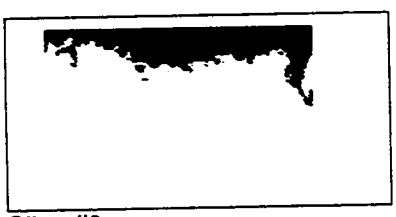
Fracture Stains: Sample FT-4

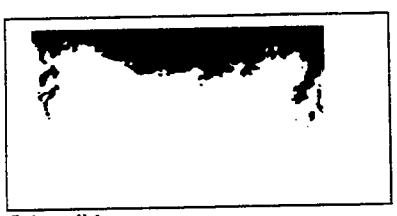
Sample Info: Permeant - Rhodamine Red Dye
Size - 4" diameter; 2" thick

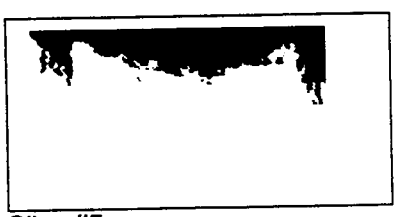
Soil - Compacted Kaolinite
Sample state - 3 freeze/thaw cycles

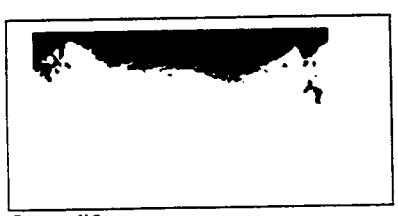

Slice #1

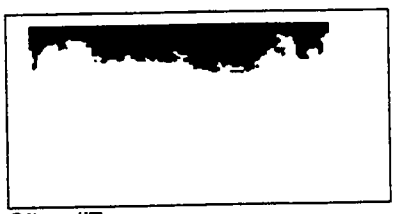

Slice #2

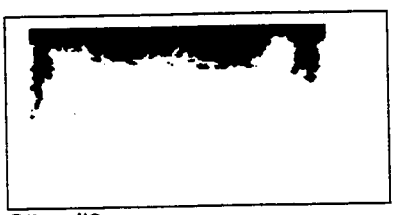

Slice #3

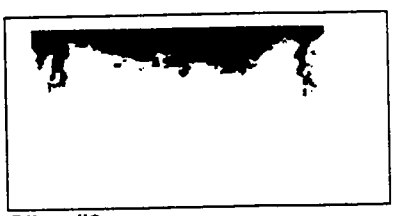

Slice #4

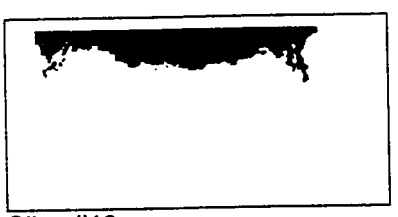

Slice #5

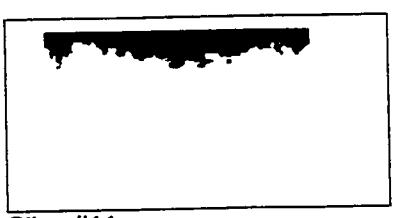

Slice #6

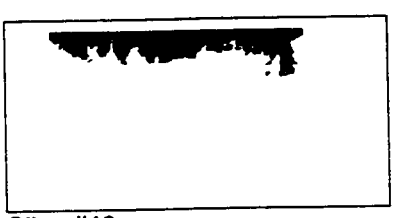

Slice #7


Slice #8

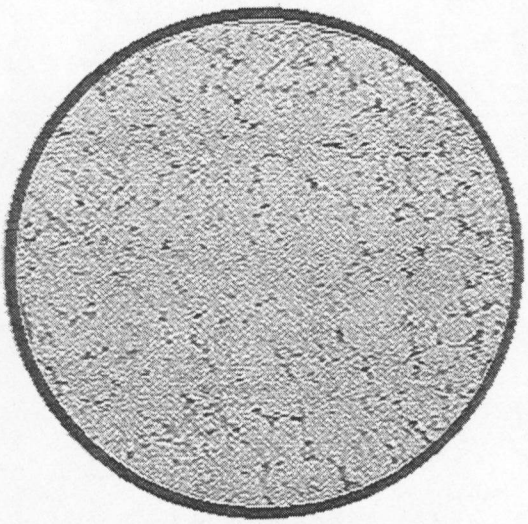

Slice #9


Slice #10


Slice #11


Slice #12

Infiltration Test: Sample FT-5



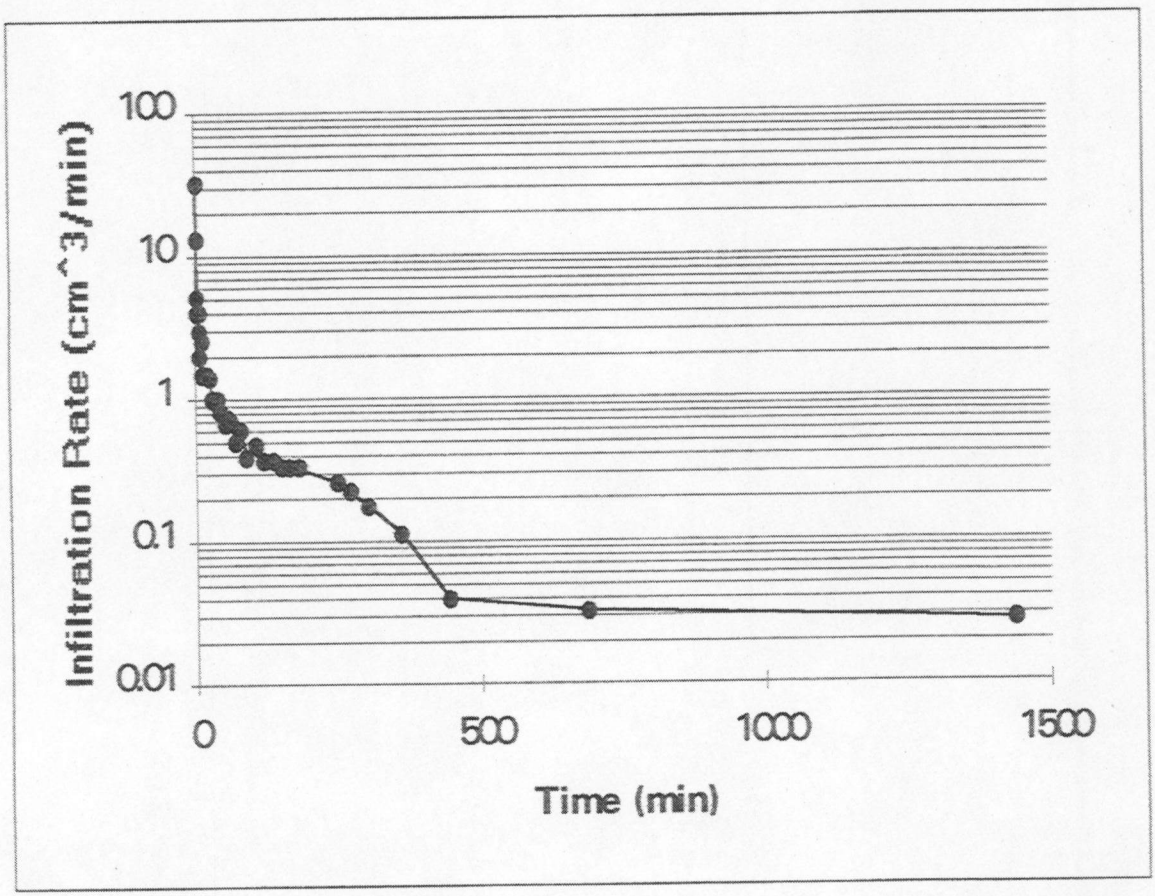
Sample just before test

Sample Information

Compacted Water Content = 36.9%
Compacted Dry Density = 1.34 g/cm^3

Sample History

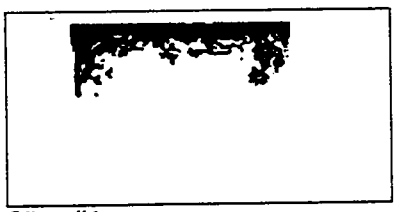
The sample was subjected to three freeze-thaw cycles. It was saturated before these cycles. It was cracked upon infiltration.

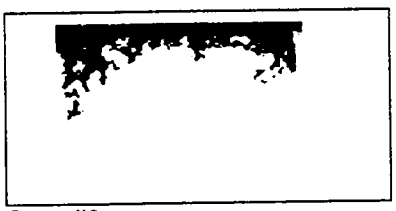


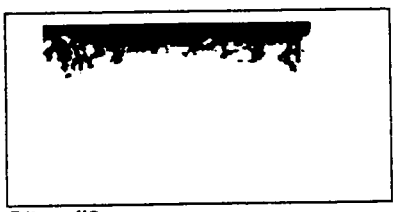
Fracture Stains: Sample FT-5

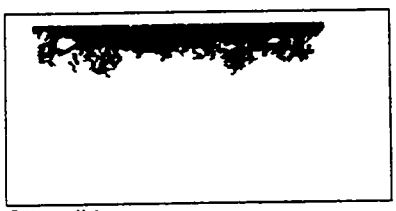
Sample Info: Permeant - Rhodamine Red Dye
Size - 4" diameter; 2" thick

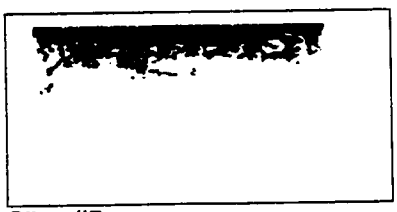
Soil - Compacted Kaolinite
Sample state - 3 freeze/thaw cycles

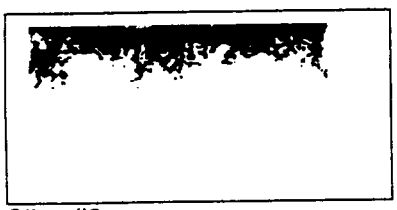

Slice #1

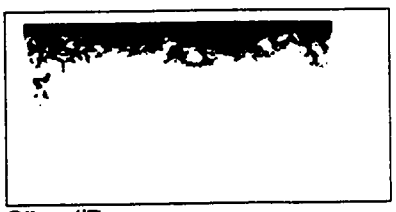

Slice #2

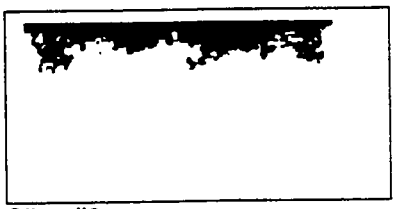

Slice #3

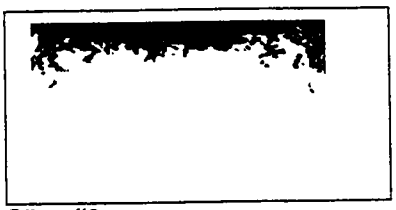

Slice #4

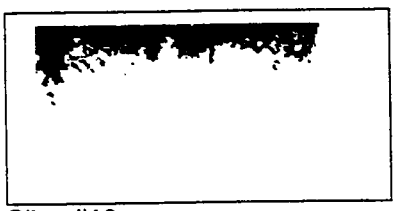

Slice #5

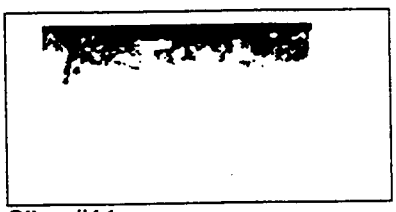

Slice #6

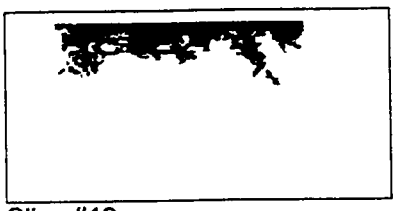

Slice #7


Slice #8

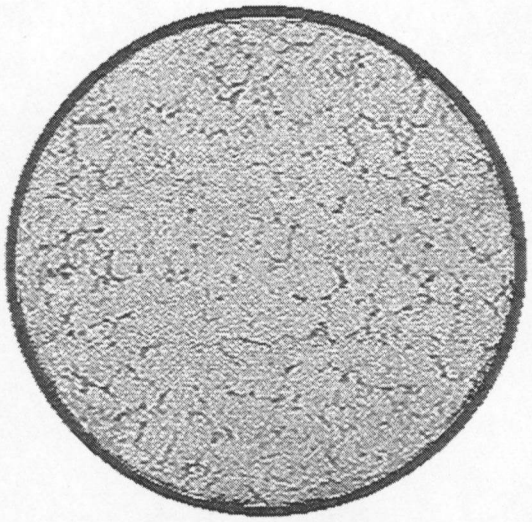

Slice #9


Slice #10


Slice #11


Slice #12

Infiltration Test: Sample FT-6



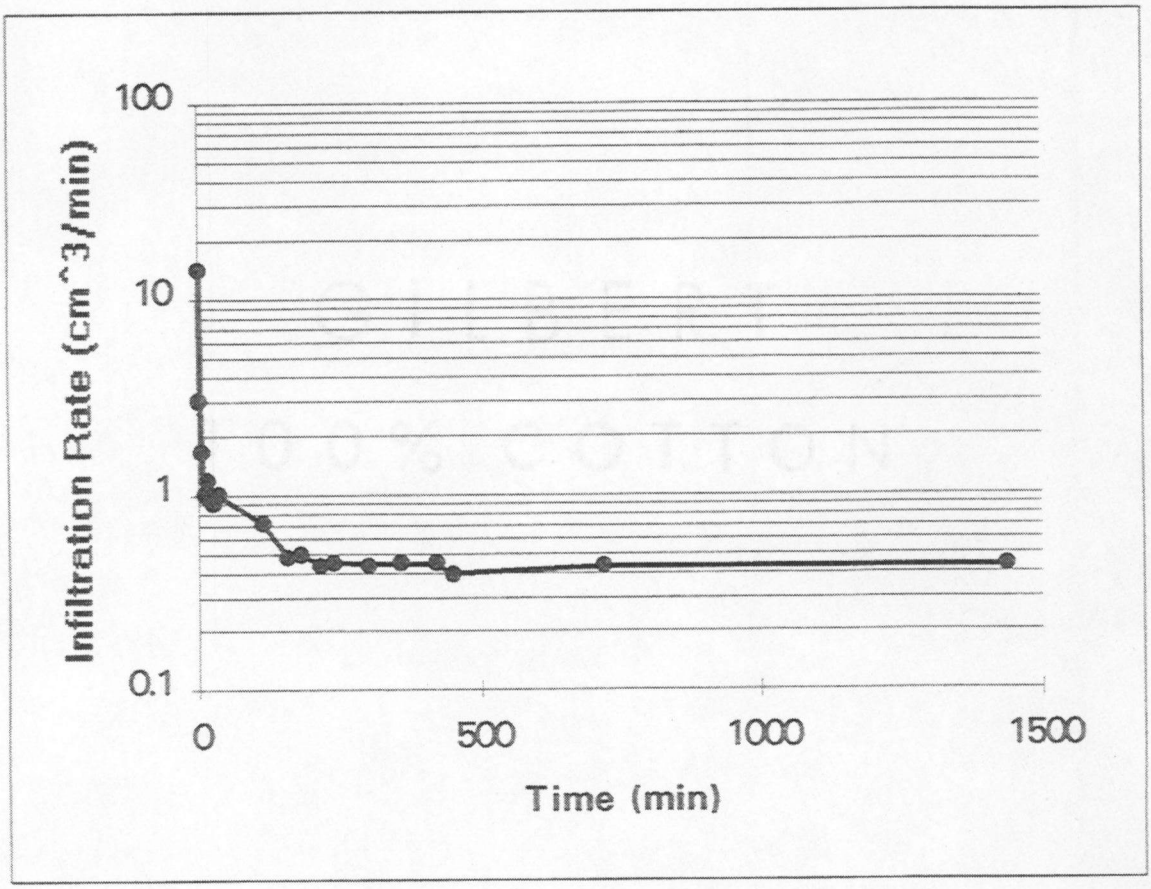
Sample just before test

Sample Information

Compacted Water Content = 36.9%
Compacted Dry Density = 1.35 g/cm^3

Sample History

The sample was subjected to three freeze-thaw cycles. It was saturated before these cycles. Water was applied for the first 20 minutes of infiltration followed by the dye. It was cracked upon infiltration.



Fracture Stains: Sample FT-6

Sample Info: Permeant - Rhodamine Red Dye
Size - 4" diameter; 2" thick

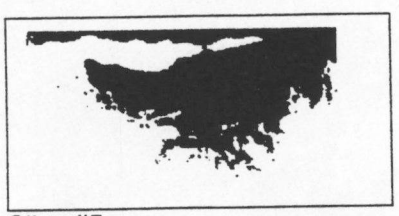
Soil - Compacted Kaolinite
Sample state - 3 freeze/thaw cycles


Slice #1


Slice #2


Slice #3


Slice #4


Slice #5


Slice #6


Slice #7


Slice #8

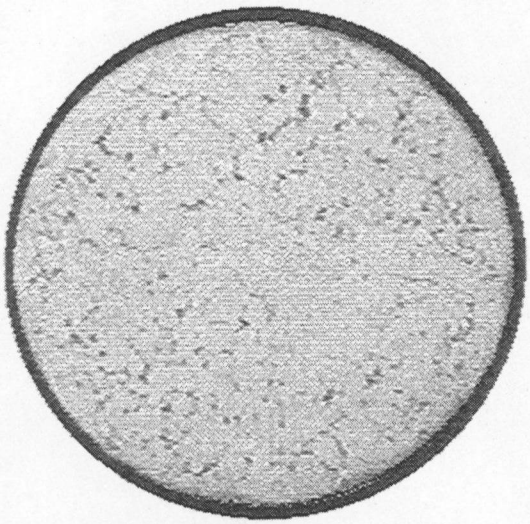

Slice #9


Slice #10


Slice #11


Slice #12

Infiltration Test: Sample FT-7



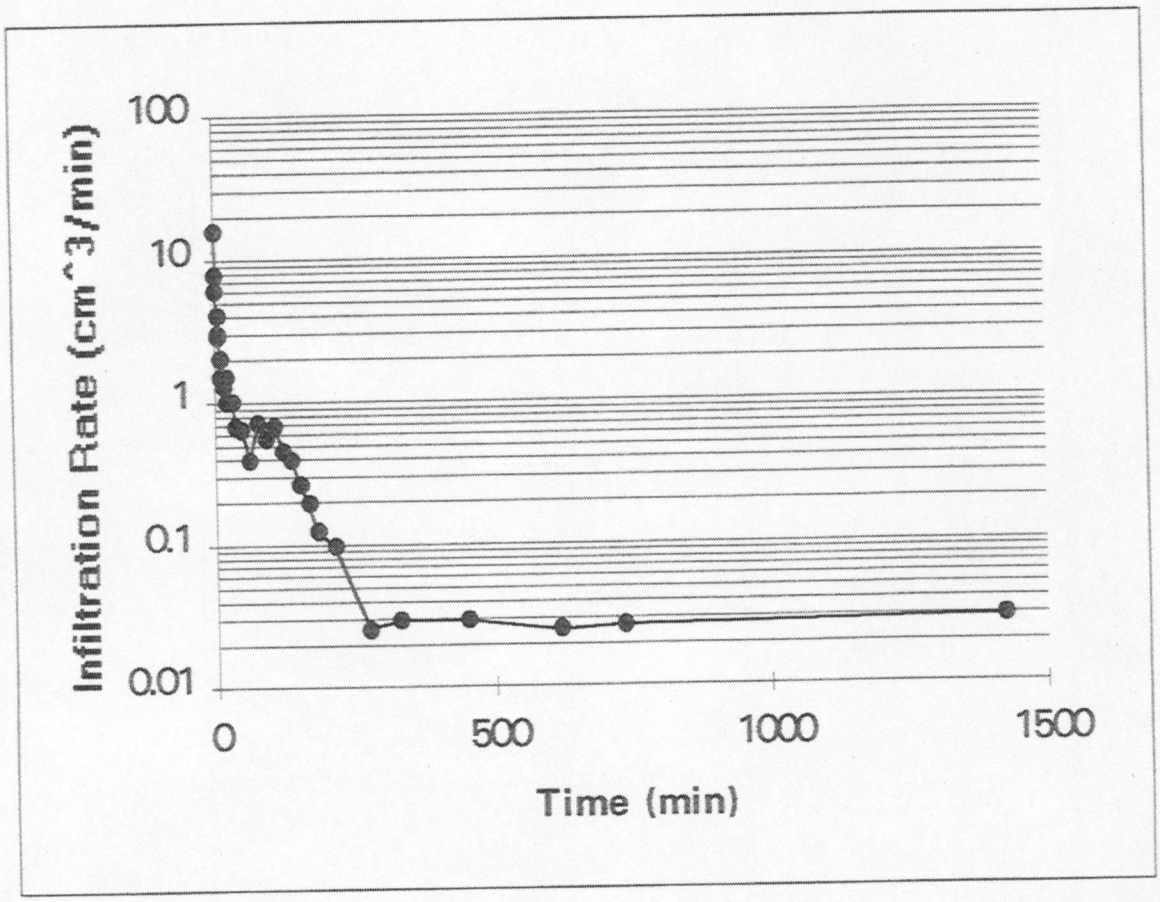
Sample just before test

Sample Information

Compacted Water Content = 36.9%
Compacted Dry Density = 1.35 g/cm^3

Sample History

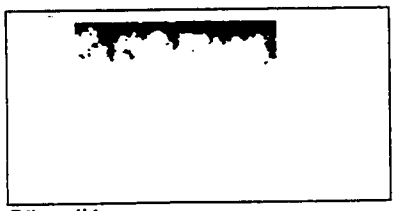
The sample was subjected to three freeze-thaw cycles. It was not saturated at the beginning of the cycles. The sample was cracked upon infiltration.

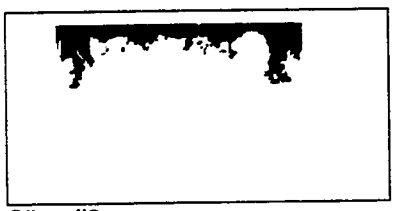


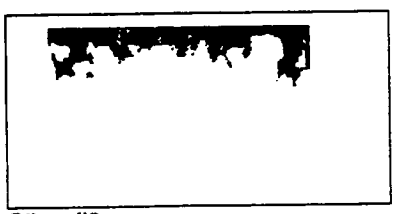
Fracture Stains: Sample FT-7

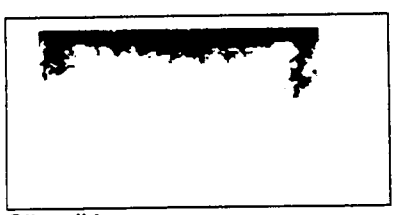
Sample Info: Permeant - Rhodamine Red Dye
Size - 4" diameter; 2" thick

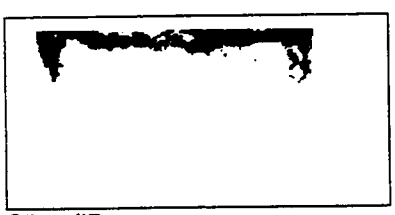
Soil - Compacted Kaolinite
Sample state - 3 frreze/thaw cycles

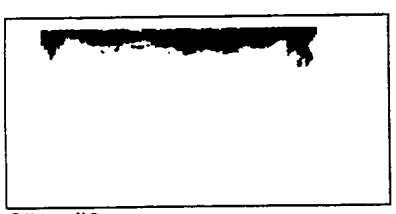

Slice #1

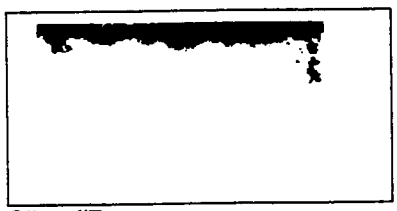

Slice #2

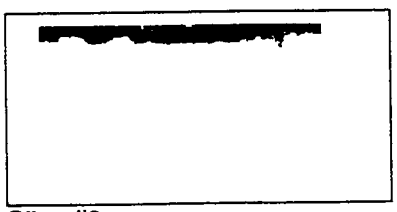

Slice #3

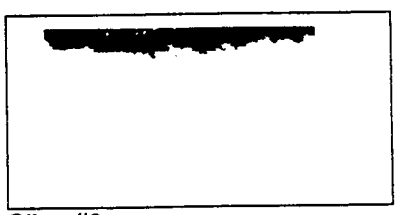

Slice #4

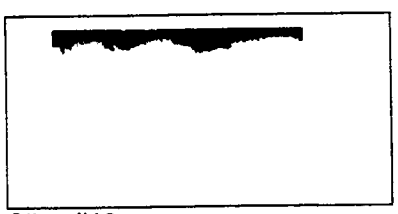

Slice #5

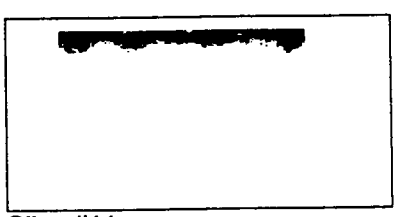

Slice #6

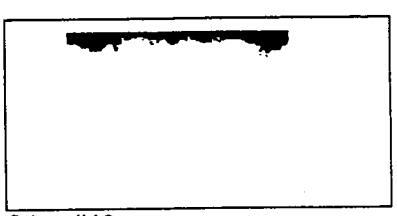

Slice #7


Slice #8


Slice #9


Slice #10


Slice #11


Slice #12

VITA

Mickey Charles McBrayer was born in Rome, Georgia on August 1, 1970. He grew up in Cartersville, Georgia. He graduated as salutatorian from Cass Comprehensive High School in June, 1988. He attended the Georgia Institute of Technology from 1988 to 1993 and received his Bachelor of Science degree in Civil Engineering. During this time he was also a Co-op student with LAW Engineering Company in Atlanta, Georgia. He went on to attend graduate school at the University of Tennessee, Knoxville. He graduated in May 1995 with his Master of Science in Civil Engineering. In the spring of 1995 he will begin work in pursuit of a Doctor of Philosophy.